Remote plasma deposition of hydrogenated amorphous silicon : plasma processes, film growth, and material properties

Citation for published version (APA):
Kessels, W. M. M. (2000). *Remote plasma deposition of hydrogenated amorphous silicon : plasma processes, film growth, and material properties*. [Phd Thesis 1 (Research TU/e / Graduation TU/e), Applied Physics and Science Education]. Technische Universiteit Eindhoven. https://doi.org/10.6100/IR536418

DOI:
10.6100/IR536418

Document status and date:
Published: 01/01/2000

Document Version:
Publisher's PDF, also known as Version of Record (includes final page, issue and volume numbers)

Please check the document version of this publication:

- A submitted manuscript is the version of the article upon submission and before peer-review. There can be important differences between the submitted version and the official published version of record. People interested in the research are advised to contact the author for the final version of the publication, or visit the DOI to the publisher's website.
- The final author version and the galley proof are versions of the publication after peer review.
- The final published version features the final layout of the paper including the volume, issue and page numbers.

Link to publication

General rights
Copyright and moral rights for the publications made accessible in the public portal are retained by the authors and/or other copyright owners and it is a condition of accessing publications that users recognise and abide by the legal requirements associated with these rights.

- Users may download and print one copy of any publication from the public portal for the purpose of private study or research.
- You may not further distribute the material or use it for any profit-making activity or commercial gain
- You may freely distribute the URL identifying the publication in the public portal.

If the publication is distributed under the terms of Article 25fa of the Dutch Copyright Act, indicated by the "Taverne" license above, please follow below link for the End User Agreement:

www.tue.nl/taverne

Take down policy
If you believe that this document breaches copyright please contact us at:

openaccess@tue.nl

providing details and we will investigate your claim.

Download date: 16. Nov. 2023

REMOTE PLASMA DEPOSITION OF HYDROGENATED AMORPHOUS SILICON

PLASMA PROCESSES, FILM GROWTH, AND MATERIAL PROPERTIES

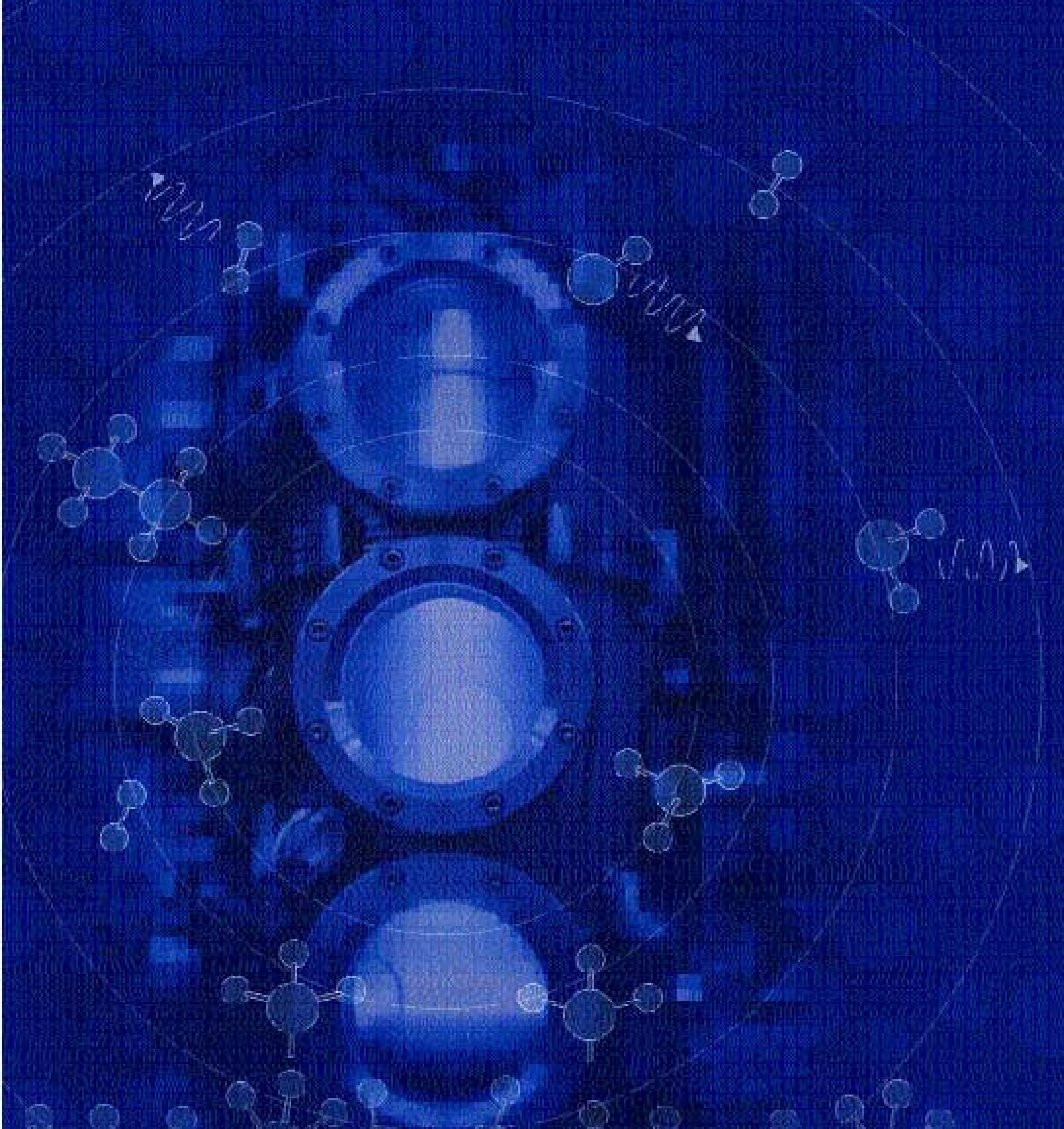

ERWIN KESSELS

REMOTE PLASMA DEPOSITION OF HYDROGENATED AMORPHOUS SILICON ERWIN KESSELS

Remote Plasma Deposition of Hydrogenated Amorphous Silicon

Plasma Processes, Film Growth, and Material Properties

PROEFSCHRIFT

ter verkrijging van de graad doctor
aan de Technische Universiteit Eindhoven,
op gezag van de Rector Magnificus, prof.dr. M. Rem,
voor een commissie aangewezen door het College
voor Promoties in het openbaar te verdedigen op
woensdag 13 September 2000 om 16.00 uur

door

Wilhelmus Mathijs Marie Kessels

geboren te Venlo

Dit proefschrift is goedgekeurd door de promotoren:

prof.dr.ir. D.C. Schram

en

prof.dr. W.F. van der Weg

en de copromotor:

prof.dr.ir. M.C.M. van de Sanden

The work described in this thesis was supported by the Netherlands Organization for Scientific Research (NWO) in the project entitled *Solar Cells for the 21st century*.

Printed and bound by Universiteitsdrukkerij Technische Universiteit Eindhoven
Cover design by Sjors Tuithof

CIP-DATA LIBRARY TECHNISCHE UNIVERSITEIT EINDHOVEN

Kessels, Wilhelmus Mathijs Marie

Remote Plasma Deposition of Hydrogenated Amorphous Silicon: Plasma Processes, Film Growth, and Material Properties / by Wilhelmus Mathijs Marie Kessels.-
Eindhoven: Eindhoven University of Technology, 2000.-
Thesis.- With summary in Dutch.-
ISBN 90-386-1579-5
NUGI 812
Trefw.: plasmadepositie / plasmadiagnostiek / plasmachemie / materiaalonderzoek / siliciumhalfgeleiders
Subject headings: plasma deposition / plasma diagnostics / plasma chemistry / material properties / amorphous semiconductors / silicon

Preface

This thesis deals with remote plasma deposition of hydrogenated amorphous silicon (a-Si:H), and in particular with high rate deposition as well as with the relation between plasma and surface processes and the a-Si:H film properties. The thesis is organized into two main sections. Part A describes the framework in which the thesis work has been performed as well as the motivation of the research. Furthermore, an overview of the results, their implications, and the conclusions is presented, thereby placing the work in a broader context and perspective. In Part B, the basis of the thesis work is presented in several articles that give a full, detailed description of the results obtained in the various sub-areas of the research. These articles have been published or will be published in international scientific journals and they are listed approximately in chronological order.

Erwin Kessels
Tilburg, April 2000

Contents

Part A: Framework and Overview of the Research

A.1 Introduction and framework of the research 3

I. Solar cells for the 21st century 3
II. a-Si:H, plasma deposition, and issues in a-Si:H (solar cell) technology 4
III. Goal of this thesis and outline 6

A.2 Overview of the research, the present status, and outlook 9

I. Introduction to the expanding thermal plasma technique 9
II. Good quality a-Si:H at 10 nm/s?! 9
III. Plasma processes and growth precursors versus a-Si:H film quality 14
IV. Surface reactions and the growth mechanism of a-Si:H 21

A.3 General conclusions 23

Part B: Articles

B.1 Temperature and growth-rate effects on the hydrogen incorporation in hydrogenated amorphous silicon 29
W.M.M. Kessels, R.J. Severens, M.C.M. van de Sanden, and D.C. Schram, J. Non-Cryst. Solids **227-230**, 133 (1998).

B.2 Hydrogen poor cationic silicon clusters in an expanding argon-hydrogen-silane plasma 35
W.M.M. Kessels, M.C.M. van de Sanden, and D.C. Schram, Appl. Phys. Lett. **72**, 2397 (1998).

B.3 Formation of large positive silicon-cluster ions in a remote silane plasma 39
W.M.M. Kessels, C.M. Leewis, M.C.M. van de Sanden, and D.C. Schram, J. Vac. Sci. Technol. A **17**, 1531 (1999).

B.4 Formation of cationic silicon clusters in a remote silane plasma and their contribution to hydrogenated amorphous silicon film growth 45
W.M.M. Kessels, C.M. Leewis, M.C.M. van de Sanden, and D.C. Schram, J. Appl. Phys. **86**, 4029 (1999).

B.5 Surface reaction probability during fast deposition of hydrogenated amorphous silicon with a remote silane plasma 59
W.M.M. Kessels, M.C.M. van de Sanden, R.J. Severens, and D.C. Schram, J. Appl. Phys. **87**, 3313 (2000).

B.6 Film growth precursors in a remote SiH_4 plasma used for high rate deposition of hydrogenated amorphous silicon 69
W.M.M. Kessels, M.C.M. van de Sanden, and D.C. Schram, accepted for publication in J. Vac. Sci. Technol. A **18**, (2000).

Contents (*continued*)

B.7 Hydrogenated amorphous silicon deposited at very high growth rates by an expanding Ar-H_2-SiH_4 plasma 83
W.M.M. Kessels, R.J. Severens, A.H.M. Smets, B.A. Korevaar, G.J. Adriaenssens, D.C. Schram, and M.C.M. van de Sanden, submitted for publication in J. Appl. Phys.

B.8 Cavity ring down detection of SiH_3 in a remote SiH_4 plasma and comparison with model calculations and mass spectrometry 95
W.M.M. Kessels, A. Leroux, M.G.H. Boogaarts, J.P.M. Hoefnagels, M.C.M. van de Sanden, and D.C. Schram, submitted for publication in J. Vac. Sci. Technol. A.

B.9 Improvement of hydrogenated amorphous silicon properties with increasing contribution of SiH_3 to film growth 107
W.M.M. Kessels, M.G.H. Boogaarts, J.P.M. Hoefnagels, M.C.M. van de Sanden, and D.C. Schram, submitted for publication in J. Vac. Sci. Technol. A.

B.10 Cavity ring down study of the densities and kinetics of Si and SiH in a remote Ar-H_2-SiH_4 plasma 111
W.M.M. Kessels, J.P.M. Hoefnagels, M.G.H. Boogaarts, D.C. Schram, and M.C.M. van de Sanden, submitted for publication in J. Appl. Phys.

B.11 *In situ* probing of surface hydrides on hydrogenated amorphous silicon using attenuated total reflection infrared spectroscopy 121
W.M.M. Kessels, D.C. Marra, M.C.M. van de Sanden, and E.S. Aydil, submitted for publication in J. Vac. Sci. Technol. A.

B.12 *In situ* infrared study of the role of ion flux and substrate temperature on a-Si:H surface composition 133
D.C. Marra, W.M.M. Kessels, M.C.M. van de Sanden, K. Kashefizadeh, and E.S. Aydil, submitted for publication in J. Vac. Sci. Technol. A.

B.13 On the growth mechanism of hydrogenated amorphous silicon 147
W.M.M. Kessels, A.H.M. Smets, D.C. Marra, E.S. Aydil, D.C. Schram, and M.C.M. van de Sanden, accepted for publication in Thin Solid Films.

Summary 155

Samenvatting 157

List of other publications related to this work 159

Dankwoord/Acknowledgments 160

Curriculum vitae 161

Part A

Framework and Overview of the Research

A.1 Introduction and framework of the research

I. SOLAR CELLS FOR THE 21ST CENTURY

"Solar cells for the 21st century" is the title of the research program started in 1995 by The Netherlands Organization for Scientific Research (NWO) on behalf of the Ministry of Education and Science. This program forms the framework of the research described in this thesis. Together with the Netherlands Program for Photovoltaic Solar Energy, as carried out by the Netherlands Agency for Energy and the Environment (NOVEM) on behalf of the Ministry of Economical Affairs, it forms the basis of the Dutch effort to attain large-scale implementation of photovoltaic energy (PV) in the 21st century. The programs are concentrated on research, development and demonstration projects, and they should enable the realization of a Dutch PV facility with a cumulative power of 1450 MWp[a] (~10 PJ or 0.5% of the forecast energy need) in 2020 as targeted by the Dutch government.[1-3] The efforts on PV, and renewable energy sources in general, are initiated by the worldwide growing energy demands, the increasing environmental problems, and declining fossil fuel resources. For example, in a recent study by Shell International[4] it has been forecast that by 2020–2030 fossil fuels will no longer be able to contribute to the growth in energy requirements necessary to fuel the economic development of the world population. Renewable energy sources on the other hand, will gradually take an increasing market share and are believed to have a significant contribution by 2020–2030 on the world energy market. In the sustained growth scenario of the energy demand it is even expected that PV accounts for 15–20% of the world energy production in 2060!

For the time being, the worldwide market for PV is still rather small (see Table I), but growing considerably. An improving price/performance ratio of solar cell systems, due to technological breakthroughs in combination with increasing interest from industry and consumers, has herein a crucial role. At present, more than 80% of the solar cells produced are crystalline silicon (c-Si) solar cells. These have relatively high efficiencies (commercial modules 12–15%) but also high production costs. The module price is presently about 4 Euro per Wp corresponding roughly with an energy price of about 0.65 Euro per kWh. A significant price reduction can be obtained on relatively short term for the well-established c-Si solar cell technology by large-scale production (economy-of-scale) and innovations in cell design, materials and production.

A lot is also expected from the upcoming thin film technologies.[5] Solar cells based on thin films (thickness is ~0.3–3 μm) of cadmium telluride (CdTe), copper indium (gallium) diselenide (CIS or CIGS), and especially of hydrogenated amorphous, micro- and poly-crystalline silicon (a-Si:H, μc-Si:H, and poly-Si:H) are ascribed a high potential to become competitive with grid electricity consumer prices. This can be attributed mainly to lower raw material needs and lower production costs, but the fact that these cells are easier to implement and to integrate in building materials and constructions is also an important advantage. With respect to thin film solar cells, the amorphous silicon technology is the most mature and has the highest capability for large-scale worldwide PV solar energy production. Hydrogenated amorphous silicon based solar cells already have a market share of about 15% in commercial PV modules and consumer electronics, while a drastic growth in production facility is presently taking place, especially in Japan and the United States. At present, the commercially available modules have a stabilized efficiency of 4–8%, while the laboratory record on a small area cell is 13% for a "sophisticated" triple junction cell (a-Si:H/a-SiGe:H/a-SiGe:H).[6] Irrespective of these low efficiencies, a-Si:H based solar cells appear to be an ideal future candidate for PV applications, where low costs are more important than efficiency (i.e., for the greater part of the applications). Especially when they are produced in large volumes by innovated techniques in roll-to-roll production processes on cheap materials, such as foils.

TABLE I. Development of the worldwide market for photovoltaic (PV) modules (Ref. 7).

Year	Worldwide market (MWp/year)
1995	78
1996	89
1997	126
1998	153
1999	198

---

[a] The unit Wp or Watt-peak represents the power generated by a solar cell under maximum irradiation, i.e., 1 kW/m^2 with AM1.5 spectrum. In the Netherlands, a PV module with a capacity of 1 Wp delivers roughly 1 kWh per year.

For example, in The Netherlands, Akzo Nobel has started a project[b] to come to a large-scale commercial production of a-Si:H solar cells and with the objective to reduce the actual solar cell module price by a factor of 3–5. By producing cells in tandem configuration (a-Si:H/a-SiGe:H)[8] on a temporary foil in a roll-to-roll process[9,10] at a production level of 1 million m^2 per year,[c] it is projected that total costs approach 40 Euro per m^2 PV foil.[8,9] This corresponds approximately with a price of 0.5 Euro/Wp and is a good starting point to achieve a PV solar energy price that is competitive with the grid electricity consumer price of about 0.13 Euro/kWh.[9]

However, before coming to large scale, cost-effective production of a-Si:H based solar cells, several problems need to be solved. This requires continuation of the ongoing fundamental research on the materials and production processes, with simultaneously, attention for industrially relevant issues. In the following section, after an introduction to the a-Si:H material and its production process, an overview of the most important current issues in a-Si:H (solar cell) technology will be given.

II. a-Si:H, PLASMA DEPOSITION, AND ISSUES IN a-Si:H (SOLAR CELL) TECHNOLOGY

Hydrogenated amorphous silicon or a-Si:H, is a semiconducting alloy of silicon and hydrogen in an amorphous matrix, whereas the corresponding materials which contain a (small) crystalline fraction are called hydrogenated microcrystalline silicon (μc-Si:H) or polycrystalline silicon (poly-Si:H). In solar cells, these intrinsic materials are used as the active photovoltaic layer for the conversion of photon energy into free electron-hole pairs. Their main advantage over c-Si is the fact that they have a higher optical absorption coefficient in the visible range of the spectrum. For a-Si:H, the selection rules for optical absorption are completely relaxed due to its amorphous nature leading to a direct optical bandgap. Therefore films with a much smaller thickness than in c-Si solar cells are sufficient to absorb the same amount of light. Furthermore, the optical bandgap of a-Si:H of 1.6–1.8 eV leads to a better use of the energy of the photons within the solar spectrum, while combinations of a-Si:H with lower bandgap materials, such as μc-Si:H (1.1 eV) or a-SiGe:H (1.45 eV), in tandem or triple-junction cells enable an optimum use of the solar spectrum.

A disadvantage in comparison with c-Si is that the amorphous nature of the material leads a considerable amount of defect states (i.e., mainly dangling bonds) in the bandgap. These form recombination centers for the electrons and holes and lead to a rather small diffusion length of the charge carriers. Therefore charge separation needs to be enhanced by an electric field that is created by thin n-type and p-type doped layers, sandwiching the intrinsic film (see Fig. 1). Because both the electrons and holes need to be collected, the efficiency of a-Si:H solar cells is mainly determined by the product of lifetime and drift mobility of the minority charge carriers, i.e., the holes.

Apart from thin film solar cells, a-Si:H has also applications in other devices. Intrinsic a-Si:H is used as the channel material in thin film transistors (TFTs) that are used for addressing pixels of liquid crystal displays (LCDs) and scanner arrays. It is used in detectors, for light sensing but also for high energy radiation (x-ray) imaging, and as the photoreceptor in photocopiers and laser printers. Furthermore, a-Si:H can be applied in light emitting diodes (LEDs), where photoluminescence leads to emission in the near-infrared (pure a-Si:H) or in the visible (e.g., alloy with carbon). These applications, however, set different demands on the a-Si:H material properties than solar cells.

Although there exist several deposition techniques, a-Si:H is generally produced by means of plasma deposition in radio-frequency (rf) driven parallel plate reactors. In this particular method of plasma enhanced chemical vapor deposition (PECVD) a silicon containing precursor gas, usually SiH_4, is ionized and dissociated by electron impact and secondary induced chemical reactions. The deposition process is carried out under low-pressure conditions (within the range 0.01–1 mbar), and the precursor gas is often diluted by noble gases and/or H_2. A high dilution of SiH_4 in H_2 is usually used to obtain μc-Si:H and poly-Si:H films. An important advantage of plasma deposition is the fact that it can take place at relatively low temperatures. The energy for SiH_4 dissociation is mainly put in the electrons in the plasma (electron temperature ~3 eV) while the gas remains relatively cold (typically ~0.05 eV or 500 K). The substrate temperature is typically 200–300 °C and permits the use of low-cost substrate materials. A disadvantage of rf PECVD is, however, the relatively low deposition rate of typically 0.1–0.3 nm/s. For an intrinsic a-Si:H film of 400 nm, as typically used in a-Si:H solar cells, this leads to deposition times between ½ and 1 hour.

Currently there are several issues in a-Si:H (solar cell) technology which are important to the potential of manufacturing a-Si:H solar cells cost-effectively. These can be divided into performance related and production cost related issues, as the price-performance ratio is decisive on the energy market.

---

[b] This project "Helianthos" started in 1997 and is a cooperation between Akzo Nobel, TNO Institute of Applied Physics, Eindhoven University of Technology, Delft University of Technology, and Utrecht Univerisity.

[c] With the expected stabilized efficiency of 7% this is equivalent to a production level of 70 MWp/year.

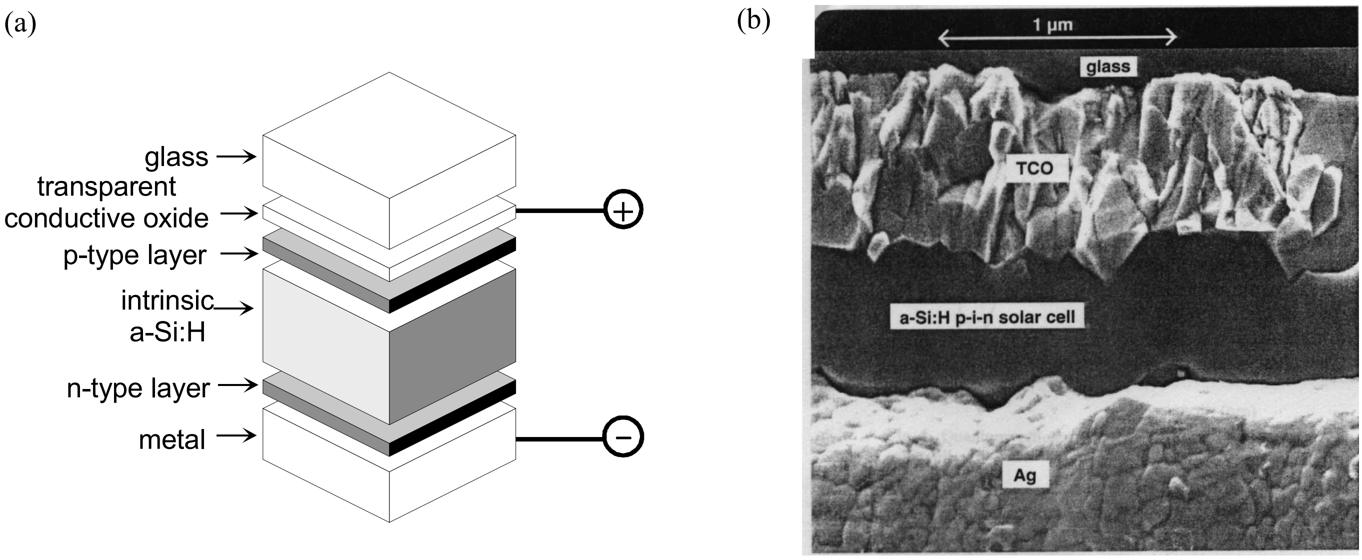

FIG. 1. (a) Schematic representation of a typical thin film a-Si:H solar cell on glass. Incoming photons [passing glass and transparent conductive oxide (TCO)] with sufficient energy, i.e., larger than the bandgap, are absorbed in the a-Si:H layer creating electron-hole pairs. The electrons and holes are separated by the internal electric field generated by the p- and n-type doped layers and the charge is collected at the electrodes. The intrinsic a-Si:H layer of this single junction "p-i-n cell" is typically ~400 nm thick, the doped layers have typically a thickness in the range of 10–30 nm. (b) Cross-sectional transmission electron micrograph of a p-i-n a-Si:H solar cell on glass. The highly reflective silver back electrode acts as a back reflector.

Concentrating on the a-Si:H film and its production process, the most important issues are:

- *cell efficiency*: As already mentioned, the efficiency of an a-Si:H solar cell is mainly limited by the collection of the charge carriers at the electrodes. The presence of defect states in the bandgap leads to recombination centers for the electrons and holes. This results in a small mobility-lifetime product and consequently small diffusion length, especially for the holes. Depositing films with a low defect density (~10^{16} cm^{-3}, i.e., at the level of <10^{-6} of the Si atomic density in the film) is therefore crucial for the application of the material in solar cells. A related point is to obtain maximum light absorption in a film that is as thin as possible. Due to the relatively small diffusion length of the holes (100–200 nm) it is important to have a high internal electric field over the complete intrinsic layer. Therefore the intrinsic film is preferentially kept as thin as possible, while absorption is enhanced by light trapping using textured surfaces and by the application of a back reflector (see Fig. 1).
- *stability against light-induced degradation*: A very important issue in a-Si:H solar cell technology is the degradation of the cell efficiency during light exposure, the so-called Staebler-Wronski effect.[11] This effect typically leads to an efficiency that is 20–30% lower than the initial value.[d] The degradation arises from the creation of additional dangling bonds, which are metastable as they can be annealed out. The origin of the creation of these defects is not yet completely understood. It has, among other things, been attributed to the breaking of weak Si-Si bonds present in the band tails by the recombination of light-generated electron-hole pairs,[12] to the breaking of strained Si-Si bonds by mobile hydrogen atoms released by the recombination of light-generated electron-hole pairs,[13] and to the formation of dangling bonds by the release of two hydrogen atoms from two Si-H bonds and the subsequent formation of two new Si-H bonds by breaking a Si-Si bond.[14] The effect of these additional dangling bonds on the solar cell's efficiency can be restricted by going to very thin intrinsic films (<250 nm). But in order to maintain efficient light absorption, it is advantageous to use tandem or triple junction cell configurations. Furthermore, it is claimed that a low hydrogen concentration in the film is favorable for reducing the Staebler-Wronski effect.[15]
- *deposition rate*: As already mentioned, the low deposition rate is an important bottleneck for the production of a-Si:H in industrial processes. To obtain a high production throughput with a typical deposition time of one hour, it is necessary to go to large electrode areas for the conventional

---

[d] For this reason stabilized efficiencies have explicitly been mentioned in the previous section.

deposition techniques. This results in very large investments in equipment and hence leads to high production costs. For this reason, industry is very interested in increasing the deposition rate, possibly even at the expense of the film quality, for example by depositing at higher pressure and higher plasma power. Another possibility is to use alternative deposition techniques, such as very high frequency (VHF) PECVD, hot wire chemical vapor deposition (HWCVD), or the expanding thermal plasma (ETP), which is the subject of this thesis.

- *large-volume production process technology*: Related to the deposition technique and the deposition rate, is the process technology used to obtain large-volume production. Important issues are, for example: a good homogeneity of film thickness and other film properties over large areas when using large electrodes, batch or roll-to-roll processing and compatibility of substrate material, demands on vacuum systems (ultra-high or high vacuum), the reliability of the process, a high production up time (continuous production) and yield, reactor cleaning (plasma clean with, e.g., CF_4 or SF_6, scrubbing, wet etch), etc.
- *material costs*: In the present a-Si:H technologies the materials costs have a considerable contribution to the cost price of the cells, especially when glass panels are used as substrates. Therefore cheaper, thin metal or even polymer foils are preferred which can also be used in roll-to-roll processes.[8,16,17] This sets demands on process temperatures and processing steps. Furthermore, the gas utilization in the deposition process is important. The use of high purity gases and the possible necessity of applying additional gas purification bring about high costs. It is also important to obtain a high gas efficiency, especially for the rather expensive SiH_4 gas.

III. GOAL OF THIS THESIS AND OUTLINE

The relatively low deposition rate of a-Si:H obtained by conventional plasma deposition techniques, has initiated a lot of research on alternative production techniques, including the expanding thermal plasma that is addressed in this thesis. The expanding thermal plasma, or ETP, is a remote plasma deposition technique, developed at the Eindhoven University of Technology,[18] which is capable of depositing good quality films of several materials at very high growth rates. In the recent years' work on this technique, a central question has therefore been whether it is possible to deposit a-Si:H with film properties suitable for the application in solar cells at such high deposition rates.[19,20]

In addition to optimization of the film and the process properties, the research on the deposition of a-Si:H by the ETP technique has a more fundamental and general goal. Important and possibly essential for (full) optimization of a-Si:H and its production process is a profound insight into all aspects playing a role in a-Si:H deposition. As schematically illustrated in Fig. 2, it is expected that the final film properties are ruled by an interplay between the plasma reactions, plasma composition, surface composition, and (sub-)surface reactions. The main goal of this thesis is therefore to obtain a better understanding of these different aspects in a-Si:H deposition and to understand their interrelations. Concerning the expanding thermal plasma, this research has mainly been concentrated on high rate deposition of a-Si:H, whereby the remote nature of the technique enables a profound and independent study of the different aspects. The results of this study are not only relevant for the ETP technique nor for high rate deposition of a-Si:H only. They also have implications for a-Si:H deposition by other (low growth-rate) methods and they yield a better understanding of the physics and chemistry involved in plasma processing and film growth in general.

With respect to a-Si:H solar cell technology, the issues mentioned in the previous section can be translated into several important and interesting fundamental issues, which can possibly be addressed by the ETP technique. The work described in this thesis has been focussed on the following questions:

- What is the relation between the deposition rate and the film properties? Is it even possible to deposit a-Si:H at very high rates while maintaining good film quality? Under which conditions is this possible and what are the limitations?
- Which plasma and gas phase reactions take place in SiH_4 plasmas used for a-Si:H deposition? How can these reactions be controlled or influenced by the plasma settings? Which species (ions, radicals, etc.) contribute to film growth and in which proportion?
- What is the role of the different species contributing to growth in terms of resulting film properties? Are the film properties determined by the species from the plasma and to which extent? Which species are beneficial and which are detrimental for the a-Si:H film quality? What is the role of the substrate conditions (substrate temperature, bias voltage, etc.) in this respect? Can appropriate substrate conditioning compensate for "detrimental" growth precursors?
- How do the plasma species lead to a-Si:H film growth? What is the nature of the a-Si:H surface during deposition and how is it affected by the substrate conditions and plasma composition?

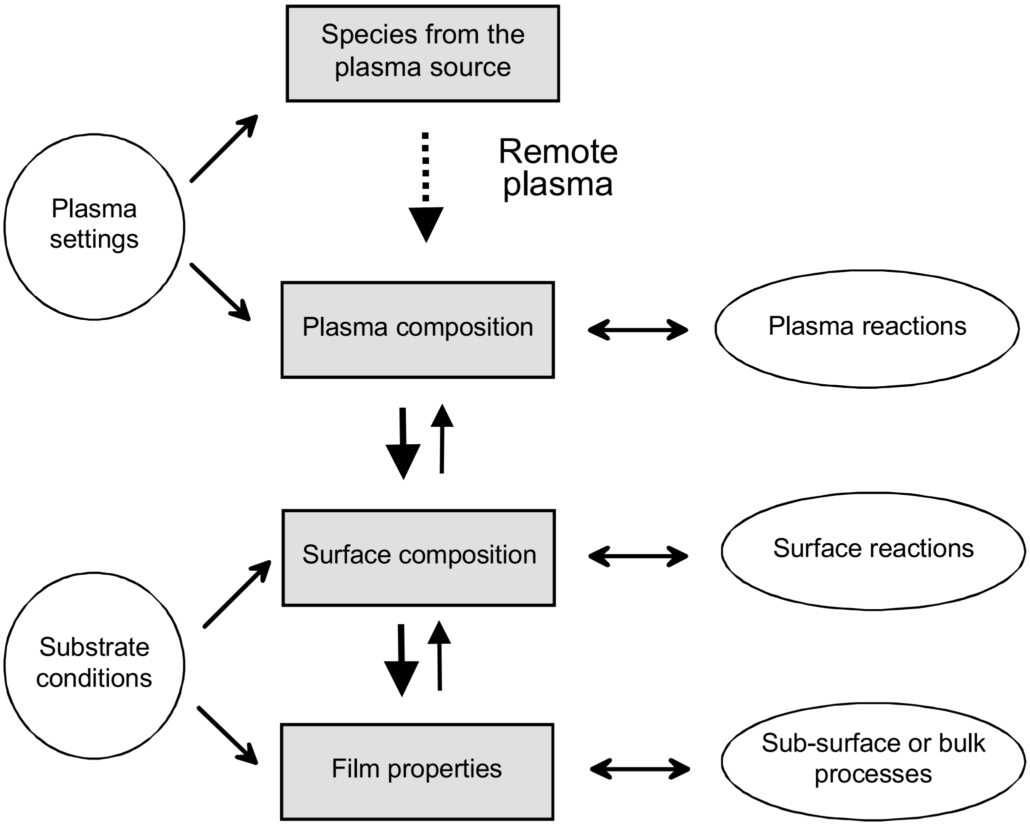

FIG. 2. Schematic and simplified representation of the deposition process of thin films by means of a (remote) plasma. The different aspects of the process, i.e., concerning plasma, surface, and film properties, are indicated together with their most important relations. The different aspects correspond to different "areas of research" and are therefore often studied separately. For the optimization of the film properties, this leads usually to the trial-and-error approach where the film properties are studied for a full range of plasma settings and substrate conditions. The complexity of the deposition process, however, requires an approach where the process is studied in its entirety. This leads finally to basic understanding enabling "sophisticated" and full optimization of the deposition process.

What are the reactions taking place on the surface and how do they lead to dense film growth, hydrogen incorporation, and what is their role in defect generation?

- And finally, with respect to Fig. 2, what are the (presumably) most important aspects of the a-Si:H deposition process?

A medium to reach these goals, as well as an important goal itself within this study, is the further development and improvement of the diagnostic techniques used for the investigation of (processing) plasmas and plasma-surface interactions. Their application is, of course, not limited to the expanding thermal plasma nor is it specific for studies of SiH_4 plasmas and a-Si:H film growth.

With the above-mentioned questions in mind, a systematic study has been performed in which all three (supposedly) major aspects in Fig. 2, i.e., plasma composition and reactions, surface composition and reactions, and the a-Si:H film properties, have been addressed. Most of the experiments have been performed with the ETP technique. A part of the work, however, has been carried out in the group of Prof. E. S. Aydil at the University of California Santa Barbara, where a sensitive surface-diagnostic technique, along with expertise in the field, was available. The results of the different studies are described in detail in the chapters of Part B of this thesis. In this part, every chapter is a journal article which deals with a certain aspect of the a-Si:H deposition process. The articles are given approximately in chronological order and represent all together a period of almost 4 years.

Concerning the expanding thermal plasma, the work has mainly been focussed on the plasma processes and the contribution of different species to film growth. This information is required for interpretation of the a-Si:H film properties in terms of reactions taking place on the surface as was realized when considering the influence of the substrate temperature and deposition rate on the structural film properties (Chapter B.1). For these investigations, several (plasma) diagnostic techniques were implemented.

First, the electrons and ions emanating from the plasma source as well as the $Si_nH_m^+$ ions created when SiH_4 is admixed were investigated by Langmuir probe measurements and ion mass spectrometry (Chapters B.2, B.3, and B.4). Subsequently, the contribution of radicals to film growth were considered by the aperture-well technique (Chapter B.5) and by direct radical detection techniques such as threshold ionization mass spectrometry and optical emission spectroscopy (Chapter B.6). This revealed clear insight into the plasma reactions for various plasma settings and also into the contribution of different species to film growth. The latter was related to the a-Si:H film properties obtained using different conditions and it was demonstrated that device quality a-Si:H can be obtained at 10 nm/s by the ETP technique (Chapter B.7). The understanding of the reactions in the plasma was further refined by radical measurements using the relatively new cavity ring down spectroscopy technique (Chapters B.8, B.9, and B.10). Furthermore, it was shown that the basic reactions in the plasma under "optimum" conditions can be captured in a fluid dynamics model with very simplified chemistry (Chapter B.8).

Furthermore, to gain insight into the nature of the a-Si:H surface during deposition, a study in another "remote" deposition technique was performed at the University of California Santa Barbara. By *in situ* studies using attenuated total reflection infrared spectroscopy the composition of the surface silicon hydrides on a-Si:H during film growth were studied. This revealed information on the surface reactions taking place during deposition (Chapters B.11 and B.12)

Finally, the prevailing kinetic growth model for a-Si:H from SiH_3 was reviewed. From the results obtained in this thesis work, the incorporation of hydrogen in a-Si:H, as also addressed in Chapter B.1, was (re)considered (Chapter B.13).

This section has been only a very brief overview of the work described in this thesis. In order to obtain a clear and total "final" picture of the work, a summary of the most important results described in Part B will be presented in the following chapter. This will also elucidate the outline of the research and the particular considerations made for the different experiments. First an introduction to the ETP technique will be given and an overview of the "optimized" a-Si:H film properties will be presented. The latter gives the present status of the work with respect to the film quality. The opportunities of the application of the ETP technique in solar cell production will also be briefly considered. Subsequently, the results of the investigation of the plasma processes and growth precursors in relation to the a-Si:H properties will be summarized. Finally, the experiments related to the surface reactions and growth mechanism of a-Si:H will be considered in brief and the general conclusions of this thesis work will be presented.

A.2 Overview of the research, the present status, and outlook

I. INTRODUCTION TO THE EXPANDING THERMAL PLASMA TECHNIQUE

Besides the deposition of a-Si:H, the expanding thermal plasma (ETP) setup has been used for the deposition of diamond,[21,22] hydrogenated amorphous carbon[18,23,24] and carbon nitride,[25] zinc oxide,[26] silicon oxide,[27] and silicon nitride.[28] The main advantage of the expanding thermal plasma is the high deposition rate that can be obtained for the different materials. Herein, the compatibility of high rate deposition with good film quality is of major concern.

An important feature of the ETP technique is the fact that it is a remote plasma. This means that plasma production, plasma transport, and surface treatment (e.g., deposition) are geometrically separated. The ETP is actually the ultimate remote plasma technique, because in contrast with, e.g., electron cyclotron resonance plasmas (ECR), remote microwave (μ-wave) and inductively coupled (ICP) plasmas, the downstream properties have no influence on the plasma production zone at all. This is due to the large pressure difference between both regions as will be discussed below. A major advantage of remote plasmas with respect to so-called direct plasmas, such as rf PECVD, is the fact that the substrate holder or electrode does not play a role in plasma production. Furthermore, it is important that direct plasma contact with the substrate is absent, leading to absence and/or a better control of ion bombardment and ultraviolet light exposure. A remote plasma also enables independent variation of plasma parameters and plasma properties. This simplifies optimization of the process and makes higher deposition rates easier accessible. The geometrical separation of the different processes and independent parameter control facilitate also fundamental studies of plasma reactions and film growth mechanisms.

The expanding thermal plasma setup, schematically depicted in Fig. 3, consists of a high-pressure plasma source and a low-pressure deposition chamber. The plasma source is a cascaded arc [see Figs. 3 and 4(a)]. It is used to create reactive species for the dissociation of the deposition precursor gas (SiH_4 for a-Si:H) in the downstream region. It is operated on high flows (tens of sccs/several slm[e]) of non-depositing gases (Ar or Ar-H_2 mixture for a-Si:H) leading to pressures of 0.2–0.6 bar when the plasma is ignited. The discharge in the cascaded arc is current controlled by a dc power supply and the power dissipated is typically within the 2–5 kW range. The plasma in the arc is thermal with an electron density of $\sim 10^{22}$ m^{-3} and with an electron and heavy particle temperature of both ~1 eV.[29] The high heavy particle temperature leads to almost full dissociation of molecular gases when these are injected in the arc.

The plasma emanates from the cascaded arc source through a nozzle and expands into the deposition chamber which is typically at a pressure of 0.1–0.3 mbar. Due to the large difference in pressure between the arc and the chamber, the plasma is accelerated leading to a supersonic expansion. At a few centimeters from the arc outlet there is a stationary shock, after which the plasma expands subsonically. In the supersonic expansion and shock, the electron temperature is reduced to ~0.1–0.3 eV and the electron density to $\sim 10^{17}$–10^{19} m^{-3}. The directed velocity after the shock is typically 1000 m/s. The reactive species emanating from the arc will be discussed in more detail below for different plasma settings. The supersonic expansion, shock region, and subsonic expansion region have been investigated in detail for Ar[30,31] and Ar-H_2 mixtures.[32-36] Figure 4(b) shows an Ar-H_2 plasma close to the arc outlet and Fig. 4(c) shows a plasma for the complete downstream region.

At 5 cm from the arc outlet, a precursor gas can be added to the plasma by an injection ring [see Fig. 4(b)]. This precursor gas is ionized and dissociated by the reactive species emanating from the plasma source. Deposition can subsequently take place by the growth precursors at a temperature-controlled yoke with substrate holder. The substrates and substrate holder are loaded into the deposition chamber from a loadlock system by means of a magnetic transfer arm. More details on the deposition setup are given in Chapters B.4 and B.7 of this thesis.

II. GOOD QUALITY a-Si:H AT 10 nm/s?!

The investigation of the deposition of a-Si:H by the ETP technique was started approximately ten years ago (1989) in the thesis work of Meeusen.[19] After this initial phase, it was fully concentrated on the characterization and optimization of the material properties in the thesis work of Severens.[20] The ETP material deposited at very high growth rates turned out to be very promising for the application in thin film solar cells. From that point, around 1996–1997, the research on the deposition process and a-Si:H material has been intensified and the number of people working on this subject has considerably been

---

[e] 1 sccs or 1 standard cubic centimeter per second = 1 cm^3 gas at 273 K and 1 atm. per second. This corresponds to $\sim 2.5\times 10^{19}$ particles per second. 1 slm or 1 standard liter per minute = 16.7 sccs.

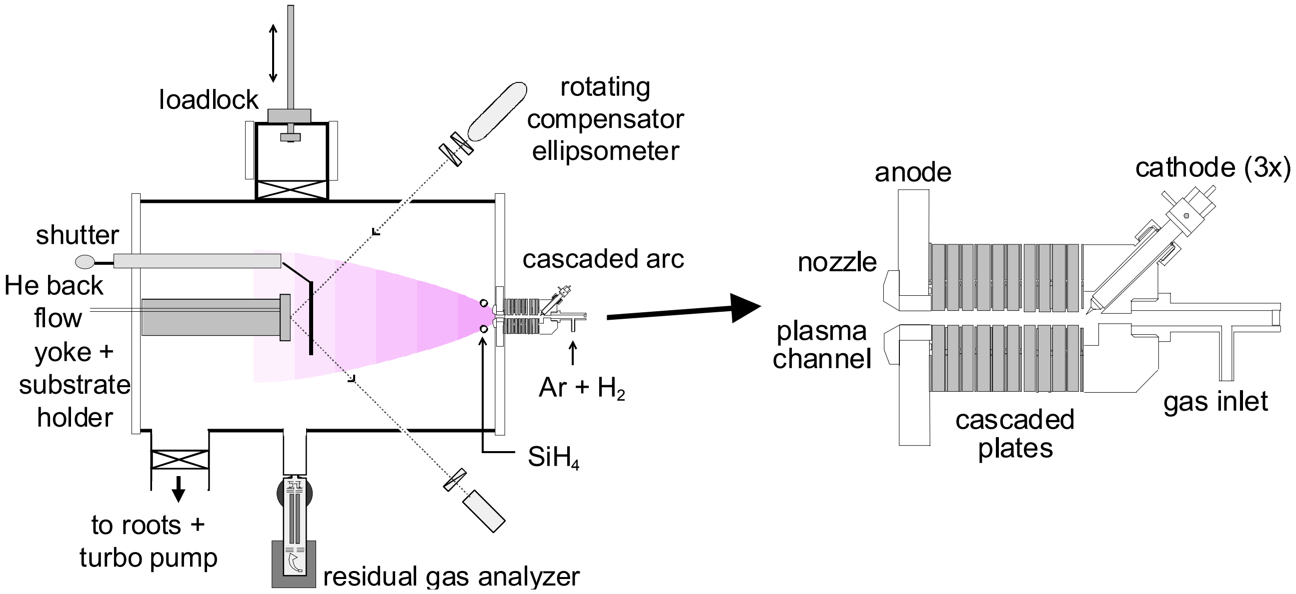

FIG. 3. The expanding thermal plasma setup consisting of a cascaded arc plasma source and a low-pressure deposition chamber. In the cascaded arc a dc discharge in a non-depositing gas is sustained in the plasma channel between three cathodes (only one cathode is shown for clarity) and a grounded anode. The electrically insulated cascaded plates lead to a gradual potential drop. All parts are of copper, except for the cathode tips (tungsten with 2% lanthanum), the PVC and boronnitride spacers between the cascaded plates, and the boronnitride cover of the cathode feedthrough. The arc is vacuum-sealed with O-rings and the cathode, anode, and plates are all water-cooled. The diameter of the plasma channel is 4 mm, the length of a cascaded arc with ten plates is about 10 cm. The typical dimensions of the deposition chamber are a length of 80 cm and a diameter of 50 cm. The distance between arc outlet and precursor gas (e.g., SiH$_4$) injection ring is 5 cm, and the distance between arc outlet and yoke with substrate holder is 35 cm. The substrates are accurately temperature controlled (100–500 ºC) by a He back flow and protected from the plasma during plasma ignition by a shutter. During processing the system is pumped by roots blowers, and overnight it is pumped by a turbo pump reaching a base-pressure of 10^{-6} mbar. A loadlock chamber with magnetic transfer arm is used to put the substrates into the system without venting it. The deposition system is standard equipped with a residual gas analyzer (Balzers QMS200 Prisma) at the side of the reactor and a home-made single wavelength (632.8 nm) rotating compensator ellipsometer. In this study, the setup has also been equipped with a mass spectrometer (Hiden Analytical Epic 300, PSM upgrade) at the position of the substrate holder, an optical emission spectroscopy setup, Langmuir probes, and a cavity ring down absorption spectroscopy system.

extended. This has finally lead to the conclusive notion that the high rate deposited a-Si:H is suitable as the intrinsic layer in thin film solar cells. In this section, the present status of the continuing work will be given.

With the ETP setup, a-Si:H can be deposited at rates varying over more than two orders of magnitude, i.e., at rates ranging from ~0.2–60 nm/s.[37] This enables several well-defined studies as, for example, shown in Chapter B.1 and B.13 and it will be fully exploited in future studies. However, concerning the material quality, the investigations have mainly been concentrated on high rate deposited a-Si:H. After an extensive investigation using different plasma settings, it has been found that the conditions yielding "optimized" a-Si:H at high deposition rates are: an Ar and H$_2$ flow of 55 and 10 sccs, respectively, in the cascaded arc, an arc current of 45 A, a voltage of 140 V, an arc pressure of ~400 mbar, a SiH$_4$ flow of 10 sccs, and a pressure of 0.20 mbar in the downstream region. The corresponding deposition rate is 7–11 nm/s.[f] In Chapter B.7 of this thesis, the results of a part of the plasma parameter space investigated (i.e., H$_2$ flow variation) are presented and the film properties of the "optimized" a-Si:H are discussed in detail. In this section, the properties of the "state-of-the-art" a-Si:H deposited at high rate are summarized in Table II and the most important and prominent properties will be briefly addressed.

A first aspect that draws attention is the relatively high substrate temperature of 400 °C for which the "optimum" properties are obtained. In several studies (Refs. 37 and 41, Chapters B.1 and B.7), it has been observed that substrate temperatures higher than 350 °C are required for obtaining sufficiently dense films

---

[f] The deposition rate for the mentioned conditions is actually 7 nm/s at a substrate temperature of 400 °C. However throughout the work, the output of the SiH$_4$ mass flow controller has drifted, such that some depositions were carried out at slightly higher SiH$_4$ flows and deposition rates. There is evidence that the latter has a negligible influence on the film properties within the range concerned.

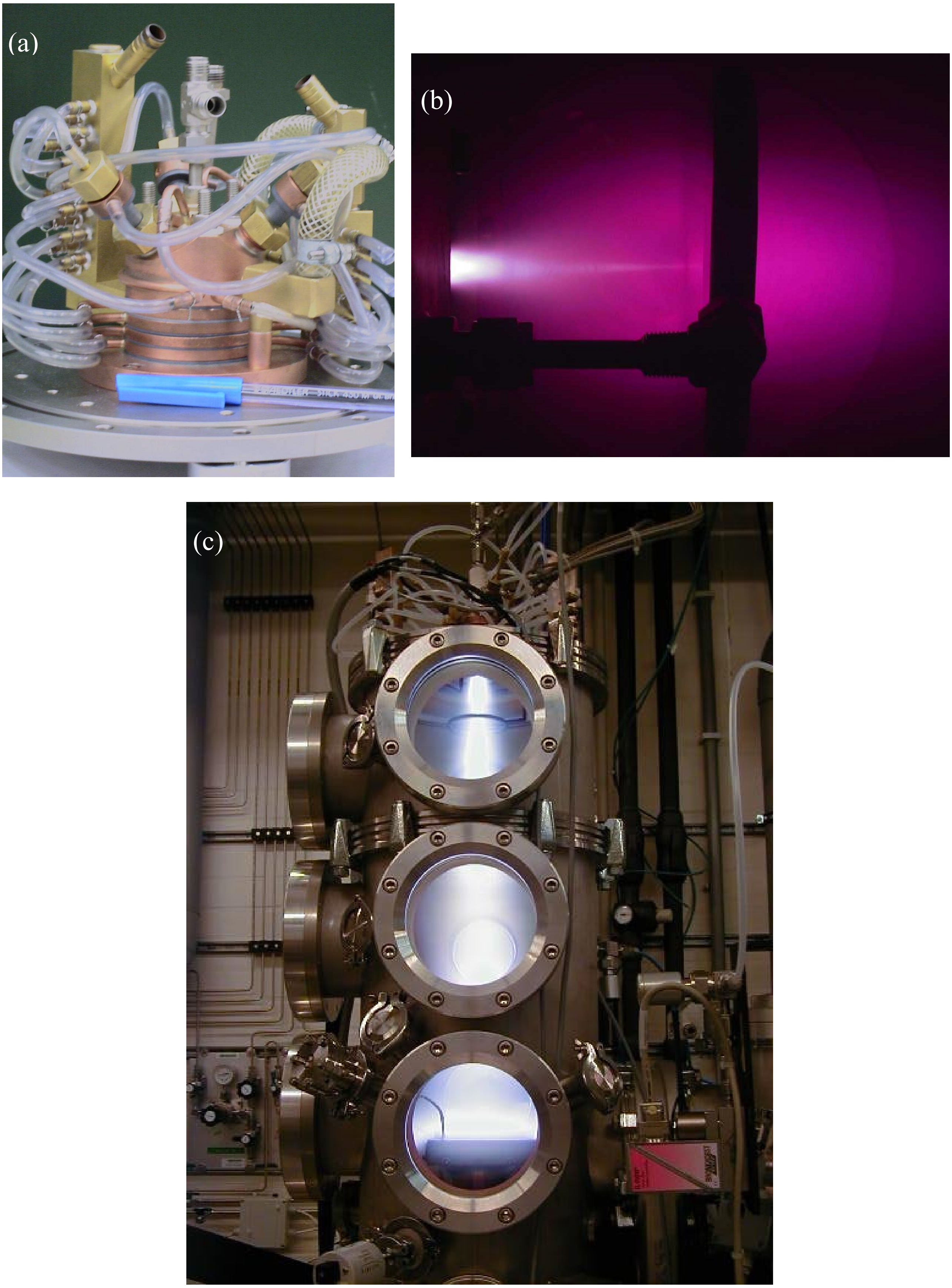

FIG. 4. (a) A cascaded arc plasma source with its plasma channel in vertical direction. This arc is disconnected from the deposition reactor and it has only four cascaded plates. (b) The supersonic expansion region of the expanding thermal plasma for an Ar-H_2 plasma. At approximately 5 cm from the arc outlet the precursor injection ring is visible. (c) Complete overview of the downstream expansion region of the expanding thermal plasma. The deposition reactor shown is part of the new solar cell production system CASCADE.

TABLE II. Room temperature properties of a-Si:H films deposited at a substrate temperature of 400 ºC by means of the expanding thermal plasma.

deposition rate	7–11 nm/s	a,b
SiH_4 consumption	10–12%	c
refractive index (at infrared)	3.6	a
refractive index (at 2 eV)	4.3	d
Si atomic density	5.1×10^{22} cm^{-3}	e
hydrogen content	6–7 at.%	a
microstructure parameter R^*	0.20	a
photoconductivity (under 100 mW/cm^2 AM1.5)	4×10^{-6} Ω^{-1}cm^{-1}	a
dark conductivity	10^{-9} Ω^{-1}cm^{-1}	a
activation energy	0.75 eV	a
Tauc band gap	1.67 eV	a
cubic band gap	1.51 eV	a
hole drift mobility (at 10^4 V/m)	1.1×10^{-2} cm^{2}V^{-1}s^{-1}	a,f
electron drift mobiltiy (at 10^4 V/m)	0.81 cm^{2}V^{-1}s^{-1}	a,f
Urbach energy	50–55 meV	f,g
defect density	10^{16} cm^{-3}	f
RMS surface roughness (at 500 nm thickness)	4 nm	a,d

a: Chapter B.7; b: Kessels *et al.* (Ref. 38); c: Chapter B.6; d: Smets *et al.* (Ref. 39); e: Kessels *et al.* (Ref. 40); f: films were deposited at 450 ºC, Korevaar *et al.* (Ref. 41) and Adriaenssens *et al.* (Ref. 43); g: Smets *et al.* (Ref. 42).

at high deposition rates with the ETP technique. The lower Si atomic density obtained at lower substrate temperatures is directly related to the relatively high hydrogen content of the ETP deposited films at these temperatures. The hydrogen content of the films deposited at 250 °C is ~17 at.% while it is typically 10–12 at.% for rf PECVD films deposited at this temperature.[44,45] The decrease in hydrogen content with increasing substrate temperature is mainly reflected in the decrease of the infrared absorption peak centered at ~2100 cm^{-1}.[41] This absorption peak is attributed to stretching vibrations of SiH_2 and clustered SiH in the film. At 400 °C, the relative magnitude of the 2100 cm^{-1} peak compared to the 2000 cm^{-1} peak (isolated SiH) is still relatively large, as can be concluded from the R^* value. At this high temperature usually values of $R^*<0.1$ are reported.[44,45] Furthermore, based on Raman spectroscopy no indications of micro-crystallinity have been observed for the material, which is also plausible from the relatively low atomic hydrogen flux during deposition (see Chapter B.8).

The photoconductivity is also higher at higher substrate temperatures and it has maximum at 400–450 °C. The maximum value is somewhat lower than those reported for rf PECVD films (~10^{-5} Ω^{-1}cm^{-1}).[44,45] The dark conductivity shows an increase with increasing substrate temperature as well. The value of ~10^{-9} Ω^{-1}cm^{-1} obtained for the optimum quality material is relatively high compared to the values <10^{-10} Ω^{-1}cm^{-1} preferentially obtained for films deposited at 250 °C.[44,45] This difference is at least partially related to the relatively low hydrogen content of 7% at 400 °C. A low hydrogen content is generally accompanied by a relatively small bandgap and low activation energy of the thermally activated dark conductivity as can be observed in Table II (see discussion in Chapter B.7).

It is easier to judge the film quality with respect to solar cell applications when considering the electron and hole drift mobility from time-of-flight experiments and the defect density from the corresponding post-transit photocurrent analysis (Chapter B.7 and Refs. 38, 41, and 43). As shown in Fig. 5, the electron drift mobility is a factor of 3–6 smaller than for typical solar grade rf PECVD films,[46] while the hole mobility is about a factor of 10 larger.[46] The high hole drift mobility is of course advantageous for solar cell applications, as the electronic transport is limited by the holes. The combination of a 10 times higher hole drift mobility and a slightly lower electron drift mobility, is also an explanation for the lower photoconductivity of the material in comparison with rf PECVD films (see Chapter B.7).

The density of states determined from post-transit photocurrent analysis of the time-of-flight measurements[43] has revealed some other distinct differences from conventional rf PECVD material. In Fig. 6, it is shown that the density of states between the band tail and the mid-gap states is three orders of magnitude lower than the density of the mid-gap states. This is the case for both the valence and conduction band sides of the gap. For rf PECVD a-Si:H, this difference is usually only one order of magnitude. For the ETP material, this particular distribution of density of states makes the deep defects at the mid-gap states to stand out prominently above

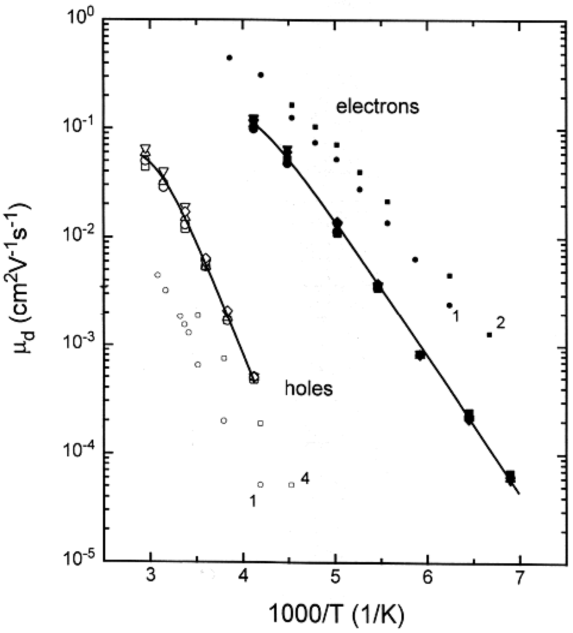

FIG. 5. The drift mobilities μ_d of the electrons and holes in ETP deposited a-Si:H for electric fields of 0.5, 1.0, 1.5, 2.0, and 2.5×10^4 V/cm across the sample. Typical data for rf PECVD a-Si:H films are also shown (by smaller symbols and for electric fields indicated in 10^4 V/cm) (Ref. 43).

the background and it is most probably the reason for the field independence of the mobilities as observed in Fig. 5.[43] The total integrated defect density is ~10^{16} cm^{-3}, similar to the defect densities in solar grade rf PECVD a-Si:H.[41,43]

From the presented film properties, it can be concluded that the a-Si:H films deposited at rates of 7–10 nm/s are suitable for the application in solar cells. However, it appears that higher substrate temperatures than for rf PECVD a-Si:H are necessary. This has implications for the substrate material used during solar cell production, but also for the solar cell structure that can be applied. The commonly used p-i-n structure, where the intrinsic a-Si:H is deposited on a p-type, boron-doped a-Si:H layer, is not applicable at high temperatures due to boron and/or hydrogen out-diffusion. Instead, the n-i-p structure can be used in which the a-Si:H is deposited on a thermally stable n-layer. This cell structure is also applied for hot-wire chemical vapor deposition of a-Si:H, in which high rate deposited films (up to 2 nm/s) generally require high substrate temperatures as well.[47,48]

In order to test the feasibility of the application of the high rate deposited a-Si:H in solar cells, cells with intrinsic a-Si:H deposited at 7 nm/s have been produced using both cell structures (see Fig. 7). These preliminary experiments have been carried out together with the groups of the Delft University of Technology and Utrecht University. They supplied the substrates with doped layers and finished the cells after the deposition of the intrinsic a-Si:H (see Chapter B.7, Refs. 38 and 41). Using this procedure, transport through air during the fabrication process was inevitably. Furthermore, for the simple, single junction solar cells, no special light-absorption enhancement techniques were applied, nor was the thickness of the intrinsic layer optimized. The p-i-n cell with the intrinsic a-Si:H deposited at 300 °C had an initial efficiency of 4.1 % (under 100 mW/cm^2 AM1.5 illumination), while the cell suffered already from degradation of the p-layer. The n-i-p cell with the intrinsic a-Si:H deposited at 400 °C had an initial

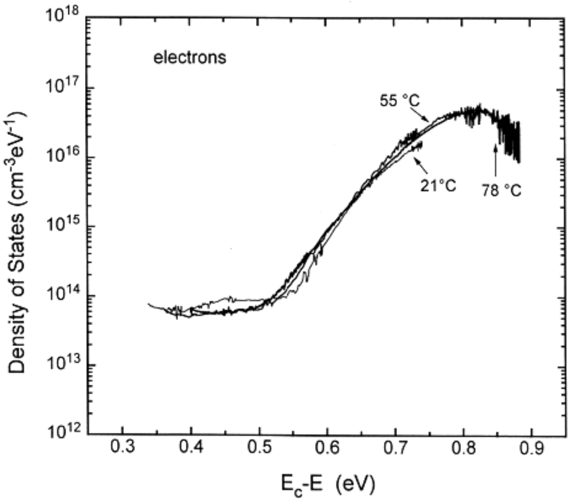

FIG. 6. Density of localized electron states on the conduction band side of the gap as derived from the post-transit photocurrent analysis (Refs. 41 and 43).

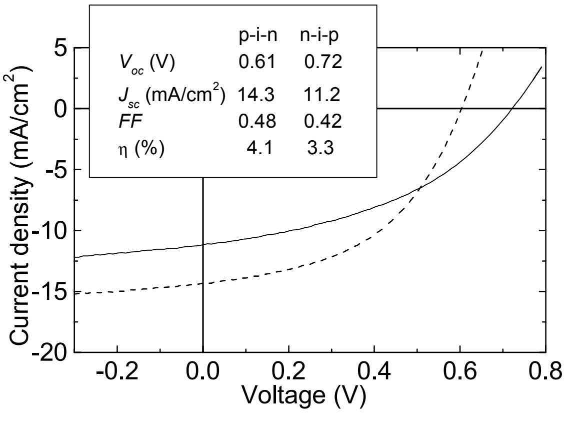

	p-i-n	n-i-p
V_{oc} (V)	0.61	0.72
J_{sc} (mA/cm^2)	14.3	11.2
FF	0.48	0.42
η (%)	4.1	3.3

FIG. 7. Solar cells with intrinsic a-Si:H deposited by the expanding thermal plasma at a rate of 7 nm/s. The p-i-n cell contained a 400 nm thick i-layer deposited at 300 °C and the n-i-p cell a 500 nm thick i-layer deposited at 400 °C. For the n-i-p cell a thermally stable n-layer and an indium tin oxide (ITO) top contact was used. The open-circuit voltage (V_{oc}), short-circuit current density (J_{sc}), fill-factor (FF), and efficiency (η) are listed in the figure for 100 mW/cm^2 AM1.5 illumination (see Chapter B.7).

efficiency of 3.3%. This efficiency is lower than the one of the p-i-n cell, despite the superior properties of the individual intrinsic layer in the n-i-p cell. This can be attributed to the fact that the n-i-p structure was not yet completely refined. For example, the indium tin oxide, used as TCO top contact, was not optimized for optical transmission (Chapter B.7 and Ref. 38).

The stability of the solar cells against light-induced degradation has not been tested yet. Although the performance of the cells still needs to be improved considerably, these first experiments with non-optimized solar cells indicate the potential for very high rate deposited a-Si:H solar cells.

The next step towards the implementation of the expanding thermal plasma in a solar cell production process is the full optimization of solar cells with ETP deposited intrinsic a-Si:H. For this reason, a completely new deposition system has recently been constructed. This has been done in a project in conjunction with DIMES of the Delft University of Technology, where the setup has been installed. In the system CASCADE (Cascaded-Arc-Solar-Cell-Apparatus-Delft-Eindhoven)[49] complete solar cells can be produced: doped layers can be deposited in a rf PECVD chamber and intrinsic layers in an ETP chamber [see Fig. 4(c)]. Furthermore, a loadlock system is present for the transfer of the samples between the two chambers without exposing the films to air. An initial aim is to deposit high quality a-Si:H at high deposition rates under conditions with reduced Ar carrier gas in the cascaded arc plasma source. This reduces the required pumping capacity and makes the technique more feasible for industrial applications. The main goal, however, is to produce high efficiency n-i-p, and even p-i-n solar cells at deposition rates in the range of 1–10 nm/s.

Hopefully, this new project will finally lead to the implementation of the expanding thermal plasma technique in an industrial solar cell production line. Anticipating such an implementation, a high throughput in solar cell production over a large foil area can most probably be obtained when combining several cascaded arc sources in a roll-to-roll deposition system. The higher substrate temperature, which may remain necessary, is not an insurmountable drawback but requires the application (and further investigation) of new solar cell device structures. As mentioned above, this investigation has already been initiated because higher substrate temperatures seem to be necessary in other alternative production techniques as well. Besides the intrinsic advantage of a high rate deposition process (i.e., high throughput with lower investments in equipment), the high deposition rate is also advantageous for low level incorporation of contamination due to leakage of air in the vacuum system. Kroll *et al.* have shown that the incorporation of oxygen in the film is inversely proportional with the deposition rate.[50] This relaxes the demands on the vacuum necessary in the solar cell production system.

III. PLASMA PROCESSES AND GROWTH PRECURSORS VERSUS a-Si:H FILM QUALITY

In the previous section, it has been shown that a-Si:H films with properties suitable for the application in solar cells can be deposited at rates up to 10 nm/s. In order to obtain insight into the fundamental conditions under which high rate deposition of a-Si:H is possible, the plasma processes, the plasma composition, and the contribution of species to film growth (growth precursors) have been investigated. From this investigation performed using different plasma settings, relations have been derived between the processes in the plasma and the growth precursors on one hand and the film properties on the other hand. Moreover, the investigation has yielded information on fundamental limitations and opportunities of high rate deposition of a-Si:H in general and the knowledge obtained can be very useful for the optimization of the growth rate in other a-Si:H deposition techniques.

The above-mentioned investigation forms the main part of the work described in this thesis. It has been concentrated on the implications of the variation of the H_2 flow in the cascaded arc because in an early stage of the work on a-Si:H it was recognized that admixing H_2 to the Ar was essential to obtain good quality a-Si:H with the ETP technique.[51] In Chapter B.7, the film properties of the a-Si:H deposited using different H_2 flows have systematically been investigated. As shown in Fig. 8, good quality a-Si:H is obtained when a considerable flow of H_2 is used. Conditions with no or a very small H_2 flow lead to inferior film properties (i.e., high void fraction, poor electronic performance) with respect to solar cell applications. It is, of course, not excluded that the

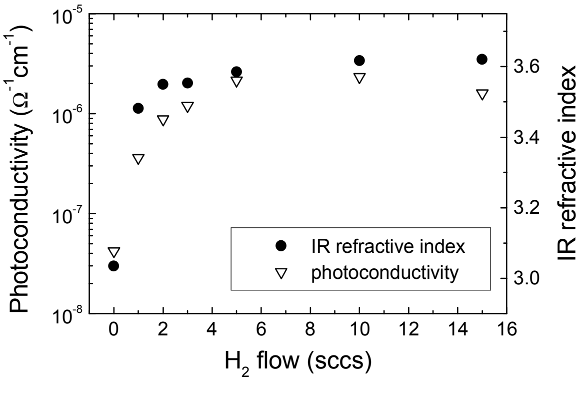

FIG. 8. The photoconductivity (AM1.5, 100 mW/cm^2) and the refractive index in the infrared as a function of the H_2 flow in the cascaded arc plasma source. The conditions are 55 sccs Ar, 10 sccs SiH_4, 45 A arc current, and 0.20 mbar downstream pressure. The substrate temperature was 400 °C. The data are taken from Chapter B.7.

material deposited without H_2 or at low H_2 flows is very well suited for other applications.

The choice for admixing H_2 to the Ar in the cascaded arc was based on expectations with respect to the reactive species emanating from the arc and the subsequent SiH_4 dissociation mechanism. From experimental observations and from considerations based on data in the literature, it was expected that for high H_2 flows atomic hydrogen would be the most abundant reactive species emanating from the arc. This H would subsequently react with SiH_4 leading to SiH_3 radicals.[51,52] The improvement of the film quality with increasing H_2 flow could therefore be related to the beneficial effect to the film properties attributed to SiH_3 dominated growth.[53-55] The inferior film properties of the a-Si:H deposited without H_2 or with only a small H_2 flow in the arc was attributed to a large contribution of radicals such as SiH_2, SiH, and Si. Due to their hydrogen deficiency and consequently high reactivity, a large contribution of these radicals is expected to be detrimental to the film properties.[53,55] In order to test these "expectations" and to verify whether SiH_3 really dominates film growth for high H_2 flows, several plasma species and related parameters have been investigated for the expanding thermal plasma. These will be addressed successively.

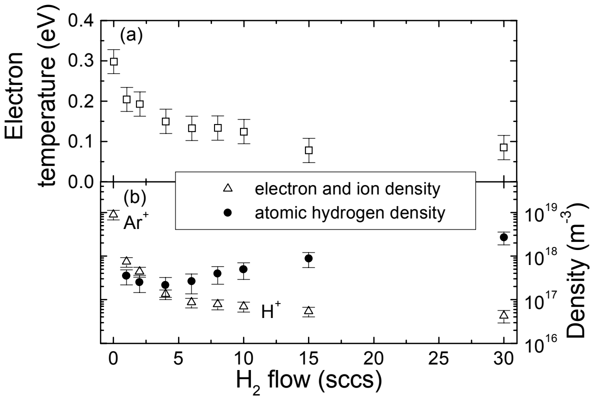

FIG. 9. (a) Electron temperature as determined from single Langmuir probe measurements at a position of 6 cm from the arc outlet. Further downstream (at 2 cm from the substrate holder), similar values have been obtained. (b) Corresponding ion and electron density at 2 cm from the substrate holder and the density of H at the position of the substrate holder. The most abundant ion changes from Ar^+ at 0 sccs H_2 to H^+ at high H_2 flows. The density of H has been determined by threshold ionization mass spectrometry and has been quantified by two-photon-absorption laser-induced fluorescence measurements in a slightly different setup and under slightly different conditions [50 sccs Ar, 8 sccs H_2, 40 A arc current, 0.20 mbar (Ref. 35)]. The plasma settings are equal to those in Fig. 8. The data on the ions and electrons are taken from Chapter B.4.

Reactive species from the plasma source

Obtaining information on the reactive species emanating from the Ar-H_2 operated cascaded arc, such as, electrons, ions, metastable atoms, and atomic hydrogen H, is the first step towards a good comprehension of the dissociation reactions of the SiH_4 as illustrated in Fig. 2. In Chapter B.4, the ions and electrons in the downstream Ar-H_2 plasma have been investigated for the a-Si:H deposition setup. In combination with threshold ionization mass spectrometry measurements on H in this setup and the results obtained in a similar setup by advanced spectroscopic studies,[30-36,56-58] these investigations have lead to a clear insight into the reactive species emanating from the arc. In Fig. 9, the most important results obtained for the a-Si:H deposition setup are summarized. The most important conclusions are:

- the electron temperature is very low in the downstream region. In this region, power is no longer coupled to the plasma and therefore the plasma is recombining, comparable to the situation in an afterglow plasma. The low electron temperature is an important feature of the ETP and, in contrast to most other plasmas, it implies that electron-induced reactions are ineffective for dissociation and ionization of SiH_4.
- the ion and electron density depend strongly on the H_2 flow admixed in the arc. The reason for this is that fast molecular processes become an important recombination channel for the ions when H_2 is admixed to the Ar.[32,33] The amount of ions emanating from the arc per second, expressed in ion fluence, decreases from ~3 sccs for pure Ar down to ~0.08 sccs for 10 sccs H_2. Furthermore, the most abundant ions change from Ar^+ at 0 sccs H_2, to ArH^+ at low H_2 flows, and to H^+ at higher H_2 flows.
- the H density increases with increasing H_2 flow in the cascaded arc, except for H_2 flows between 1 and 4 sccs. The forward flux of H behind the shock front is however much smaller than expected on the basis of full H_2 dissociation in the arc. This has been attributed to very effective radial escape of H atoms in the supersonic expansion that is driven by large radial density gradients induced by effective wall recombination of H.[35]

From these investigations, it has been concluded that SiH_4 dissociation reactions in the ETP technique are governed by reactive ionic and atomic species emanating from the arc. In this respect, the arc changes basically from an (Ar) ion source to an H source when going from zero to a high H_2 flow.

This information on the species emanating from the arc, in conjunction with data in the literature, has lead to a reaction scheme for the plasma processes in the ETP Ar-H_2-SiH_4 plasma. Throughout this thesis work, the scheme has been tested and continuously been refined by several diagnostic studies on the plasma species that are expected to be most important. An overview of the species investigated and the diagnostic techniques applied is given in Table III. These investigations have lead to a fairly good understanding of the plasma processes and they have revealed the contribution of different species to a-Si:H film growth. The currently presumed global reaction scheme for the Ar-H_2-SiH_4 plasma is schematically represented in the frame given below and the results on the contribution of several species are summarized in Fig. 10.

SiH_4 consumption and deposition rate

As pointed out in Refs. 20 and 59, the behavior of the SiH_4 consumption as a function of the H_2 flow in the arc [Fig. 10(a)] reveals already a great deal about the SiH_4 dissociation process. Two regimes are clearly distinguishable: firstly, a high SiH_4 consumption at very low H_2 flows that subsequently decreases with increasing H_2 flow, and secondly, a gradual increase of the SiH_4 consumption with increasing H_2 flow at high H_2 flows. On the basis of the dominant species from the arc, these two regimes can be attributed to ion-induced dissociation of SiH_4 and H-induced dissociation, respectively.[20,59] The SiH_4 consumption correlates very well with the Si growth flux (i.e., deposition rate in terms of Si atoms deposited). This suggests that the consumed SiH_4 is mainly converted into film. In the results presented below, it is corrected for the amount of SiH_4 consumed or, equivalently, the Si growth flux when considering the importance of species to the deposition process.

Positive ions/cationic clusters

The mass spectrometry studies in Chapters B.2, B.3, and B.4 have revealed the presence of relatively large and hydrogen-poor positive ions or cationic clusters ($Si_nH_m^+$ with n up to 10) in the plasma. Their formation has been attributed to sequential ion-SiH_4 reactions [reaction 3(a) and 3(b) in frame]. As shown in Fig. 10(c), these ions have only a small contribution to a-Si:H film growth. Moreover, this contribution is almost independent of the H_2 flow. At first sight this is rather remarkable because at low H_2 flows many more ions emanate from the cascaded arc than at high H_2 flows [see Fig. 9(b)]. The reason for this behavior is that the ion flux at very low H_2 flows is strongly reduced by fast dissociative recombination reactions of the molecular ions formed when SiH_4 is admixed [reaction (2a)]. It is also important to note that the energy of the ions gained in the plasma sheath is relatively small (<2 eV) in the ETP technique. Consequently, the ions do not supply a considerable amount of kinetic energy to the film. Ion-induced rearrangement of (sub)surface atoms and ion-induced elimination of hydrogen is therefore insignificant in the ETP technique in contrast with most other plasma deposition techniques.

SiH_3 radicals

Based on the contribution of the ions, it can be concluded that more than 90% of the film growth is due to neutral species. Due to its presumed importance, the density of SiH_3 has been extensively investigated in Chapters B.6, B.8, and B.9. The contribution of SiH_3 to film growth is given in Fig. 10(b). It shows that at high H_2 flows, the remainder of the film growth can almost completely be explained by the contribution of SiH_3. As expected, SiH_4 dissociation is governed by the hydrogen abstraction reaction by H from the arc [reaction (4)] under these conditions.

A dominant contribution of SiH_3 is also suggested by the value of the overall surface reaction probability at high H_2 flows [see Fig. 10(e)]. As discussed in Chapter B.5, the value of ~0.3 approaches the values within the range ~0.2–0.3 reported for SiH_3 in the literature.

TABLE III. Plasma species and related parameters studied for the ETP Ar-H_2-SiH_4 plasma and the diagnostic techniques applied.

SiH_4 consumption	mass spectrometry	a,b
$Si_nH_m^+$	ion mass spectrometry & Langmuir probe	c,d,e
SiH_3	threshold ionization mass spectrometry (TIMS)	b,f
	cavity ring down spectroscopy (CRDS)	f,g,h,i
SiH_2	threshold ionization mass spectrometry (TIMS)	b
Si*, SiH*	optical emission spectroscopy (OES)	b,j
Si, SiH	cavity ring down spectroscopy (CRDS)	j
surface reaction probability β	aperture-well experiment	b,f,k
Si_2H_6, Si_3H_8	mass spectrometry	a,e

a: Van de Sanden *et al.* (Ref. 59); b: Chapter B.6; c: Chapter B.2; d: Chapter B.3; e: Chapter B.4; f: Kessels *et al.* (Ref. 60); g: Boogaarts *et al.* (Ref. 61); h: Chapter B.8; i: Chapter B.9; j: Chapter B.10; k: Chapter B.5.

The ETP Ar-H$_2$-SiH$_4$ plasma: global reaction scheme

The global reaction scheme proposed for the ETP Ar-H$_2$-SiH$_4$ plasma is schematically represented below. The reactions are only given for very low and for relatively high H$_2$ flows added to the Ar in the cascaded arc plasma source. For intermediate H$_2$ flows there is a transition region.

At zero or very low H$_2$ flows, SiH$_4$ dissociation is governed by dissociative charge transfer of Ar$^+$ with SiH$_4$ leading to SiH$_n^+$ ($n \leq 3$) ions. Because the electron density is very high for these conditions, these reactions are almost directly followed by dissociative recombination reactions with electrons. This leads to SiH$_m$ ($m \leq 2$) radicals that, in contrast with SiH$_3$,[62] are rather reactive with SiH$_4$.[63-67] These radicals will therefore create polysilane radicals. When the dissociative recombination reactions have reduced the electron density to a sufficient extent (approximately down to 10^{17} m^{-3}, i.e., when the ratio of the electron density and the silane density becomes ~10^{-3}), ion-molecule reactions between the silane ions and SiH$_4$ can become significant as well. This initiates a reaction channel with sequential ion-SiH$_4$ reactions leading to cationic clusters containing up to 10 Si atoms.

When the H$_2$ flow is further increased, the influence of ion-induced reactions decreases because the ion fluence from the arc is drastically reduced. For sufficiently high H$_2$ flows ($\gtrsim$5 sccs), reactions with H emanating from the arc are more effective, and SiH$_4$ dissociation is governed by hydrogen abstraction leading to SiH$_3$. However, besides H, there is still a small flow of H$^+$ from the plasma source. The H$^+$ ions undergo charge transfer reactions with SiH$_4$ and initiate sequential ion-molecule reactions. Under these conditions, dissociative recombination with electrons will take place as well. These reactions, however, are much less important than for the conditions with very low H$_2$ flows because of the much lower electron density.

H$_2$ flow $\lesssim$ 2 sccs:

$$(1)\quad Ar^+ + SiH_4 \xrightarrow{ch.\ tr.} Ar + SiH_n^+ + ..\ (n\leq 3) \quad \overset{n_e \text{ high}}{\Rightarrow} \quad (2a)\quad SiH_n^+ + e \xrightarrow{dis.\ rec.} SiH_m + ..\ (m\leq 2)$$

$$\Downarrow$$

$$(2b)\quad SiH_m + SiH_4 \xrightarrow{rad.\text{–}mol.} Si_2H_p + ..\ \text{etc.}$$

$$\overset{n_e \text{ reduced}}{\Rightarrow} \quad (3a)\quad SiH_n^+ + SiH_4 \xrightarrow{ion\text{–}mol.} Si_2H_m^+ + ..$$

$$\Downarrow$$

$$(3b)\ Si_pH_q^+ + SiH_4 \xrightarrow{ion\text{–}mol.} Si_{p+1}H_r^+ + ..\ \text{etc.}$$

H$_2$ flow $\gtrsim$ 5 sccs:

$$(4)\quad H + SiH_4 \xrightarrow{H\ abs.} H_2 + SiH_3$$

$$(5)\quad H^+ + SiH_4 \xrightarrow{ch.\ tr.} SiH_n^+ + ..\ (n\leq 3) \quad \Rightarrow \quad (3a)\quad SiH_n^+ + SiH_4 \xrightarrow{ion\text{–}mol.} Si_2H_m^+ + ..$$

$$\Downarrow$$

$$(3b)\ Si_pH_q^+ + SiH_4 \xrightarrow{ion\text{–}mol.} Si_{p+1}H_r^+ + ..\ \text{etc.}$$

In these reactions, the total amount of H is presented unbalanced for simplicity. n_e is electron density; *ch.tr.*: charge transfer, reaction rate for (1) 4×10^{-17} m^{3}s^{-1} mainly leading to SiH$_3^+$ at thermal energies (Refs. 66 and 68, Chapter B.4), proposed reaction rate for (5) 5×10^{-15} m^{3}s^{-1} leading to SiH$_3^+$ (Ref. 66 and Chapter B.4); *dis. rec.*: dissociative recombination, reaction rates typically ~10^{-13} m^{3}s^{-1} (Ref. 66 and Chapter B.4); *rad.-mol.*: radical-molecule reactions, reaction rates typically ~10^{-17}–10^{-16} m^{3}s^{-1} (Ref. 66, Chapters B.6 and B.10); *ion-mol.*: ion-molecule reactions, reaction rates estimated at ~10^{-17}–10^{-16} m^{3}s^{-1} for present conditions (Chapter B.3); *H abs.*: H abstraction reaction, thermally activated reaction rate of 2×10^{-16} m^{3}s^{-1} at 2000 K and 5×10^{-17} m^{3}s^{-1} at 1000 K (Ref. 69 and Chapter B.6).

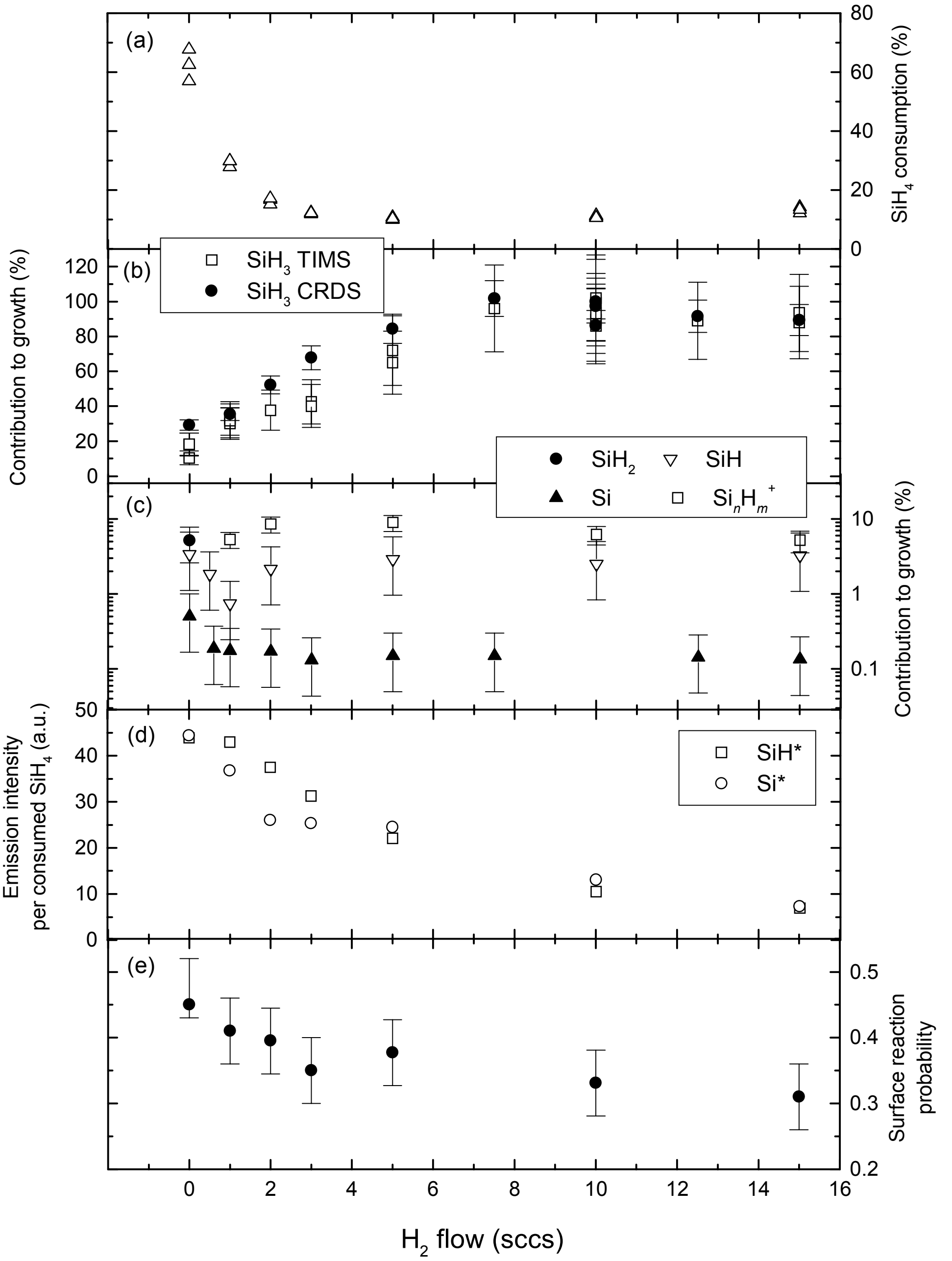

FIG. 10. (a) The relative consumption of SiH_4 as determined by mass spectrometry (Chapter B.6, Refs. 20 and 59). (b) Contribution of SiH_3 to a-Si:H film growth as estimated from threshold ionization mass spectrometry (TIMS) (Chapter B.6) and cavity ring down spectroscopy (CRDS) (Chapters B.8 and B.9). (c) Contribution of SiH_2 to film growth as determined from TIMS at 0 sccs H_2 (Chapter B.6), the contribution of SiH and Si as determined from CRDS measurements (Chapter B.10), and the contribution of cationic clusters $Si_nH_m^+$ to film growth. The contribution of the ions is calculated from the ion flux as measured by a Langmuir probe and corrected for the average number of Si atoms in the ions as determined from the ion mass spectra (Chapter B.4). A sticking probability of one has been assumed for the ions, as validated by a molecular-dynamics study (Ref. 70). (d) Emission intensity of Si I 4s $^1P_1^0$–$3p^2$ $^1S_0$ (at 390.6 nm) and SiH A $^2\Delta$–X $^2\Pi$ (around 414 nm) divided by the amount of SiH_4 consumed for the particular plasma setting. The emission intensity is obtained from non-local optical emission spectroscopy measurements (Chapter B.6 and B.10). (e) The overall surface reaction probability β determined using the "aperture-well" technique. The overall surface reaction probability depends on the flux of the different species to the substrate and on each of their particular surface reaction probabilities (Chapters B.5 and B.6). For all experiments, the Ar flow was 55 sccs, the SiH_4 flow 10 sccs, the arc current 45 A, and the pressure in the deposition chamber ~0.20 mbar.

Furthermore, it is expected that the contribution of SiH_3 observed at low H_2 flows arises from the production of SiH_3 by H [reaction (4)] that is generated in the dissociation of SiH_4 by reactions (1) and (2a).

SiH_2, SiH, and Si radicals

Figure 10(b) clearly illustrates that there is an important contribution of neutral species other than SiH_3 at low H_2 flows. In Chapter B.4 and B.6, this contribution has been associated with the strong recombination of ions by reaction (2a) when using very low H_2 flows in the arc. Evidence for this recombination process is given in Fig. 10(d). Radiative decay of the excited silane radicals SiH and Si indicates the recombination of silane ions SiH_n^+ ($n \leq 3$), because recombination is the only significant production pathway for electronically excited states in the ETP technique. This is due to the low electron temperature in the downstream region. The figure reveals that relatively more Si and SiH are produced at very low H_2 flows. This is most probably also the case for SiH_2 as expected from reaction (2a). However, the relatively higher production rate at very low H_2 flows does not yield information on the final reaction products contributing to growth.

The possible higher contribution of Si, SiH and SiH_2 at very low H_2 flows has been tested by direct radical measurements (see Chapters B.6 and B.10). Their contribution to film growth is given in Fig. 10(c). Remarkably, the contribution of SiH and Si are almost H_2 flow independent: it is only slightly higher at 0 sccs H_2. This implies that not only the production of Si and SiH is relatively more important at low H_2 flows but that also their loss is more important for these conditions.

Polysilane radicals

Because the above-mentioned SiH_m ($m \leq 2$) radicals have a high reactivity with SiH_4 [reaction (2b)], a considerable amount of these radicals probably react with SiH_4 to form polysilane radicals before reaching the substrate or reactor wall. This presumption is corroborated by a study presented in Chapter B.10. In the reactions with SiH_4, it is expected that primarily hydrogen deficient disilane and polysilane radicals are created. This is also suggested by the higher value of the overall surface reaction probability at low H_2 flows [see Fig. 10(e)]. As discussed in Chapters B.5 and B.6, the increase of the overall surface reaction probability at low H_2 flows indicates a significant contribution of very reactive species to film growth. Hydrogen deficient polysilane radicals, such as Si_2H_n ($n \leq 4$), produced in reaction (2b) are likely candidates. For these radicals, a high reactivity similar to SiH_m ($m \leq 2$) radicals is expected. For SiH_m ($m \leq 2$) radicals surface reaction probability values within the range 0.6–1 have been reported (see Chapter B.5).

Polysilane molecules, negative ions, and dust particulates

Species which can be present in the plasma but which have not been addressed so far are polysilane molecules, negative ions, and particulates or dust. Their possible relevancy for the ETP technique will be briefly considered.

Polysilane molecules, such as Si_2H_6 and Si_3H_8, have been measured by means of mass spectrometry at the position of the substrate and at the side wall of the reactor (see Chapter B.4 and Ref. 59). These measurements revealed that the density of these species in the plasma is relatively low. For the condition with 10 sccs H_2, it has been found that approximately 10% of the SiH_4 that is consumed is converted into Si_2H_6. The amount of Si_3H_8 was hardly measurable and estimated to be even a factor of 10 lower.

Preliminary mass spectrometry experiments have not revealed any negative ions in the Ar-H_2-SiH_4 plasma within the mass range of 1–300 amu. Their detection, however, is known to be complicated because negative ions are confined in the plasma due to the plasma sheath. In the expanding thermal plasma, the sheath potential is relatively small (<2 eV) and due to drag forces negative ions might relatively easily be extracted into the mass spectrometer. Negative ions in ETP Ar-O_2 plasmas could also be measured by means of mass spectrometry. Furthermore, a relatively low density of negative ions is expected on the basis of the electron temperature in the ETP technique.[59] Unless the SiH_4 is considerably vibrationally excited, the electrons do not have enough energy for dissociative attachment of SiH_4.[66]

The possible presence of particulates or dust in the expanding thermal plasma has not been experimentally investigated yet. The expected very low density of negative ions and the less efficient confinement of negatively charged particles in this plasma makes the generation of particulates less probable than, e.g., in rf plasmas. This might be an important advantage of the expanding thermal plasma because particulates have a detrimental influence on the film quality and can cause serious problems and limitations during processing.[71] The presence of particulates, however, cannot be completely excluded (see also Chapter B.10). For example, in addition to the negative ion route,[72,73] radical-SiH_4 reactions and radical-radical reactions have been proposed as a formation pathway for these species.[74-76] Such a formation pathway could become particular significant under conditions with heavy SiH_4 consumption, e.g., at very low H_2 flows where a large amount of very reactive (poly)silane radicals is created.

From the results presented, some important conclusions can be drawn:

It can be concluded that the a-Si:H growth in the expanding thermal plasma in terms of growth precursors is fairly well understood. This is especially the case at high H_2 flows at which SiH_3 can almost completely explain the deposition rate. For these conditions, the ions, Si, and SiH have only a minor contribution and, together with SiH_2 and possibly polysilane radicals, they account for the remaining part of the deposition rate. Herein, the contribution of SiH_2 is expected to be lower than ~5% at 0 sccs H_2 because its contribution is expected to have a dependence on the H_2 flow similar to that of Si and SiH. A small contribution of polysilane radicals is expected since even under these conditions radical-SiH_4 reactions [reactions (2b)] will occur. Moreover, polysilane radicals are also created by recombination of cationic clusters with electrons.

For no and very low H_2 flows in the cascaded arc, the measurements have also yielded considerable insight into the growth process. However, a large part of the deposition rate can still not be attributed to specific growth precursors. On the basis of the observed larger production rate of SiH_x ($x \leq 2$) radicals at low H_2 flows and their high reactivity with SiH_4, it is very plausible that polysilane radicals have a large contribution to film growth under these conditions. Measurements of these polysilane radicals are, however, necessary to further elucidate the most important growth precursors under these conditions.

Another very important conclusion in itself is that for high H_2 flows the deposition process is by far dominated by SiH_3. This dominance of SiH_3 is demonstrated by three independent measurements. A conclusion about the exact value of its contribution is difficult, but a contribution of approximately 90% is estimated. This is larger than the contribution of SiH_3 to rf PECVD deposited a-Si:H as determined by Kae-Nune *et al.*[77] and Itabashi *et al.*[78] For deposition rates of 0.1–0.2 nm/s, a contribution by SiH_3 of about 60% has been obtained while for higher deposition rates it was even lower.[77] The fact that films can be grown by almost only SiH_3 at deposition rates up to 10 nm/s in the expanding thermal plasma is therefore certainly noteworthy.

Additional evidence for the dominance of reaction (4) and consequently for the dominance of SiH_3 at high H_2 flows is obtained from fluid dynamics simulations in Chapter B.8. These simulations revealed that the measured SiH_3 density and deposition rate, could easily be explained by the amount of H from the arc (as available behind the shock front) when assuming a simplified chemistry: production of SiH_3 by H in reaction (4) and surface loss of H and SiH_3 on the walls and substrate.

Finally, the improvement of the film properties with increasing H_2 flow can be understood from the increasing contribution of SiH_3 to film growth. Actually, the often suggested relation between film quality and the contribution of SiH_3 is clearly demonstrated by these results. The favorable influence of SiH_3 on the film quality has been attributed to its relatively low surface reaction probability in comparison with other silane radicals, as well as to its (presumed) ability to diffuse over the surface. One particular cause of the deterioration of the film properties at very low H_2 flows can be understood from the high contribution of very reactive (poly)silane radicals under these conditions. These radicals stick (almost) immediately at impact on the surface due to their high surface reaction probability. This leads to a high surface roughness and consequently to columnar film growth and the incorporation of voids (see Chapter B.7). SiH_3 radicals on the other hand can have several reflections at the surface before sticking and have therefore a higher probability to reach so-called “valleys” at the surface. Accordingly, SiH_3 dominated film growth forms a good starting point for the deposition of smooth and dense a-Si:H films.

Although there is already a fairly good insight into the plasma composition and processes, future experiments will be required to obtain a full understanding of the film growth under all plasma settings. Although determination of the contribution of SiH_2 for all H_2 flows is not expected to yield surprising results, it is useful and should be relatively simple using the cavity ring down technique. Measuring the polysilane radicals might reveal more insight into the a-Si:H growth process, especially for low H_2 flows in the cascaded arc. However, it may be difficult to use cavity ring down since the density of polysilane radicals is expected to be low. This is due not only to their high reactivity, but also due to the fact that they can be distributed over several different kinds of radicals and even over different isomeric states. Additionally, the application of cavity ring down requires information about their spectral transitions, which is currently not available for most of these radicals. The application of threshold ionization mass spectrometry will eliminate the latter disadvantage but requires the addition of a second partial pumping stage to the mass spectrometer. Use of threshold ionization mass spectrometry would enable also a comparison of mass spectrometry measurements with cavity ring down data for other radicals than SiH_3.

Other experiments that are recommended are measurements of atomic hydrogen, negative ions, and particulates in the Ar-H_2-SiH_4 plasma. Although their densities are expected to be low as discussed above, in-depth measurements are required in order to settle this issue conclusively. Furthermore, determination of the surface reaction probability for the species in the plasma separately and using different plasma settings would contribute considerably to the understanding of their reactions on the a-Si:H surface. These kinds of measurements will be addressed in more detail in the next section.

IV. SURFACE REACTIONS AND THE GROWTH MECHANISM OF a-Si:H

A specific goal of the work on a-Si:H at the Eindhoven University of Technology is to analyze the atomistic reactions during a-Si:H film growth, and in particular the reactions which lead to film growth and/or have an important effect on the resulting film properties. In this section, the part of the thesis work dealing with surface reactions and the growth mechanism will be briefly considered. It only forms a minor part of the investigations presented, but actually it has been an important underlying motive for most of the experiments. The investigations described in this thesis yield the required foundation for future detailed *in situ* studies on a-Si:H film growth.

Chapter B.1 deals with an investigation of the structural a-Si:H properties, and especially of the hydrogen content, as a function of substrate temperature and deposition rate. The experiments revealed that at higher deposition rates, higher substrate temperatures are necessary in order to obtain sufficiently dense films. This is a very relevant observation for high rate deposition of a-Si:H because it is generally found that films deposited at higher rates require higher temperatures in order to attain the same quality as at lower deposition rates. For most plasma techniques, the reason why higher substrate temperatures are required is difficult to trace because increasing the deposition rate generally affects the plasma reactions and composition drastically. For the ETP technique on the other hand, SiH_3 dominance was expected for the full range of the plasma settings used. Consequently, the observations were interpreted in the prevailing kinetic growth model of a-Si:H with SiH_3 as the growth precursor.

At that point, it was realized that well-defined studies of the surface reactions and of the growth mechanism of a-Si:H require detailed knowledge of the species contributing to growth. This has initiated the extensive investigations of the plasma composition as presented in this thesis. Finally, it has been established that film growth using the ETP technique is indeed dominated by SiH_3 under conditions with high H_2 flows in the cascaded arc. On the basis of the experiments described in Chapter B.13, it is expected that SiH_3 is also dominant for conditions with the lower deposition rates when relatively “high” H_2 flows are used. The incorporation of hydrogen in the film, or more appropriate, the elimination of hydrogen from the film can indeed be interpreted in terms of mechanisms involving SiH_3.

Essential insight into the nature of the a-Si:H surface during deposition and into the reactions taking place has been obtained from *in situ* attenuated total reflection Fourier transform infrared spectroscopy (ATR-FTIR) studies.[79] These have been performed in the group of Prof. E. S. Aydil at the University of California Santa Barbara and are described in Chapters B.11 and B.12. The experiments have been carried out in an inductively coupled plasma reactor under somewhat less well-defined conditions as for the ETP technique (i.e., concerning the growth precursors). Although not conclusive, there are indications that in this plasma SiH_3 also plays a dominant role in the film formation process (see Chapter B.12). The experiments have demonstrated the role of (energetic) ions during deposition with respect to surface dangling bond formation and the subsequent decomposition of surface hydrides. Furthermore, a thermally activated, series decomposition reaction set for the surface hydrides has been observed in which surface SiH_3 decomposes into SiH_2 and subsequently into SiH with increasing substrate temperature.

In Chapter B.13, the decomposition processes of the surface silicon hydrides have been related to the substrate temperature dependence of the hydrogen content of a-Si:H. It is pointed out that the underlying surface reactions most probably play an important role in hydrogen elimination during a-Si:H film growth. Moreover, the thermally activated decomposition of surface SiH_3 into surface SiH_2 does not conflict with the hydrogen elimination process proposed in Chapter B.1. Yet, the proposed reaction is not unique in this sense and other reactions are possible as well. Although from these experiments the hydrogen elimination is not yet completely unraveled, the experiments illustrate the relevancy of these kind of studies for obtaining clear insight into this important step in film formation.

From this perspective, it is also expected that future experiments with the expanding thermal plasma can contribute significantly to the debate on the different film growth mechanisms proposed (the most important mechanisms are reviewed in Chapter B.13). The ETP technique is actually very well suited for these kinds of experiments. The contribution of different species to film growth is rather well known and the growth process is largely dominated by SiH_3. Moreover, using the ETP technique the deposition rate can be varied over two orders of magnitude while varying basically only the flux of SiH_3. Furthermore, the a-Si:H is saved from ion bombardment and there are strong indications that the flux of H towards the a-Si:H film during deposition is much lower than the flux of SiH_3 (see Chapter B.8). In order to enhance the “SiH_3-purity” of the growth precursors even more, it is also possible to block the line-of-sight beam between plasma source and substrate.[80] In this way, film growth can only take place indirectly by growth precursors that survive several wall collisions. It is expected that in this case only SiH_3 reaches the substrate due to its relatively low surface reaction probability. The advantage of the ETP technique herein is that due to the high “initial” flux of SiH_3, a reasonable deposition rate can even be obtained under these conditions.

All together, these issues enable detailed future studies on the surface reactions and growth mechanism of a-Si:H with the ETP technique. Some examples are:

- a study of the hydrogen elimination process under largely SiH_3 dominated conditions when applying ATR-FTIR in the expanding thermal plasma technique,
- a study of the influence of the deposition rate on the film properties under pure SiH_3 conditions. This might yield a conclusive answer to the question whether the requirement of a higher substrate temperature at higher deposition rates is inherent to the deposition rate itself,
- a study of the influence of ion bombardment on the film properties by applying an external rf bias to the substrate. In this way, it can possibly be tested whether hydrogen elimination can be promoted by the kinetic energy supplied by the ions and whether the required high substrate temperature can subsequently be reduced,
- a study of the evolution of the surface roughness of the films during growth for SiH_3 dominated conditions.[39] This reveals information on possible surface diffusion processes of species,
- a study of the surface reaction probability of SiH_3 or other radicals by time-resolved cavity ring down measurements close to the substrate. This can be done as a function of the growth rate revealing a possible flux dependence (e.g., for Si_2H_6 formation on the surface) but also under different substrate conditions (temperature, ion bombardment, etc.) by simultaneously monitoring the nature of the surface by ATR-FTIR.

A.3 General conclusions

In this thesis, a variety of aspects related to the deposition process of a-Si:H is addressed. The investigated subjects range from a-Si:H film properties to plasma processes and from surface reactions to growth precursors. These different aspects are presented in a set of journal articles, each with their own conclusions, and which are also summarized in the previous chapter. Finally, by reconsidering the "questions" posed when presenting the goal of this work, conclusions of general interest for a-Si:H deposition will be drawn.

- Hydrogenated amorphous silicon films with properties suitable for application in solar cells can be deposited at very high deposition rates (up to 10 nm/s). With the expanding thermal plasma, this high deposition rate can be achieved using a high H_2 dilution of the Ar in the cascaded arc plasma source in which film growth is by far dominated by SiH_3. However, to obtain dense, device quality films relatively high substrate temperatures (~400 ºC) are currently necessary. The promising material properties and results on preliminary solar cells have initiated a full investigation of ETP deposited solar cells that is currently taking place.

- The plasma composition and plasma reactions have been investigated extensively for the ETP technique. For this particular remote plasma, the reactions taking place in the downstream Ar-H_2-SiH_4 plasma depend strongly on the operation of the cascaded arc plasma source. Under conditions with no or low H_2 flows in this source, SiH_4 dissociation is dominated by charge transfer reactions with ions and dissociative recombination reactions with electrons. This leads finally to a large contribution of very reactive polysilane radicals created by SiH_x ($x \leq 2$) radical-SiH_4 interactions. Under conditions with relatively high H_2 flows on the other hand, ions play only a minor role and SiH_4 is mainly dissociated by atomic hydrogen. The growth precursors are therefore predominantly SiH_3 radicals. Furthermore, sequential ion-SiH_4 reactions play an important role in this remote plasma but the contribution of ions to film growth is relatively small in all cases.

- The a-Si:H film properties are considerably affected by the species contributing to film growth. Smooth and dense films with good opto-electronic properties can be obtained under conditions in which the deposition process is by far dominated by SiH_3. Inferior film properties with respect to solar cell applications are obtained under conditions in which very reactive (poly)silane radicals contribute significantly to film growth. The relatively large contribution of these species leads to void-rich, columnar films with much poorer opto-electronic performance. The substrate temperature has an important and essential influence on the film properties. A high substrate temperature can furthermore compensate largely for poor structural film properties originating from the growth precursors, but not for poor opto-electronic properties.

- The reactions of the plasma species on the a-Si:H surface which lead to film growth are not completely unraveled yet. Good film properties are directly related to SiH_3 dominated reactions. In this respect, the relatively low surface reactivity of SiH_3 and its presumed ability to sample several surface sites before sticking seem to be essential. The hydrogen surface coverage also plays an important role and it can be significantly affected by plasma species such as energetic ions. Furthermore, thermally activated surface reactions leading to a decomposition of higher surface hydrides into lower surface hydrides (i.e., $SiH_3 \rightarrow SiH_2 \rightarrow SiH$) are expected to have an important contribution to hydrogen elimination from the film. In this respect, the higher substrate temperature necessary at higher deposition rates seems to be related to "failing" hydrogen elimination reactions on the time scale of the deposition rate. This can be interpreted as an intrinsic effect of the high deposition rate by SiH_3 radicals.

- For plasma deposition of a-Si:H, it appears that both the supply of the "right" growth precursors to the surface and the "proper" conversion of these precursors by surface reactions into bulk film are essential for obtaining good quality a-Si:H films.

References

[1] *Derde Energienota,* SDU Uitgevers, ‘s-Gravenhage, The Netherlands (1995).

[2] *Duurzame energie in opmars. Actieprogramma 1997-2000*, Ministry of Economical Affairs, ‘s-Gravenhage, The Netherlands (1997).

[3] *Duurzame energie in uitvoering. Voortgangsrapportage*, Ministry of Economical Affairs, ‘s-Gravenhage, The Netherlands (1999).

[4] *The Evolution of World’s Energy Systems*, Shell International Ltd., 1996.

[5] A. Shah, P. Torres, R. Tscharner, N. Wyrsch, and H. Keppner, Science **285**, 692 (1999).

[6] J. Yang, A. Banerjee, and S. Guha, Appl. Phys. Lett. **70**, 2975 (1997).

[7] P.D. Maycock, PV News, February 2000.

[8] R.E.I. Schropp, C.H.M. van de Werf, M. Zeman, M.C.M. van de Sanden, C.I.M.A. Spee, E. Middelman, L.V. de Jonge-Meschaninova, P.M.G.M. Peters, A.A.M. van der Zijden, M.M. Besselink, R.J. Severens, J. Winkeler, and G.J. Jongerden, Mater. Res. Soc. Symp. Proc. **557**, 713 (1999).

[9] R.E.I. Schrop and M. Zeman, *Proceedings SAFE 1998, Mierlo, The Netherlands*, ed. by J.P. van Veen (STW technology foundation, Utrecht, The Netherlands, 1998), p. 497.

[10] *Zonnecelonderzoek in Nederland*, DV 1.1.137.99.06, NOVEM 1999

[11] D.L. Staebler and C.R. Wronski, Appl. Phys. Lett. **31**, 292 (1977).

[12] M. Stutzmann, Philos. Mag. B **56**, 63 (1987); Philos. Mag. B **60**, 531 (1989).

[13] P.V. Santos, N.M. Johnson, and R.A. Street, Phys. Rev. Lett. **67**, 2686 (1991).

[14] H.M. Branz, Phys. Rev. B **59**, 5498 (1999).

[15] H. Fritzsche, Mater. Res. Soc. Symp. Proc. **467**, 19 (1997).

[16] Y. Ichikawa, S. Fujikake, K. Tabuchi, T. Sasaki, T. Hama, T. Yoshida, H. Sakai, and M. Saga, Mater. Res. Soc. Symp. Proc. **557**, 703 (1999).

[17] S. Guha, J. Yang, A. Banerjee, and S. Sugiyama, Mater. Res. Soc. Symp. Proc. **507**, 99 (1999).

[18] G.M.W. Kroesen, D.C. Schram, and M.J.F. van de Sande, Plasma Chem. & Plasma Proc. **10**, 49 (1990).

[19] G.J. Meeusen, PhD thesis, Eindhoven University of Technology (1994).

[20] R.J. Severens, PhD thesis, Eindhoven University of Technology, to be published.

[21] J.J. Beulens, A.J.M. Buuron, and D.C. Schram, Surf. Coat. Technol. **47**, 401 (1991).

[22] A.J.M. Buuron, PhD thesis, Eindhoven University of Technology (1993).

[23] J.W.A.M. Gielen, P.R.M. Kleuskens, M.C.M. van de Sanden, L.J. van IJzendoorn, D.C. Schram, E.H.A. Dekempeneer, and J. Meneve, J. Appl. Phys. **80**, 5986 (1996).

[24] J.W.A.M. Gielen, W.M.M. Kessels, M.C.M. van de Sanden, and D.C. Schram, J. Appl. Phys. **82**, 2643 (1997).

[25] A. de Graaf, G. Dinescu, J.L. Longueville, M.C.M. van de Sanden, D.C. Schram, E.H.A. Dekempeneer, and L.J. van IJzendoorn, Thin Solid Films **333**, 29 (1998); A. de Graaf, PhD thesis, Eindhoven University (2000).

[26] R. Groenen, J.L. Linden, H.R.M. van Lierop, D.C. Schram, A.D. Kuypers, and M.C.M. van de Sanden, submitted for publication.

[27] M.F.A.M. van Hest, M.C.M. van de Sanden, and D.C. Schram, *Proceedings of 12th International Colloquium on Plasma Processes* (Antibes, France, 1999), p 259.

[28] W.M.M. Kessels, T. Lauinger, J.D. Moschner, D.C. Schram, and M.C.M. van de Sanden, to be published.

[29] J.J. Beulens, M.J. de Graaf, and D.C. Schram, Plasma Sources Sci. Technol. **2**, 180 (1993).

[30] M.C.M. van de Sanden, J.M. de Regt, and D.C. Schram, Plasma Sources. Sci. Technol. **3**, 501 (1994).

[31] M.C.M. van de Sanden, R. van den Bercken, and D.C. Schram, Plasma Sources. Sci. Technol. **3**, 511 (1994).

[32] R.F.G. Meulenbroeks, M.F.M. Steenbakkers, Z. Qing, M.C.M. van de Sanden, and D.C. Schram, Phys. Rev. E **49**, 2272 (1994).

[33] R.F.G. Meulenbroeks, R.A.H. Engeln, M.N.A. Beurskens, R.M.J. Paffen, M.C.M. van de Sanden, J.A.M. van de Mullen, and D.C. Schram, Plasma Source Sci. Technol. **4**, 74 (1995).

[34] R.F.G. Meulenbroeks, R.A.H. Engeln, J.A.M. van der Mullen, and D.C. Schram, Phys. Rev. E **53**, 5207 (1996).

[35] S. Mazouffre, M.G.H. Boogaarts, J.A.M. van der Mullen, and D.C. Schram, Phys. Rev. Lett. **84**, 2622 (2000).

[36] R. Engeln, N. Sadeghi, S. Mazouffre, and D.C. Schram, to be published.

[37] R.J. Severens, W.M.M. Kessels, L. Gabella, F. van de Pas, M.C.M. van de Sanden, and D.C. Schram, *Proceedings of the 13th International Symposium on Plasma Chemistry* (Beijing, 1997), p. 1059; R.J. Severens, F. van de Pas, J. Bastiaanssen, W.M.M. Kessels, L.J. van IJzendoorn, M.C.M. van de Sanden, and D.C. Schram, *Proceedings of 14th European Photovoltaic Solar Energy Conference and Exhibition* (Barcelona, Spain, 1997), p. 582.

[38] W.M.M. Kessels, A.H.M. Smets, B.A. Korevaar, G.J. Adriaenssens, M.C.M. van de Sanden, and D.C. Schram, Mater. Res. Soc. Symp. Proc. **557**, 25 (1999).

[39] A.H.M. Smets, M.C.M. van de Sanden, and D.C. Schram, to be published.

[40] W.M.M. Kessels, M.C.M. van de Sanden, R.J. Severens, L.J. Van IJzendoorn, and D.C. Schram, Mater. Res Soc. Symp. Proc. **507**, 529 (1998).

[41] B.A. Korevaar, G.J. Adriaenssens, A.H.M. Smets, W.M.M. Kessels, H.–Z. Song, M.C.M. van de Sanden, and D.C. Schram, J. Non-Cryst. Solids. **266-269**, 380 (2000).

[42] A.H.M. Smets, B.A. Korevaar, C. Smit, W.M.M. Kessels, M.C.M. van de Sanden, and D.C. Schram, to be published.

[43] G.J. Adriaenssens, H.-Z. Song, V.I. Arkhipov, E.V. Emelianova, W.M.M. Kessels, A.H.M. Smets, B.A. Korevaar, and M.C.M. van de Sanden, Journal of Optoelectronics and Advanced Materials **2**, 31 (2000).

[44] W. Luft and Y. Simon Tsuo, *Hydrogenated amorphous silicon alloy deposition processes*, (Marcel Dekker, New York, 1993).

[45] R.E.I. Schropp and M. Zeman, *Amorphous and Microcrystalline Silicon Solar Cells: Modeling, Materials and Device Technology* (Kluwer Academic Publishers, Boston 1998).

[46] G.J. Adriaenssens, in *Properties of Amorphous Silicon and its Alloys*, ed. by Tim Searle (Inspec, The Institution of Electrical Engineers, London, 1998), p. 199.

[47] Q. Wang , E. Iwaniczko, Y. Xu, B.P. Nelson, and A.H. Mahan, Mater. Res. Soc. Symp. Proc. **557**, 163 (1999).

[48] K.F. Feenstra, J.K. Rath, C.H.M. van der Werf, Z. Hartman, and R.E.I. Schropp, *Proceedings of the 2nd World Conference on Photovoltaic Energy Conversion* (Vienna, Austria, 1998), p. 956.

[49] B.A. Korevaar, C. Smit, A.H.M. Smets, R.A.C.M.M. van Swaaij, D.C. Schram, and M.C.M. van de Sanden, to be published.

[50] U. Kroll, J. Meier, H. Keppner, A. Shah, S.D. Littlewood, I.E. Kelly, and P. Giannoules, J. Vac. Sci. Technol. **13**, 2742 (1995).

[51] R.J. Severens, G.J.H. Brussaard, H.J.M. Verhoeven, M.C.M. van de Sanden, and D.C. Schram, Mater. Res. Soc. Symp. Proc. **377**, 33 (1995).

[52] R.J. Severens, M.C.M. van de Sanden, H.J.M. Verhoeven, J. Bastiaanssen, and D.C. Schram, Mater. Res. Soc. Symp. Proc. **420**, 341 (1996).

[53] A. Gallagher, Mater. Res. Soc. Symp. Proc. **70**, 3 (1986).

[54] A. Matsuda and K. Tanaka, J. Appl. Phys. **60**, 2351 (1986).

[55] R.A. Street, *Hydrogenated Amorphous Silicon* (Cambridge University Press, New York, 1991).

[56] G.M.W. Kroesen, D.C. Schram, A.T.M. Wilbers, and G.J. Meeusen, Contrib. Plasma Phys. **31**, 27 (1991).

[57] A.J.M. Buuron, D.K. Otorbaev, M.C.M. van de Sanden, and D.C. Schram, Diamond Rel. Mater. **4**, 1271 (1995).

[58] H.W.P. van der Heijden, M.G.H. Boogaarts, S. Mazouffre, J.A.M. van der Mullen, and D.C. Schram, Phys. Rev. E **61**, 4402, (2000).

[59] M.C.M. van de Sanden, R.J. Severens, W.M.M. Kessels, R.F.G. Meulenbroeks, and D.C. Schram, J. Appl. Phys. **84**, 2426 (1998); J. Appl. Phys. **85**, 1243 (1999).

[60] W.M.M. Kessels, A.H.M. Smets, B.A. Korevaar, G.J. Adriaenssens, M.C.M. van de Sanden, and D.C. Schram, Mater. Res. Soc. Symp. Proc. **609**, A4.2.1 (2000).

[61] M.G.H. Boogaarts, P.J. Böcker, W.M.M. Kessels, D.C. Schram, and M.C.M. van de Sanden, submitted for publication.

[62] S.K. Loh, and J.M. Jasinski, J. Chem. Phys. **95**, 4914 (1991).

[63] J.M. Jasinski, Mater. Res. Soc. Symp. Proc. **165**, 41 (1990).

[64] T. Tanaka, M. Hiramatsu, M. Nawata, A. Kono, and T. Goto, J. Phys. D **27**, 1660 (1994).

[65] H. Nomura, K. Akimoto, A. Kono, and T. Goto, J. Phys. D **28**, 1977 (1995).

[66] J. Perrin, O. Leroy, and M.C. Bordage, Contrib. Plasma Phys. **36**, 1 (1996).

[67] A. Kono, S. Hirose, and T. Goto, Jpn. J. Appl. Phys., Part 1 **38**, 4389 (1999).

[68] E.R. Fisher and P.B. Armentrout, J. Chem. Phys. **93**, 4858 (1990).

[69] A. Goumri, W.-J. Yuan, L. Ding, Y. Shi, and P. Marshall, Chem. Phys. **177**, 233 (1993).

[70] S. Ramalingam, E.S. Aydil, and D. Maroudas, submitted for publication.

[71] A. Bouchoule, in *Dusty Plasmas - Physics, Chemistry and Technological Impacts in Plasma Processing*, ed. by A. Bouchoule (John Wiley & Sons Ltd., Chichester, 1999).

[72] A.A. Howling, L. Sansonnens, J.-L. Dorier, and Ch. Hollenstein, J. Appl. Phys. **75**, 1340 (1994).

[73] A.A. Howling, C. Courteille, J.-L. Dorier, L. Sansonnens, and Ch. Hollenstein, Pure and Appl. Chem. **68**, 1017 (1996).

[74] M. Shiratani, T. Fukuzawa, and Y. Watanabe, Jpn. J. Appl. Phys., Part 1 **38**, 4542 (1999).

[75] Y. Watanabe, M. Shiratani, T. Fukuzawa, H. Kawasaki, Y. Ueda, S. Singh, and H. Ohkura, J. Vac. Sci. Technol. A **14**, 995 (1996).

[76] A. Gallagher, Mater. Res. Soc. Symp. Proc. **557**, 3 (1999).

[77] P. Kae-Nune, J. Perrin, J. Guillon, and J. Jolly, Plasma Sources Sci. Technol. **4**, 250 (1995).

[78] N. Itabashi, N. Nishiwaki, M. Magane, S. Naito, T. Goto, A. Matsuda, C. Yamada, and E. Hirota, Jpn. J. Appl. Phys, Part 2 **29**, L505 (1990).

[79] D.C. Marra, E.A. Edelberg, R.L. Naone, and E.S. Aydil, J.Vac. Sci. Technol. A **16**, 3199 (1998).

[80] A. von Keudell and J.R. Abelson, Phys. Rev. B **59**, 5791 (1999).

Part B
Articles

Temperature and growth-rate effects on the hydrogen incorporation in hydrogenated amorphous silicon

W. M. M. Kessels, R. J. Severens, M. C. M. van de Sanden,[a)]
and D. C. Schram
Department of Applied Physics, Eindhoven University of Technology, P.O. Box 513, 5600 MB Eindhoven, The Netherlands

Hydrogen incorporation in hydrogenated amorphous silicon produced by the expanding thermal plasma is investigated as a function of substrate temperature at three different deposition rates of 0.3, 3, and 11 nm/s. The increase of the refractive index with increasing substrate temperature is attributed to the decreasing hydrogen concentration. The latter result is explained by a model which assumes a thermally activated hydrogen cross-linking step immediately after the chemisorption of a silyl radical. The activation energy for this process is about 150 meV. For growth rates larger than 1 nm/s the hydrogen content is significantly growth-rate dependent.

I. INTRODUCTION

One way of reducing the costs of thin film solar cells made of hydrogenated amorphous silicon (a-Si:H) is by increasing the deposition rate. The a-Si:H-films produced by expanding thermal plasma chemical vapor deposition (ETP-CVD),[1] which uses a source gas mixture of argon and hydrogen with silane injected downstream, are very promising in that sense. Device quality films (AM 1.5 photo-conductivity of 6×10^{-5} Ω^{-1} cm^{-1}, defect density of 10^{16} cm^{-3}, and an Urbach energy of 50 meV) have been deposited at a rate of 10 nm/s.[1]

Furthermore, the growth of a-Si:H from atomic hydrogen and silyl radicals can be easily studied using ETP-CVD: due to the remote type of deposition, a large range of growth rates can be produced under similar relative gas flows by tuning the source properties. In the literature several attempts have been made to develop a growth model for a-Si:H. The surface-diffusion model proposed by Matsuda and Ganguly,[2] Gallagher,[3] and Perrin *et al.*[4] has been successful in explaining several features of a-Si:H growth. In this MGP model it is assumed that only silyl radicals (SiH_3 radicals) contribute to film growth. From silane depletion measurements with a residual gas analyzer on the expanding thermal plasma, it has been concluded that under the conditions of interest mainly silyl radicals are produced.[5] Therefore the MGP model, which is usually applied to film deposition in conventional RF diode and triode reactors, will be used as a basis in this paper. The incorporation of hydrogen in a-Si:H is not explained by the MGP-model. This contribution is aimed at an extension of the model on this point by studying temperature and growth-rate effects during ETP-CVD of a-Si:H.

II. EXPERIMENTAL SETUP

The setup (Fig. 1) consists of a DC thermal plasma source, the cascaded arc, which is operated at a pressure of 0.5 bar and a power of typical 1–5 kW. In this cascaded arc an argon/hydrogen plasma (at a ratio of 5:1) is created at typical flows of 6–10 slm (standard liter per minute). The arc is mounted on a deposition chamber which is held at a pressure of about 0.2 mbar and in which the plasma expands. Just behind the plasma inlet silane is admixed by means of an injection ring. The reactive particles formed by the interaction of the plasma and the silane flow towards the substrate which is positioned 32 cm downstream of the arc outlet and temperature controlled within 10 K.[1] *In situ* information about the film growth is obtained by a rotating compensator ellipsometer (RCE) at 632.8 nm. Information on the composition of the plasma is obtained by a residual gas analyzer (RGA). The hydrogen content of the films is determined by a combination of elastic recoil detection analysis (ERDA) and Rutherford backscattering (RBS)[6] as well as by Fourier transform infrared transmission spectroscopy (FTIR). The latter also gives information about the bonding types.

The conditions under which the films presented in this paper were grown are shown in Table I. The conditions were chosen such that the relative silane consumption was the same for all depositions.

[a)] Corresponding author. E-mail: m.c.m.v.d.sanden@phys.tue.nl

J. Non-Cryst. Solids 227-230, 133 – 137 (1998).

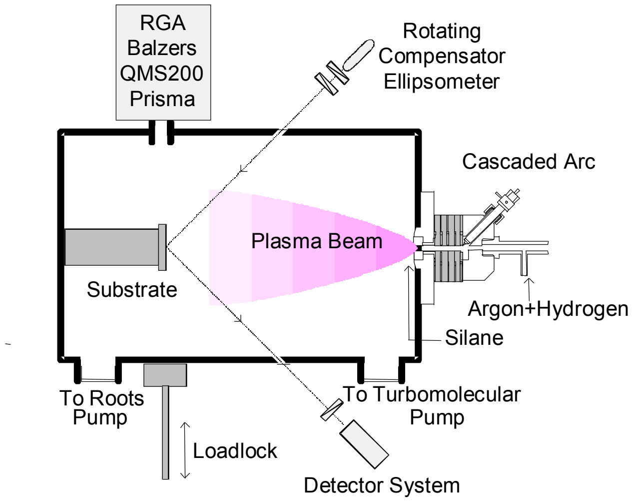

FIG. 1. The expanding thermal plasma setup for a-Si:H deposition.

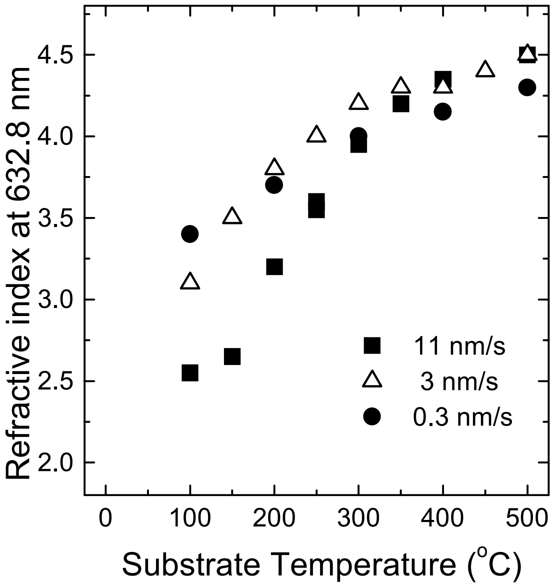

FIG. 2. Refractive index at 632.8 nm as a function of the substrate temperature for a-Si:H films deposited under the conditions of Table I.

III. RESULTS

Films have been deposited at substrate temperatures between 100 and 500 °C under the conditions shown in Table I. The growth rate is nearly temperature independent and is equal to, respectively, 11, 3, and 0.3 nm/s for the conditions 1, 2, and 3. Although this temperature independence has implications for the MGP-model, it is not discussed here but elsewhere.[1,7] The refractive index at 632 nm as determined with *in situ* ellipsometry is shown in Fig. 2. Although the growth rate varies over a wide range material with good structural quality is obtained especially at high substrate temperatures, as indicated by the refractive index. At higher growth rates the refractive index depends strongly on the temperature. The refractive index for the lowest rate is the same at higher temperatures, within the experimental uncertainty of about 0.1.

The hydrogen content of the films is given in Fig. 3. The relative experimental accuracy is about 10%. From the combination of the nuclear techniques RBS and ERDA it was concluded that the total atomic density is constant within 10% for the observed range of the refractive index and equal to about 5×10^{28} m^{-3}. This agrees very well with the value reported by Langford *et al.*[8] The hydrogen content itself is determined with FTIR spectroscopy after recalibration of the conversion factors for the SiH and SiH_2 absorption peaks. The obtained conversion factors differ considerably from those of Langford[8] and will be reported elsewhere.[9] The hydrogen content decreases drastically as a function of the substrate temperature. Although it can not be seen in this figure, mainly the SiH_2-bonded hydrogen decreases and is partly converted into SiH-bonded hydrogen. The hydrogen content shows also a dependence on the plasma condition, i.e., it also increases with increasing growth rate. Only for the two lowest rates and for temperatures above 250 °C, the hydrogen content is equal within the experimental accuracy. This is exactly within the range of 0.01 to 1 nm/s for 250 and 400 °C for which Ganguly and Matsuda[2] also reported a growth-rate independent hydrogen content.

IV. DISCUSSION

The observed increase of the refractive index as a function of substrate temperature is due to the fact that less hydrogen is incorporated into the film at higher temperatures. As mentioned before the atomic density

TABLE I. Gas flows and arc current used for film deposition.

	Argon flow (slm)	Hydrogen flow (slm)	Silane flow (slm)	Arc current (A)	Growth rate (nm/s)
Condition 1	3.3	0.6	0.6	45	11
Condition 2	3.3	0.3	0. 2	25	3
Condition 3	2.1	0.12	0.04	12.5	0.3

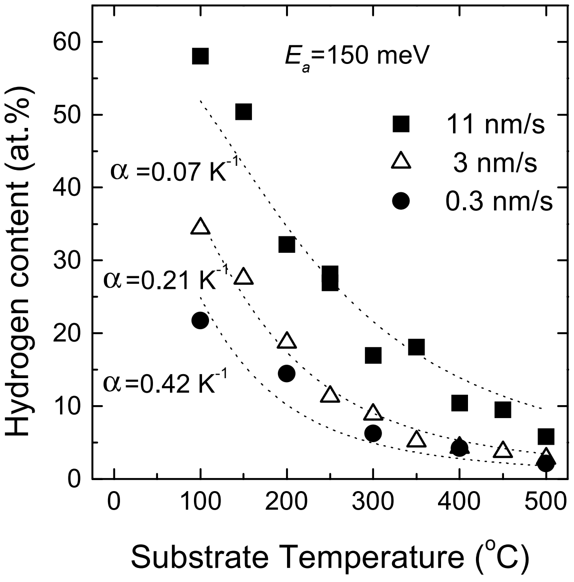

FIG. 3. Hydrogen content as determined with FTIR spectroscopy as a function of the substrate temperature. The curves are fits to Eq. (3).

of the film remains nearly constant but the higher the temperature is the more hydrogen is eliminated which leads to a higher silicon density and therefore to a higher refractive index. Hydrogen can be eliminated by a cross-linking step[10] immediately after a physisorbed SiH_3-radical has chemisorbed on a surface dangling bond. The cross-linking probability is thermally activated but due to the energy released at the chemisorption of the SiH_3 radical (about 2 eV) the activation energy is quite low.[11] If this cross-linking reaction does not occur immediately after chemisorption it is assumed that hydrogen is incorporated into the film. The cross-linking step is unlikely to occur in two situations that have the same origin, namely the energy available being too small to eliminate hydrogen. In the first situation there are two hydrogen atoms, which could actually desorb as a hydrogen molecule but the temperature is too low for the cross-linking to occur (Fig. 4a). In the second situation there is no second hydrogen atom on a surface site next to the dangling bond with which to form molecular hydrogen. Consequently, the lack of H_2-formation energy prevents cross-linking (Fig. 4b). We suggest that surface dangling bonds are built in as defects in this way. Although this last process is very important for the electronic properties of the film, it has a negligible contribution to the hydrogen content, at least for the temperature range studied. Therefore the hydrogen content incorporated into the film can be described only on the basis of the first process.

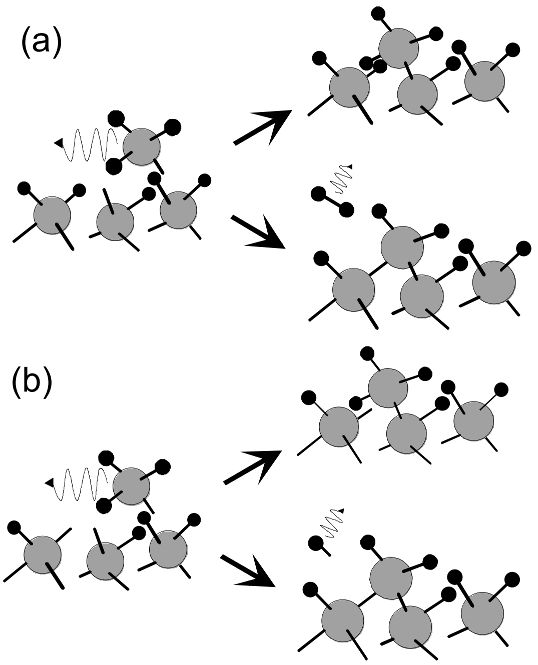

FIG. 4. Schematic representation of the hydrogen incorporation. In situation (a) molecular hydrogen is released after cross-linking or two hydrogen atoms are incorporated into the film. In situation (b) the incorporation of a defect and a hydrogen atom is more probable than cross-linking and desorption of a hydrogen atom.

The hydrogen content, c_H, is equal to two times the rate of incorporated non-cross-linked silicon, $j_{Si\text{-}H}$, (two hydrogen atoms are incorporated at once) divided by the sum of this term and the rate of silicon incorporation j_{Si}. The incorporation rate of silicon is equal to the rate of silicon incorporated without cross-linking, $j_{Si\text{-}H}$, and the rate of silicon incorporated with cross-linking, $j_{Si\text{-}Si}$. Thus:

$$c_H = \frac{2 j_{Si-H}}{j_{Si} + 2 j_{Si-H}} = \frac{2 j_{Si-H}}{j_{Si-Si} + 3 j_{Si-H}} . \tag{1}$$

This equation is analogous to the relation derived by Kampas and Griffith[12] who assumed that SiH_2 was the depositing radical. The equation shows that the hydrogen content is 2/3 when no cross-linking occurs, i.e., deposition of polysilane, and zero if every incorporated silicon atom cross-links. We assume that the quantities $j_{Si\text{-}Si}$ and $j_{Si\text{-}H}$ are related by the Arrhenius expression

$$\frac{j_{Si\text{-}Si}}{j_{Si\text{-}H}} = \alpha T \exp(-E_a/kT) \tag{2}$$

and thus obtain

$$c_H = \frac{2}{3 + \alpha T \exp(-E_a / kT)} . \tag{3}$$

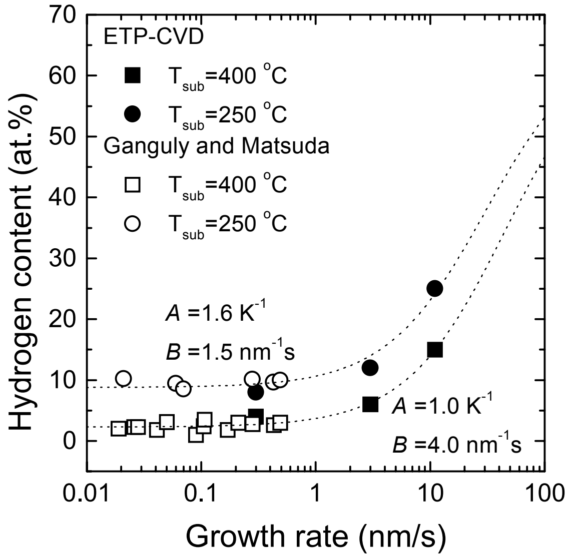

FIG. 5. Hydrogen content as a function of the growth rate for two different substrate temperatures. The values reported by Ganguly and Matsuda (Ref. 2) are also shown (open squares and circles). The curves are fits to Eq. (3).

Here is T the substrate temperature in Kelvin, α a temperature independent pre-exponential factor, and E_a the activation energy. The assumed Arrhenius expression is based on the so-called 'transition-state theory' in which a transition involves an intermediate state, the 'transition state'.[13] Fitting the data in Fig. 3 by Eq. (3) we find that the activation energy E_a, which is assumed to be growth-rate independent, is about 150 meV. The pre-exponential factor α is assumed to be growth-rate dependent and is equal to, respectively, 0.42, 0.21, and 0.07 K^{-1} for the growth rates 0.3, 3, and 11 nm/s. Ganguly and Matsuda[2] observed a temperature dependence of the hydrogen content and no growth-rate dependence at least for the range 0.01−1 nm/s. This has some implications for the growth-rate dependent pre-exponential factor: its dependence on the growth rate should be minimal in the above range. To be more specific, the hydrogen content is shown in Fig. 5 as a function of the growth rate for two different temperatures, namely 250 and 400 °C. The hydrogen content for these temperatures as reported by Ganguly and Matsuda are also shown in Fig. 5. These hydrogen contents agree well with our values obtained by ETP-CVD. To determine the growth-rate dependence of α the data points have been fitted by Eq. (3). The restrictions for the fit are a hydrogen content of 66% at an infinite growth rate (no time left for cross-linking) and an almost growth-rate independent hydrogen content at low growth rates. These conditions are achieved by a fit in which the pre-exponential factor α of the Arrhenius expression has the form

$$\alpha = \frac{A}{1 + R_g / B} \tag{4}$$

where R_g is the growth rate and A and B are fit parameters indicated in Fig. 5. Although the expression α is purely empirical it gives an appropriate description for the hydrogen content at the growth rates studied. It also accounts for the result that the growth rate is of no importance at the smallest R_g since there is no competition between the time for the formation of a monolayer, which is proportional to $1/R_g$, and the characteristic time needed for cross-linking. The hydrogen content is only significantly influenced by high growth rates where also the time to grow a monolayer becomes comparable to the time needed for a cross-linking step.

V. CONCLUSION

We demonstrate that a model which assumes a thermally activated cross-linking step immediately after the chemisorption of the silyl radical can give a plausible description of the hydrogen incorporation in a-Si:H films and can be used to fit the hydrogen content in the film as a function of substrate temperature. While the hydrogen content shows an almost growth-rate independent behavior at low growth rates between 0.01 and 0.1 nm/s, it increases at higher growth rates. Although this growth-rate dependence is not completely understood at the moment it suggests a kind of competition between the time to deposit a monolayer and the characteristic time for cross-linking which depends on temperature.

ACKNOWLEDGMENTS

This research is financially supported by the Netherlands Agency for Energy and the Environment (NOVEM), the Netherlands Organization for Scientific Research (NWO-Prioriteit), the Foundation for Fundamental Research on Matter (FOM-Rolling Grant). L. van IJzendoorn and F. van de Pas are thanked for performing the RBS/ERDA measurements. M. J. F van de Sande, A. B. M. Hüsken, and H. M. M. de Jong are thanked for their skillful technical assistance.

[1] M.C.M. van de Sanden, R.J. Severens, W.M.M. Kessels, F. van de Pas, L. Van IJzendoorn, and D.C. Schram, Mater. Res. Soc. Symp. Proc. **467**, 621 (1997).

[2] G. Ganguly and A. Matsuda, Mater. Res. Soc. Symp. Proc. **258**, 39 (1992).

[3] A. Gallagher, Mater. Res. Soc. Symp. Proc. **70**, 3 (1986).

[4] J. Perrin, Y. Takeda, N. Hirano, Y. Takeuchi, and A. Matsuda, Surface Scienc **210**, 114 (1989).

[5] W.M.M. Kessels, L. Gabella, J. Bastiaansen, R.J. Severens, M.C.M. van de Sanden, and D.C. Schram, *Proceedings of the 2nd Conference on Low Temperature Plasma Diagnostics* (Bad-Honnef, Germany, 1997).

[6] L. van IJzendoorn, Analytica Chimica Acta **297**, 55 (1994).

[7] R.J. Severens, W.M.M. Kessels, L. Gabella, F. van de Pas, M.C.M. van de Sanden, and D.C. Schram, *Proceedings of 13th International Symposium on Plasma Chemistry* (Beijing, China, 1997), p. 1059.

[8] A.A. Langford, M.L. Fleet, B.P. Nelson, W.A. Langford, and N. Maley, Phys. Rev. B **45**, 13367 (1992).

[9] W.M.M. Kessels, M.C.M. van de Sanden, R.J. Severens, L.J. van IJzendoorn, and D.C. Schram, Mater. Res. Soc. Symp. Proc. **507**, 529 (1998).

[10] G.H. Lin, J.R.. Doyle, M. He, and A. Gallagher, J. App. Phys. **64**, 188 (1988).

[11] R.J. Severens, M.C.M. van de Sanden, H.J.M. Verhoeven, J. Bastiaanssen, and D.C. Schram, Mater. Res. Soc. Symp. Proc. **420**, 341 (1996).

[12] F.J. Kampas, R.W. Griffith, Appl. Phys. Lett. **39**, 407 (1981).

[13] G.M. Barrow, *Physical Chemistry* (McGraw-Hill Kogakusha Ltd. Tokyo, 1979), p. 693.

J. Non-Cryst. Solids 227-230, 133 – 137 (1998).

Hydrogen poor cationic silicon clusters in an expanding argon-hydrogen-silane plasma

W. M. M. Kessels,[a] M. C. M. van de Sanden,[b] and D. C. Schram
Department of Applied Physics, Eindhoven University of Technology, P.O. Box 513, 5600 MB Eindhoven, The Netherlands

Cationic silicon clusters $Si_nH_m^+$ with up to ten silicon atoms have been detected mass spectrometrically in an expanding argon-hydrogen-silane plasma used for fast deposition of amorphous hydrogenated silicon. A reaction pathway is proposed in which initial silane ions are produced by dissociative charge exchange between argon and hydrogen ions emanating from the plasma source and the admixed silane followed by chain reactions of the created ions with silane. The silicon clusters are hydrogen poor, which is ascribed to the high gas temperature as the initial argon-hydrogen plasma is thermal in origin.

The formation of large positive ions in silane plasmas used for the deposition of amorphous hydrogenated silicon is of interest as they are expected to have a detrimental influence on the film quality. These ions, or more appropriate, cationic clusters can lead to disturbances in the film stochiometry and to defects.[1] Until now several authors have reported about the detection and formation of positive silicon ions and clusters in mainly conventional dc and rf silane discharges.[2-4] To our knowledge, only Theil and Powell[5] report about the detection of positive silicon clusters in a remote type of plasma, but do not deal with their growth mechanism. This letter deals with the detection and formation of positive silicon clusters in an expanding thermal plasma.

The expanding thermal plasma is a remote plasma assisted deposition technique that allows for the deposition of solar grade quality amorphous silicon at a growth rate of 10 nm/s.[6] In this technique (cf. Fig. 1) a thermal argon-hydrogen plasma (electron density ≈ 10^{22} m^{-3}, electron temperature ≈ 1 eV) is created in a dc arc discharge operating at subatmospheric pressure and expanded into a reactor chamber at 0.2 mbar. The argon flow is 55 sccs (standard cubic centimeters per second) and the hydrogen flow is varied between 0 and 15 sccs. Silane is admixed by means of an injection ring at 6 cm from the arc exit at a flow of 10 sccs. No power is coupled in downstream leading to a low electron temperature (≈0.2–0.3 eV) in the expansion. The admixed silane is therefore ionized and dissociated by argon and hydrogen ions as well as by atomic hydrogen created in the arc. The electron density downstream ranges from 10^{19} to 10^{16} m^{-3} depending on the admixed flows of molecular gases. For the present study the substrate holder is replaced by a Hiden Analytical EPIC 300 mass spectrometer.

In Fig. 2 positive ion mass spectra are shown obtained with ionizer off for 1 sccs and 10 sccs hydrogen admixed in the arc. Both spectra, which are not corrected for mass dependent gas extraction and spectrometer transmission, show positive ions with up to 10 silicon atoms whereby the observation is limited by the mass range of the spectrometer. In the condition with 1 sccs hydrogen admixture the ion count rates are smaller than with 10 sccs hydrogen admixture and the smallest clusters observed contain four silicon atoms. Compared to the spectra obtained in rf and dc plasmas it is striking that the clusters are relatively hydrogen poor with the higher silicon ions containing dominantly one hydrogen atom. The ion spectra presented by Theil and Powell, which have a similar silicon number distribution as in our situation, suggest the dominance of the clusters containing two hydrogen atoms.[5]

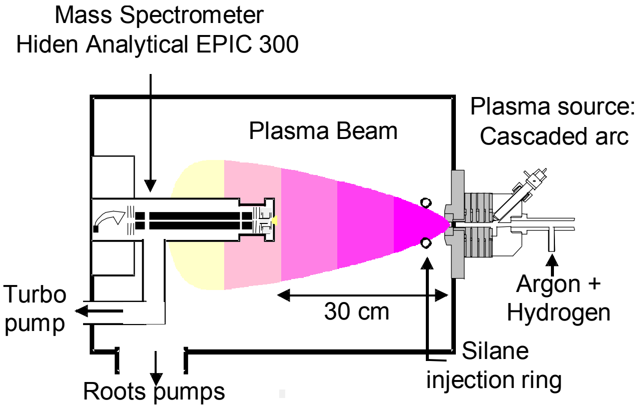

FIG. 1. The expanding thermal plasma setup used for fast deposition of hydrogenated amorphous silicon. The substrate holder is replaced by a mass spectrometer with a similar geometry.

---

[a] Electronic mail: w.m.m.kessels@phys.tue.nl
[b] Electronic mail: m.c.m.v.d.sanden@phys.tue.nl

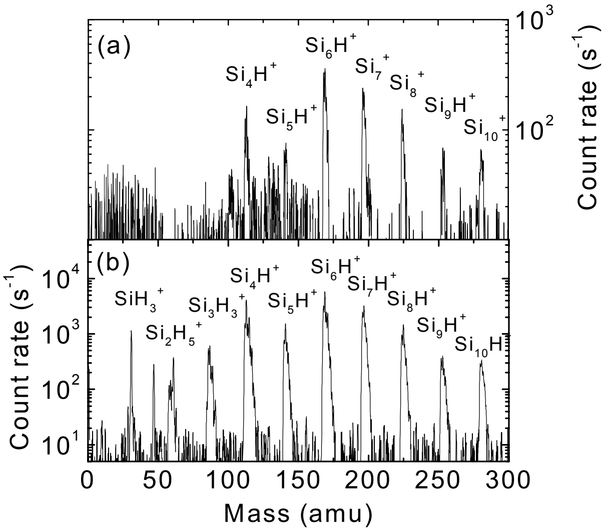

FIG. 2. Positive ion mass spectra as obtained in the expanding argon-hydrogen-silane plasma for (a) 1 sccs hydrogen and (b) 10 sccs hydrogen admixed in the arc. The most dominant ions are indicated. The spectra are corrected for a small background level caused by photons.

The basic difference between the two plasma conditions in Fig. 2, as reported in Refs. 7 and 8, are the reactive species emanating from the arc. If a small hydrogen flow is admixed the ion fluence emanating from the arc is large and the silane dissociation (dissociation degree about 50%) is dominated by argon and hydrogen ions. If the hydrogen flow is increased the ion fluence is effectively quenched and silane is dominantly dissociated by atomic hydrogen. The silane dissociation degree is reduced to about 10% due to a smaller reaction rate of atomic hydrogen with silane.[9]

In both conditions in Fig. 2, ions that leave the arc will undergo dissociative charge exchange with the admixed silane leading to silane ions, dominantly SiH_3^+.[9] These silane ions can either recombine dissociatively with electrons or react with silane. The latter reaction will be favored if the electron density is or gets sufficiently low. In both conditions the reaction pathway proposed for the creation of the cationic silicon ions is the chain reaction:

$$Si_nH_m^+ + SiH_4 \rightarrow Si_{n+1}H_p^+ + qH_2 \tag{1}$$

where $n \geq 1$ and $m+4 = p+2q$. Reactions in which atomic hydrogen is created are neglected as they are energetically less favorable. The direct ionization of higher silanes is ruled out due to the fast fall off in the density of these higher silanes.[8] From the proposed point of view the cluster size depends on the product of the silane density and the distance between the point where the initial silane ion is created and the mass spectrometer. In the case of 1 sccs hydrogen admixture dissociative recombination with an electron will be much larger as the initial ion and electron fluence emanating from the arc is larger.[8] This, in combination with a smaller silane density due to the higher dissociation degree, leads to smaller cluster count rates than for the condition in which a smaller ion fluence emanates from the arc as is observed in Fig. 2. The ions with less than four silicon atoms are probably absent due to their higher recombination rate with electrons in comparison with larger ions.

To produce more evidence for the reaction pathway, a simple computer code was written for the reactions of the cationic clusters with silane, regardless of the number of hydrogen atoms present in the clusters. The distance between the arc outlet and the mass spectrometer was divided into a large number of points and at every point $x + \Delta x$ the flux φ_n (i.e., product of density and velocity) of a certain cationic cluster with n silicon atoms was calculated from the flux both surviving and created while traveling the distance Δx. This was done by the following discretized mass balance equation:

$$\begin{aligned} \varphi_n(x+\Delta x) = \varphi_n(x)\left(1 - \frac{k_n N_{SiH4}}{v_n}\Delta x\right) \\ + \varphi_{n-1}(x)\frac{k_{n-1}N_{SiH4}}{v_{n-1}}\Delta x. \end{aligned} \tag{2}$$

In Eq. (2), Δx is the distance between two successive points, k_n and v_n are, respectively, the reaction rate with silane and the directed velocity of the cationic cluster or ion with n silicon atoms and N_{SiH4} is the silane density which is assumed homogeneous. Outward diffusion turned out to be relatively unimportant and was therefore not taken into account. The code was applied to the condition of 10 sccs hydrogen admixture as in this case the ion-silane chain reactions are believed to be dominant and the assumption of a homogeneous silane density (10^{20} m^{-3}) is best fulfilled due to the small silane dissociation degree. The ion flux into the reactor is dominated by hydrogen ions[8] and was set equal to 8×10^{20} $m^{-2}s^{-1}$ [the measured hydrogen ion density and directed velocity are respectively 8×10^{17} m^{-3} (Ref. 8) and 1000 m/s (Ref. 10)]. The reaction rate of hydrogen ions with silane was set to 5×10^{-15} m^3s^{-1}.[9] Taking 1000 m/s as an upper limit for the directed velocity of the clusters it can be shown that the observed positive ion mass spectrum can very well be obtained by the proposed reaction pathway if reaction rates for the chain reactions are of the order of 10^{-16} m^3s^{-1}. Smaller rates would not lead to the large cationic clusters observed while larger rates would lead to a relative smaller abundance of the smaller clusters. Although the simplifications and the lack of data allow no further conclusions, these reaction rates correspond very well with those as proposed by Weakliem[3] and Kushner.[11] On the other hand Mandich and Reents, who determined various silicon cluster ion-silane reaction rates either experimentally or theoretically, distanced themselves from these proposed rates. Their measurements revealed reaction rates that depend strongly (from 10^{-15} to 10^{-19} m^3s^{-1}) on the number of silicon and hydrogen atoms present in the cluster and on its isomeric state.[12] According to Mandich and Reents simplifying and generalizing assumptions on the rates should be postponed.[13] On the other hand, the conditions under which our experiments were performed are quite distinct from theirs. Moreover, our results are difficult to reconcile with their observations. For example, a termination in the chain reactions at a certain isomeric state or cluster size (they observe no clusters containing more than 6 silicon atoms)[12] is not observed in our spectrum. The results in Fig. 2 only suggest a bottleneck in the reaction from $Si_4H_m^+$ to $Si_5H_n^+$. Kushner[11] already mentioned that possible activation barriers in the reaction of silicon ions and clusters with silane can be overcome by internal energy of particles in a plasma. Such a possible influence was also suggested by Mandich and Reents who obtained their results at low pressure and at room temperature. In our plasma the kinetic and internal energy of the species is even higher than in conventional silane plasmas due to the fact that the argon-hydrogen plasma is thermal in origin.[10] This is probably also the reason of the specific hydrogen distribution observed in the clusters as will be discussed next.

In Fig. 3 the distribution in hydrogen content of cationic clusters containing six silicon atoms is given at a higher resolution. This distribution is typical for the clusters containing more than three silicon atoms: the clusters with odd numbers and even numbers of hydrogen atoms are decoupled due to the fact that no atomic hydrogen can be created in the chain reactions [cf. Eq. (1)]. Furthermore, the clusters are hydrogen poor and those with only one hydrogen atom are dominant. Although this is in relative agreement with the observations of Theil and Powell[5] it is totally different compared to rf or dc silane plasmas.[2-4] For example, Haller reports a mean hydrogen to silicon ratio of 1.5 for cationic silicon clusters.[2] In these types of plasmas normally the addition of SiH_2 is proposed in the chain reactions accompanied by the loss of one hydrogen molecule [i.e., $p = m+2$, $q=1$ in Eq. (1)]. Our results indicate that the addition of only Si-atoms with the release of two hydrogen molecules is by far dominant. This was confirmed by a simple computer code which showed that the probability for only Si-atom addition is larger than 95%. This code was started at clusters containing four silicon atoms and not at the initial silane ions as their distribution in hydrogen content suggests also other ion-molecule reactions than given in Eq. (1). We will not go into these reactions but it should be mentioned that a certain ion or cluster can be dominant either due to a high production rate or due to a reduced reactivity of the ion or cluster and thus a lower loss rate. However, if, e.g., the large bare silicon clusters Si_n^+ would have a reduced reactivity the distribution in hydrogen content for larger clusters would imply that even more than two hydrogen molecules are released in the reaction with silane.

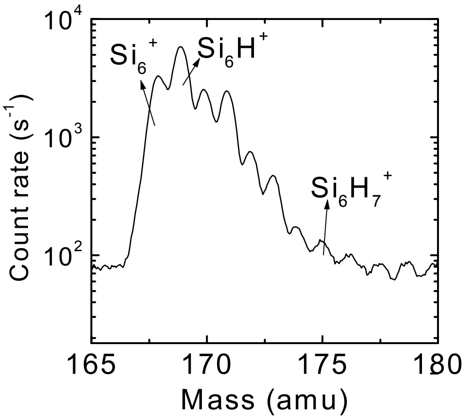

FIG. 3. High resolution mass spectrum of six silicon atoms containing clusters.

In summary, it has been shown that cationic silicon clusters are present in an expanding argon-hydrogen-silane plasma having possible implications for other remote plasmas. These clusters are inevitably created if the product of the silane density and the geometrical interaction pathway is large, even when the ion fluence emanating from the plasma source is relatively low. Furthermore, our results suggest that the reaction rates as determined by Mandich and Reents are not appropriate for our plasma conditions due to the higher gas temperature, the latter probably leading also to hydrogen poor clusters. Future studies of cationic silicon cluster formation are in progress as well as the determination of their influence on the quality of hydrogenated amorphous silicon.

The authors acknowledge N. van der Beek, S. van Egmond, and C. Leewis for their contributions to the measurements and M. J. F. van de Sande, A. B. M. Hüsken, and H. M. M. de Jong for their skillful technical assistance. This work has been financially supported by the Netherlands Organization for Scientific Research (NWO-Prioriteit), the Netherlands Agency for Energy and the Environment (NOVEM) and the Foundation for Fundamental Research on Matter (FOM-Rolling Grant).

[1] W. Luft and Y. Simon Tsuo, *Hydrogenated amorphous silicon alloy deposition processes*, (Marcel Dekker, New York, 1993).

[2] I. Haller, Appl. Phys. Lett. **37**, 282 (1980).

[3] H.A. Weakliem, R.D. Estes, and P.A. Longeway, J. Vac. Sci. Technol. A **5**, 29 (1987).

[4] A.A. Howling, L. Sansonnens, J.-L. Dorrier, and Ch. Hollenstein, J. Appl. Phys. **75**, 1340 (1994).

[5] J.A. Theil and G. Powell, J. Appl. Phys. **75**, 2652 (1994).

[6] M.C.M. van de Sanden, R.J. Severens, W.M.M. Kessels, L. van IJzendoorn, F. van de Pas, and D.C. Schram, Mater. Res. Soc. Symp. Proc. **467**, 621 (1997).

[7] R.F.G. Meulenbroeks, R.A.H. Engeln, M.N.A. Beurskens, R.M.J. Paffen, M.C.M. van de Sanden, J.A.M. van der Mullen, and D.C. Schram, Plasma Sources Sci. Technol. **4**, 74 (1995).

[8] M.C.M. van de Sanden, R.J. Severens, W.M.M. Kessels, R.F.G. Meulenbroeks, and D.C. Schram, J.Appl. Phys. **84**, 2426 (1998).

[9] J. Perrin, O. Leroy, and M.C. Bordage, Contrib. Plasma Phys. **36**, 1 (1996).

[10] M.G.H. Boogaarts, G.J. Brinkman, H.W.P. van der Heijden, P. Vankan, S. Mazouffre, J.A.M. van der Mullen, D.C. Schram, and H.F. Döbele, *Proceedings of the Eigth International Symposium Laser-aided Plasma Diagnostics*, (Doorwerth, The Netherlands 1997), p. 109.

[11] M.J. Kushner, J. Appl. Phys. **63**, 2532 (1988).

[12] See, e.g., W.D. Reents, Jr. and M.L. Mandich, Plasma Sources Sci. Technol. **3**, 373 (1994).

[13] M.L. Mandich and W.D. Reents, Jr., J. Chem. Phys. **90**, 3121 (1989).

Appl. Phys. Lett. 72 (19), 2397 – 2399 (1998).

Formation of large positive silicon-cluster ions in a remote silane plasma

W. M. M. Kessels,[a] C. M. Leewis, A. Leroux, M. C. M. van de Sanden,[b] and D. C. Schram
Department of Applied Physics, Eindhoven University of Technology, P.O. Box 513, 5600 MB Eindhoven, The Netherlands

The formation of hydrogen poor cationic silicon clusters $Si_nH_m^+$ with up to ten silicon atoms in an expanding argon-hydrogen-silane plasma has been studied by mass spectrometry and Langmuir probe measurements. Sequential clustering reactions with silane, initiated by silane ions, cause their size to depend on the product of silane density and geometrical path length having possible implications for a-Si:H films deposited by remote plasmas. Reaction rates, estimated by an one-dimensional model, show no strong dependence on the number of silicon and hydrogen atoms present in the ions in contrast with rates determined by ion-cyclotron resonance mass spectrometry studies. Possible causes of the discrepancy are discussed as well as the hydrogen poverty of the clusters. The maximum contribution of the cationic clusters to the growth flux is about 6% for the conditions investigated.

I. INTRODUCTION

Today's studies concerning silane plasma chemistry and deposition mechanism of hydrogenated amorphous silicon (a-Si:H) are mainly concentrated on silane radical processes. However, the chemistry of silicon containing ions and their impact on the deposition process should not be underestimated. Although their contribution to the silicon growth flux can be limited, they can for example supply a considerable amount of potential and kinetic energy to the surface as they are accelerated in the plasma sheath. Furthermore, silicon containing ions can reach a considerable size as sequential ion-molecule reactions with silane are relatively fast. This clustering can particularly be important in remote silane plasmas as it will be shown that the size of silicon containing ions depends on the product of silane density and distance between plasma source and substrate.

In this paper the formation of large positive ions containing up to ten silicon atoms in an expanding argon-hydrogen-silane plasma as reported in Ref. 1 is further investigated. The plasma under consideration is a thermal plasma source created argon-hydrogen plasma to which silane is injected downstream. With this setup it is possible to deposit solar grade quality a-Si:H at a growth rate of 10 nm/s at a substrate temperature of 400 °C.[2] Furthermore, this plasma is very well suited to study the plasma chemistry as the downstream plasma properties can be varied without influencing the source properties. In the present study, the silane flow admixed to the plasma and consequently the silane density has been varied for constant source properties and the consequences for cationic cluster formation have been investigated. Results concerning the ion chemistry in the plasma are compared to fundamental ion-molecule reactions as, e.g., studied by Mandich and Reents[3-6] and the extrapolation of such results to silane plasmas is discussed. Moreover, the contribution of the cationic clusters to film growth has been determined and their impact on film quality is considered.

II. EXPERIMENT

The setup is schematically illustrated in Fig. 1. A thermal argon-hydrogen plasma is created in a cascaded arc operating at a current of 45 A, a voltage of about 180 V, and a pressure of about 400 mbar. The argon and hydrogen flow are, respectively, 55 and 10 sccs (standard cubic centimeter per second). The plasma in the arc has typically an electron density of 10^{22} m^{-3} and an electron temperature of 1 eV. The plasma expands supersonically into the low pressure (0.20 mbar) deposition chamber, and after a stationary shock at about 4 to 5 cm from the arc exit the plasma flows subsonically (with about 1000 m/s) into the direction of the substrate holder.[7] Silane is injected about 5 cm from the arc exit by means of an injection ring and at flows varied between 1 and 15 sccs.

The substrate holder is positioned at 38 cm from the arc exit and is replaced by a mass spectrometer (Hiden Analytical EPIC 300) with similar geometry in the present study. The setup is also equipped with a double cylindrical Langmuir probe positioned at 2 cm

---

[a] Electronic mail: w.m.m.kessels@phys.tue.nl
[b] Electronic mail: m.c.m.v.d.sanden@phys.tue.nl

J. Vac. Sci. Technol. A 17 (4), 1531 – 1535 (1999).

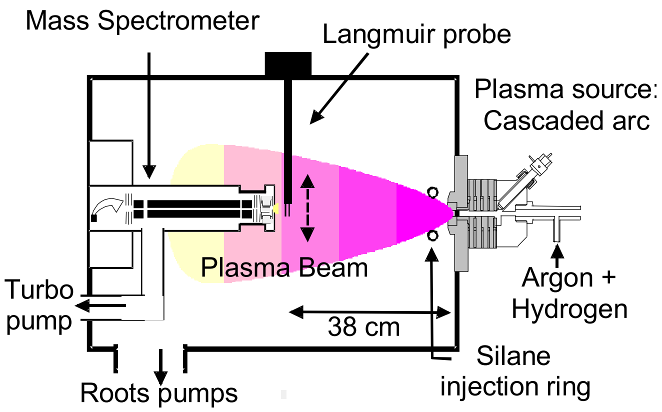

FIG. 1. Experimental arrangement for high rate deposition of a-Si:H showing plasma source, deposition chamber, mass spectrometer (at usual position of substrate holder), and Langmuir probe.

in front of the substrate holder or mass spectrometer and which can be scanned in radial direction. As measurements have been performed in a depositing plasma the probe characteristics obtained have been carefully checked. It turned out that the current to the probe in the depositing plasma was sufficient low to avoid a significant voltage drop over the resistive a-Si:H film formed. Yet severe disturbances occurred in measurements at the electron current branch of single probe measurements, particularly in the saturation region. Before every measurement the probe was cleaned by drawing high currents to each of the probes separately. The probe characteristics obtained were analyzed by the method proposed by Peterson and Talbot.[8] A more detailed description about the measurements in the depositing plasma and the analysis can be found in Ref. 9.

III. RESULTS AND DISCUSSION

As presented in an earlier paper[10] the dissociation of silane is determined by ions (either Ar^+ or H^+) and atomic hydrogen emanating from the arc as the electron temperature is too low (0.1–0.3 eV) for electron induced ionization. In the plasma condition described a large atomic hydrogen flux emanates from the plasma source and its interaction with silane leads to a large SiH_3 flux towards the substrate. The presence of both atomic hydrogen in the argon-hydrogen plasma and SiH_3 in the argon-hydrogen-silane plasma have been demonstrated by appearance potential mass spectrometry using the same mass spectrometer as mentioned above. Yet no quantitative information has been obtained by this technique and therefore an indirect way was used showing that SiH_3 is the dominant species contributing to film growth.[10] Nevertheless, also a small flux of mainly atomic hydrogen ions (about a factor 100 lower than the atomic hydrogen flux) emanates from the arc creating silane ions by charge transfer with silane, most probably by:[11]

$$H^+ + SiH_4 \rightarrow SiH_3^+ + H_2. \qquad (1)$$

It is expected that sequential clustering reactions of these primary silane ions lead to the cationic clusters as shown by ion mass spectrometry scans in Fig. 2. This figure shows peaks due to silicon cluster ions $Si_nH_m^+$, containing up to 10 silicon atoms for silane flows of 10 and 15 sccs. Possible larger clusters can not be observed due to the limited range of the mass spectrometer. Around 47 amu also silanol ions are observed most probably caused by oxygen remaining in the deposition chamber after a plasma clean with an argon-carbontetrafluoride-oxygen mixture. The mass spectra, obtained with ionizer off, are not corrected for mass dependent transmittance and detector efficiency of the spectrometer. The background signal is caused by photons from the plasma source arriving at the mass spectrometer's detector which is almost in line-of-sight with the plasma source. As can be seen in Fig. 2 the cluster size increases with silane flow and consequently silane density. This dependency on silane density confirms the proposed reaction mechanism:[1,12,13]

$$Si_nH_m^+ + SiH_4 \rightarrow Si_{n+1}H_p^+ + qH_2 \qquad (2)$$

with $n \geq 1$ and $m+4 = p+2q$. Reactions leading to the formation of atomic hydrogen are neglected as they are endothermic.[14] According to Haller,[12,15] and copied by Weakliem,[13] also charge transfer can occur between the cationic clusters and silane molecules. Calculations[16] showed, however, that the ionization potential of bare silicon clusters Si_n with $n \geq 2$ is at most 8 eV which is smaller than the ionization potential of silane. Assuming a similar ionization potential for silicon clusters containing few hydrogen atoms makes charge transfer with silane very unlikely even when the silane is rovibrationally excited.

Another possible production mechanism of the cationic clusters is by means of ionization of polysilanes. This mechanism is very unlikely as the polysilane density is very low in the expanding plasma. The disilane density is about a factor 100 lower than the silane density,[10] whereas trisilane and tetrasilane are estimated to be respectively a factor 10^3 and 10^4 lower. Larger polysilanes have not been observed.[9]

As reported earlier, it is remarkable that the hydrogen content of the cationic clusters in Fig. 2 is distinct from the hydrogen content in positive ions and cluster ions generally observed in silane plasmas.[12,13,15,17] For all clusters containing more than three silicon atoms the most abundant ion contains

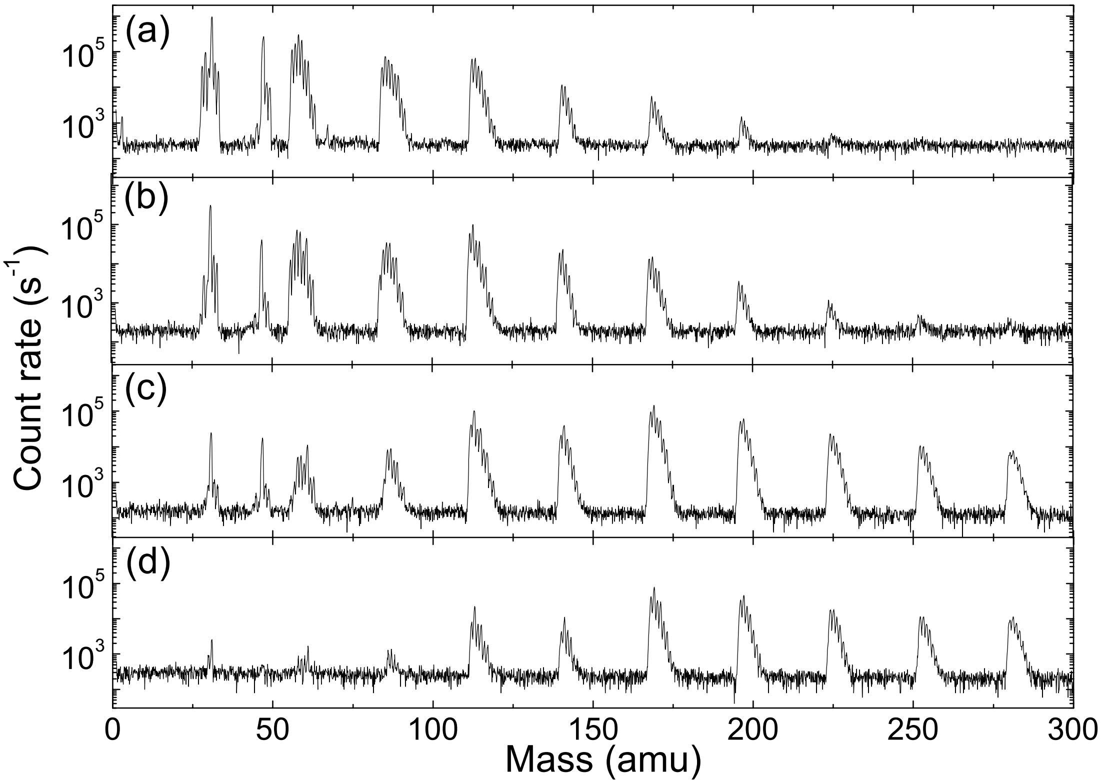

FIG. 2. Ion mass spectra for constant source properties of 55 sccs argon, 10 sccs hydrogen and 45 A arc current with silane flows of (a) 1, (b) 3, (c) 10 and (d) 15 sccs.

only one or no hydrogen atom and only ions containing up to seven hydrogen atoms, $Si_nH_7^+$, are clearly observable. The clusters with even and odd number of hydrogen atoms appear also to be decoupled,[1] which can be understood from the endothermicity of the elimination of atomic hydrogen in reaction (2). Furthermore, the distribution of hydrogen in the clusters suggests that the ion-molecule reactions of Eq. (2) occur mostly with elimination of two hydrogen molecules, i.e., q=2. Assuming the reaction pathway in Eq. (2), the release of hydrogen has been studied by a simple computer code as proposed by Hollenstein.[18] The code starts at clusters containing four silicon atoms as smaller ions are more hydrogen saturated which is possibly due to side effects as charge transfer reactions between the ions emanating from the arc and the small quantity of disilane and trisilane present in the plasma. A comparison between experimental and calculated results has demonstrated that the probability for elimination of two hydrogen molecules and therefore the addition of only a Si atom is larger than 95%.[1] This is in strong contrast with cluster ions in conventional radio-frequency (rf) and direct-current (dc) silane plasmas[12,13,15,17] where the hydrogen to silicon ratio is about constant for larger cluster ions. In these plasmas the observed cationic cluster growth can satisfactorily be explained by sequential addition of SiH_2 and consequently the release of only one hydrogen molecule. For remote plasmas only little information about cationic clusters is available, apart from the observation by Theil and Powell[19] that the degree of hydrogenation of the cluster ions decreased (leading dominantly to $Si_nH_2^+$) with increasing discharge power in 13.56 MHz and 2.45 GHz generated discharges in helium. Therefore we attribute the hydrogen poverty of the cationic silicon clusters to the high gas temperature (1000–1500 K[20]) in the expanding plasma compared to conventional silane plasmas which is due to the fact that the plasma is created in a thermal plasma source. This is in agreement with the expectation of Mandich and Reents,[5] observing mainly SiH_2 addition in their ion-silane studies at thermal energies,[3-6] that more hydrogen is eliminated when additional energy is present. Furthermore, Henis *et al.*[14] postulated that the probability for reactions between silicon containing ions and silane leading to products requiring extensive rearrangement and bond breaking, necessary to create two hydrogen molecules, is increased at higher kinetic energies of the involved species. This corresponds also with the structure of the cluster ions as the limited hydrogen content implies very compact clusters. Such compact structure is particularly stable and is in fact the ground state geometry for dehydrogenated neutral and ionic clusters.[16] Their hydrogenated counterparts show also a particular stability at compact structures, but at intermediate and fully hydrogen-terminated bulk-like tetrahedral coordinated structures as well.[21,22] The compact structure is most probably created in the expanding plasma with relatively high gas temperature, whereas the other two structures are dominantly observed in conventional silane plasmas.

Quantitative information on the presence of the cationic clusters has been determined from Langmuir probe measurements. In Fig. 3 the ion flux at 2 cm in front of the substrate is shown for different silane flows. The ion flux for the non-depositing argon-hydrogen plasma is given for comparison. The ion flux decreases considerably when silane is admixed due to dissociative recombination of the silicon containing ions with electrons. The rate for this reaction is assumed to be $10^{-13}T_e^{-1/2}$ m^{3}s^{-1} (T_e: electron temperature in eV) and to be rather independent of ion size.[11] The electron temperature obtained is in the range 0.2–0.3 eV.[9] Notice that the ion flux increases with silane flow as the source properties are kept constant. Although small differences in dissociative recombination rates for the different clusters can not be excluded, it can probably be attributed mainly to a decrease of beam width. While no beam properties are observed for the non-depositing plasma, the beam diameter decreases with increasing silane flow and consequently increasing cluster size for the depositing plasma. The beam radius scales with $1/\sqrt[4]{M}$ (M: the average ion mass) showing reduced outward diffusion of the heavy ions for a more or less constant forward velocity in the beam.

From these results a simple one-dimensional model has been set up to obtain information about the reaction rates for the reactions in Eq. (2). This model, an extension of the model presented in Ref. 1, is based on sequential clustering reactions starting from an initial atomic hydrogen ion flux of 0.08 sccs[9] including dissociative recombination of the molecular species with electrons. Different silane flows were modeled (cf. Fig. 3). It is assumed that the silane density is homogeneous throughout the deposition chamber and proportional to the silane flow. The total ion flux at the position of the substrate holder is given by the probe measurements and it fixes more or less the directed velocity of the clusters due to the fact that the magnitude of dissociative recombination depends most critically on the time it takes to travel from the silane injection point to the substrate. The obtained directed velocity is about 900 m/s which is in good agreement with other experiments on a similar setup.[23] The relative distribution of the cationic clusters is determined from the mass spectra without distinguishing between the different numbers of hydrogen atoms present. Setting the reaction rate of the hydrogen ions with silane at 5×10^{-15} m^{3}s^{-1} [11] the reaction rates for the sequential reactions have been estimated by matching the calculated densities to the experimental values. It has turned out that the reaction rates obtained for the different silane flows are in relative good agreement despite the very simple model. The averaged reaction rates are shown in Fig. 4 where k_n denotes the reaction rate of a cluster ion containing n silicon atoms with silane.

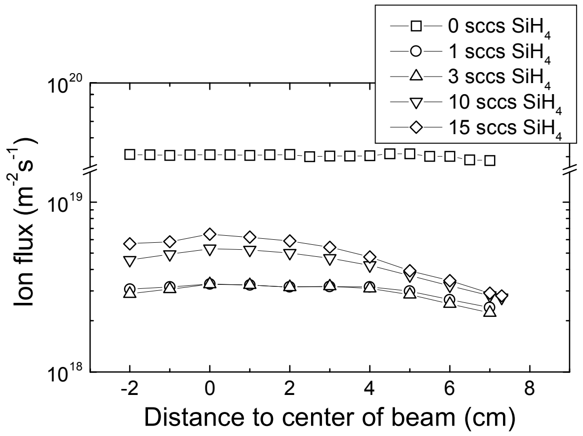

FIG. 3. Radial ion flux at 2 cm from substrate holder for different silane flows as obtained from Langmuir probe measurements.

Figure 4 shows that the reaction rates are in the range of 10^{-17}–10^{-16} m^{3}s^{-1} and that the rates do not depend critically on the number of silicon atoms present in the clusters. These near-collisional rates are in accordance with the ones suggested by Haller,[15] Weakliem,[13] and Kushner[24] and are about a factor 5–10 smaller than the Langevin rates.[11] They are, however, not in agreement with the rates proposed by Mandich and Reents.[3-6] From both ion-cyclotron resonance mass spectrometry at thermal energies and theoretical considerations they derived rates which span three orders of magnitude as the rates show a strong dependence on the number of silicon and hydrogen atoms present in the cluster and on their isomeric state. Moreover, they do not observe production of clusters containing more than six silicon atoms in their ion-silane reactions,[3-6] although such ions are observed in silane plasmas as shown in this paper as well as in others.[17-19] Possible causes of the differences between their observations and those in silane plasmas will be discussed below.

First of all, the experimental conditions between both cases are very different. In their ion-cyclotron resonance mass spectrometer the pressure is roughly six orders of magnitude lower than in silane plasmas and the only gas used is pure silane. The fact that they use mostly SiD_4 instead of SiH_4 is not expected to

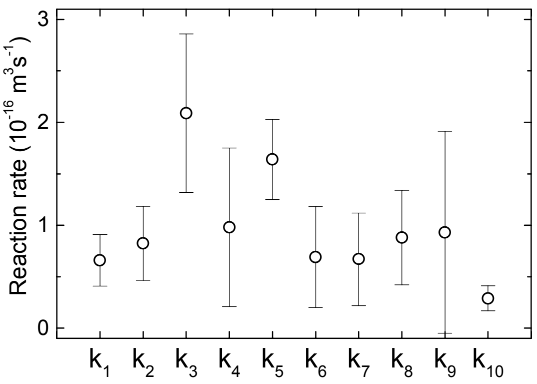

FIG. 4. Reaction rates for the sequential ion-silane reactions as determined from an one-dimensional model. For further explanation refer to the text.

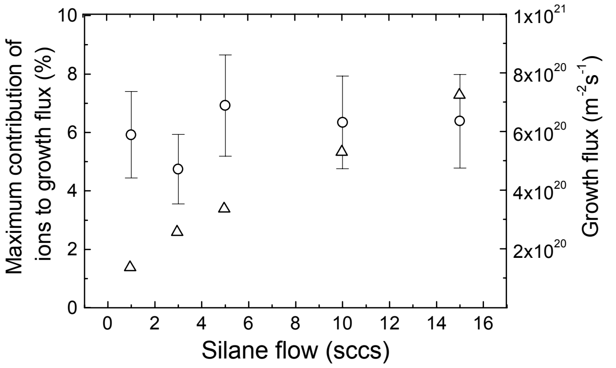

FIG. 5. Total silicon growth flux (Δ) and contribution of cationic clusters to growth flux (O) as a function of silane flow.

cause significant differences.[3] In silane plasmas on the other hand also silane radicals are present which can influence the clustering reactions.[21] Their lower abundance can possibly be compensated for by their higher reactivity. Furthermore, also polysilanes like disilane and trisilane are present in silane plasmas. Mandich and Reents show for example that reactions between silicon cluster ions and disilane can proceed to clusters with up to eight silicon atoms and then terminate.[25] Although this can explain the observation of cationic clusters with more than six atoms it would probably cause a sharper transition in the mass spectrum between the clusters with six and seven silicon atoms as silane is much more abundant. Another aspect is the influence of small amounts of water which are always present in processing silane plasmas. Mandich and Reents observed that the growth of ions is significantly enhanced and does not terminate for ions below 400 amu in mixtures of silane containing 7% water.[25] In this mixture, however, also some large ions containing oxygen atoms were observed. In the expanding plasma such amount of water is surely not present and the size and magnitude of cationic cluster did not change with the presence of silanol ions. The influence of water is therefore probably limited though it cannot totally be excluded.

Another aspect is the presence of higher kinetic energies and excited species in plasmas. The rates presented by Mandich and Reents apply to ground state reactions with silane at room temperature. Additional energy can possibly increase the ion-molecule reaction rates and overrule the bottle-necks observed as also suggested by Kushner.[24] It would for instance explain the observation of Weakliem *et al.* who found that at higher gas temperatures larger cluster ions were formed.[13] That additional energy can have an effect has already been concluded from the compactness and hydrogen poverty of the cationic silicon clusters in the expanding plasma. Mandich and Reents observed even intriguing effects in the reaction of hot side products, created by nonthermal energy species, with silane. Yet they expect the enhanced elimination of molecular hydrogen due to additional energy to lead finally to highly stable compact structures at limited size which are chemically unreactive with silane.[5] They do not expect large differences from the presence of vibrationally excited silane as concluded from an analogy with the reactions with disilane.[25] Nevertheless, a considerable influence of the presence of higher kinetic and internal energies cannot be excluded to our opinion. For example, in their case the sequential reactions terminate either at bare silicon clusters or at ions with a large number or hydrogen atoms created by association reactions with silane.[25] These reactions have a strong negative temperature dependence[4] and will therefore not occur in the expanding plasma. The reaction rates of the hydrogen poor clusters with silane are however not thoroughly investigated. It can therefore be concluded that the straightforward application of the reaction rates determined by techniques like ion-cyclotron resonance mass spectrometry in silane plasmas can be rather troublesome and can lead to erroneous results when any of the above mentioned aspects are neglected.

Finally, from the ion flux in Fig. 3 the contribution of the cationic clusters to the silicon growth flux has been calculated. This, as well as the total growth flux, is shown in Fig. 5. The total growth flux is determined from the growth rate and the silicon density in the film. The latter is derived from a relation between refractive index of the films and the silicon density.[26] The contribution of the cationic clusters to this growth flux is obtained by multiplying the ion flux with the average number of silicon atoms in the clusters as estimated from the mass spectra. As it is assumed that the clusters have unity sticking probability this is the maximum contribution cationic clusters can have to the growth flux.

Figure 5 shows that the maximum contribution of the ions is rather independent of the silane flow. Under the condition where device quality a-Si:H is deposited, i.e., with 10 sccs silane, the maximum contribution is about 6%. This relatively small contribution is not in contrast with the dominant contribution of SiH_3 to deposition. Nevertheless the cationic clusters can have a significant impact on the film quality. Their compactness can for example lead to disturbances in film stochiometry as they have no perfect tetrahedral bond coordination.[16] Also the electronic defect density, preferably on the order of 10^{-6}–10^{-7} of the film density, can be very sensitive for their incorporation as the clusters are hydrogen poor. Furthermore, it should be noted that the ion energy flux towards the film in the expanding plasma is relatively small due to the small self-bias (< 2 V). The absence of this energy flux can be one of the reasons that a higher substrate temperature is necessary to obtain solar grade material with the expanding argon-hydrogen-silane plasma. Another point of interest are the dissociatively recombined ions. When a significant fraction of cationic clusters recombines with electrons possibly large polysilane radicals are created which can have a similar impact on film growth as cluster ions. These aspects considered have also some implications for other remote plasmas. Depending on silane density and distance between plasma source and substrate holder the creation of relatively large silicon cluster ions cannot be neglected, even not when the ion or metastable fluence from the plasma source is relatively low.

IV. CONCLUSION

It is shown that cationic clusters are created in silane plasmas by sequential ion-molecule reactions with silane. In a plasma these reactions proceed at near-collisional rates rather independent of the number of silicon and hydrogen atoms present in the ions and even clusters larger than expected from ion-cyclotron resonance mass spectrometry studies can be created. The hydrogen content of the clusters is probably related to the kinetic energy of the species involved in the reactions. The cationic clusters can also have a significant impact at the film quality despite the fact that their maximum contribution to the growth flux is in the order of percents.

ACKNOWLEDGMENTS

The authors greatly acknowledge B. A. Korevaar and A. H. M. Smets for their contribution to the work and M. J. F van de Sande, A. B. M. Hüsken, and H. M. M. de Jong for their outstanding technical assistance. This work has been financially supported by The Netherlands Organization for Scientific Research (NWO), The Netherlands Agency of Energy and the Environment (NOVEM), and the Foundation for Fundamental Research on Matter (FOM-RG).

[1] W.M.M. Kessels, M.C.M. van de Sanden, and D.C. Schram, Appl. Phys. Lett. **72**, 2397 (1998).

[2] W.M.M. Kessels, R.J. Severens, M.C.M. van de Sanden, D.C. Schram, J. Non-Cryst. Solids **227-230**, 133 (1998).

[3] M.L. Mandich and W.D. Reents, Jr., J. Chem. Phys. **90**, 3121 (1989).

[4] M.L. Mandich, W.D. Reents, Jr., and K.D. Kolenbrander, J. Chem. Phys. **92**, 437 (1990).

[5] M.L. Mandich, and W.D. Reents, Jr., J. Chem. Phys. **95**, 7360 (1991).

[6] W.D. Reents, Jr., and M.L. Mandich, J. Chem. Phys. **96**, 4429 (1992).

[7] M.C.M. van de Sanden, J.M. de Regt, and D.C. Schram, Plasma Sources. Sci. Technol. **3**, 501 (1994).

[8] E.W. Peterson and L. Talbot, AIAA Journal **8**, 2215 (1970).

[9] W.M.M. Kessels, C.M. Leewis, M.C.M. van de Sanden, and D.C. Schram, J. Appl. Phys. **86**, 4029 (1999).

[10] M.C.M. van de Sanden, R.J. Severens, W.M.M. Kessels, R.F.G. Meulenbroeks, and D.C. Schram, J. Appl. Phys. **84**, 2426 (1998).

[11] J. Perrin, O. Leroy, and M.C. Bordage, Contrib. Plasma Phys. **36**, 1 (1996).

[12] I. Haller, Appl. Phys. Lett. **37**, 282 (1980).

[13] H. A. Weakliem, R.D. Estes, and P.A. Longeway, J. Vac. Sci. Technol. A **5**, 29 (1987).

[14] J.M.S. Henis, G.W. Stewart, M.K. Tripodi, and P.P. Gaspar, J. Chem. Phys. **57**, 389 (1972).

[15] I. Haller, J. Vac. Sci. Technol. A **1**, 1376 (1983).

[16] K. Raghavachari and V. Logovinsky, Phys. Rev. Lett. **55**, 2853 (1985).

[17] Ch. Hollenstein, A.A. Howling, C. Courteille, J.L. Dorier, L. Sansonnens, D. Magni, and H. Müller, Mater. Res Soc. Symp. Proc. **507**, 547 (1998).

[18] Ch. Hollenstein, A.A. Howling, C. Courteille, D. Magni, S. Scholz Odermatt, G.M.W. Kroesen, N. Simons, W. de Zeeuw, and W. Schwarzenbach, J. Phys. D **31**, 74 (1998).

[19] J.A. Theil and G. Powell, J. Appl. Phys. **75**, 2652 (1994).

[20] G.M.W. Kroesen, D.C. Schram, A.T.M. Wilbers, and G.J. Meeusen, Contrib. Plasma Phys. **31**, 27 (1991).

[21] H. Murakami and T. Kanayama, Appl. Phys. Lett. **67**, 2341 (1995).

[22] M.O. Watanabe, H. Murakami, T. Miyazaki, and T. Kanayama, Appl. Phys. Lett. **71**, 1207 (1997).

[23] M.G.H. Boogaarts, G.J. Brinkman, H.W.P. van de Heijden, P. Vankan, S. Mazouffre, J.A.M. van der Mullen, D.C. Schram, and H.F. Döbele, *Proceedings of the Eighth International Symposium, Laser-Aided Plasma Diagnostics* (Doorwerth, The Netherlands, 1997), p. 109.

[24] M.J. Kushner, J. Appl. Phys. **63**, 2532 (1988).

[25] W.D. Reents, Jr. and M.L. Mandich, Plasma Sources Sci. Technol. **3**, 373 (1994).

[26] W.M.M. Kessels, M.C.M. van de Sanden, R.J. Severens, L.J. Van IJzendoorn, and D.C. Schram, Mater. Res Soc. Symp. Proc. **507**, 529 (1998).

J. Vac. Sci. Technol. A 17 (4), 1531 – 1535 (1999).

Formation of cationic silicon clusters in a remote silane plasma and their contribution to hydrogenated amorphous silicon film growth

W. M. M. Kessels,[a] C. M. Leewis, M. C. M. van de Sanden,[b] and D. C. Schram

Department of Applied Physics, Eindhoven University of Technology, P.O. Box 513, 5600 MB Eindhoven, The Netherlands

The formation of cationic silicon clusters $Si_nH_m^+$ by means of ion-molecule reactions in a remote Ar-H_2-SiH_4 plasma is studied by a combination of ion mass spectrometry and Langmuir probe measurements. The plasma, used for high growth rate deposition of hydrogenated amorphous silicon (a-Si:H), is based on SiH_4 dissociation in a downstream region by a thermal plasma source created Ar-H_2 plasma. The electron temperature, ion fluence and most abundant ion emanating from this plasma source are studied as a function of H_2 admixture in the source. The electron temperature obtained is in the range of 0.1 to 0.3 eV and is too low for electron induced ionization. The formation of silicon containing ions is therefore determined by charge transfer reactions between ions emanating from the plasma source and SiH_4. While the ion fluence from the source decreases about a factor 40 when a considerable flow of H_2 is admixed in the source, the flux of cationic silicon clusters towards the substrate depends only slightly on this H_2 flow. This implies a strong dissociative recombination of silicon containing ions with electrons in the downstream region for low H_2 flows and it causes the distribution of the cationic silicon clusters with respect to the silicon atoms present in the clusters to be rather independent of H_2 admixture. The average cluster size increases however strongly with the SiH_4 flow for constant plasma source properties. Moreover, it leads to a decrease of the ion beam radius and due to this, to an increase of the ion flux towards the substrate, which is positioned in the center of the beam. Assuming unity sticking probability the contribution of the cationic clusters to the total growth flux of the material is about 6% for the condition in which solar grade a-Si:H is deposited. Although the energy flux towards the film by ion bombardment is limited due to the low electron temperature, the clusters have a very compact structure and very low hydrogen content and can consequently have a considerable impact on film quality. The latter is discussed as well as possible implications for other (remote) SiH_4 plasmas.

I. INTRODUCTION

The possibility to apply hydrogenated amorphous silicon (a-Si:H) successfully and at relatively low costs in devices such as thin film solar cells and thin film transistors by means of SiH_4 dissociation by a plasma, has initiated numerous studies to reveal the underlying plasma and surface chemical aspects of the film growth. In most of the work nowadays in this field, it is assumed that the dominant specie contributing to film growth is the silyl (SiH_3) radical. The dominance of SiH_3 is either concluded from experimental results,[1-4] in which the arguments are usually based on measured densities instead of net fluxes towards the substrate, or from more or less indirect deductions from other experiments.[5-8] Presently usually only little or even no attention is paid to the contribution of positive ions to the deposition process. In, e.g., the model for a-Si:H growth in rf and very high frequency, VHF discharges proposed by Gallagher *et al.*, Matsuda *et al.*, and Perrin *et al.*[4] no contribution of positive ions to film growth is included. Neglecting the contribution of positive ions is frequently based on the low electron density usually found in these types of plasmas. However in this reasoning it is passed over that the ions have presumably unity sticking probability[9,10] and that the ions can also contain more than one silicon atom.[11] Moreover, apart from this direct contribution to film growth, the positive ions can have also an indirect contribution. They have a much higher kinetic energy than radicals do as they are accelerated in the plasma sheath. This can lead to ion bombardment and, consequently, in possible film densification and/or growth site creation.[12] In the deposition of hydrogenated amorphous carbon (a-C:H) for example,

---

[a] Electronic mail: w.m.m.kessels@phys.tue.nl

[b] Electronic mail: m.c.m.v.d.sanden@phys.tue.nl

J. Appl. Phys. 86 (7), 4029 – 4039 (1999).

ions are even often expected to be inevitable for dense film growth.[13-15] Furthermore, Ganguly and Matsuda[16] and Kato *et al.*[17] have observed an increase in room temperature hole drift mobility in their material of 2 orders of magnitude compared to the conventional value when the ions have an energy between 23 and 24 eV. Recently, Hamers *et al.*[18,19] concluded from mass resolved ion energy measurements that the best structural properties, in terms of hydrogen bonding configuration and film density, are obtained above an ion threshold energy of 5 eV per deposited atom. Moreover, they estimated that the ion flux in a conventional rf/VHF SiH_4 discharge can at least account for 10% of the observed growth rate. Accordingly, the contribution of ions to a-Si:H film growth in SiH_4 plasmas is still matter of debate.

The contribution of ions to film growth has also been investigated in so-called remote plasmas. As a matter of fact these plasmas, in which plasma generation, plasma transport and film deposition are spatially separated, even facilitate the study of the flux of ions as well as of other reactive species towards the substrate. Theil and Powell[20] observed rather large positive silicon containing ions in 13.56 MHz and 2.45 GHz generated helium discharges in which SiH_4 was injected downstream. On the other hand, Jasinkski[10] reports only on positive ions containing one Si atom in a He-SiH_4 afterglow plasma created by a microwave discharge in pure helium. Assuming unity sticking probability for the ions Jasinkski estimates a contribution of 10% to the growth rate. In an expanding Ar-H_2-SiH_4 plasma, the remote plasma which is the subject of this article, also large positive silicon ions or, more appropriate, positive cluster ions have been observed.[21,22] This plasma is created by the so-called expanding thermal plasma technique and uses a thermal Ar-H_2 plasma to dissociate SiH_4 in a downstream region. The high efficiency plasma source, a cascaded arc, enables the use of high SiH_4 flows and solar grade a-Si:H can be deposited at a rate of 10 nm/s.[23,24] Apart from the interesting properties as good film quality at a high growth rate, the technique is well suited for studies concerning a-Si:H film growth. From such studies it was concluded that in this plasma a-Si:H deposition is dominated by SiH_3 radicals.[8] However, we have to admit that the influence of positive ions on the SiH_4 dissociation and film growth in our deposition technique was formerly dealt with on an inaccurate basis: neglecting ion-molecule reactions and expecting that silane ions created by a charge transfer reaction between hydrogen and/or argon ions with SiH_4 would immediately recombine dissociatively with electrons it was estimated that the total contribution of species created by ionic processes was about 6% of the growth rate and mainly in the form of SiH_x radicals ($x<3$) and Si_2H_y radicals ($y<6$).[8]

Recent experiments revealed that positive ions can possibly contribute significantly to film growth as ions containing several Si atoms were observed.[21] Their formation, attributed to sequential ion-molecule reactions, has already been addressed in another paper[22] as well as their hydrogen poverty, the reaction rates for the ion-molecule reactions, and the discrepancy between these rates and rates determined from ion cyclotron resonance mass spectrometry. In this article more data obtained from ion mass spectrometry and Langmuir probe measurements will be given for a variety of plasma conditions. The Langmuir probe measurements and the calculated ion fluxes replace thereby previous measurements[25,26] in which the nature of the ions in the plasma was not revealed and which were performed for less appropriate plasma conditions with respect to film quality obtained. Furthermore the contribution of the cationic clusters to a-Si:H film growth is determined emphasizing the implications of the ion chemistry in SiH_4 plasmas.

II. EXPERIMENT

A. Deposition setup

The expanding thermal plasma setup consists of two parts: a thermal plasma source, a cascaded arc, and a low-pressure deposition chamber. The cascaded arc consists of three cathodes, a stack of 10 copper plates with a central bore of 4 mm, and an anode plate with a conical shaped nozzle. All parts are water cooled and made of copper except the cathode tips, which are of tungsten with 2% lanthanum. The plates are separated by boron-nitride and PVC spacers. Under the conditions of interest, pure Ar or a mixture of Ar and H_2 is introduced into the arc. The Ar flow is fixed at 55 sccs (1 standard cubic centimeter per second corresponds to 2.5×10^{19} particles per second) and the H_2 flow is varied between 0 and 15 sccs (purity of both gases >99.9995%). The dc discharge is current controlled at 45 A and the voltage over the arc ranges from 70 to 140 V depending on the H_2 concentration in the mixture. The pressure in the upstream part of the arc is about 400 mbar and varies only slightly with gas mixtures used. Typical arc plasma parameters are an electron density of about 10^{22} m^{-3} and an electron temperature of about 1 eV. Due to the high electron density there is a good energy coupling between the electrons and the heavy particles, which leads to a high heavy particle temperature (~1 eV).[27] As a result of the high pressure gradient between the plasma source and the deposition chamber (at 0.20 mbar) the plasma expands supersonically from the nozzle into this chamber. After a stationary shock front at about 5 cm behind the nozzle, the plasma expands subsonically and the

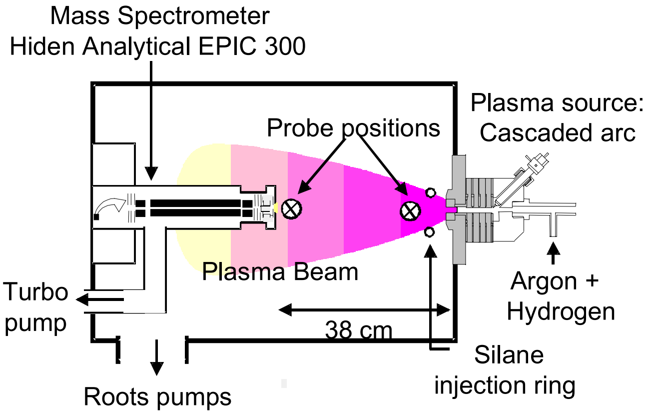

FIG. 1. Expanding thermal plasma deposition setup. The axial positions of the Langmuir probe are indicated. The mass spectrometer is situated at the usual position of the substrate holder.

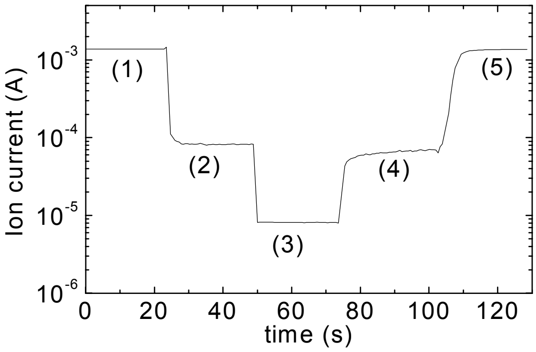

FIG. 2. Time-dependent ion current scan with a single cylindrical probe at -10 V for Ar plasma (1) and (5), Ar-H_2 plasma (2) and (4) and Ar-H_2-SiH_4 plasma (3). The gas flows used are 55 sccs Ar, 10 sccs H_2 and 10 sccs SiH_4.

tron temperature and electron density are heavily reduced in comparison with those in the arc.[28] As will be shown in this article, the electron temperature is in the range of 0.1 to 0.3 eV and the electron density in the range of 10^{16}–10^{19} m^{-3} depending on the gas mixture used. The typical directed velocity of the particles downstream is 1000 m/s.[29] Pure SiH_4 (Praxair Silane Ultraplus, purity >99.995%) is admixed to the expanding plasma by a stainless steel injection ring located at 5 cm from the nozzle. The injection ring has a diameter of 7.5 cm and contains 8 holes with a diameter of 1 mm each. Throughout this article, SiH_4 flows in the range of 0–25 sccs are used. All flows are controlled by mass flow controllers. The deposition chamber has a volume of 180 ℓ and is pumped by a stack of two roots blowers and one forepump. The pumping capacity at the reactor chamber is ~1500 m^3/h for a pressure of 0.20 mbar. The residence time of stable particles in the low-pressure chamber is typical 0.4–0.5 s as concluded from mass spectrometry measurements. Overnight the reactor is pumped by a 450 ℓ/s turbopump reaching a base pressure of 10^{-6} mbar. Films are deposited on a substrate holder located at 38 cm from the arc exit, which is replaced by a mass spectrometer (see Sec. II C) for the current study.

B. Langmuir probe measurements

Cylindrical single and double Langmuir probe measurements have been applied to determine the ion and electron density, the electron temperature and, where possible, the effective mass of the ions in the downstream region (i.e., in the deposition chamber). The probes consist of tungsten wires with a diameter of 0.2 mm and a length of 3 mm protruding from a ceramic (Al_2O_3) tube. The two probes in the double probe configuration are separated about 3 mm. The voltage on the single probe, or between the probes in the double probe, is swept between -10 and 10 V with a step size of 0.05–0.2 V by means of a Keithley 2400 source-measure unit.

In the Ar-H_2 plasma, single probe measurements have been performed at axial positions of ~6 cm from the arc nozzle and at ~2 cm from the substrate (see Fig. 1). At both positions, radial profiles of the electron and ion density are obtained by moving the probe in radial direction. The plasma sheath thickness in the plasma under investigation is in the range 10^{-4}–10^{-5} m which means that the sheath is collisionless (ions' mean free paths ~10^{-1}–10^{-3} m). The thin sheath limit,[30] which has been assumed in previous studies using cylindrical probes,[8,31] is not completely valid within the total range of the above mentioned electron densities. Therefore the probe measurements have not been analyzed by applying linear extrapolation of the saturation currents to plasma potential, but by the procedure proposed by Peterson and Talbot.[32,33] This yields somewhat lower electron densities than reported in previous studies for similar plasma conditions.[8] The procedure gives the electron and ion saturation current at plasma potential, the electron temperature, the plasma potential, and the ratio of probe radius and Debye length. The electron density is calculated from the electron saturation current at plasma potential.[34] From the ratio of electron and ion saturation current the effective ion mass is calculated, giving an indication which ions are dominantly present in the plasma.[34] The latter procedure has been verified in different types of plasmas as Ar, (Ar-)H_2, Ar-D_2, (Ar-)N_2[34,35] by comparison with ion mass spectrometry.

In the Ar-H_2-SiH_4 plasma only double probe measurements have been performed. The reason is that the electron saturation current collected by a single probe cannot be measured appropriately due to the formation of a resistive layer on the probe during deposition. The a-Si:H film deposited on the probe has a limited conductivity, which can generate a considerable voltage drop over the film. In simplified terms, the voltage V_{probe} applied to the probe is lowered by the product of current I drawn and the resistance R of the film, i.e., the voltage on the surface exposed to the plasma is equal to V_{probe}-IR. This means that depending on the current drawn and the resistivity of the film, the voltage on the surface exposed to the plasma can deviate considerably from the voltage applied.[30] This is of course most pronounced at higher currents, like the electron saturation current. The ion saturation current does not necessarily suffer from a voltage drop over the film, as it is relatively small. This was already addressed by Mosburg *et al.*[36] They showed that the voltage drop over the film at low currents can be insignificant due to a decreased resistivity of the a-Si:H caused by irradiation with photons, and/or by an increased probe temperature. The latter is easily obtained in the expanding thermal plasma as the gas temperature is relatively high compared to other plasmas.[37,38] Whether the ion saturation current does not suffer from a serious voltage drop has been checked by performing time-resolved measurements at a fixed negative potential of -10 V in single probe configuration. Starting with a clean probe the current is measured in an Ar plasma to which, successively, H_2 and SiH_4 are introduced. Subsequently the SiH_4 is removed and then the H_2. In Fig. 2 such a scan is shown and it is clear that the ion current is constant for all conditions including the plasma in which deposition takes place. Moreover, when the SiH_4 is switched off the current rises immediately to almost the usual level of the current in an Ar-H_2 plasma. This shows that the current in the plasma with SiH_4 is not limited by the deposited film. However the fact that it does not rise immediately to the full current drawn in the Ar-H_2 plasma (before admixing SiH_4) shows that the probe suffers slightly from the a-Si:H film in that case. This time-dependent scan was checked for all conditions, while in between the probe was cleaned. The cleaning of the probes was performed by applying +10 V to the probes in an Ar plasma for 30 s resulting in a large current of about 0.7 A. This cleaning procedure has been executed before every measurement. The currents drawn with the double probe and in the time-dependent measurements showed good agreement. The double probe measurements were again analyzed by an appropriate procedure proposed by Peterson and Talbot,[32] yielding the electron temperature, the ion saturation current at plasma potential, the voltage difference between floating and plasma potential, and the ratio of probe radius and Debye length. Comparison of single and double probe measurements in Ar and Ar-H_2 plasmas revealed an agreement in electron density within 15%. Analysis of double probe measurements yields no information on the effective mass of the ions, however, the latter is required to analyze the double probe measurements. Information on the effective mass of the ions in SiH_4 plasmas is therefore deduced from ion mass spectrometry as will be dealt with in more detail in Sec. II C. The total error in ion saturation current is estimated at 25% as also suggested by the reproducibility measurements. The error in electron density is larger as it is relatively more sensitive to the effective ion mass. Fortunately, knowledge on the ion saturation is sufficient to determine the flux of silicon containing ions to the a-Si:H film as will be shown in Sec. III.

C. Ion mass spectrometry

To obtain information on the different ions present in the plasma ion mass spectrometry has been applied at the position of the substrate holder. The mass spectrometer used is a Hiden Analytical EPIC 300,[39] which outer geometry is adjusted such that it roughly resembles the geometry of the substrate holder. Gas extraction takes place by a 50 μm thin, knife-edged extraction orifice with a diameter of 50 μm. The ionizer, located just behind the orifice, is switched off in the present study. The mass filter is preceded and followed by an only rf driven pre- and postfilter. The mass range of the mass spectrometer is 300 amu. Mass filter transmitted particles are finally accelerated to a DeTech 415 channeltron with the first-dynode voltage set at -1200 V and which is operated in the pulse-counting mode. The masses are scanned in steps of 0.02–0.1 amu and the integration time at every step is typically 100 ms. The mass spectrometer is differentially pumped by a turbopump leading to a pressure of 5×10^{-7} mbar during processing (reactor pressure ~0.20 mbar) and a base pressure of 10^{-9} mbar.

The diameter of the orifice for gas extraction is much smaller than the mean free path of the species present in the plasma and therefore the flow of particles into the mass spectrometer is effusive. Only for a pure Ar plasma the thickness of the plasma sheath does not exceed half the orifice diameter and therefore only in this case the plasma in front of the orifice as well as the ion extraction can be disturbed to some extent. The physical acceptance angle of the mass spectrometer for the ions is limited to 12.7° with respect to the normal of the orifice flange. During processing the extraction hole can be become plugged due to deposition and therefore a plasma clean is applied regularly using an Ar-CF_4 plasma followed by an Ar-H_2 plasma.

A problem with the interpretation of mass spectrometry data is mass discrimination by the mass spectrometer as both the mass filter transmittance and detector efficiency are usually mass dependent.[40] The transmittance of the mass filter was estimated for masses up to 132 amu by comparing an ion spectrum with a so-called "rf-only" spectrum.[41-43] In the 'rf-only' case the dc voltage on the mass filter rods is omitted and the mass spectrometer acts as a high pass filter. Although only information up to 132 amu was obtained and although the data showed considerable scattering, it turned out that the transmittance of the mass filter is best estimated by a decrease with ion mass M proportional to $M^{-1/2}$. This rather small mass discrimination can possibly be attributed to the presence of a pre- and postfilter reducing the influence of the dc fringing fields. Furthermore, it turned out that the detection efficiency of the channeltron used decreases approximately in a similar way with mass.[44] This leads to an overall mass discrimination proportional to M^{-1}. Throughout this article mass spectrometry data is given uncorrected for this mass discrimination unless stated otherwise.

Another complication in this study is the presence of a signal at the spectrometers detector generated by plasma photons: the cascaded arc plasma source, which produces a large photon flux covering the total spectral range,[45] is perfectly aligned with the mass spectrometers orifice (see Fig. 1). This leads to a background signal in the mass spectra (see Fig. 6) which depends on the plasma created in the cascaded arc (the photon signal decreases for increasing H_2 admixture). For the present case it is much smaller than the signals created by plasma ions. Therefore it does not disturb the measurements and in fact enables monitoring the plugging of the gas extraction orifice by a-Si:H deposition.

III. RESULTS

A. Argon-hydrogen plasma

Different plasmas generated by the cascaded arc have been investigated thoroughly by spectroscopic diagnostics[28,29,46-49] and Langmuir probe measurements[31,34,35] as they are used to dissociate precursor gases like SiH_4 for thin film deposition. In this section, the knowledge of the Ar and Ar-H_2 plasma is enlarged by applying Langmuir probe measurements and ion mass spectrometry to the specific conditions used for a-Si:H deposition. Furthermore, the probe measurements have been analyzed by a more appropriate and accurate method in comparison with a previous study[8] (see Sec. II B). The electron temperature obtained by the single probe at 6 cm from the arc exit is given in Fig. 3(a) and is about 0.3 eV for pure Ar and decreases for increasing H_2 admixtures. This is in good agreement with Thomson scattering results.[28,46-48] The low electron temperature arises from the fact that no power is coupled to the plasma in the downstream region and it makes electron induced ionization of the atomic and molecular species in this region improbable.[8] The plasma is therefore recombining and this means that the ion fluence in the downstream region is totally determined by the ion fluence emanating from the arc. Ionization in the downstream region occurs by means of charge transfer reactions between ions emanating from the arc and the species downstream like SiH_4.[8] In order to investigate the formation of silicon containing ions, the ion fluence and the type of ions emanating from the arc have been determined.

The total ion fluence, expressed in standard cubic centimeters per second, is given in Fig. 3(b). It has been derived by integrating Gaussian fits applied to the radial electron density profiles at an axial position of 6 cm from the arc exit and assuming a directed velocity of the ions of 1000 m/s.[29] Electron density profiles are given in Fig. 4 for an Ar plasma and an Ar-H_2 plasma with 10 sccs H_2. The expansion of the plasma is clearly observable: at 6 cm from the arc the electron density shows a clear Gaussian profile, whereas nearby at 2 cm from the substrate holder the electron densities are smeared out due to expansion. They are only slightly peaked at the source axis. The electron densities for the pure Ar plasma show a good correspondence with Thomson scattering[28,49] after correction for differences in pressure. The accuracy of the ion fluence is mainly limited by the accuracy of the Gaussian fits applied and by the assumptions about the ion directed velocity. Furthermore, this method has also been applied in Ref. 8, although less appropriate analysis of the Langmuir probe data (see Sec. II B) lead to a too high ion fluence in that case (up to ~50%).

In agreement with earlier observations the ion fluence decreases strongly for increasing H_2 flow due to charge transfer and dissociative recombination reactions.[47] The ion fluence decreases less drastically as suggested by electron densities determined at the plasma source axis due to a slight increase of the width of the profiles with increasing H_2 flow. The latter can be understood from Fig. 5(a), which shows the effective mass of the ions as obtained from the ratio of electron and ion saturation current. For pure Ar the ion mass is equal to about 40 amu corresponding to Ar^+. For increasing H_2 admixture, the effective ion mass decreases, finally down to about 1 amu corresponding to H^+. This behavior is confirmed by ion mass spectra, obtained at an axial position of 38 cm, as shown in Fig. 5(b). The ArH^+ present in the spectrum when H_2 is admixed is created by associative charge exchange between Ar^+ and H_2.[47]

In summary, it can be concluded that for a pure Ar plasma the ion fluence is large and that the dominant ion is Ar^+. The dissociation and ionization of the SiH_4 is therefore governed by Ar^+ emanating from the arc leading to a high dissociation degree.[8] It should be noted that the argon metastable density is of little importance,[8] because the metastable density is about a

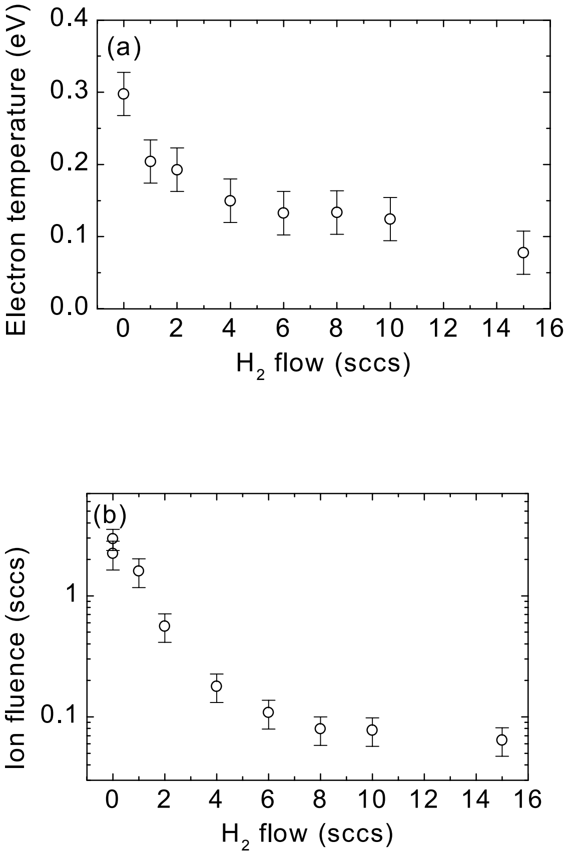

FIG. 3. (a) Electron temperature in the downstream region and (b) the ion fluence emanating from the arc determined at 6 cm from the arc exit for an Ar flow of 55 sccs and varying H_2 flow.

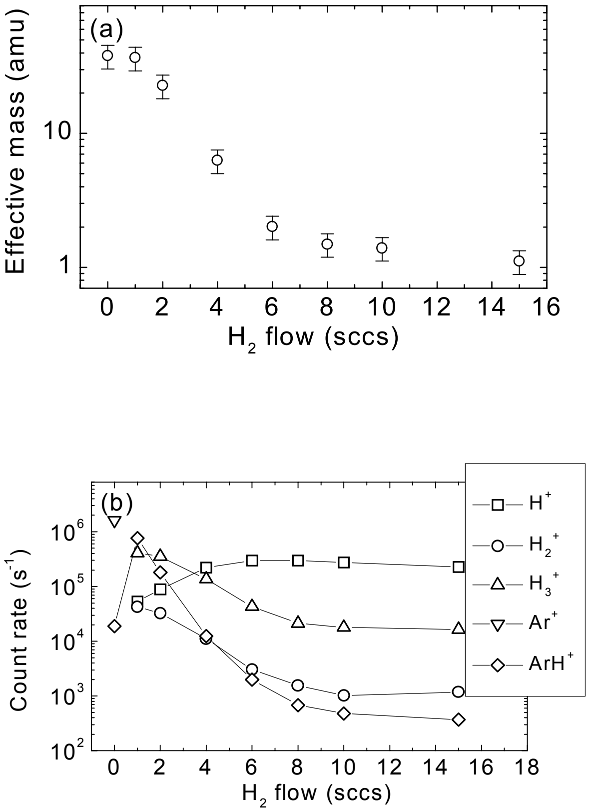

FIG. 5. (a) Effective mass (in amu) of ions emanating from the arc determined from the ratio of electron and ion saturation current and (b) ions measured by mass spectrometry at a distance of 38 cm from the arc exit for different H_2 flows.

factor of 10 lower than the ion density.[50] When H_2 is admixed in the arc the most abundant ion changes from Ar^+ or ArH^+ to H^+, while at the same moment the ion fluence is strongly reduced. Subsequently, for larger H_2 flows the dissociation of SiH_4 is therefore not dominated by ions but by the large fluence of H atoms emanating from the arc leading to an overall smaller dissociation degree of SiH_4.[8] However for the formation of silicon containing ions the relative small ion fluence under these conditions is still important as will be shown in Sec. III B.

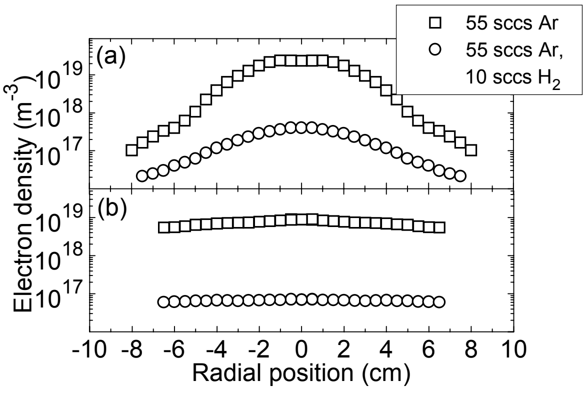

FIG. 4. Radial profiles of electron density determined at (a) 6 cm from the arc exit and (b) 2 cm from the substrate.

B. Argon-hydrogen-silane plasma

As already reported, adding SiH_4 to the Ar-H_2 plasma leads to the observation of large and hydrogen-poor positive silicon ions as shown in Fig. 6.[21,22] These ion mass spectra consist of raw data without any correction for mass discrimination. In the spectra the signal generated by plasma photons can be clearly seen. Furthermore, ion peaks are observed around mass 47 due to silanol ions $SiH_nOH_2^+$ ($0 \leq n \leq 3$). The oxygen in these ions probably comes from contamination as at first the deposition chamber was cleaned with an Ar-CF_4-O_2 plasma. After omitting O_2 in the gas mixture, silanol ions were hardly observable.

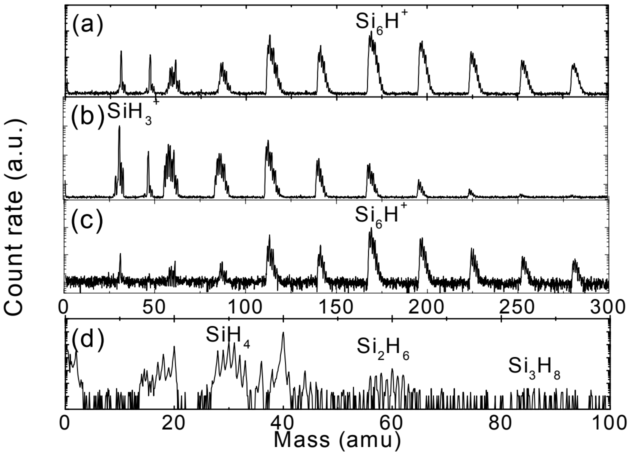

FIG. 6. Mass spectra for different SiH_4 and H_2 flows: ion spectrum for (a) 10 sccs SiH_4 and 10 sccs H_2, (b) 3 sccs SiH_4 and 10 sccs H_2, (c) 10 sccs SiH_4 and 3 sccs H_2 (most abundant ions are indicated), (d) neutral mass spectrum showing SiH_4 and polysilanes for plasma with 10 sccs SiH_4 and 10 sccs H_2.

To draw conclusions about the relative abundance of ions throughout different plasma conditions and to avoid problems by day-to-day changes in the absolute count rates so-called multiple-ion-detection (MID) scans have been performed. This means that the most abundant ion within every major peak was selected and the combination of these masses was monitored as a function of time wherein the plasma conditions were varied. Changes of the relative distribution of hydrogen within the different clusters with plasma conditions have been neglected, justified by the ion mass spectra. Furthermore, corrections have been applied for decreasing signals due to plugging of the gas extraction orifice. A finally obtained multiple-ion-detection scan is given in Fig. 7 as a function of SiH_4 flow at a constant H_2 flow of 10 sccs.

From Fig. 6(a), 6(b) and 7 it is very clear that the cluster size increases with increasing SiH_4 flow and consequently downstream SiH_4 density. For low SiH_4 flows, mainly clusters with only a few Si atoms are observed and their signals decrease drastically when the SiH_4 flow is increased. On the other hand, the signals due to clusters containing six or more Si atoms increase rapidly. Unfortunately, the mass range of the mass spectrometer limits the observation of the cluster ions for large SiH_4 flows.

The results of Fig. 6 and 7 confirm the earlier proposed reaction pathway for the formation of cationic silicon clusters under the plasma conditions considered, i.e., the ion-molecule chain reactions[21,22]

$$Si_nH_m^+ + SiH_4 \rightarrow Si_{n+1}H_p^+ + qH_2, \tag{1}$$

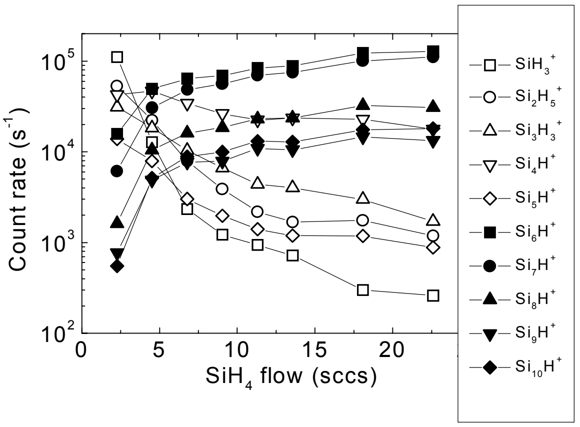

FIG. 7. Multiple-ion-detection scan as a function of SiH_4 flow for a H_2 flow of 10 sccs.

with $n \geq 1$ and $m+4 = p+2q$, neglecting endothermic reactions leading to the formation of H atoms.[51] The possibility that the cluster ions are created by ionization of polysilanes present in the plasma can be ruled out as only a small amount of Si_2H_6 and a hardly observable amount of Si_3H_8 are present in the plasma beam [see Fig. 6(d)]. The sequential ion-silane reactions of Eq. (1) are initiated by Ar^+ or H^+ emanating from the arc (see Sec. III A). These ions undergo charge transfer reactions with SiH_4 admixed by ring injection

$$Ar^+ + SiH_4 \rightarrow SiH_n^+ + mH_2 + pH + Ar \tag{2}$$

with $n+2m+p = 4$ and, respectively,

$$H^+ + SiH_4 \rightarrow SiH_n^+ + mH_2 + pH, \tag{3}$$

with $n+2m+p = 5$. For reaction (2) the reaction rates are still subject of debate but in the order of 10^{-16}–10^{-17} m^3s^{-1}, leading probably dominantly to ions with $n=3$.[52] For reaction (3) only a reaction rate is proposed for the reaction leading to ions with $n=3$ which is 5×10^{-15} m^3s^{-1}.[52] Reaction rates for the sequential ion-molecule reactions have been estimated from a simple one-dimensional model. It revealed near-collisional rates (10^{-16}–10^{-17} m^3s^{-1}), which are rather independent of silicon and hydrogen content of the clusters.[22] However Fig. 7 indicates that the ion-molecule reactions of Eq. (1) cannot be as straightforward as proposed and that also another kind of reaction must take place. This is suggested by the remarkable fact that the count rate due to clusters containing four Si atoms decreases only slightly with increasing SiH_4 flow, whereas the count rate due to clusters containing five Si atoms behaves rather similar to the clusters containing less than four Si atoms. For the moment no information is available on a underlying reaction and no conclusive information can be distracted from fundamental ion-molecule reaction studies, e.g.,

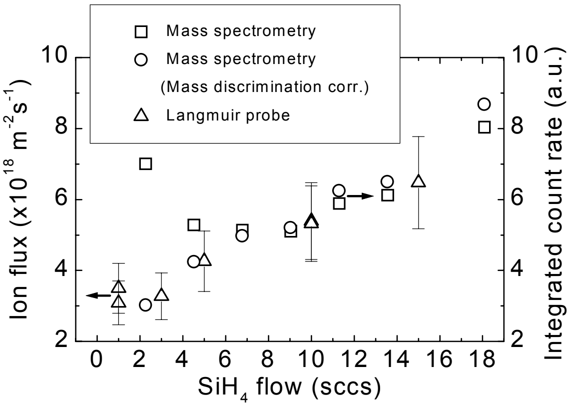

FIG. 8. Ion flux as obtained from Langmuir probe measurements and mass spectrometry (in arbitrary units) for a H_2 flow of 10 sccs and a varying SiH_4 flow.

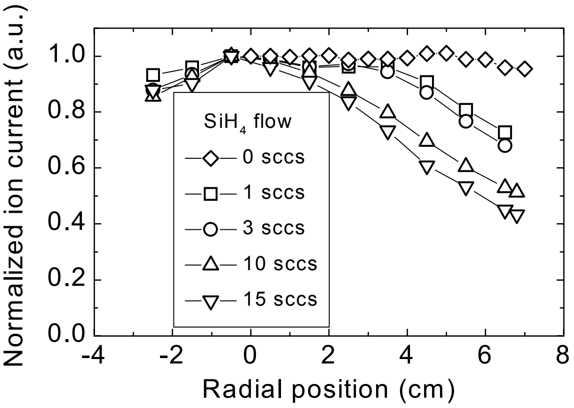

FIG. 9. Normalized radial scans of ion current for different SiH_4 flows at 2 cm in front of substrate holder. The ion current scan for the Ar-H_2 plasma (55 sccs Ar, 10 sccs H_2) is given for comparison.

performed by Mandich and Reents,[53] as discussed in Ref. 22. Therefore, a computer code is applied to obtain more insight.[54]

Quantitative information on the total ion flux arriving at the substrate has been obtained from Langmuir probe measurements (see Sec. II B). The ion flux towards the substrate as a function of SiH_4 flow is given in Fig. 8. Also the total sum of the count rates (in arbitrary units) of Fig. 7 is displayed for a SiH_4 flow up to about 15 sccs. For larger SiH_4 flows cluster ions containing more than 10 Si atoms are probably very important. Apart from the simple integrated count rate, the integrated count rate with a correction for the overall mass discrimination of the mass spectrometer is also shown. Despite the doubts about the accuracy of this correction, it shows a much better correspondence with the probe data. Both methods show an increase of ion flux towards the substrate for increasing SiH_4 flow. As the initial ion fluence is independent of the amount of SiH_4 injected, at first sight the difference could be accounted for by differences in recombination rates of the different cluster ions with electrons. However, another effect becomes clear from radial scans of the single Langmuir probe in front of the substrate holder. Fig. 9 shows the radial ion current scans normalized to their center value for different SiH_4 flows injected. It is clear that the ion current scans are profiled and that the width of the profiles decreases for increasing SiH_4 flow. It has been carefully checked that the observed profile is not due to probe contamination. From the profiles and from a comparison with the scans obtained in Ar(-H_2) plasmas (see Fig. 4), it is suggested that the width of the ion current profiles is determined by the mass of the ions present in the plasma. For an Ar-H_2 plasma with H^+ as dominant ion, the ion current is not significantly peaked. The current profiles for small SiH_4 flows have about a similar width as the ion current profile in a pure Ar plasma, whereas the profiles for larger SiH_4 flows and consequently large cluster ions are considerably more pronounced. An increase of ion current due to the slightly increasing pressure with SiH_4 flow appeared to be insignificant. This leads to the conclusion that the expansion of the ion beam is limited by the outward diffusion of the ions. Hereby the directed velocity of the ions towards the substrate, estimated at 900 m/s,[22] is inevitably coupled to the one of the neutral species.[29] When, for example, both the diffusion velocity as well as the directed velocity would scale with the ion mass no difference in profile width should be observed.

The ion flux towards the substrate as a function of H_2 flow admixed in the arc is given in Fig. 10. The ion flux shows a slight decrease for increasing H_2 flow. Furthermore, MID-scans for varying H_2 flow (data not shown) yield that the relative abundance of the ions does not considerably change with H_2 flow. This is also suggested by radial scans of the ion current, similar to those in Fig. 9, which show no significant dependence of the profile width on the H_2 flow. This fact, which leads to an almost constant average ion mass, prevents us from drawing conclusions about the spectrometers mass discrimination correction in this case. The slight decrease of the ion flux and the rather similar mass spectra for all H_2 flows are surprising as the ion fluence from the arc decreases drastically when H_2 is admixed [see Fig. 3(b)] and the dominant ion emanating from the arc changes from Ar^+ or ArH^+ to H^+ (see Fig. 5).[55] It can be explained by a competition of the ion-molecule reactions (1) with dissociative recombination reactions of the ions with electrons:

$$Si_nH_m^+ + e \rightarrow Si_nH_p + qH + rH_2 \qquad (4)$$

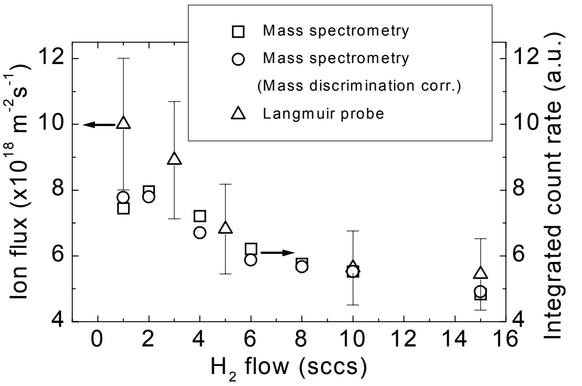

FIG. 10. Ion flux as obtained from Langmuir probe measurements and mass spectrometry (in arbitrary units) for a SiH_4 flow of 10 sccs and a varying H_2 flow.

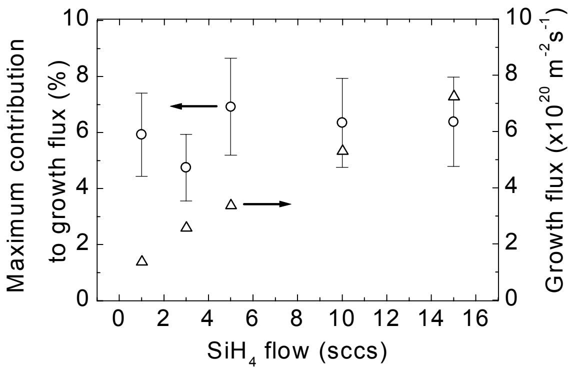

FIG. 11. Total growth flux and maximum contribution of cationic silicon clusters to this growth flux as a function of SiH_4 flow (10 sccs H_2).

with $p+q+2r = m$ and whereby in fact it is not excluded that the silicon cluster breaks apart. Analogous to hydrocarbon ions, the reaction rate of dissociative recombination is estimated at $10^{-13}T_e^{-1/2}$ (in m^3s^{-1} with T_e the electron temperature in eV),[52] while the rate can possibly increase slightly with ion size.[56] Depending on the proportion of this reaction rate to the reaction rates for the ion-molecule reactions and on the proportion of the density of electrons to the density of SiH_4 either dissociative recombination or ion-molecule reactions are more favored. This means that at high electron density, i.e., for a low H_2 flow in the arc, first dissociative recombination is more probable and when the electron density is decreased to a sufficient extent by recombination, the ion-silane reactions get as important. This most probably causes the apparent small influence of H_2 admixture in the arc on the ion spectrum [see Fig. 6(a) and 6(c)], although the amount of ions emanating from the arc is strongly changed. The recombination takes presumably place in the initial region where SiH_4 is admixed immediately after charge transfer with Ar^+ or H^+ has occurred by the reaction

$$SiH_3^+ + e \rightarrow SiH_n + pH + qH_2 \qquad (5)$$

with $n \leq 2$ and $n+p+2q = 3$. The radicals created in this way are very reactive both with SiH_4 as with surfaces.

The electron temperature and ion density in the depositing plasma have also been determined from the Langmuir double probe measurements, yet with limited accuracy. The electron temperatures obtained are about 0.3 eV for the H_2 flow series. For the SiH_4 flow variation it is in the range of 0.2–0.3 eV, with the electron temperature increasing slightly with SiH_4 flow. The electron density is in the order of 10^{16} m^{-3} and shows roughly the same trend as the ion fluxes in Figs. 8 and 10. For all SiH_4 flows the electron density is smaller than for the plasma without SiH_4, despite a smaller beam radius for the conditions with SiH_4. This can be attributed to dissociative recombination of the cluster ions with electrons [Eq. (4)].

From the ion flux towards the substrate,[57] the contribution of the cationic clusters to a-Si:H film growth in the expanding thermal plasma can be determined. To calculate this contribution in terms of number of Si atoms deposited, the ion fluxes have to be multiplied by the average number of Si atoms in the clusters. These averages have been estimated from ion mass spectra as given in Fig. 6. In this reasoning, it is essential that hydrogen ions do not contribute significantly to the ion flux measured by the Langmuir probe. Under any condition, hydrogen ions have not been observed in ion mass spectra for SiH_4 plasmas. This was checked by changing the admixed H_2 for D_2, neither showing a peak corresponding to deuterium ions.

To calculate the contribution of the cationic clusters, knowledge about their sticking probability is also necessary. As no data is available yet, unity sticking probability is assumed following the literature.[9,10] For this reason the contribution calculated and depicted in Figs. 11 and 12 is called the maximum contribution of the cluster ions to film growth. In Fig. 11 and 12 the growth fluxes obtained at a substrate temperature of 400 °C are also shown, i.e., the net flux of Si atoms contributing to growth and leading to the deposition rate. The growth flux is calculated by the product of deposition rate (in the range of 2–60 nm/s) and silicon density in the film obtained for the particular plasma condition.[58]

The maximum contribution of the cationic silicon clusters ranges from 4 to 7% for varying SiH_4 flow (see Fig. 11) and from 5 to 9% for varying H_2 flow (see Fig. 12). The contribution is rather independent of both the SiH_4 and H_2 flow. The latter case is again surprising because for no or small H_2 admixture in the arc the ion fluence into the chamber is very large and the dissociation is mainly governed by charge transfer reactions with the Ar^+ and ArH^+ ions emanating from

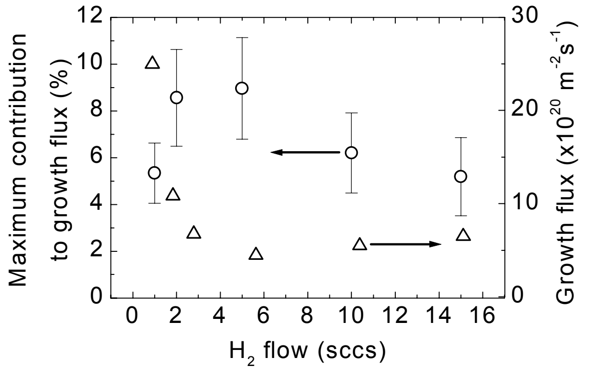

FIG. 12. Total growth flux and maximum contribution of cationic silicon clusters to this growth flux as a function of H_2 flow (10 sccs SiH_4).

the arc. The H atom fluence is still low under these conditions and the charge transfer reactions have a relatively high reaction rate compared to the reaction rate of H atoms with SiH_4 as well.[8] So the peculiar situation occurs that a high ion fluence from the arc is used for efficient SiH_4 dissociation, consequently leading to a high growth rate but with only a relatively small contribution of positive ions. As already mentioned this requires a strong dissociative recombination of molecular ions finally creating very reactive radicals and leading presumably to the rather poor film properties (e.g., low film density) obtained at low H_2 flows. The best material so far has been obtained at conditions (H_2 and SiH_4 flow both 10 sccs) in which the film growth is dominated by SiH_3 radicals[8] and where the cluster ions have a maximum contribution of about 6%. The a-Si:H obtained under this condition fulfills the demands for its application in thin film solar cells.[23,24] The impact of the cationic clusters on the film quality will be discussed in Sec. IV, but it is already mentioned that the energy flux of the clusters to the film in the expanding thermal plasma is limited. Due to the low electron temperature the difference between plasma potential and floating potential is only 1.5–2 V and the ions are therefore not highly energetic when they hit the surface in contrast with, e.g., ions in rf SiH_4 plasmas.[16,18,19]

IV. DISCUSSION

In Sec. III it is shown that the maximum contribution of the cationic silicon clusters to the growth flux is in the range 4%–9% for the conditions investigated. As already mentioned, especially the fact that the contribution is rather independent of the H_2 flow is very interesting: the ion fluence emanating from the source is heavily depending on the H_2 flow and for no or small H_2 flows the initial chemistry is totally determined by this ion fluence. This apparent contradiction has been explained by dissociative recombination reactions, Eq. (4) and in particular, Eq. (5). These reactions are favored over clustering as long as the electron density is high. Now it is interesting to examine what happens with the reaction products created by this dissociative recombination as they are in fact also generated by ion-silane reactions. When a silane ion immediately recombines with an electron most probably very reactive silane radicals SiH_n with $n<3$ are created, which can react rapidly with SiH_4. The reaction of SiH_2 with SiH_4 can lead, for instance, to Si_2H_6 or to disilane radicals. The production of Si_2H_6 requires a stabilization reaction, favorably by collisions with SiH_4.[8,59] However when such stabilization reaction does not occur, reactive disilane radicals are created, such as Si_2H_4, which can possibly react with SiH_4 again. In this way, silane radicals created by dissociative recombination of silane ions can induce also clustering reactions by means of sequential radical-silane reactions (the few rates reported for these reactions have the same order of magnitude as the ion-silane reactions[52]). Unfortunately, the detection of such radicals at relative low densities is difficult due to their reactive nature and due to the fact that they need to be ionized in the mass spectrometer. But it shows that the role of ion chemistry is not limited to the contribution of cationic clusters to the growth flux. In Ref. 8 it was shown that approximately two SiH_4 molecules are consumed per Ar^+ when a pure Ar plasma is used. This is an average value and does not exclude that (cationic) clusters are created with more than two Si atoms: a part of the Ar^+ can be lost by reactions with H_2 generated by SiH_4 dissociation, a part of the SiH_4 can be dissociated by H atoms created by other SiH_4 dissociation reactions and some of the reactive silane radicals react at the chamber walls before clustering with SiH_4. In Ref. 8 it was also shown that the polysilanes and particularly the Si_2H_6 creation, which are low in this type of plasma, are even lower when a pure Ar plasma is used instead of an Ar-H_2 plasma. This can be attributed to failing stabilization reactions as more SiH_4 is consumed in a pure Ar plasma leading to a lower SiH_4 density. Another possibility is that the Si_2H_6 is immediately dissociated by either ions from the source or by H atoms created by SiH_4 dissociation. The latter reaction, which has a larger reaction rate than the reaction between H atoms and SiH_4,[52] leads most probably to SiH_3 and SiH_4 and consumes in fact only one SiH_4 because SiH_3 is unreactive with SiH_4. Consequently, sequential radical-silane reactions cannot be excluded, especially in conditions in which dissociative recombination is important, and the importance of ion induced reactions is not limited to cationic clusters contributing to growth. A significant contribution of reactive (poly)silane radicals can therefore be a reason for the relative poor properties of the films produced when no or a small H_2 flow is admixed in the arc.

For higher H_2 flows the deposition is dominated by SiH_3 and under these circumstances the best quality material is obtained. For a SiH_4 and H_2 flow of both 10 sccs, solar grade material is deposited while the maximum contribution of cationic silicon clusters is about 6%. Also under these conditions the total contribution of reactive species generated by ion induced reactions can be larger as inferred from the same reasoning as above. Dissociative recombination will relatively occur more for cationic clusters and less for silane ions, especially due to the already low electron density. This most probably leads to a relative larger contribution of polysilane radicals.

A rough estimate of the total contribution of ion-silane interactions to the SiH_4 dissociation and a-Si:H film growth for this condition can be obtained by considering the initial ion flux emanating from the arc (about 0.08 sccs). A lower limit is obtained if it assumed that on the average two SiH_4 molecules are dissociated per ion as is the case for the pure Ar plasma.[8] This assumption leads to a dissociation of ~0.16 sccs SiH_4 (~13% of the SiH_4 dissociated under this condition). This is a lower limit because an average value, obtained in a plasma in which relatively more reactions will occur consuming only one SiH_4 per ion (as discussed above), is used. Furthermore, the contribution to film growth at the substrate is probably larger than 13% due to a preferentially more directed velocity of the heavier particles towards the substrate holder (see Sec. III B). An upper limit can be obtained by assuming that all the ions emanating from the source lead to clusters containing on the average six Si atoms, as is the case for the cationic clusters. This would mean that dissociatively recombined ions and recombined cationic clusters continue to react with SiH_4 at the same rate as for the ion-silane reactions. In this case, 40% of the SiH_4 flow is dissociated due to reactions initiated by ions. In conclusion, the real part of SiH_4 dissociated by ion induced reactions will probably be somewhere in between these percentages while the growth is still dominated by SiH_3. Yet the contribution of species created by ion induced processes to film growth can still be important for, e.g., the film quality as will be discussed next.

It is generally accepted that the deposition of a-Si:H in most types of SiH_4 plasmas is dominated by SiH_3. Furthermore, a correlation between the high film quality and dominance of SiH_3 is often suggested. A relatively small contribution of cationic clusters (and possibly reactive polysilane radicals) to film growth can have important implications for the film quality. First of all the clusters have a very compact structure as discussed in Ref. 22 and can possibly create disturbances in the a-Si:H film stochiometry. The clusters do not have the perfect tetrahedral crystalline structure to create nano- or micro-crystalline sites,[60] which is in agreement with the fact that this has also not been observed by Raman scattering on the films.[58] Furthermore the clusters are hydrogen-poor and contain consequently many overcoordinated or unsaturated bonds.[22] Therefore they can have a significant contribution to the dangling bond density in the film. Their contribution to film growth is on the order of 10^{-1}–10^{-2} while a defect density on the order of 10^{-6}–10^{-7} of the film density is required for solar grade material. Nonetheless, as already mentioned the defect density of the material deposited with a considerable flow of H_2 in the arc is sufficiently low ($<10^{16}$ cm^{-3}) for the application in solar cells. So it is still difficult to draw conclusions on detrimental or possibly even advantageous influences of the cationic clusters on the film quality up to now.

The possible implications mentioned above depend strongly on the sticking probability of the clusters, which is of no importance when the energy flux towards the film is considered. Due to the low electron temperature in the expanding plasma the energy flux of the clusters is small compared to other types of plasmas. In, for example, rf plasmas the energy flux of the ions could even be very important for the film quality. For example, the structural properties of the a-Si:H films deposited by an rf SiH_4 plasma, which improve with ion energy as observed by Hamers,[18,19] might be totally explained by the additional energy supplied to the film by the ions. The absence of this additional energy supply in the expanding Ar-H_2-SiH_4 plasma can be one reason for the relatively high substrate temperature required to obtain good quality a-Si:H. The best solar grade properties are obtained at substrate temperatures in the range of 400–450 °C which are at least 150 °C higher than the optimum substrate temperature in rf SiH_4 plasmas. This can possibly be clarified by the application of an external bias voltage.

The observation of cationic clusters in the expanding Ar-H_2-SiH_4 plasma and their formation mechanism has some possible implications for other SiH_4 plasmas. Especially in remote SiH_4 plasmas where the product of geometrical path length between source and substrate is usually relatively high, the creation of reactive species by ions and sequential ion-molecule reactions cannot be neglected. Even when the ion or metastable fluence from the source is relatively small in comparison with, e.g., the H atom fluence (as in the expanding Ar-H_2-SiH_4 plasma) the clustering reactions can lead to clusters with a considerable size and can have a significant contribution to the growth flux or impact on film properties. The fact that for a certain technique a-Si:H deposition is dominated by SiH_3 is therefore most probably no guarantee for a good film quality. A reduction of the contribution of large (cationic) clusters in remote SiH_4 plasmas can possibly be obtained by putting the substrates not in line-of-sight with the source. The fact that the substrate in the microwave setup of Jasinski[10] is placed in a tube at 90° with the plasma source is perhaps the reason that he only observes small silane ions, whereas Theil and Powell do observe large cationic clusters.[20]

V. CONCLUSIONS

It has been shown that the combination of ion mass spectrometry and Langmuir probe measurements is very powerful to study ion formation and ion fluxes in a reactive plasma. Both techniques are in principle ion flux measurements, yet the interpretation of their data separately can lead to problems, whereas their combination yields complimentary information. Furthermore, it is shown that probe measurements in depositing plasmas can very well be possible although great care is required.

The results obtained in the expanding Ar-H_2-SiH_4 plasma confirm that the observed cationic clusters are created by sequential ion-molecule clustering reactions and not by direct ionization of polysilanes. After charge exchange reactions between ions emanating from the plasma source and SiH_4, these reactions compete with dissociative recombination reactions with electrons. Especially when the electron density is sufficiently low (or reduced) they can lead to large cationic clusters whose average size depends on the product of SiH_4 density and distance between plasma source and substrate holder.

The ion flux towards the substrate has distinct beam properties for larger SiH_4 flows. The width of the ion beam decreases with increasing SiH_4 flow and consequently increasing cluster size. This leads to an ion flux towards the substrate increasing with SiH_4 flow. The influence of the H_2 flow admixed in the arc on the ion flux to the substrate and on the cluster size is small, although the initial ion flux emanating from the arc is strongly dependent on this H_2 flow. This is attributed to a strong dissociative recombination of the initially created silane ions with electrons at the position of SiH_4 injection.

The maximum contribution of the cationic clusters to the silicon growth flux is in the range of 4%–9% and rather independent of SiH_4 and H_2 flow. It has been discussed that cationic clusters and reactive species created by ion induced processes in general can still have a significant impact on the film growth. In (remote) silane plasmas they cannot be simply neglected both in terms of contribution to growth flux or influence on a-Si:H film quality

ACKNOWLEDGMENTS

The authors greatly acknowledge Dr. A. A. Howling, Dr. Ch. Hollenstein, and H. Müller from the Ecole Polytechnique Fédérale de Lausanne for their many valuable suggestions and their information about the Hiden mass spectrometer. Dr. A. Leroux, B. A. Korevaar, and A. H. M. Smets are thanked for their important contribution to the work and M. J. F van de Sande, A. B. M. Hüsken, and H. M. M. de Jong for their outstanding technical assistance. This work has been financially supported by the Netherlands Organization for Scientific Research (NWO-Prioriteit), the Netherlands Agency of Energy and the Environment (NOVEM), and the Foundation for Fundamental Research on Matter (FOM-Rolling Grant).

[1] R. Robertson and A. Gallagher, J. Appl. Phys. **59**, 3402 (1986).

[2] N. Itabashi, N. Nishiwaki, M. Magane, S. Naito, T. Goto, A. Matsuda, C. Yamada, and E. Hirota, Jpn. J. Appl. Phys. Part 2 **29**, L505 (1990).

[3] P. Kae-Nune, J. Perrin, J. Guillon, and J. Jolly, Plasma Sources Sci. Technol. **4**, 250 (1995).

[4] A good overview is, e.g., given in J. Perrin, M. Shiratani, P. Kae-Nune, H. Videlot, J. Jolly, and J. Guillon, J. Vac. Sci. Technol. A **16**, 278 (1998).

[5] A. Matsuda and A. Tanaka, J. Appl. Phys. **60**, 2351 (1986).

[6] D.A. Doughty, J.R. Doyle, G.H. Lin, and A. Gallagher, J. Appl. Phys. **67**, 6220 (1990).

[7] G. Ganguly and A. Matsuda, Phys. Rev. B **47**, 3661 (1993).

[8] M.C.M. van de Sanden, R.J. Severens, W.M.M. Kessels, R.F.G. Meulenbroeks, and D.C. Schram, J. Appl. Phys. **84**, 2426 (1998).

[9] J. Perrin, Y. Takeda, N. Hirano, H. Matsuura, and A. Matsuda, Jpn. J. Appl. Phys. Part 1 **28**, 5 (1989).

[10] J.M. Jasinski, J. Vac. Sci. Technol. A **13**, 1935 (1995).

[11] A.A. Howling, L. Sansonnens, J.-L. Dorier, and Ch. Hollenstein, J. Appl. Phys. **75**, 1340 (1994), Ch. Hollenstein, A.A. Howling, C. Courteille, D. Magni, S.Scholz Odermatt, G.M.W. Kroesen, N. Simons, W. de Zeeuw, and W. Schwarzenbach, J. Phys. D **31**, 74 (1998).

[12] D.M. Mattox, J. Vac. Sci. Technol. A **7**, 1105 (1989).

[13] P. Reinke, W. Jacob, and W. Möller, J. Appl. Phys. **74**, 1354 (1993).

[14] J.L. Lee, Y.H. Lee, and B. Farouk, J. Appl. Phys. **79**, 7676 (1996).

[15] A. von Keudell and W. Jacob, J. Appl. Phys. **81**, 1531 (1997).

[16] G. Ganguly and A. Matsuda, Mater. Res. Soc. Symp. Proc. **336**, 7 (1994).

[17] K. Kato, S. Iizuka, G. Ganguly, T. Ikeda, A. Matsuda, and N. Sato, Jpn. J. Appl. Phys. Part 1 **36**, 4547 (1997).

[18] E.A.G. Hamers, W.G.J.H.M. van Sark, J. Bezemer, W.F. van der Weg, and W.J. Goedheer, Mater. Res. Soc. Symp. Proc. **420**, 461 (1996).

[19] E.A.G. Hamers, W.G.J.H.M. van Sark, J. Bezemer, H. Meiling, and W.F. van der Weg, J. Non-Cryst. Solids **226**, 205 (1998).

[20] J.A. Theil and G. Powell, J. Appl. Phys. **75**, 2652 (1994).

[21] W.M.M. Kessels, M.C.M. van de Sanden, and D.C. Schram, Appl. Phys. Lett. **72**, 2397 (1998).

J. Appl. Phys. 86 (7), 4029 – 4039 (1999).

[22] W.M.M. Kessels, C.M. Leewis, A. Leroux, M.C.M. van de Sanden, and D.C. Schram, J. Vac. Sci. Technol. A **17**, 1531 (1999).

[23] R.J. Severens, F. van de Pas, J. Bastiaanssen, W.M.M. Kessels, L.J. van IJzendoorn, M.C.M. van de Sanden, and D.C. Schram, *Proceedings of 14th European Photovoltaic Solar Energy Conference and Exhibition* (Barcelona, Spain, 1997), p. 582.

[24] W.M.M. Kessels, R.J. Severens, M.C.M. van de Sanden, and D.C. Schram, J. Non-Cryst. Solids **227-230**, 133 (1998).

[25] G.J. Meeusen, R.P. Dahiya, M.C.M. van de Sanden, G. Dinescu, Zhou Qing, R.F.G. Meulenbroeks, and D.C. Schram, Plasma Sources Sci. Technol. **3**, 521 (1994).

[26] M.C.M. van de Sanden, R.J. Severens, R.F.G. Meulenbroeks, M.J. de Graaf, Z. Qing, D.K. Otorbaev, R. Engeln, J.W.A.M. Gielen, J.A.M. van der Mullen, and D.C. Schram, Surf. Coat. Technol. **74-75**, 1 (1995).

[27] J.J. Beulens, M.J. de Graaf, and D.C. Schram, Plasma Sources Sci. Technol. **2**, 180 (1993).

[28] M.C.M. van de Sanden, J.M. de Regt, and D.C. Schram, Plasma Sources. Sci. Technol. **3**, 501 (1994).

[29] M.G.H. Boogaarts, G.J. Brinkman, H.W.P. van de Heijden, P. Vankan, S. Mazouffre, J.A.M. van der Mullen, D.C. Schram, and H.F. Döbele, *Proceedings of te Eighth International Symposium, Laser-Aided Plasma Diagnostics* (Doorwerth, The Netherlands, 1997), p. 109.

[30] N. Hershkowitz, in *Plasma diagnostics,* Vol 1: Discharge parameters and chemistry, ed. by O. Auciello and D.L. Flamm (Academic Press, Inc., London, 1989), p. 113.

[31] Zhou Qing, D.K. Otorbaev, G.J.H. Brussaard, M.C.M. van de Sanden, and D.C. Schram, J. Appl. Phys. **80**, 1312 (1996).

[32] E.W. Peterson and L. Talbot, AIAA Journal **8**, 2215 (1970).

[33] G.J.H. Brussaard, PhD thesis, Eindhoven University of Technology (1999).

[34] G.J.H. Brussaard, M. van der Steen, M. Carrère, M.C.M. van de Sanden, and D.C. Schram, Phys. Rev. E **54**, 1906 (1996).

[35] G.J.H. Brussaard, M.C.M. van de Sanden, and D.C. Schram, Phys. Plasmas **4**, 3077 (1997).

[36] E.R. Mosburg, Jr., R.C. Kerns, and J.R. Abelson, J. Appl. Phys. **54**, 4916 (1983).

[37] R.F.G. Meulenbroeks, P.A.A. van der Heijden, M.C.M. van de Sanden, and D.C. Schram, J. Appl. Phys. **75**, 2775 (1994).

[38] G.M.W. Kroesen, D.C. Schram, A.T.M. Wilbers, and G.J. Meeusen, Contrib. Plasma Phys. **31**, 27 (1991).

[39] Hiden Analytical Limited, Gemini Business Parc, Warrington WA5 5TN, United Kingdom.

[40] P.H. Dawson, in *Quadrupole mass spectrometry and its applications*, edited by P.H. Dawson (Elsevier, Amsterdam, 1976).

[41] A.N. Hayhurst, and H.R.N. Jones, Int. J. Mass Spectrom. Ion Processes **148**, L29 (1995).

[42] H. Eppler, N. Müller, and G. Rettinghaus, Balzers Instruments, Liechtenstein (private communication).

[43] Ch. Hollenstein, A.A. Howling, C. Courteille, J.L. Dorier, L. Sansonnens, D. Magni, and H. Müller, Mater. Res Soc. Proc. **507**, 547 (1998).

[44] H. Müller and A.A. Howling (private communication).

[45] A.T.M. Wilbers, G.M.W. Kroesen, C.J. Timmermans, and D.C. Schram, Meas. Sci. Technol. **1**, 1326 (1990).

[46] M.C.M. van de Sanden, R. van den Bercken, and D.C. Schram, Plasma Sources. Sci. Technol. **3**, 511 (1994).

[47] R.F.G. Meulenbroeks, M.F.M. Steenbakkers, Z. Qing, M.C.M. van de Sanden, and D.C. Schram, Phys. Rev. E **49**, 2272 (1994).

[48] R.F.G. Meulenbroeks, R.A.H. Engeln, M.N.A. Beurskens, R.M.J. Paffen, M.C.M. van de Sanden, J.A.M. van de Mullen, and D.C. Schram, Plasma Source Sci. Technol. **4**, 74 (1995).

[49] R.F.G. Meulenbroeks, R.A.H. Engeln, J.A.M. van der Mullen, D.C. Schram, Phys. Rev. E **53**, 5207 (1996).

[50] A.J.M. Buuron, K.K. Otorbaev, M.C.M. van de Sanden, and D.C. Schram, Phys. Rev. E **50**, 1383 (1994).

[51] J.M.S. Henis, G.W. Stewart, M.K. Tripodi, and P.P. Gaspar, J. Chem. Phys. **57**, 389 (1972).

[52] J. Perrin, O. Leroy, and M.C. Bordage, Contrib. Plasma Phys. **36**, 1 (1996).

[53] W.D. Reents, Jr. and M.L. Mandich, Plasma Sources Sci. Technol. **3**, 373 (1994).

[54] A. Leroux, W.M.M. Kessels, M.C.M. van de Sanden, and D.C. Schram, J. Appl. Phys. **88**, 537 (2000).

[55] It even suggests that clustering reactions are initiated by the same silane ion independent of the ions emanating from the plasma source.

[56] C. Rebrion-Rowe, L. Lehfaoui, B.R. Rowe, and J.B.A. Mitchell, J. Chem. Phys. **108**, 7185 (1998).

[57] In fact the ion flux at floating potential has to be considered instead of the ion flux at plasma potential as the substrate is floating. The substrate can however be considered as a planar probe where there is no difference in current at both potentials.

[58] W.M.M. Kessels, M.C.M. van de Sanden, R.J. Severens, L.J. Van IJzendoorn, and D.C. Schram, Mater. Res Soc. Proc. **507**, 529 (1998).

[59] J.B. Hasted, *Physics of Atomic Collisions*, 2nd ed. (Butterworths, London, 1972).

[60] K. Raghavachari and V. Logovinsky, Phys. Rev. Lett. **55**, 2853 (1985).

Surface reaction probability during fast deposition of hydrogenated amorphous silicon with a remote silane plasma

W. M. M. Kessels,[a)] M. C. M. van de Sanden,[b)] R. J. Severens, and
D. C. Schram
Department of Applied Physics, Eindhoven University of Technology, P.O. Box 513, 5600 MB Eindhoven, The Netherlands

The surface reaction probability β in a remote Ar-H_2-SiH_4 plasma used for high growth rate deposition of hydrogenated amorphous silicon (a-Si:H) has been investigated by a technique proposed by D. A. Doughty *et al.* [J. Appl. Phys. **67**, 6220 (1990)]. Reactive species from the plasma are trapped in a well, created by two substrates with a small slit in the upper substrate. The distribution of amount of film deposited on both substrates yields information on the compound value of the surface reaction probability, which depends on the species entering the well. The surface reaction probability decreases from a value within the range of 0.45–0.50 in a highly dissociated plasma to 0.33±0.05 in a plasma with ~12% SiH_4 depletion. This corresponds to a shift from a plasma with a significant production of silane radicals with a high (surface) reactivity (SiH_x, $x<3$) to a plasma where SiH_3 is dominant. This has also been corroborated by Monte Carlo simulations. The decrease in surface reaction probability is in line with an improving a-Si:H film quality. Furthermore, the influence of the substrate temperature has been investigated.

I. INTRODUCTION

An important parameter in the fundamental study of thin film growth by means of (plasma enhanced) chemical vapor deposition is the sticking, or more generally, the surface reaction probability of the different gas phase species on the surface. Knowledge of these parameters yields insight in the growth process of the films, which is beneficial for process and film quality optimization. Apart from being essential for modeling studies, knowledge of these probabilities enables determination of the contribution of different species to film growth from density measurements in the gas phase.

Although sticking and surface reaction probabilities depend on the nature of the surface, which can in principle depend strongly on the substrate and gas phase or plasma conditions, multiple efforts have been made in the field of plasma enhanced chemical vapor deposition of hydrogenated amorphous silicon (a-Si:H) to determine both probabilities as more or less universal constants. This work was largely put into shape by the efforts of Gallagher, Perrin, and Matsuda.[1-5] They have tried to formulate a kinetic growth model for a-Si:H deposition, in which they concentrated on the incorporation of SiH_3 in the film. From several experiments they concluded that this radical is dominantly contributing to a-Si:H film growth. They proposed a surface reaction probability β of SiH_3 which is composed of a probability for sticking of SiH_3 on the surface (probability s) and a probability for recombination of SiH_3 at the surface to form, e.g., SiH_4 or Si_2H_6 with other species on the surface (probability γ). In reality, usually only β, the probability that a radical or ion gets lost in its original form at the surface ($\beta=s+\gamma$), is or can be experimentally determined. Many techniques have been applied to study this β under all kinds of circumstances. These techniques vary from relative approximate techniques yielding a more macroscopic β to more sophisticated methods concentrated on one type of radical. An overview of β's determined for silane radicals under different conditions is given in Table I.

Several techniques listed in Table I yield in principle only a compound value of β (referred to as "overall surface reaction probability") because probably several species in the plasma contribute to growth. The value of β found is usually assigned to a particular radical by proving or making plausible that it is far dominant in the gas phase. This can, however, be troublesome as the dominance of a certain radical is concluded from density measurements and the density itself depends on β. For instance, species with a high surface reactivity will not easily build up a

---

[a)] Electronic mail: w.m.m.kessels@phys.tue.nl
[b)] Electronic mail: m.c.m.v.d.sanden@phys.tue.nl

J. Appl. Phys. 87 (7), 3313 – 3320 (2000).

TABLE I. Overview of the surface reaction probabilities β for silane radicals obtained under different experimental conditions and by several techniques (RT = room temperature).

β (substrate temperature)	Experimental conditions	(Dominant) radical	Technique applied	Ref.
0.10±0.01 (RT) – 0.21±0.01 (350 °C)	Hg photo-CVD, SiH_4 with Hg	SiH_3	grid	6
0.26±0.02 (240 °C)	rf triode, SiH_4	SiH_3	grid	2
0.26±0.05 (RT – 480 °C)	rf triode, SiH_4	SiH_3	grid and trench	3
0.29	dc triode, SiH_4	SiH_3	aperture-well assembly	7
0.59	dc cathode, SiH_4	…		
0.33	dc anode, SiH_4	SiH_3		
0.37 (20–250 °C)	rf diode, SiH_4	SiH_3		
0.18 (RT)	rf diode, H_2-SiH_4 (63%)	SiH_3	infrared laser absorption	8,9
0.5±0.05 (RT) – 0.7±0.05 (500 °C)	rf diode, SiH_4	…	trench	4
0.05±0.01 (RT)	microwave, He-Cl_2-SiH_4 (6%)	SiH_3	appearance potential mass spectrometry	10
0.28±0.03 (300 °C)	rf diode (afterglow), SiH_4	SiH_3	appearance potential mass spectrometry	5
0.15 (RT)	rf diode, He-SiH_4 (50%)	SiH_3	infrared laser absorption	9
0.03 (RT)	in afterglow			
0.28±0.05	hollow cathode (CVD-like), SiH_4	SiH_3	macroscopic trench	11
0.95±0.05	hollow cathode (PVD-like), Ar-SiH_4 (5%)	Si, SiH, SiH_2		
0.97±0.05 (200 °C)	remote magnetron sputtering, Ar-H_2-SiH_4	Si, SiH		
0.15 (RT)	photolysis reactor, n-$C_4H_9SiH_3$/Si_2H_6	SiH_2	resonance enhanced multi-photon ionization	12
0.6	rf diode (afterglow), SiH_4	SiH_2	laser induced fluorescence	13
>0.94 (RT)	near-effusive beam from inductively coupled	SiH	laser induced fluorescence	14
0.95±0.05 (RT)	plasma, SiH_4			15
0.18		SiH_3	atomistic simulations	16
0.7		SiH_2	using molecular	17
0.95 (RT)		SiH	dynamics	18

large gas phase density just because of their high loss probability at the surface, but they can of course contribute significantly to film growth.

Table I shows that a lot of data are available for β of SiH_3. All data show agreement on the fact that β of SiH_3 is relatively low compared to β of SiH, which is measured with high accuracy. For SiH_2 up to now less convincing data are available, but it is generally accepted that its β is rather high and at least higher than for SiH_3 (Robertson and Rossi realize that their value of 0.15 is unexpectedly low[12]). Therefore, in the case of a-Si:H deposition, usually a division is made into very reactive species like SiH_2, SiH, etc., with a high β (>0.5) and SiH_3 with a smaller β (<0.3). Furthermore, it is generally accepted that good a-Si:H film quality is related to a dominant contribution of SiH_3 to film growth while a considerable contribution of the silane radicals with a high (surface) reactivity is expected to produce films with inferior quality.[1,6,7]

Because of this rather clear division in magnitude of β's in the case of a-Si:H, it can be useful to determine the overall β. Such technique is usually much easier to apply than a manifold of techniques, in order to determine β of all different species present in the plasma separately. Moreover, it is easier to link the overall β directly with film quality. By comparing the experimentally found β's to those listed in Table I information about the species contributing to film growth can be obtained. Starting from this point, an overall β can give insight in film growth and in the contribution of very reactive species. For this reason, the overall β has been determined in the expanding

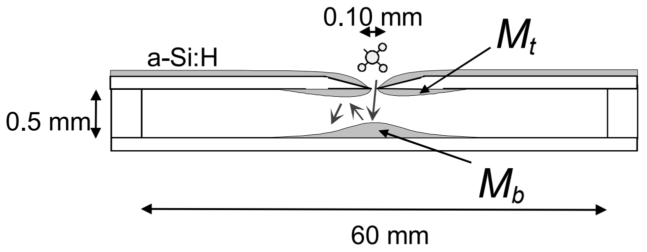

FIG. 1. Schematic illustration of the "aperture-well assembly" to determine the overall surface reaction probability β of the depositing species in a SiH_4 plasma. The figure is not to scale.

thermal plasma (ETP) setup for different plasma settings. This remote deposition technique has proven to be able to deposit solar grade a-Si:H at a growth rate of 10 nm/s.[19,20] It uses an Ar/H_2 plasma created in a thermal plasma source (cascaded arc) for downstream SiH_4 dissociation in a low-pressure region. Characteristic for this technique and, as will be shown later advantageous for the determination of β, is the absence of ion bombardment of the surface due to the low electron temperature.[21] The determination of β in this plasma is part of a project in which the plasma chemistry, the fluxes of reactive species like ions and radicals to the substrate and their contribution to film growth is investigated.[20-23] This is subsequently related with the quality of the films in terms of structural and opto-electronic properties[20] yielding more information on a-Si:H film growth, especially at elevated growth rates.

The technique used to determine β is the so-called "aperture-well assembly", which has been explored by Doughty *et al.*[7] Its principle and design are described in Sec. II as well as the method of analysis. A Monte Carlo method is presented to obtain theoretical insight in the resulting β when for example different species contribute to film growth (Sec. III). In Sec. IV, β is given for different plasma conditions as well as for different substrate temperatures. These results and their implications for a-Si:H film growth in the expanding thermal plasma are discussed in Sec. V followed by conclusions in Sec. VI.

II. EXPERIMENT

In the "aperture-well assembly" (see Fig. 1), a well is created by two substrates with in the upper substrate an aperture (slit).[7] Species in the plasma can enter the well through the aperture and collide with the bottom substrate assuming no gas phase collisions to occur inside the well. If only one type of radical (or ion) with β=1 is present in the plasma, all radicals (ions) entering the well are lost at the lower substrate and only deposition takes place at the bottom of the well (assuming a sticking probability $s\neq 0$). If β<1, the radicals can undergo reflection (probability r=1-β) towards the underside of the upper substrate where they can deposit or reflect once again to the bottom substrate, etc. For a flux F of one type of radicals entering through the aperture of area A, the number of radicals deposited at the bottom substrate M_b and at the underside of the top substrate M_t can be calculated by summing up the different contributions:

$$M_b = \frac{sFA}{1-r^2} \quad \text{and} \quad M_t = \frac{srFA}{1-r^2}. \tag{1}$$

The surface reaction probability can now either be calculated from the ratio of the total amount of film deposited inside the well and the amount which would have been deposited at the area of the aperture if it had not been there (sFA):

$$\beta = 1 - r = \frac{sFA}{M_t + M_b} \tag{2}$$

or by comparing the amount of film deposited at the underside of the top substrate to the amount of film deposited at the bottom substrate:

$$\beta = 1 - r = 1 - \frac{M_t}{M_b}. \tag{3}$$

Doughty *et al.*[7] has applied the first method, in this article, the second method is chosen.

Several criteria have to be met in the design of the aperture-well assembly for applying above equations. A 0.50 mm thick copper spacer ring (see Fig. 1) separates the two stainless steel substrates creating the well. The distance d between the two substrates is therefore smaller than the mean free path for momentum transfer of the species in the expanding thermal plasma avoiding gas phase collisions (the mean free path is 1.3 and 2.5 mm when the gas temperature is set equal to the temperature of the substrate or to the temperature in the center of the plasma beam, respectively). A comparison with experiments with d is 0.25 and 1.00 mm is made. The distance between the center of the well and its edges (formed by the copper spacer ring) is 30 mm, such that film deposition at the edges can be neglected. The aperture in the top substrate is a slit with a width of 0.10 mm and a length of 8 mm. This is sufficiently small to limit "bouncing out" of reactive species in a sufficient extent as evidenced by a three-dimensional Monte-Carlo simulation (see Sec. III). Although information on β can be obtained by applying Monte-Carlo simulations when above-mentioned restrictions are not satisfied, a method yielding direct information on β has been preferred. The top substrate is rather

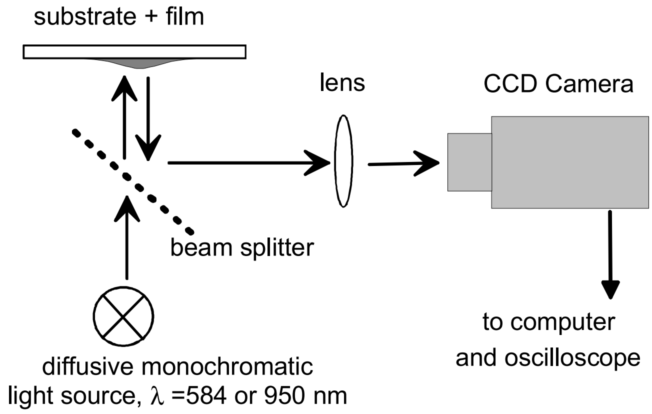

FIG. 2. Setup used for analyzing the deposited film profiles on the substrates. The light source is either a sodium or infrared lamp.

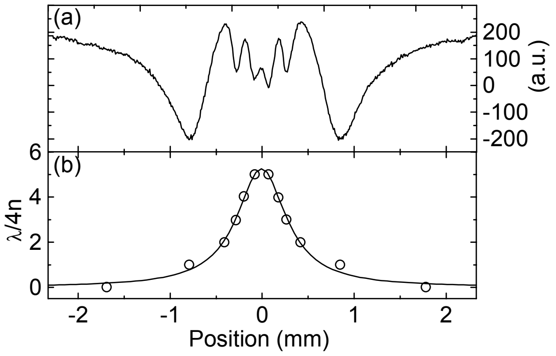

FIG. 3. (a) Fringes in intensity of light reflected from a substrate due to multiple reflection in a-Si:H film and (b) the corresponding thickness profile of the film. The symbols are the data points extracted from (a) and the line is a fitted Lorentzian.

thick (0.50 mm) to improve heat conduction and temperature control. The heat flux (~0.4 Wcm^{-2}) in the expanding thermal plasma will heat up a too thin top substrate considerably during deposition leading to substrate fracture. Furthermore, the films deposited on top of the well need to be thick (10 μm) to obtain a considerable amount of film inside the well through the small aperture and this leads consequently to a high stress. The slit in the upper substrate is knife-edged shaped (at an angle of 60°) at the side facing the plasma. This reduces the effective thickness of the upper substrate to less than 0.1 mm at the position of the slit. In this way, the angular distribution of the species arriving inside the well is not disturbed seriously. Furthermore, it reduces deposition on the edges of the slit. The latter can lead to a distorted composition of the flux of reactive species inside the well as the most reactive species will be lost more easily on these edges and will be filtered out.

The well is mounted on top of a substrate holder in the expanding thermal plasma setup, described in detail in Refs. 21 and 22. An adequate temperature control of the substrates between 100 and 500 °C is usually obtained by using a small helium back flow. The temperature control in the aperture-well assembly is inferior and therefore the temperature of both substrates was monitored by means of thermocouples under similar, but nondepositing, plasma conditions. For a substrate holder temperature of 400 °C, the temperatures are 357 and 384 °C for the upper and lower substrate, respectively, before plasma ignition. After plasma ignition, both substrates increase less than 40 °C in temperature on the time scale for deposition (6–10 min), while the difference remains smaller than 30 °C. This is supposed to be a fairly good temperature control (during the greater part of the deposition time the substrate temperatures are close to 400 °C). The determination of β is most probably not disturbed, anticipating on the fact that β is not heavily temperature dependent (see Sec. V). Most experiments have been carried out at 400 °C, which yields a-Si:H with optimum structural and opto-electronic properties for the ETP technique. At lower temperatures (250 and 325 °C), the temperature control is somewhat poorer than at 400 °C especially in the initial period of deposition.

The amount of film deposited inside the well at both substrates is determined by means of an optical technique schematically represented in Fig. 2. Diffusive, monochromatic light is projected at the substrate with film and the reflected light is projected by means of a beam splitter on a lens focussed at a charge coupled device (CCD) camera. Multiple reflections within the film lead to interference and therefore regions with maximum and minimum intensity are observed in the CCD video frame. As the cross sections of the deposition profiles perpendicular to the slit's long dimension are independent of the position along this dimension (except for the slit's ends), the deposited profiles are analyzed at only three positions. This is done by reading out one pixel line of the CCD array, corresponding with a cross-section of the profile, by means of an oscilloscope. Accurate positioning of the substrate is achieved by the computer video frame. The observed oscilloscope image shows fringes corresponding to differences in thickness[24] of the profile as illustrated in Fig. 3. The film thickness is obtained from the fringes by using Eq. (4), where the thickness between a maximum $d_{\max}$ and a minimum $d_{\min}$ of a fringe is given by

$$\left| d_{\max} - d_{\min} \right| = \frac{\lambda}{4n}, \tag{4}$$

with λ the wavelength of the light used and n the corresponding refractive index of the material. From this, a cross section of the deposition profile can be obtained (see Fig. 3) by assuming that that thickness of a-Si:H is zero at the edges of the profiles where the light is reflected by the stainless steel. Two monochromatic light sources have been used: a sodium lamp (λ=584 nm) leading to a large number of fringes but suffering from absorption for thicker parts of the a-Si:H and an infrared source. The latter is composed of light emitting diodes (LEDs) (λ=950 nm). This combination leads to an unambiguous interpretation of the fringes. The thickness profiles are fitted with Lorentzians from which the total amount of film is calculated. The refractive index and wavelength drop out in the calculation of β as only the ratio of the material deposited at both substrates is considered. Using the refractive index as obtained from ellipsometry (λ=632.8 nm) and Fourier transform infrared (FTIR) spectroscopy, the increase in thickness between a minimum and maximum in intensity is approximately 34 and 69 nm for the sodium and infrared source, respectively (for a-Si:H deposited at 400 °C). Furthermore, for one experiment, the deposition profiles at both substrates have also been determined by particle-induced x-ray emission (PIXE) analysis.[25] As shown in Fig. 4, the thickness profiles obtained show a very good agreement with those obtained by the optical technique demonstrating the adequacy of the optical analysis.

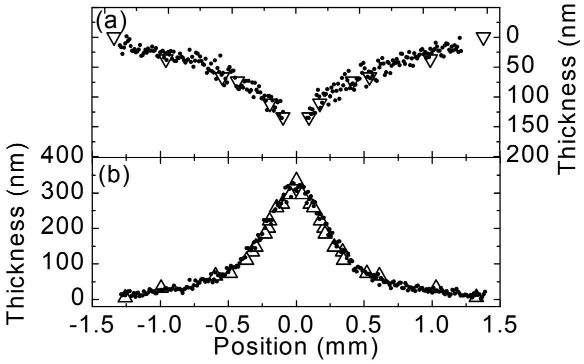

FIG. 4. Comparison between thickness profiles obtained by the optical technique using interference (open symbols) and by particle-induced x-ray emission (PIXE) (closed symbols and in arbitrary units) for the (a) top and (b) bottom substrate.

III. MONTE CARLO SIMULATION

A three-dimensional model for the aperture-well assembly using the Monte Carlo method to simulate the trajectories of reactive particles (radicals or ions) has been set up to get acquainted with the influence of different parameters and to test assumptions important for correct interpretation of the experimental data. The simulation itself is not used to retrieve β from the experimental data. Several fluxes of different reactive species with different surface reaction probabilities β and sticking probabilities *s* ($s \leq \beta$) can be implemented to get insight into the resulting overall β. Only interactions of the reactive species with the surfaces are taken into account: the particles can either react or reflect from the surface. For the latter, the cosine distribution is assumed.[14,26] The reaction probability at the surface is assumed to be independent of the angle of incidence of the particles and no surface diffusion is taken into account. Typically, 10^6–10^7 particles are used per calculation and from the distribution of the particles deposited at both substrates the (overall) β is calculated. The simulation has been tested for different cases. The cross sections of the distribution of the deposited particles can very well be approximated by Lorentzian profiles. As expected the number of particles bouncing out of the well through the slit decreases for increasing β. For β > 0.2, less than 6% of the particles bounce out and no significant influence of this effect on the calculated β has been found. Yet it illustrates the necessity of the aperture being as small as possible. Also a considerable amount of particles reach the edges of the well for very low values of β and this amount increases with increasing well height (distance between the two substrates). The width of the profiles of deposited materials show a linear increase with increasing well height. The increasing importance of gas phase reactions can however not be observed in the simulation, as these are not taken into account. The determination of β is hardly influenced by the fact that the top substrate is not infinitesimal thin. Furthermore, the overall β obtained from simulations taking several species into account with different combinations of β and *s* showed excellent agreement with theoretical calculations.

IV. RESULTS

Depositions with the aperture-well assembly have been performed under different conditions. An arc current of 45 A and an Ar, SiH_4, and H_2 flow of respectively 55, 10, and 10 sccs (standard cubic centimeters per second) are standard. The corresponding downstream pressure is 0.20 mbar and the substrate temperature is set at 400 °C. This parameter setting with a resulting growth rate of 10 nm/s yields the best film quality.[20] The typical deposition time for the aperture-well assembly is 10 min. No significant dependence of the deposition time on β has been observed, but shorter times lead to less material deposited inside the well troubling data interpretation (the growth rate is of course much smaller

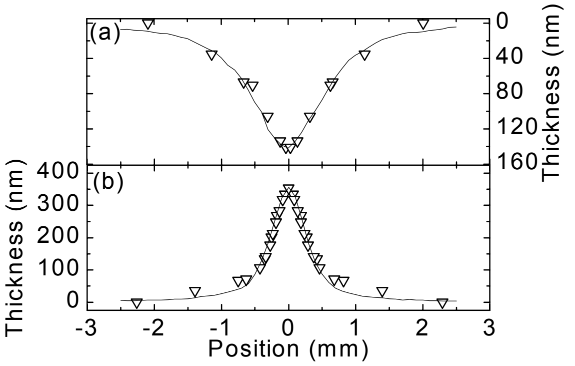

FIG. 5. Data points show experimental cross section of the thickness profile for both the (a) upper and (b) lower substrate. The corresponding β is 0.36. The profiles obtained from a Monte Carlo simulation are given by lines.

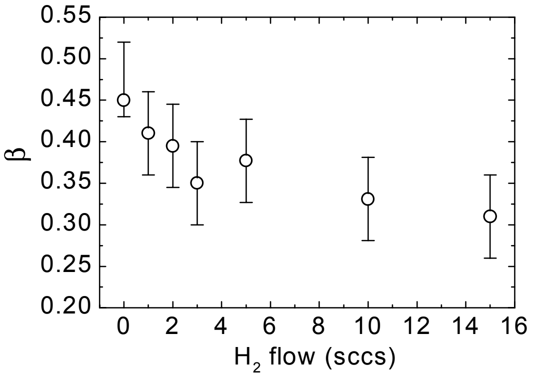

FIG. 6. Overall surface reaction probability β as a function of H_2 flow admixed in the plasma source. The Ar and SiH_4 flow are, respectively, 55 and 10 sccs. The arc current is 45 A, the downstream pressure 0.20 mbar, and the substrate temperature is 400 °C.

inside the well than at the side of the upper substrate facing the plasma). A typical distribution of the a-Si:H deposited inside the well at both the upper and lower substrate is given in Fig. 5. The value of β, calculated from Eq. (3), is 0.36. The results of the Monte Carlo simulation using one single specie with β=0.36 are given in the same figure. The simple, isotropic cos(θ) distribution for the angular distribution of the species entering the well leads to too broad profiles. Top and bottom profiles are almost 1.5 times broader than their experimental counterparts, also for the distances of 0.25 and 1.00 mm between the substrates. A “narrower” $\cos^4(\theta)$ distribution leads to a good agreement between the full width at half maximum of the simulated and experimental data. This anisotropy can be due to the presence of the “absorbing” slit or be due to beam properties of the downstream plasma.[23] The angular distribution has no influence on the value of β obtained from the simulated profiles. The fact that the experimentally obtained profiles are less broad cannot be attributed to the fact that the involved simulations use one specie (with the experimentally found β), while the experimentally observed β is a compound value made up by different species (including for example, ions with β=1). By using different species in the Monte Carlo simulation, it has been shown that the width of the profiles obtained is not greatly influenced by the fact how the fluxes of different species lead to the overall value. The width of the profiles does however decrease with increasing (overall) β. Furthermore, Fig. 5 also shows that the simulated data drop slower to zero than the experimental data. This can be attributed to the difficulty in the interpretation of the experimental data at very small film thickness (very slight changes in reflectivity).

To obtain an indication of the accuracy of the technique and to eliminate possible artifacts in the interpretation of the separate data, the aperture-well assembly experiment has been repeated at least three times for every condition. The experiment has been repeated 14 times for the standard condition. From the distribution of the values of β, the uncertainty in the data has been estimated.

The obtained β’s are shown in Fig. 6 for different H_2 flows in the plasma source while the other parameters are kept fixed at their standard values. The figure shows a decreasing overall β with increasing H_2 flow. Changing the H_2 admixture in the cascaded arc leads a drastic change in the downstream plasma chemistry.[20-22] It has been shown that increasing the H_2 flow leads to an increase in the contribution of SiH_3 to film growth. The latter is created by hydrogen abstraction of SiH_4 by atomic hydrogen emanating from the cascaded arc. The ion fluence from the arc is low for these conditions and the SiH_4 consumption is ~12%. At low H_2 flows however, a large fraction of SiH_4 is dissociated (~60%), mainly due to the large ion fluence emanating from the source. Under these conditions, very reactive (poly)silane radicals, created by ion induced reactions, contribute significantly to growth.[21] The relative contribution of SiH_3 is significantly smaller than for high H_2 flows. The contribution of silicon containing positive ions or cationic clusters $Si_nH_m^+$, created by sequential ion-silane reactions, is rather independent of the H_2 flow as discussed in Ref. 21. The decreasing value of β is in qualitative agreement with the fact that with increasing H_2 admixture the contribution of very reactive (poly)silane radicals, with high β’s, strongly decreases. The lowest β is obtained at the plasma settings with the highest SiH_3 contribution (H_2 = 10–15 sccs). Under these conditions also the best a-Si:H film quality, both in terms of structural and optoelectronic film properties is obtained. Furthermore, the film surface roughness, as determined from simulations of *in situ* ellipsometry data,[27] decreases with increasing H_2 flow. This also suggests an increasing importance of species with a low β. The interpretation of the absolute values of β is somewhat more complicated as the experimentally found values are overall values depending on the fluxes of the several species towards the substrate. For the standard condition (10 sccs H_2), β is relatively close to some of the literature data on SiH_3.[2,3,5,7,11] This would suggest that under this condition, the deposition is by far dominated by SiH_3, however, some other data on SiH_3 (Refs. 6,8–10) would suggest a considerable contribution of species with a higher β. A discussion about this interpretation, possible consequences and, e.g., the influence of species with $s < \beta$ will be given in Sec. V with the help of Monte Carlo simulations.

To investigate the influence of the substrate temperature on β, the aperture-well assembly experiment has been performed at different substrate temperatures. This is done for fixed plasma parameters, i.e., at the standard condition, where SiH_3 is dominant. In Fig. 7(a), β is given for 250, 325, and 400 °C. Although the figure shows an increase in β from 325 to 400 °C, β is constant within the experimental uncertainty. No significant temperature dependence of β has been observed in literature for cases where SiH_3 is the only depositing radical [the temperature dependence in Ref. 6 is attributed to parasitic catalytic chemical vapor deposition (CVD)[3]] and this has been explained by surface diffusion of SiH_3.[2,3,7] For the case that also other species contributed to film growth, β increased from 0.5 at room temperature to 0.7 at 500 °C.[4] The Si growth flux or Si incorporation flux as determined from a combination of elastic recoil detection (ERD) and Rutherford backscattering (RBS)[28] is given for the same plasma setting in Fig. 7(b). Assuming that the fluxes of species are independent of substrate temperature, Fig. 7(b) suggests a slightly decreasing sticking probability. The decrease is less than 8% between 250 and 400 °C. The growth flux does not show an abrupt increase at temperatures over 350 °C as observed by Matsuda *et al.*[3,4,29] and which has been attributed to additional creation of growth sites due to thermal desorption of hydrogen at the surface. An influence of thermal desorption is also not expected: the growth rate for the ETP technique is much higher (10 nm/s) than for the technique of Matsuda *et al.*[3] This means that thermal desorption will only become significant at very high temperatures and that it also cannot explain the possible increase of β for temperatures over 325 °C.

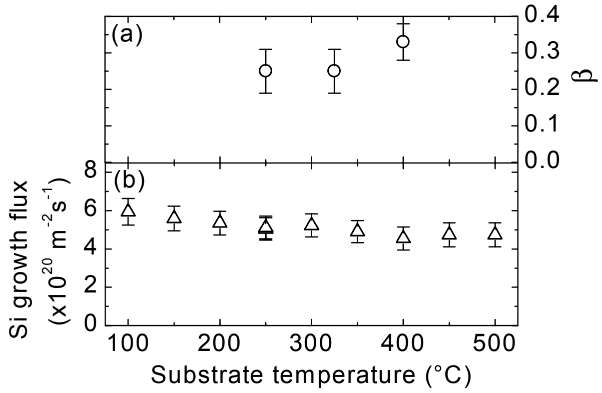

FIG. 7. (a) Overall surface reaction probability β and (b) Si growth flux as a function of substrate temperature. The plasma settings are equal to those in Fig. 6 with 10 sccs H_2.

V. DISCUSSION

It has been shown that the aperture-well assembly is a relative simple technique yielding the overall β with a fairly good reproducibility. Yet the variation of β with H_2 flow or substrate temperature is relatively small such that the interpretation of the data is somewhat limited by the experimental uncertainty. It has also been shown that the experiment is rather sensitive to certain assumptions setting critical demands on the design of the experiment and complicating the interpretation of the data. Some final aspects should still be addressed. First, it is assumed that the substrate material does not influence the experiment, which is plausible as no significant difference in a-Si:H growth rate on stainless steel and crystalline silicon substrates has been observed. Furthermore, it is assumed that the probabilities *s* and β are growth flux independent. It is, e.g., assumed that thermal desorption of surface hydrogen is also negligible for the film deposited inside the well as the growth rate in that region is still larger than 0.1 nm/s. At last, it should be remarked that the absence of a severe ion bombardment on the surface in the expanding thermal plasma is favorable for the aperture-well assembly experiment. Due to the low electron temperature in the downstream region, the energy gained by the ions in the plasma sheath is less than 2 eV,[21] and therefore the experiment is not disturbed by the fact that such a bombardment would only take place at a small region of the bottom substrate directly in line of sight with the plasma. A sudden increase in thickness at the center of the bottom profile due to enhanced growth site creation by ion bombardment is therefore also not observed in Figs. 4 and 5.

In Sec. IV, it has been shown that β decreases with increasing H_2 flow in agreement with a decreasing contribution of very reactive radicals (as measured indirectly) and an increasing contribution of SiH_3 (measured directly).[20,30] The interpretation of the overall β is complicated by the fact that no absolute fluxes of species contributing to film growth are known yet. It is nevertheless possible to go more into detail on basis of β's for the different species available in the literature. For that, it has to be assumed that β does not depend heavily on the nature of the film surface but mainly on the species contributing to growth. In literature it is assumed that β is rather temperature independent and mainly determined by steric factors of the radicals as long as the hydrogen coverage of the surface is high.[3,7] This means that the obtained values of β can be compared to those obtained in other experiments where also high quality a-Si:H is obtained.

The surface reaction probability for the plasma setting yielding the best film quality is 0.33±0.05. It approaches the reported β's for SiH_3 in the literature (see Table I). Especially when the temperature effect on β in Fig. 7(a) is real: for lower temperatures (but typical for a-Si:H deposition) even a lower β is obtained. It is, however, not reasonable to assume that the deposition under this condition is completely due to SiH_3. It is, e.g., known that for this plasma setting, the total contribution of cationic silicon clusters is about 7% of the growth flux.[21,23] This percentage is based on the assumption that for the cationic clusters and ions $s=\beta=1$, which is a fair assumption as concluded from a classical molecular dynamics study.[31] The influence of these clusters and other very reactive species on the overall β can be illustrated by Monte Carlo simulations. These showed that a flux of 5% of species with $s=\beta=1$ with a main flux of SiH_3 with $\beta=0.30$ leads to an overall value of 0.33. In this case, the contribution of the very reactive species to film growth is 15%. Under these suppositions, the β at $H_2=0$ sccs can be explained by a contribution of 50% by species with $s=\beta=1$. For both cases, a possible larger contribution of very reactive (poly)silane radicals can be compensated for by a $\beta<1$ for these species. This illustrates that the obtained overall β for the settings yielding the best film quality can very well be explained by a flux of mainly SiH_3 with a minor contribution of other radicals and ions.

Up to now, it has been assumed that for all species contributing to film growth $s=\beta$. But what are the consequences if for one type of species $s<\beta$? For example, from experiments by Matsuda *et al.*[3] it has been concluded that s/β is ~0.4 for SiH_3 at substrate temperatures lower than 350 °C.[32] This means that 60% of the SiH_3 lost at the surface does not contribute to deposition but leads for example to SiH_4 and Si_2H_6 generation at the surface. From Monte Carlo simulations, it has been derived that assuming $s=0.12$ and $\beta=0.30$ ($s/\beta=0.4$) the allowable flux of very reactive species is only 2% of the total flux to obtain an overall β of 0.33. Yet the resulting contribution of species with $s=\beta=1$ to film growth in terms of Si atoms deposited is still about 15%. From more simulations using other values for the probabilities and fluxes, it is concluded that this is generally true: the fact that for some species $s<\beta$ does not lead to other conclusions about the contribution of the specific species to film growth. It only influences the ratio of fluxes towards the substrate as the reactive species can get lost by recombination as well.

VI. CONCLUSION

The aperture-well assembly technique has been used to gain information about the (overall) surface reaction probability in a remote SiH_4 plasma generated by the expanding thermal plasma setup. It has been shown that caution in the design and the interpretation is required for this simple method but that it nonetheless gives considerable insight in the a-Si:H film growth. Especially, when the data are combined with data on fluxes or densities of species in the plasma.

For the expanding thermal plasma setup, it has been shown that the overall β increases with decreasing contribution of SiH_3 and increasing contribution of radicals with a high surface reactivity such as SiH_x, $x<3$. The overall β at a substrate temperature of 400 °C is 0.33±0.05 for plasma settings in which the a-Si:H film quality is optimal (solar grade quality). For these settings, the deposition can be explained by a dominant contribution of SiH_3 with a minor contribution of radicals and ions with a high surface reactivity as corroborated by Monte Carlo simulations. For conditions with a higher β, relatively poor a-Si:H is obtained corresponding with higher contribution of very reactive species. This shows that there is a relation between a small β, high contribution of SiH_3 and high a-Si:H film quality, for films deposited at much higher growth rates than by conventional techniques as well.

The experiments suggest a somewhat lower β at substrate temperatures of 250 and 325 °C than at 400 °C, however, not unambiguously due to the relative large experimental uncertainty. The total Si growth flux decreases slightly for increasing substrate temperature at constant plasma settings suggesting a decreasing sticking probability with temperature. However, no increase in deposition rate (Si growth flux) due to thermal desorption of hydrogen at the surface has been observed, which is explained by the high growth rate.

ACKNOWLEDGMENTS

The authors acknowledge J. Bastiaanssen, G. Toto, C. Smits, C. Vitarella, and R. ter Riet for their contribution to the measurements. Dr. P. Mutsaers is thanked for the PIXE analysis and M. J. F. van de Sande, A. B. M. Hüsken, and H. M. M. de Jong for their technical assistance. This work has financially been supported by the Netherlands Organization for Scientific Research (NWO Prioriteit), the Netherlands Agency for Energy and the Environment (NOVEM) and the Foundation for Fundamental Research on Matter (FOM-Rolling Grant).

[1] A. Gallagher, Mater. Res. Soc. Symp. Proc. **70**, 3 (1986).

[2] J. Perrin, Y. Takeda, N. Hirano, Y. Takeuchi, and A. Matsuda, Surf. Sci. **210**, 114 (1989).

[3] A. Matsuda, K. Nomoto, Y. Takeuchi, A. Suzuki, A. Yuuki, and J. Perrin, Surf. Sci. **27**, 50 (1990).

[4] J.-L. Guizot, K. Nomoto, and A. Matsuda, Surf. Sci. **244**, 22 (1991).

[5] J. Perrin, M. Shiratani, P. Kae-Nune, H. Videlot, J. Jolly, and J. Guillon, J. Vac. Sci. Technol. A **16**, 278 (1998).

[6] J. Perrin and T. Broekhuizen, Appl. Phys. Lett. **50**, 433 (1987).

[7] D.A. Doughty, J.R. Doyle, G.H. Lin, and A. Gallagher, J. Appl. Phys. **67**, 6220 (1990).

[8] N. Itabashi, N. Nishikawa, M. Magane, S. Naito, T. Goto, A. Matsuda, C. Yamada, and E. Hirota, Jpn. J. Appl. Phys., Part 2 **29**, L505 (1990).

[9] M. Shiratani, H. Kawasaki, T. Fukuzawa, Y. Watanabe, Y. Yamamoto, S. Suganuma, M. Hori, and T. Goto, J. Phys. D **31**, 776 (1998).

[10] J.M. Jasinski, J. Phys. Chem. **97**, 7385 (1993).

[11] A. Nurrudin, J.R. Doyle, and J.R. Abelson, J. Appl. Phys. **76**, 3123 (1994).

[12] R.M. Robertson and M.J. Rossi, J. Chem. Phys. **91**, 5037 (1989).

[13] M. Hertl and J. Jolly, Centre de Recherches en Physique des Plasmas, EPFL, Lausanne Report LRP 629/99, *Workshop on Frontiers in Low Temperature Plasma Diagnostics III* (Saillon, Switzerland, 1999), p. 245.

[14] P. Ho, W.G. Breiland, and R.J. Buss, J. Chem. Phys. **91**, 2627 (1989).

[15] P.R. McCurdy, K.H.A. Bogart, N.F. Dalleska, and E.R. Fisher, Rev. Sci. Instrum. **68**, 1684 (1997).

[16] S. Ramalingan, D. Maroudas, and E.S. Aydil, J. Appl. Phys. **86**, 2872 (1999).

[17] S. Ramalingan, P. Mahalingam, E.S. Aydil, and D. Maroudas, J. Appl. Phys. **86**, 5497 (1999).

[18] S. Ramalingan, D. Maroudas, and E.S. Aydil, J. Appl. Phys. **84**, 3895 (1998).

[19] R.J. Severens, F. van de Pas, J. Bastiaanssen, W.M.M. Kessels, L.J. van IJzendoorn, M.C.M. van de Sanden, and D.C. Schram, *Proceedings of 14th European Photovoltaic Solar Energy Conference and Exhibition* (Barcelona, Spain, 1997), p. 582.

[20] W.M.M. Kessels, A.H.M. Smets, B.A. Korevaar, G.J. Adriaenssens, M.C.M. van de Sanden, and D.C. Schram, Mater. Res. Soc. Symp. Proc. **557**, 25 (1999).

[21] W.M.M. Kessels, C.M. Leewis, M.C.M. van de Sanden, and D.C. Schram, J. Appl. Phys. **86**, 4029 (1999).

[22] M.C.M. van de Sanden, R.J. Severens, W.M.M. Kessels, R.F.G. Meulenbroeks, and D.C. Schram, J. Appl. Phys. **84**, 2426 (1998).

[23] W.M.M. Kessels, C.M. Leewis, A. Leroux, M.C.M. van de Sanden, and D.C. Schram, J. Vac. Sci. Technol. A **17**, 1531 (1999).

[24] The technique yields in fact a profile of the optical path length in the a-Si:H, which is more appropriate than the pure thickness as it takes also variations of the Si density into account. The latter is in good approximation linear in the refractive index.

[25] P.H.A. Mutsaers, Nucl. Instrum. and Methods Phys. Res. B **113**, 323 (1996).

[26] J.-H. Yun and S.-K. Park, Jpn. J. Appl. Phys., Part 1 **34**, 3216 (1995).

[27] A.H.M. Smets, M.C.M. van de Sanden, and D.C. Schram, Thin Solid Films **343-344**, 281 (1999).

[28] W.M.M. Kessels, M.C.M. van de Sanden, R.J. Severens, L.J. van IJzendoorn, and D.C. Schram, Mater. Res. Soc. Symp. Proc. **507**, 529 (1998).

[29] Y. Toyoshima, K. Arai, A. Matsuda, and K. Tanaka, J. Non-Cryst. Solids **137&138**, 765 (1991).

[30] W.M.M. Kessels, M.C.M. van de Sanden, and D.C. Schram, accepted for publication in J. Vac. Sci. Technol A **18**, (2000).

[31] S. Ramalingan, W.M.M. Kessels, D. Maroudas, and E.S. Aydil (unpublished).

[32] In the experiments of Matsuda *et al.* both β and s for SiH_3 have been found to be independent of substrate temperature below 350 °C. However, in the determination of s the growth rate has been used instead of the net Si growth flux. The Si density of a-Si:H usually increases with substrate temperature which means that the s and therefore s/β presumably slightly increases with temperature.

Film growth precursors in a remote SiH_4 plasma used for high rate deposition of hydrogenated amorphous silicon

W. M. M. Kessels,[a] M. C. M. van de Sanden,[b] and D. C. Schram
Department of Applied Physics, Eindhoven University of Technology, P.O. Box 513, 5600 MB Eindhoven, The Netherlands

The SiH_4 dissociation products and their contribution to hydrogenated amorphous silicon (a-Si:H) film growth have been investigated in a remote Ar-H_2-SiH_4 plasma that is capable of depositing device quality a-Si:H at 10 nm/s. SiH_3 radicals have been detected by means of threshold ionization mass spectrometry for different fractions of H_2 in the Ar-H_2 operated plasma source. It is shown that at high H_2 flows, SiH_4 dissociation is dominated by hydrogen abstraction and that SiH_3 contributes dominantly to film growth. At low H_2 flows, a significant amount of very reactive silane radicals, SiH_x ($x \leq 2$), is produced as concluded from threshold ionization mass spectrometry on SiH_2 and optical emission spectroscopy on excited SiH and Si. These radicals are created by dissociative recombination reactions of silane ions with electrons and they, or their products after reacting with SiH_4, make a large contribution to film growth at low H_2 flows. This is corroborated by the overall surface reaction probability which decreases from ~0.5 to ~0.3 with increasing H_2 fraction. The film properties improve with increasing H_2 flow and device quality a-Si:H is obtained at high H_2 fractions where SiH_3 dominates film growth. Furthermore, it is shown that at high H_2 flows the contribution of SiH_3 is independent of the SiH_4 flow while the deposition rate varies over one order of magnitude.

I. INTRODUCTION

The increasing demand for clean energy sources has initiated a lot of research on hydrogenated amorphous silicon (a-Si:H) and its application in thin film solar cells. To increase their competitiveness with conventional energy sources the work in this field is mainly focussed on increasing the solar cells' (stable) efficiency, the application of new low-cost materials, and the improvement of the production processes, which should all be compatible with large-area deposition and a high throughput. In this respect, one of the central questions is whether it is possible to deposit a-Si:H suitable for application in thin solar cells at high growth rates (preferably >1 nm/s). Several investigations have already addressed this question,[1-10] and recently it is shown that device quality a-Si:H can be obtained even at a rate of 10 nm/s with the expanding thermal plasma (ETP).[11,12] This technique combines a high-pressure thermal plasma source with a low-pressure deposition chamber and is therefore a real remote plasma. The a-Si:H obtained has some remarkable properties such as an enhanced hole drift mobility. Furthermore, the good film quality is confirmed by the results on the first, not yet optimized, solar cells which contained intrinsic a-Si:H deposited at a rate of 7 nm/s.[11,12]

In order to obtain insight into the conditions under which good quality a-Si:H can be obtained at high deposition rates as well as into possible limitations, the reactions in the plasma and at the film surface are studied for the expanding thermal plasma. This investigation yields a better understanding of the deposition process of a-Si:H and the resulting film properties, which enables further process and film quality optimization. This knowledge is also of importance for other (low deposition-rate) SiH_4 plasmas, and it can yield insight into how to increase the growth rate in these plasmas while maintaining good film quality.

This article, which is part of a project aiming at a good understanding of the plasma processes and film growth in the expanding thermal plasma, deals with the plasma chemistry which has already been addressed globally in previous work.[13] Here, the dissociation reactions of SiH_4 are considered in more detail and information on the contribution of the specific reaction products to film growth is obtained from applying several plasma diagnostics. This is done for different plasma conditions and the results are related to the obtained film properties, which are presented in detail in another article.[14] It is focussed on the silane radicals (SiH_x, $x \leq 3$) because an extensive investigation of the ion-chemistry showed that the

---

[a] Electronic mail: w.m.m.kessels@phys.tue.nl
[b] Electronic mail: m.c.m.v.d.sanden@phys.tue.nl

contribution of $Si_nH_m^+$ ions is less than 10%, in terms of Si atoms deposited, for all conditions.[15,16] The contribution of the different radicals is expected to have important implications for the film quality because the film properties are strongly dependent on the plasma parameters while the contribution of the ions remains about constant. The radicals have been studied by a combination of diagnostics, such as threshold ionization mass spectrometry, optical emission spectroscopy, and aperture-well experiments. These diagnostics have been applied to two parameter studies: the variation of the plasma source operation by changing the H_2 flow in the source and the variation of the downstream SiH_4 density.

II. EXPERIMENT

A. Deposition setup and plasma source operation

The deposition setup is depicted schematically in Fig. 1 and it consists of a cascaded arc plasma source and a deposition chamber. In the deposition chamber, SiH_4 is injected where it is dissociated by the reactive species emanating from the Ar-H_2 operated plasma source. The deposition setup and cascaded arc are described in detail in Ref. 16 and 17, respectively, and the conditions for the plasmas studied in this article are listed in Table I. Here only the characteristics of the plasma emanating from the plasma source will be described briefly for its different operation conditions and some striking differences between the expanding thermal plasma and conventional deposition plasmas will be given.

TABLE I. Setup conditions of the expanding thermal plasma for high rate deposition of a-Si:H.

Ar flow	55 sccs
H_2 flow	0–15 sccs
arc current	45 A
arc voltage	70–140 V
arc pressure	~400 mbar
SiH_4 flow	1–20 sccs
downstream pressure	0.18–0.20 mbar

The cascaded arc is a thermal plasma source and it is operated on a mixture of Ar and H_2, at high pressure and high gas flows [expressed in standard cubic centimeters per second (sccs)]. In the source, there is typically an electron density n_e=~10^{22} m^{-3} and an electron and heavy particle temperature T_e=T_h=~1 eV.[17] The pressure in the deposition chamber is kept low (~0.20 mbar) by means of roots blowers with a high pumping capacity. Therefore the plasma expands from the cascaded arc into the deposition chamber. Operated on pure Ar, the downstream plasma has a high electron density and relatively low electron temperature: both Thomson scattering experiments as well as Langmuir probe measurements have revealed n_e=~10^{19} m^{-3} and T_e=~0.3 eV for the presented conditions.[16,18] The dissociation of SiH_4 by electron processes is therefore negligible in comparison with dissociation reactions by reactive ionic and atomic particles. When the source is operated on pure Ar this is mainly by Ar^+.

When H_2 is admixed to the Ar in the arc, n_e in the downstream region is drastically reduced (a factor of 40 going from 0 to 10 sccs H_2) due to associative charge transfer reactions between Ar^+ and H_2 followed by dissociative recombination of the molecular ions with electrons.[13,16,19,20] T_e decreases to 0.1–0.2 eV [16,20] and the dominant ion in the downstream region changes to H^+.[16] Furthermore, the H_2 in the cascaded arc is effectively dissociated due to the high gas temperature (~1 eV) in the plasma source.[21] Consequently, for a considerable fraction of H_2 in the Ar-H_2 mixture, the cascaded arc acts predominantly as an atomic hydrogen source.

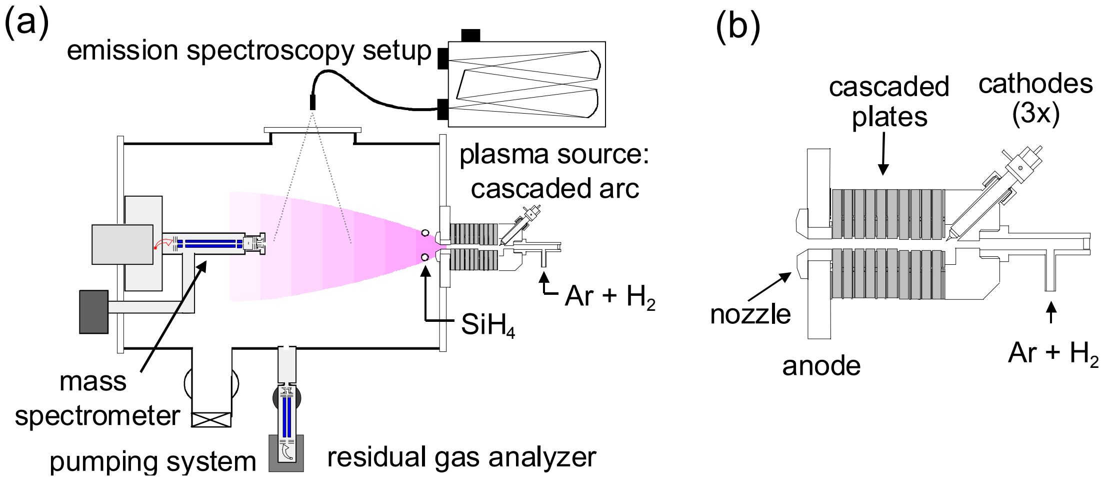

FIG. 1. (a) Schematic of the expanding thermal plasma and plasma diagnostics. The mass spectrometer is located at the usual position of the substrate holder. (b) The cascaded arc plasma source.

For different H_2 fractions, the total ion flow emanating from the arc has been determined by radial Langmuir probe measurements just after the arc exit. It revealed an ion fluence of almost 3 sccs for a pure Ar plasma and 0.08 sccs for a plasma with 10 sccs H_2.[13,16] The amount of H in the downstream region has been quantified by means of two-photon absorption laser-induced fluorescence (TALIF) under similar conditions in a different reactor.[22] The determination of the total fluence of H available for SiH_4 dissociation from these measurements is more complicated. Although it is expected that the H_2 in the cascaded arc is nearly fully dissociated, it has been shown that a significant amount of H is lost by recombination in the nozzle of the plasma source and by fast radial escape of H from the shock. The forward flow of H has been estimated at roughly 1–2 sccs for an injected H_2 flow of 10 sccs.[22]

Apart from the fact that SiH_4 is not dissociated by electrons, other important differences with conventional plasma deposition techniques are the low energy that ions gain in the plasma sheath (~1–2 eV) and the relatively high gas temperature (1000–1500 K).[23,24] The low ion energy is a consequence of the low T_e and it saves the deposited films from severe ion bombardment (additional ion energy can be obtained by applying an external rf bias on the substrate). The high gas temperature is due to the fact that the plasma is thermal in origin.

B. Threshold ionization mass spectrometry

The substrate holder has been replaced by a mass spectrometer (see Fig. 1) to analyze the flux of radicals towards the substrate. The mass spectrometer, with a similar geometry as the substrate holder, is a modified version (PSM Upgrade) of the Hiden Analytical EPIC 300, which suffered from detection of plasma photons because its detector was in direct line-of-sight with the plasma source.[16] In the upgrade, the detector is blocked from photons from the source by adding a Bessel box type of energy analyzer. Gas extraction takes place by a knife-edged extraction orifice with a diameter and thickness of 50 μm. This leads to an effusive flow of the plasma species in the mass spectrometer, which is differentially pumped by a 56 ℓ/s turbo-pump. During plasma operation with a typical pressure of 0.20 mbar, the pressure in the mass spectrometer is within the range 7×10^{-7}–10^{-6} mbar. The ionizer region with the filament is located at about 24 mm from the extraction orifice. The linear filament is made of thoriated iridium and yields a high electron emission current I_e at relatively low temperatures: I_e is actively controlled at 50 μA corresponding with a filament temperature of about 1800 K. Behind the ionizer the Bessel box is located which is followed by the mass filter (with rf driven pre- and post-filter) and a channeltron (DeTech 415).

To distinguish ionization of radicals in the mass spectrometer from dissociative ionization of SiH_4 the threshold ionization or appearance potential method has been used. This method is described in detail in the literature.[25,26] Briefly, the energy of the electrons emitted by the filament is scanned in the vicinity of the ionization potential of the radical of interest, while monitoring the intensity at the radical's mass-over-charge ratio. At electron energies E higher than the ionization potential E_i of the radical but lower than the potential for dissociative ionization of the parent molecule into the specific ionic channel (appearance potential E_a), the measured intensity $I(E)$ is a measure for the radical density n in the plasma

$$I(E) = \alpha I_e \sigma(E) n \quad \text{with} \quad E_i < E < E_a \tag{1}$$

with $\sigma(E)$ the cross-section for ionization and α a geometry and mass dependent proportionality constant. The measured radical intensity is corrected for the contribution by pyrolysis, i.e., thermal decomposition, of SiH_4 on the filament by subtracting the signal at $E<E_a$ obtained for the "plasma off" condition. Herein, differences in the SiH_4 signal at $E>>E_a$ during "plasma on" and "plasma off" (due to SiH_4 consumption and/or gas temperature effects) are taken into account.[27]

Quantification of the radical density takes place by linking the radical intensity to the measured intensity of the parent SiH_4 molecule at $E>>E_a$.[25,26] The latter can directly be related to the known partial pressure of SiH_4 during "plasma off". In this method, besides the difference in cross-sections for electron-induced ionization of the radical and parent molecule (at the appropriate electron energies), also the difference in surface reactivity should be taken into account. SiH_4 is not reactive and will lead to a residual partial pressure in the mass spectrometer whereas silane radicals SiH_x are rather reactive[28] and are easily lost on their way to and in the ionizer. Therefore, practically only SiH_x radicals in the beam of the effusive flux that reaches the ionizer without wall-collisions (determined by the acceptance angle) contribute to the SiH_x intensity (beam component) whereas the measured intensity for SiH_4 has both a beam and residual density component. This difference can be taken into account by a correction factor C that can be estimated from the density n_{beam} of SiH_4 in the beam originating directly from the extraction orifice and the density n_{res} of residual SiH_4 at the position of the ionizer

$$C = \frac{n_{beam} + n_{res}}{n_{beam}}. \tag{2}$$

For a SiH_4 density n and a thermal velocity v in front of the extraction orifice with area A, these densities in the ionizer at a position l from the extraction orifice are given by[29]

$$n_{beam} = \frac{nA}{4\pi l^2} \quad \text{and} \quad n_{res} = \frac{\frac{1}{4}nvA}{S} \tag{3}$$

where S is the pumping speed for SiH_4 at the position of the ionizer. For the present setup, this yields $C\approx35$ when using $S=56$ ℓ/s. This high value of C means that the residual SiH_4 density in the ionizer is much higher than the density of SiH_4 in the beam directly originating from the extraction orifice. The residual gas density in the ionizer can be reduced by applying double partial pumping as done by Kae-Nune *et al.*[26] Furthermore, our case differs from the one described by Singh *et al.*[30] by the fact that for silane radicals the surface loss probability is much higher than for the radicals studied in their work.

In this procedure it is important that the emission current I_e is independent of electron energy E. This requires that I_e is controlled at rather low currents because at higher currents space charge can easily build up around the filament for low E values, as described by the Child-Langmuir law. This can cause I_e to deviate considerably from the demanded I_e and to depend on E. This effect has experimentally been investigated yielding that for I_e=50 μA the influence of space charge is negligible down to E=5 eV.

Furthermore, space charge effects, as well as the thermal energy distribution of emitted electrons, the potential drop along the filament, and contact and surface potentials of the electrodes lead to an electron energy that is not purely mono-energetic. This causes an apparent onset of the signal below the ionization potential and troubles the determination of the ionization potential and/or calibration of the electron energy scale. For the Hiden system the half-width-half-maximum value is estimated to be within 0.5 eV. The electron energy scale has been calibrated by means of the ionization potential of noble gases and applying the commonly used linear extrapolation method.[31] This revealed that the electron energies are ~1.4 eV lower than indicated by the energy scale.

C. Emission spectroscopy

Emission spectroscopy has been applied to monitor the emission by excited SiH and Si radicals. For SiH the A $^2\Delta$–X $^2\Pi$ electronic transition band at around 414 nm has been analyzed and for Si I the 4s $^1P_1^0$–3p^2 $^1S_0$ transition at 390.6 nm. The emission spectroscopy setup is a modified version of the one described in Ref. 32, which dealt with measurements under less relevant plasma conditions in terms of resulting a-Si:H quality. By means of a high grade fused silica fiber (Oriel 77532) the total (i.e., non-local) emission by the plasma in the region from the substrate up to ~20 cm upstream has been collected and focussed on a Czerny-Turner monochromator (Jobin-Yvon HR 640) with a focal length of 640 mm and a dispersion of 1 nm/mm. The entrance slit used is 250 μm and a CCD camera (SBIG ST-6 Optohead), recording a wavelength range of ~11 nm, has been used as detector.

Emission by Ar in a pure Ar plasma is used as a reference to correct for reduced transmission due to deposition on the spectroscopic window. Furthermore, the integration time is chosen such that the correction for this reduced transmission is rather constant for the different plasma conditions. Moreover, the reactor is cleaned by means of an Ar-CF_4 plasma after every measurement.

Only non-local and relative measurements of the emission intensity have been performed. From fitting simulations of the SiH emission spectrum to the experimental data the vibrational and rotational temperatures of the excited radical have been extracted. This technique, explored by Perrin and Delafosse,[33] is applied by using an improved version of the program described in Ref. 32.

D. Other diagnostics

The other diagnostics will be presented only briefly as they are described extensively in previous articles. The depletion or net consumption of SiH_4 for the different plasma conditions has been determined by a residual gas analyzer (Balzers Prisma QMS 200) located at the side of the deposition chamber. The difference in the measured signal I due to SiH_4 (at m/e =28–32) when the plasma is on and off can be attributed completely to the consumption of SiH_4.[13] The equivalent flow of SiH_4 that is consumed by the plasma $\Phi_{SiH_4,cons}$, is calculated by multiplying the fraction of SiH_4 that is consumed with the initial SiH_4 flow Φ_{SiH_4}

$$\Phi_{SiH_4,cons} = \left(\frac{I_{off} - I_{on}}{I_{off}}\right)\Phi_{SiH_4} . \tag{4}$$

The overall surface reaction probability of the species contributing to growth has been determined from so-called "aperture-well" experiments.[28,34] This technique uses a well, created by two substrates, in which reactive particles from the plasma entering through a small slit in the upper substrate are trapped. From the distribution of the amount of film deposited on both substrates an overall surface reaction probability β_o can be calculated, which depends on the relative fluxes of the reactive species entering the well and each of their particular surface reaction probabilities β. More information can be found in Ref. 28.

III. RESULTS

A. H_2 flow series

In this section, the dissociation of SiH_4 is considered for different operating regimes of the cascaded arc as presented in Sec. II A. The SiH_4 flow is kept fixed at 10 sccs. The net consumed SiH_4 flow is given in Fig. 2 as a function of the H_2 flow in the cascaded arc. For zero H_2 flow, the SiH_4 consumption is very large (~60 %). This can be attributed to ion-induced reactions as mainly Ar^+ emanates from the plasma source. For increasing H_2 admixture the SiH_4 consumption first decreases due to decreasing ion fluence, while for H_2 flows >3 sccs the reactions with H take over. From that point, the SiH_4 consumption increases slightly due to an increasing H flow from the arc. Apparently the consumption of SiH_4 for the H-dominated region is lower than for the ion-dominated region. In Fig. 2, also the corresponding deposition rate for a substrate temperature of 400 ºC is given. From the fact that the deposition rate (when corrected for the Si atomic film density) scales very well with the consumption of SiH_4 it can be concluded that the consumed SiH_4 is mostly converted into a-Si:H and not into polysilanes, as also corroborated by the small fraction of Si_2H_6 and Si_3H_8 observed.[13,16]

At high H_2 flows, it is expected that mainly SiH_3 will be created as the reaction of H with SiH_4 leads to hydrogen abstraction of SiH_4

$$H + SiH_4 \rightarrow SiH_3 + H_2. \tag{5}$$

The rate of this reaction is $1.8\times10^{-16}\exp(-1925/T)$ m^3s^{-1} for a gas temperature T (in K) in the range 290–660 K. At higher temperatures, rates higher than predicted from this relation have been proposed.[35] Therefore SiH_3 has been measured by threshold ionization mass spectrometry. An electron energy scan at m/e=31 corresponding with the SiH_3^+ ion is given in Fig. 3. The used integration time per step in E is 1.5 s. At low values of E a hump due to direct ionization of SiH_3 can clearly be seen, while at higher energies the signal due to dissociative ionization of SiH_4 comes up. The depicted electron energy scale is not re-scaled, and the too high ionization and appearance potential of SiH_3 and SiH_4 are in fair agreement with the shift of +1.4 eV obtained from the calibration procedure. For high E, the signal for “plasma on” is normalized to the one for “plasma off” such that the signal for “plasma off” due to pyrolysis (at $E<E_a$) can be subtracted directly from the radical signal.

The densities of SiH_3 obtained for different H_2 flows in the arc are given in Fig. 4(a). A complication arises from the fact that the gas extraction orifice becomes easily clogged due to the high deposition rate. This is (partially) circumvented by monitoring a reference signal, but especially the SiH_3 measurements at very low H_2 flows, with deposition rates up to 60 nm/s, were cumbersome. The absolute values of the SiH_3 densities have been estimated by the method described in Sec. II B. The partial ionization cross sections of SiH_4 have been taken from Ref. 36. Information about ionization cross-sections for SiH_x radicals is only recently available from work by Tarnovsky *et al.* who determined ionization cross sections for SiD_x radicals.[37] The latter cross-sections for SiD_3 and SiD_2 radicals at E=10 eV are, respectively, a factor of ~4 smaller and ~2 larger than those estimated by Kae-Nune *et al.*[26] from ionization cross sections of CD_x radicals.[38,39] We note that the absolute scale of the SiH_3 density in Fig. 4(a) has a

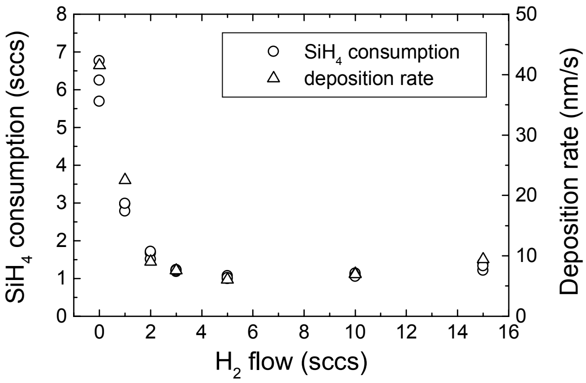

FIG. 2. Consumption of SiH_4, expressed in equivalent flow, as a function of H_2 admixture in the cascaded arc. The SiH_4 flow is 10 sccs. The corresponding deposition rate for a substrate temperature of 400 °C is given on the right axis.

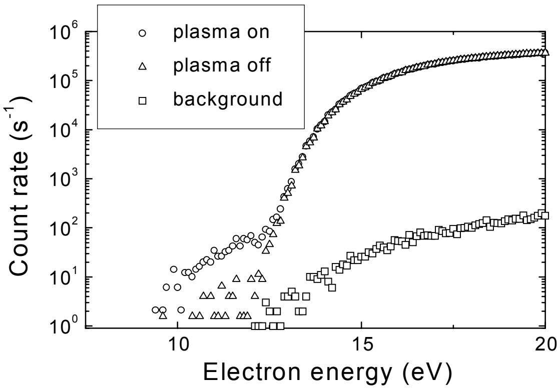

FIG. 3. Electron energy scan at m/e=31 for determination of the SiH_3 density. The values for “plasma off” are normalized to those of “plasma on” at high electron energies. Both the H_2 and SiH_4 flow are 10 sccs. The background signal, obtained with SiH_4 flow = 0 sccs, is due to an (unknown) contaminant in the mass spectrometer.

considerable uncertainty, mainly due to the uncertainty in the pumping speed S (and consequently C) for SiH_4 at the position of the ionizer.

The SiH_3 density shows a steep decrease going from zero to a small H_2 flow, followed by a gradual increase for higher H_2 flows. The latter increase is in agreement with an increasing flow of H from the cascaded arc. For the interpretation of the SiH_3 density at low H_2 flows it is important to realize that at these flows much more SiH_4 is consumed. The SiH_3 density at 0 sccs H_2 is about equal to the one at 15 sccs H_2, yet the net consumed SiH_4 flow is at least a factor of four higher. It is therefore better to consider the contribution of SiH_3 to film growth. Determination of the absolute value of the contribution from the densities[26] in Fig. 4(a) is however cumbersome. First, there are uncertainties in the absolute density itself. Second, estimations on the thermal velocity v and sticking probability s of SiH_3 are required, where especially s is not accurately known within a factor of two. Therefore another method is proposed which is, to our opinion, more reliable, however, not generally applicable: as the increase of the H_2 flow from 10 to 15 sccs leads only to more H from the arc (the ion flow decreases slightly),[16] it is plausible that the *increase* in SiH_4 consumption and a-Si:H deposition rate between 10 and 15 sccs (see Fig. 2) is completely due to a higher SiH_3 density. Linking the increase in deposition rate to the increase in SiH_3 signal, a direct relation between SiH_3 signal and the deposition rate is obtained, from which the contribution of SiH_3 to film growth, as given in Fig. 4(b), can be calculated. The absolute value of the presented contribution relies, of course, fully on the above-mentioned assumption with respect to the increase in deposition rate between 10 and 15 sccs H_2. However, as will shown below, this assumption is also plausible on the basis of the other results with respect to the plasma chemistry and the surface reaction probability. It is therefore expected that the presented values of the absolute contribution are much more accurate than estimations on the basis of the SiH_3 density. We note however, that both methods yield the same relative dependence of the contribution of SiH_3 to film growth, while the absolute values of the contributions in Fig. 4(b) are not in contradiction with those calculated from the SiH_3 densities in Fig. 4(a) when reasonable values for v and s of SiH_3 are applied. In Fig. 4(b), there is still some uncertainty in the exact contribution, mainly due to the fact that the deposition rate and SiH_3 density have been determined in different experiments, but it is clear that the contribution of SiH_3 increases with H_2 flow and saturates at higher H_2 flows (where it dominates film growth with a contribution of around 90%).

Figure 4(b) shows that at low H_2 flows, other species than SiH_3 contribute significantly to film growth. As mentioned above, at these flows SiH_4 dissociation is governed by reactions induced by positive ions emanating from the plasma source. Ar^+ and H^+ can undergo dissociative charge exchange with SiH_4 leading to silane ions SiH_n^+ ($n \le 3$, SiH_4^+ is unstable[40])

$$Ar^+ (H^+) + SiH_4 \rightarrow SiH_n^+ + pH_2 + qH + Ar \quad (n \le 3). \qquad (6)$$

The reported reaction rates $k_{ch.ex.}$ for Ar^+ are in the order of 10^{-16} m^3s^{-1} and at thermal energies mainly SiH_3^+ is created.[40] For H^+ only a rate for the reaction leading to SiH_3^+ has been proposed which is equal to 5×10^{-15} m^3s^{-1}.[40] Silane ions initiate cationic cluster $Si_nH_m^+$ formation by sequential ion-molecule reactions with SiH_4[15,16,41]

$$Si_nH_m^+ + SiH_4 \rightarrow Si_{n+1}H_p^+ + qH_2 \qquad (7)$$

with rates $k_{ion\text{-}mol}$ estimated at $\sim 10^{-16}$ m^3s^{-1}. It has been shown that the contribution of the positive ions to film growth is less than 10% in terms of Si atoms deposited.[16] The previously used assumption that s=1 for these ions has recently been justified by molecular dynamics studies which yielded s>0.85 for all types of

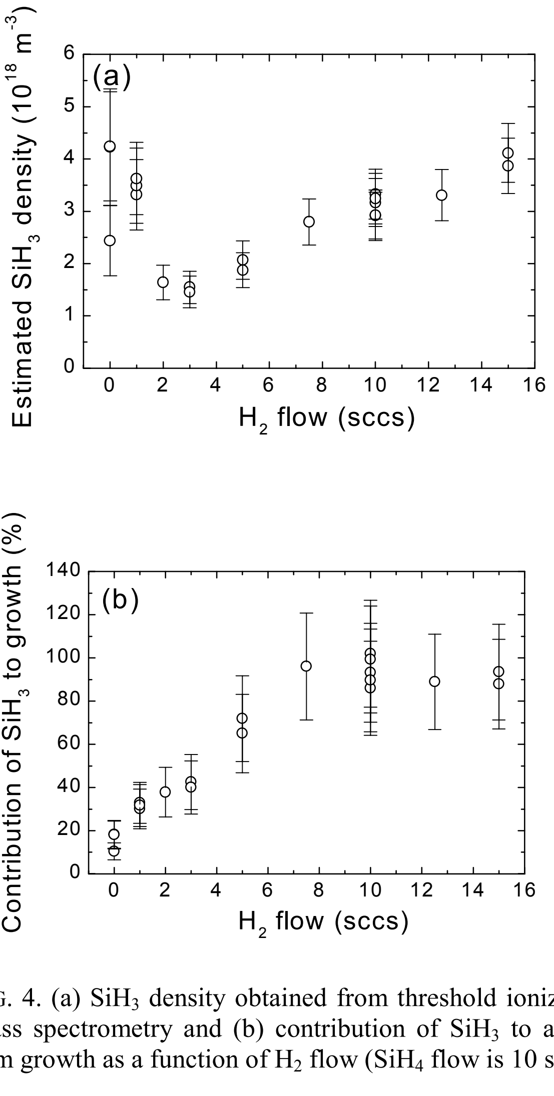

FIG. 4. (a) SiH_3 density obtained from threshold ionization mass spectrometry and (b) contribution of SiH_3 to a-Si:H film growth as a function of H_2 flow (SiH_4 flow is 10 sccs).

hydrogenated Si surfaces.[42] Remarkable is that the contribution of the ions is rather independent of the H_2 flow admixed in the arc while the ion fluence from the arc is heavily dependent on this H_2 flow.[16] This can be understood from dissociative recombination reactions of silane ions with electrons

$$SiH_n^+ + e \rightarrow SiH_m + pH + qH_2 \quad (n\leq 2) \qquad (8)$$

with reaction rates k_{rec} in the order of $10^{-13}T_e^{-1/2}$ m^3s^{-1} (T_e in eV).[40] These reactions compete with the ion-molecule reactions (7), but as long as the product of the reaction rate for dissociative recombination and the electron density is much larger than the product of the reaction rate for ion-molecule reactions and the SiH_4 density, i.e., $k_{rec}\, n_e >> k_{ion\text{-}mol}\, n_{SiH4}$, dissociative recombination will prevail. This is certainly the case at low H_2 flows where n_e is high.[16] For these conditions dissociative recombination reactions occur almost instantaneously after reaction (6), leading to a significant production of radicals like SiH_2, SiH, and Si. The rather constant contribution of the cationic clusters is explained by the fact that the ion-molecule reactions can only get important when n_e is significantly reduced by reaction (8). For a SiH_4 density of $\sim 10^{20}$ m^{-3} this is expected to occur at $n_e \approx 10^{17}$ m^{-3}. This value is roughly equal to the value of n_e at higher H_2 flows.

From reaction (6) and (8), the relatively high SiH_3 density at low H_2 flows can also be understood. In both reactions, H can be generated that subsequently can react with SiH_4 creating SiH_3 [reaction (5)]. This can lead to a considerable density of SiH_3 under conditions where the SiH_4 consumption is high and it explains the initial decrease of the SiH_3 density at low H_2 flows. Another possible reaction that can generate SiH_3 from the reaction products of reaction (6) is

$$SiH_2^+ + SiH_4 \quad \rightarrow \quad SiH_3^+ + SiH_3. \qquad (9)$$

On the basis of the aforementioned reasoning, this reaction with a rate of $\sim 10^{-15}$ m^3s^{-1} [40] will become as important as dissociative recombination when n_e is reduced to $\sim 10^{18}$ m^{-3}.

In order to measure the radicals created in reaction (8) threshold ionization mass spectrometry has been applied. SiH_2 radicals could only be detected for H_2=0 sccs where the SiH_2 production is also expected to be at maximum. As shown in Fig. 5, the radical signal is rather weak (an estimation of the density on the basis of the procedure described in Sec. II B yields $\sim 10^{18}$ m^{-3} at 0 sccs H_2) and the SiH_2 density in front of the substrate holder is apparently too low for the measurements at non-zero H_2 flows. It should be noted that detection of SiH_2 is more complicated than the detection of SiH_3. First, SiH_2 has a higher surface reaction probability than SiH_3,[28] which can lead to a higher loss of SiH_2 during extraction from the plasma. Second, the difference between the ionization potential of SiH_2 and the appearance potential of SiH_2^+ from SiH_4 is smaller,[26] while at m/e=30 a strong residual signal due to contamination in the mass spectrometer appears at slightly lower electron energies than the appearance potential (see Fig. 5). This residual signal, which is not related to the SiH_4 flow, is measured in pure Ar. Although its origin is still unclear, NO^+ created by ionization of NO is a likely candidate. This radical, possibly created at the hot filament from residual N_2 and O_2, has an ionization potential around 10 eV.[43]

The presence of contamination together with a relatively low density in front of the mass spectrometer are probably also the reasons why SiH and Si radicals could not be detected. The low radical densities can be due to a small production rate or to a large loss rate, e.g., by fast reactions with SiH_4 as will be addressed in Sec. IV. Furthermore, for the present setup the detection limit of the radicals is rather high due to the interfering high residual gas density in the mass spectrometer as discussed in Sec. II B.

Although the reaction pathway proposed is not counter to the fact that SiH_2 has only been detected for 0 sccs H_2 and that SiH and Si could not be observed at all, optical emission spectroscopy has been applied to find more confirmation. The A $^2\Delta$–X $^2\Pi$ electronic transition band of SiH at ~414 nm and the 4s $^1P_1^0$–3p^2 $^1S_0$ transition at 390.6 nm, represented by SiH* and Si*, respectively, have been studied. Unlike conventional plasmas, T_e in the downstream region is too low for the creation of these electronically excited species by electron-induced excitation or dissociation to be significant. Accordingly, Si* and SiH* are mainly created by dissociative recombination of SiH_n^+ with electrons [reaction (8)], where enough energy is available for electronic excitation of the produced

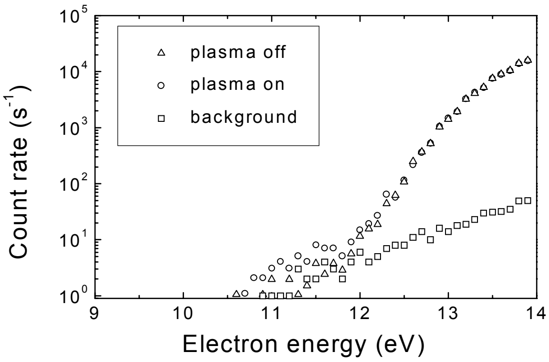

FIG. 5. Electron energy scan at m/e=30 for detection of SiH_2. The values for “plasma off” are normalized to those of “plasma on” at high electron energies. The H_2 flow is 0 sccs and SiH_4 flow 10 sccs. The background signal, obtained with SiH_4 flow = 0 sccs, is due to a contaminant in the mass spectrometer.

silane radicals. Therefore it is believed that the emission of these excited species is an indication of the occurrence of reaction (8). Because of their fast radiative decay (radiative lifetime τ for Si I 4s $^1P_1^0$ and SiH A $^2\Delta$ is 4.1 ns and 534 ns, respectively[44]) their emission is expected to be proportional to the number of recombination events. On the basis of this, the emission intensity per unit of time displayed in Fig. 6(a), reveals that more dissociative recombination reactions take place at low H_2 flows when more ions emanate from the arc. The fact that both the SiH* and Si* emission show the same dependence validates the assumption that a fixed percentage (i.e., independent of H_2 flow) of the reaction products in reaction (8) are SiH* and Si*. In Fig. 6(b), the emission intensity is corrected for the total amount of SiH_4 consumed showing that reactions (6) and (8) are, relatively, more important at low H_2 flows, in agreement with the reaction pathway proposed.

The assumption that the emission by SiH* and Si* displays in fact the recombination of silane ions can roughly be validated by relating the emission intensity to the ion fluence from the arc. From stationary rate equations for reactions (6), (7), and (8) a local radiative decay rate for the excited species can be calculated

$$\frac{n_{\mathrm{SiH}x^*}}{\tau} = \frac{n_{\mathrm{Ar^+/H^+}}\, n_{\mathrm{SiH4}}\, k_{ch.ex.}}{n_e k_{rec} + n_{\mathrm{SiH4}}\, k_{ion-mol}}\, n_e k_{rec} \qquad (10)$$

where $n_{\mathrm{SiH}x^*}$ is the density of the excited species and $n_{\mathrm{Ar^+/H^+}}$ the density of Ar^+ and H^+ from the arc. At low H_2 flows the ion-molecule reactions (second term in denominator) can be neglected compared to dissociative recombination leading to a radiative decay rate linear in the Ar^+/H^+ ion density. Assuming a similar *global* behavior, it is expected that at low H_2 flows the total radiative decay rate is linear in the ion fluence from the arc. This is indeed true for the emission intensity per unit of time (integrated over a large part of the downstream region) as can be seen in Fig. 7 where the slope of the fit in the double-log plot is almost equal to one (0.90).

The rotational and vibrational temperatures of the excited SiH radical are shown in Fig. 8 and do not show a clear dependence on the H_2 flow. This implies an excitation mechanism that is independent of the H_2 flow. The vibrational temperature is around 3000 K and the rotational temperature is between 1400 and 1500 K. The gas temperatures in the expanding thermal plasma are in the range 1000–1500 K.[23,24]

The increasing contribution of SiH_3 and the decreasing production of SiH_x ($x\leq 2$) radicals for increasing H_2 flow are expected to affect the overall surface reaction probability β_o. For SiH_3 the reported values of surface reaction probability β are within the range 0.1–0.3, while for SiH_x ($x\leq 2$) values in the range 0.6–1 have been reported.[28] The difference in these β values explains the decrease of β_o with increasing H_2 flow as shown in Fig. 9. Values of β_o estimated on the basis of the presented contributions of SiH_3 and $Si_nH_m^+$

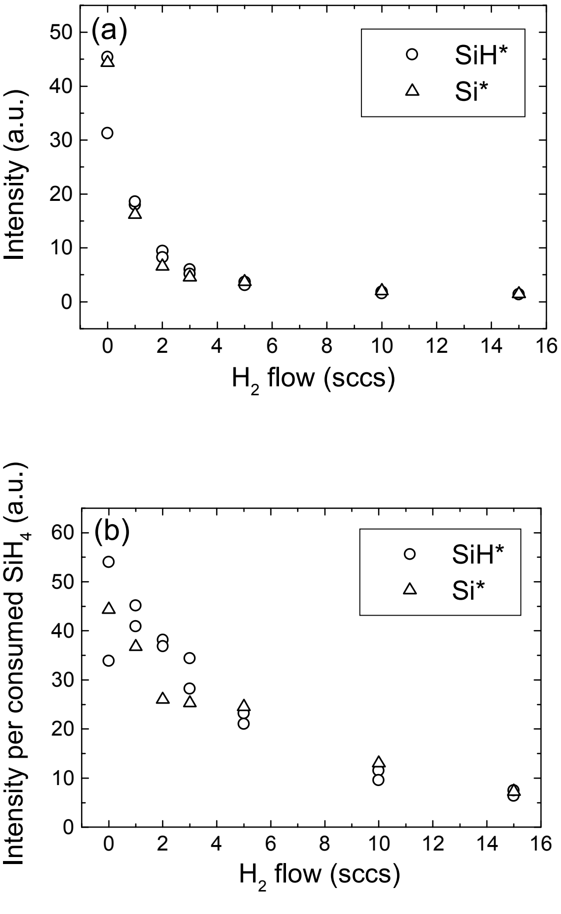

FIG. 6. (a) Emission intensity of SiH* (A $^2\Delta$–X $^2\Pi$) and Si* (4s $^1P_1^0$–3p^2 $^1S_0$) per unit of time. The SiH_4 flow is 10 sccs. (b) Emission intensity divided by SiH_4 consumption (in arbitrary units).

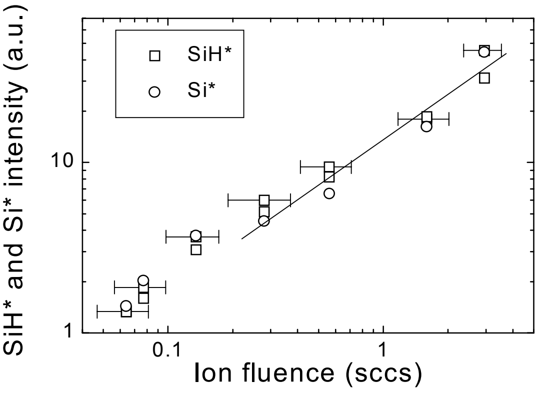

FIG. 7. Emission intensity of SiH* and Si* from Fig. 6(a) as a function of the ion fluence emanating from the arc. The line is a fit to the data points for H_2 <5 sccs where the ion-molecule reactions can be neglected compared to dissociative recombination reactions.

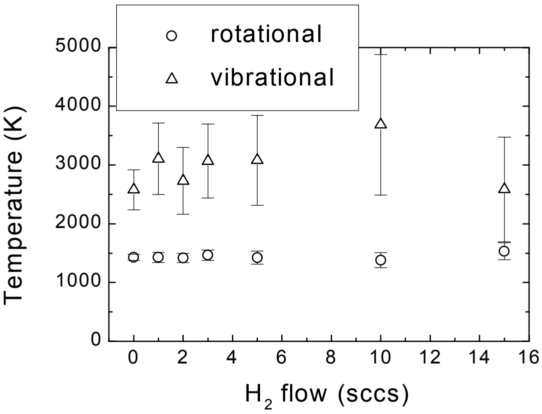

FIG. 8. Vibrational and rotational temperature of SiH* obtained from a fit to the experimental spectrum of the $A\,^2\Delta – X\,^2\Pi$ transition. The SiH_4 flow is 10 sccs.

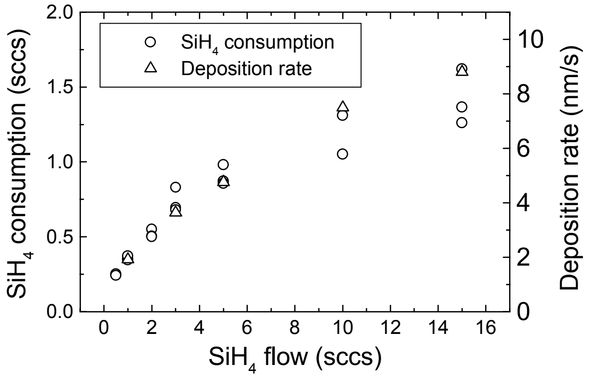

FIG. 10. Consumption of SiH_4, expressed in equivalent flow, for a constant H_2 flow (10 sccs) in the arc. The corresponding deposition rate for a substrate temperature of 400 °C is given on the right axis.

and the presented production of SiH_x ($x \le 2$) radicals are also given in Fig. 9. These values are determined by the procedure described in Ref. 28 using $s=\beta=0.28$ for SiH_3, $s=\beta=1$ for $Si_nH_m^+$, and $s=\beta=0.6$ for SiH_x ($x \le 2$), all independent of the H_2 flow. The values obtained from this simplified estimation show fairly good agreement. The rather low β which needs to be assumed for SiH_x ($x \le 2$) can possibly be explained by the fact that these radicals are very reactive with SiH_4 and can have reacted to polysilane radicals, with possibly a lower β, before reaching the substrate (see Sec. IV).

B. SiH_4 flow series

The influence of the partial pressure of SiH_4 on the plasma processes has been studied by varying the SiH_4 flow while keeping the plasma source conditions fixed. The H_2 flow in the arc is set at 10 sccs because for this condition mainly H emanates from the source and the best a-Si:H film properties have been obtained.

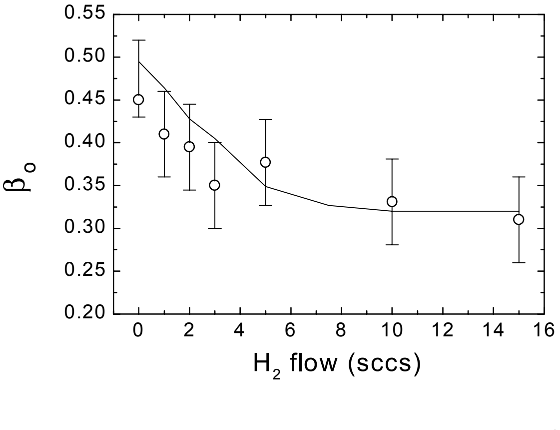

FIG. 9. The overall surface reaction probability β_o as determined from aperture-well experiments for 10 sccs SiH_4 and varying H_2 flows. The line represents estimations of β_o on the basis of the contributions of the different species to film growth. Further explanation is given in the text.

The consumed SiH_4 flow and corresponding deposition rate are given in Fig. 10. The SiH_4 consumption increases with SiH_4 flow and its dependence on the SiH_4 flow can roughly be divided into two regions. Up to ~3 sccs the increase is steeper than at higher flows where the SiH_4 consumption increases only gradually with SiH_4 flow. It means that at low SiH_4 flows a larger fraction of the SiH_4 is consumed than at higher flows. This behavior suggests that the amount of H available for SiH_4 dissociation is the limiting factor whereas the total flow of SiH_4 consumed at high SiH_4 flows is about equal to the forward flow of H as estimated from the TALIF measurements (see Sec. II A). These observations corroborate that a considerable amount of H from the cascaded arc is lost before the H can dissociate SiH_4.[22]

In Fig. 11(a), the SiH_3 density is given showing the same dependence on the SiH_4 flow as the SiH_4 consumption in Fig. 10. Consequently, the contribution of SiH_3 to film growth as shown in Fig. 11(b) and calculated by the method described in Sec. III A is fairly constant for the different SiH_4 flows. This means that SiH_3 dominates film growth independent of the SiH_4 flow and for deposition rates ranging from 1 to 10 nm/s.

The rather constant contribution of SiH_3 has implications for reactions that affect the SiH_3 density. Hydrogen abstraction by H from SiH_3

$$H + SiH_3 \quad \rightarrow \quad SiH_2 + H_2 \qquad (11)$$

has a considerable reaction rate at 300 K (2×10^{-17} m^3s^{-1})[45] in comparison with reaction (5), and the rate for the disproportion reaction between two SiH_3 radicals

$$SiH_3 + SiH_3 \rightarrow SiH_2 + SiH_4 \qquad (12)$$

is even higher (~10^{-16} m^3s^{-1} at 300 K).[40,45] These reactions lead to SiH_2 production and especially reaction (12) can become very important at high SiH_4 flows as it is quadratically dependent on the SiH_3 density. These reactions are apparently not very important, as they would lead to an increasing contribution of SiH_2 [or its reaction products (polysilane radicals) with SiH_4] to film growth at the expense of the contribution of SiH_3. This is not obvious in Fig. 11(b).

The missing fraction of film growth in Fig. 11(b) takes place by positive ions and radicals other than SiH_3. As addressed in Ref. 15 and 16, the contribution of ions is almost independent of the SiH_4 flow and less than 7%, while the average number of Si atoms per ion increases with increasing SiH_4 flow. The ion size has implications for the products created by dissociative recombination of the ions. Although less frequent, recombination will still take place under this condition with relatively low n_e and it is expected that the rate for dissociative recombination of the ions with electrons does not heavily depend on the size of the ions.[16,40] At low SiH_4 flows there are relatively more silane ions SiH_n^+ and their recombination leads to SiH_x ($x \leq 2$) radicals (and thus to SiH* and Si*), while the recombination of the cationic clusters at larger SiH_4 flows most probably leads to larger neutral fragments. It is therefore expected that the emission of SiH* and Si* is relatively stronger at low SiH_4 flows. This is indeed the case as can be seen in Fig. 12, providing more evidence for the reaction pathway for cationic cluster formation proposed in Ref. 15. Furthermore, the rotational and vibrational temperature of the excited SiH radical (not shown) do not show a clear dependence on the SiH_4 flow and are about 1500 K and 3000 K, respectively, like in Fig. 8.

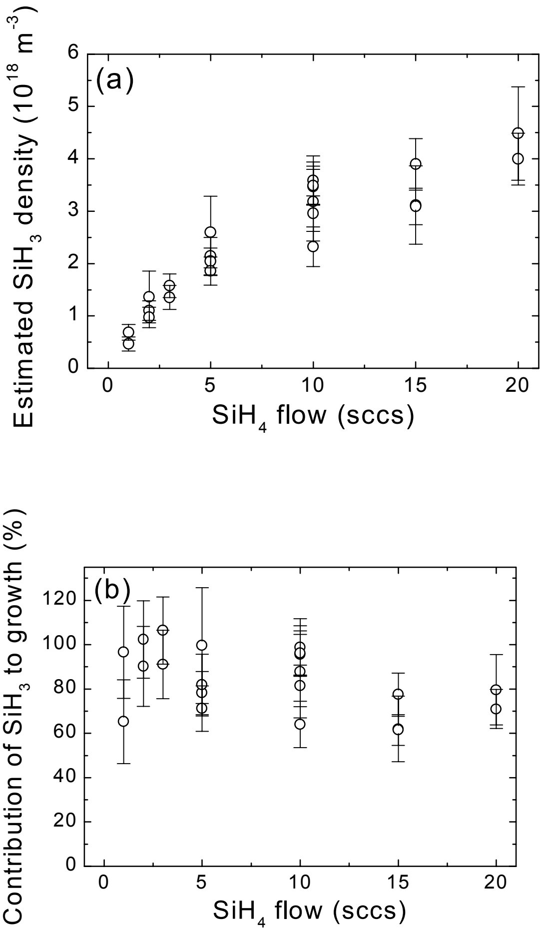

FIG. 11. (a) SiH_3 density obtained from threshold ionization mass spectrometry and (b) contribution of SiH_3 to a-Si:H film growth as a function of SiH_4 flow (H_2 flow is 10 sccs).

IV. DISCUSSION

From the combination of the results obtained by the different diagnostics, the dissociation mechanisms of SiH_4 in the expanding thermal plasma are fairly well understood. For the H_2 flow series, it is convincingly shown that the contribution of SiH_3 increases with increasing H_2 flow and becomes constant for H_2 flows >7.5 sccs. This is independent of the assumption used to determine the absolute contribution to film growth (see Sec. III A). This particular assumption, which leads to the conclusion that SiH_3 dominates the deposition process for high H_2 flows with an estimated absolute contribution of ~90%, seems however very plausible and is corroborated by the value of the overall surface probability β_o of ~0.3 at high H_2 flows. The absolute SiH_3 density in Fig. 4(a) can fully account for the presented contribution of SiH_3 to film growth, but the calculation of the contribution of SiH_3 on the basis of this density leaves too much freedom in the absolute value due to uncertainties in the absolute density of

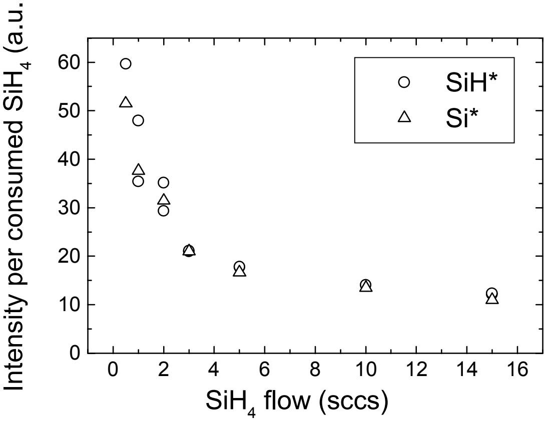

FIG. 12. Emission intensity of SiH* (A $^2\Delta$–X $^2\Pi$) and Si* (4s $^1P_1^0$–3p^2 $^1S_0$) per unit of time and divided by SiH_4 consumption (in arbitrary units). H_2 flow is fixed at 10 sccs.

SiH_3 itself [mainly due to the factor C, see Eq. (2)] as well as in v and s. It is therefore expected that the presented method is much more accurate, although the estimation of the exact contribution is, of course, very sensitive on the accuracy and reproducibility of the deposition rate and SiH_3 signal.

At lower H_2 flows, it is shown that there needs to be a significant contribution of radicals other than SiH_3 as the contribution of positive ions does not compensate for the lower contribution of SiH_3. Figure 6 suggests that the production of SiH_x ($x \leq 2$) from dissociative recombination is about a factor of six larger at 0 sccs H_2 than at 10 sccs H_2. This difference roughly compensates the decrease in contribution of SiH_3 as shown in Fig. 4(b) but it is premature to conclude that SiH_x ($x \leq 2$) radicals govern film growth at low H_2 flows. First of all, the emission intensity in Fig. 6 is not collected in the whole deposition chamber making it difficult to speculate about how much more recombination events take place at low H_2 flows. Secondly, in the determination of the contribution of SiH_3 it is assumed that β and s of SiH_3 are independent of the H_2 flow. It can however not be excluded that β and s are somewhat higher at low H_2 flows due to a higher reactivity of the a-Si:H surface. For example, the higher contribution of SiH_x ($x \leq 2$) radicals can lead to more surface dangling bonds. This would also contribute to the increase of β_o in Fig. 9. But most important is that the emission intensity is only an indication of the recombination of silane ions. It does not reveal information on the specific species created and finally contributing to film growth. As mentioned before, the radicals produced in reaction (8) have a rather high reactivity with SiH_4 and can be converted into other species before reaching the substrate or wall. In contrast with SiH_3, which is not very reactive with SiH_4 (reaction rate $<4\times10^{-20}$ m^3s^{-1} at 300 K),[45] reaction rates in the order 10^{-16}–10^{-17} m^3s^{-1} (at ~0.2 mbar and 300 K)[40,46,47] have been proposed for SiH_2, SiH, and Si. This means that for a typical SiH_4 density of ~10^{20} m^{-3}, the radicals have reacted with SiH_4 within 50–500 μs and this is shorter than the transport time of the radicals to the substrate (~500–1000 μs). This shows that the influence of the radicals created from reaction (8) cannot be derived simply from Fig. 6 and that additional, more extensive investigations are required.

Although still some questions remain unanswered, a correlation between the reaction products of SiH_4 dissociation and the a-Si:H film quality can already be made. This will be discussed only briefly, as it will be addressed more extensively in another article where also the film properties for the different plasma conditions are given.[14] As mentioned earlier, a considerable H_2 flow in the arc is necessary to obtain good film properties (the optimum film quality is obtained with 10 sccs H_2 and 10 sccs SiH_4 flow) showing the importance of the contribution of SiH_3 to film growth. The opto-electronic film properties depend strongly on the H_2 flow while the structural film properties only become inferior at very low H_2 flows (<2 sccs). Under these conditions, a-Si:H is obtained that contains a considerable void fraction. This can be understood from a significant contribution of radicals with a very high β and is also in line with the higher surface roughness of the films as obtained by *in situ* ellipsometry.[48] That film growth dominated by SiH_3 does not automatically lead to good film quality can be seen from the deterioration of the film properties for decreasing SiH_4 flow. Under these conditions, the contribution of SiH_3 to film growth is about constant while both structural and opto-electronic properties are inferior at low SiH_4 flows (<3 sccs). This is less understood, but it can possibly be attributed to the fact that at low SiH_4 flows the reaction products from dissociative recombination are smaller. Their impact on the film quality could be different from the impact of larger neutral fragments created by recombination of cationic clusters at larger SiH_4 flows. For example, the small Si and SiH radicals can penetrate the subsurface region[49] and introduce dangling bonds into the film, which can degrade the film properties.

V. CONCLUSION

The dissociation of SiH_4 in the expanding thermal plasma used for high rate deposition of device quality a-Si:H has been investigated by different plasma diagnostics. The density of SiH_3 has been determined by threshold ionization mass spectrometry and the contribution of SiH_3 to a-Si:H film growth has been determined without using estimates on the SiH_3 thermal velocity and sticking probability. It has been shown that at high H_2 flows SiH_4 dissociation mainly takes place by hydrogen abstraction by H emanating from the Ar-H_2 operated plasma source. Under these conditions, film growth is dominated by SiH_3 (estimated contribution ~90%) and the best a-Si:H film quality is obtained.

The contribution of SiH_3 decreases with decreasing H_2 flow and at low H_2 flows the dissociation of SiH_4 is dominated by reactions with ions from the plasma source. As confirmed by optical emission spectroscopy on excited Si and SiH, this causes strong dissociative recombination of silane ions producing a considerable amount of very reactive radicals, such as SiH_2, SiH, and Si. The contribution of these radicals and/or their reaction products is expected to cause the inferior a-Si:H film properties obtained at low H_2 flows. This is corroborated by the increase in overall surface reaction probability for decreasing H_2 flow, while the overall surface reaction probability of ~0.3

at high H_2 flows corresponds to film growth dominated by SiH_3.

For a fixed H_2 flow of 10 sccs in the cascaded arc, the consumption of SiH_4 has been investigated for varying SiH_4 flows. That SiH_3 dominated film growth does not guarantee good film quality is shown from the fact that the contribution of SiH_3 is independent of the SiH_4 flow, while the film properties are inferior at low SiH_4 flows. Furthermore, it has been demonstrated that the neutral products created by dissociative recombination of positive ions are smaller at low SiH_4 flows as expected from the smaller size of the ions at low SiH_4 flows.

ACKNOWLEDGMENTS

Dr. G. Dinescu and Dr. E. Aldea of the National Institute of Lasers and Plasma Physics Romania are gratefully acknowledged for providing the program for simulating the emission data and for their help on the analysis. A. H. M. Smets, B. A. Korevaar, F. H. M. Hammen, and I. Aarts are thanked for their contributions to the measurements and M. J. F. van de Sande, A. B. M. Hüsken, and H. M. M. de Jong for their skilful technical assistance. This work was supported by The Netherlands Organization for Scientific Research (NWO-prioriteit), The Netherlands Foundation for Fundamental Research on Matter (FOM-Rolling Grant) and The Netherlands Agency for Energy and the Environment (NOVEM).

[1] K. Kobayashi, M. Hayama, S. Kawamoto, and H. Miki, Jpn. J. Appl. Phys., Part 1 **26**, 202 (1987).

[2] J. Perrin, P. Roca i Cabarrocas, B. Allain, and J.M. Friedt, Jpn. J. Appl. Phys., Part 1 **88**, 2041 (1988).

[3] A.H. Mahan, J. Carapella, B.P. Nelson, R.S. Crandall, and I. Balberg, J. Appl. Phys. **69**, 6728 (1991).

[4] J.-H. Lee, S.K. Park, and C.S. Kim, Jpn. J. Appl. Phys., Part 2 **34**, L1191 (1995)

[5] M. Goto, H. Toyoda, M. Kitagawa, T. Hirao, and H. Sugai, Jpn. J. Appl. Phys., Part 1 **36**, 3714 (1997).

[6] S. Will, H. Mell, M. Poschenrieder, and W. Fuhs, J. Non-Cryst. Solids **227-230**, 29 (1998).

[7] A. Heya, K. Nakata, A. Izumi, and H. Matsumura, Mater. Res. Soc. Symp. Proc. **507**, 435 (1998).

[8] S. Morrison, J. Xi, and A. Madan, Mater. Res. Soc. Symp. Proc. **507**, 559 (1998).

[9] R. Platz, C. Hof, S. Wieder, B. Rech, D. Fisher, A. Shah, A. Payne, and S. Wagner, Mater. Res. Soc. Symp. Proc. **507,** 565 (1998).

[10] Y.-B. Park, X. Li, S.-W. Rhee, and D.-W. Park, J. Phys. D **32**, 1955 (1999).

[11] W.M.M. Kessels, A.H.M. Smets, B.A. Korevaar, G.J. Adriaenssens, M.C.M. van de Sanden, and D.C. Schram, Mater. Res. Soc. Symp. Proc. **557**, 25 (1999).

[12] B.A. Korevaar, G.J. Adriaenssens, A.H.M. Smets, W.M.M. Kessels, H.–Z. Song, M.C.M. van de Sanden, and D.C. Schram, J. Non-Cryst. Solids. **266-269**, 380 (2000).

[13] M.C.M. van de Sanden, R.J. Severens, W.M.M. Kessels, R.F.G. Meulenbroeks, and D.C. Schram, J. Appl. Phys. **84**, 2426 (1998); J. Appl. Phys. **85**, 1243 (1999).

[14] W.M.M. Kessels, R.J. Severens, A.H.M. Smets, B.A. Korevaar, G.J. Adriaenssens, D.C. Schram, and M.C.M. van de Sanden, submitted for publication.

[15] W.M.M. Kessels, C.M. Leewis, A. Leroux, M.C.M. van de Sanden, D.C. Schram, J. Vac. Sci. Technol. A **17**, 1531 (1999).

[16] W.M.M. Kessels, C.M. Leewis, M.C.M. van de Sanden, D.C. Schram, J. Appl. Phys. **86**, 4029 (1999).

[17] J.J. Beulens, M.J. de Graaf, and D.C. Schram, Plasma Sources Sci. Technol. **2**, 180 (1993).

[18] M.C.M. van de Sanden, J.M. de Regt, and D.C. Schram, Plasma Sources Sci. Technol. **3**, 501 (1994).

[19] R.F.G. Meulenbroeks, M.F.M. Steenbakkers, Z. Qing, M.C.M. van de Sanden, and D.C. Schram, Phys. Rev. E **49**, 2272 (1994).

[20] R.F.G. Meulenbroeks, R.A.H. Engeln, M.N.A. Beurskens, R.M.J. Paffen, M.C.M. van de Sanden, J.A.M. van der Mullen, and D.C. Schram, Plasma Source Sci. Technol. **4**, 74 (1995).

[21] M. Boulos, P. Fauchais, and E. Pfender, *Thermal plasmas: Fundamentals and applications, Vol. 1*, (Plenum Press, New York, 1994).

[22] S. Mazouffre, M.G.H. Boogaarts, J.A.M. van der Mullen, and D.C. Schram, Phys. Rev. Lett. **84**, 2622 (2000).

[23] G.M.W. Kroesen, D.C. Schram, A.T.M. Wilbers, and G.J. Meeusen, Contrib. Plasma Phys. **31**, 27 (1991).

[24] R.F.G. Meulenbroeks, R.A.H. Engeln, J.A.M. van der Mullen, and D.C. Schram, Phys. Rev. E **53**, 5207 (1996).

[25] H. Sugai and H. Toyoda, J. Vac. Sci. Technol. A **10**, 1193 (1992).

[26] P. Kae-Nune, J. Perrin, J. Guillon, and J. Jolly, Plasma Sources Sci. Technol. **4**, 250 (1995).

[27] Consumption of SiH_4 usually leads to a decrease of the SiH_4 signal when the plasma is turned on. This is however not the case for all measurements reported here. This effect, which can not be explained by a change in SiH_4 flux into the mass spectrometer due to a change in gas temperature, has no implications for the radical measurements.

[28] W.M.M. Kessels, M.C.M. van de Sanden, R.J. Severens, and D.C. Schram, J. Appl. Phys. **87**, 3313 (2000).

[29] J.W. Coburn and E. Kay, J. Vac. Sci. Technol. **8**, 738 (1971).

[30] H. Singh, J.W. Coburn, and D.B. Graves, J. Vac. Sci. Technol. A **17**, 2447 (1999).

[31] A.J.B. Robertson, *Mass Spectrometry*, (Methuen & Co. LTD, London, 1954).

[32] G.J. Meeusen, E.A. Ershov-Pavlov, R.F.G. Meulenbroeks, M.C.M. van de Sanden, and D.C. Schram, J. Appl. Phys. **71**, 4156 (1992).

[33] J. Perrin and E. Delafosse, J. Phys. D **13**, 759 (1980).

[34] D.A. Doughty, J.R. Doyle, G.H. Lin, and A. Gallagher, J. Appl. Phys. **67**, 6220 (1990).

[35] A. Goumri, W.-J. Yuan, L. Ding, Y. Shi, and P. Marshall, Chem. Phys. **177**, 233 (1993).

[36] R. Basner, M. Schmidt, V. Tarnovsky, K. Becker, and H. Deutsch, Int. J. Mass. Spectrom. Ion Phys. **171**, 83 (1997).

[37] V. Tarnovsky, H. Deutsch, and K. Becker, J. Chem. Phys. **105**, 6315 (1996).

[38] F.A. Baiocchi, R.C. Wetzel, and R.S. Freund, Phys. Rev. Lett. **53**, 771 (1984).

[39] This has consequences for the radical densities determined by Kae-Nune *et al.* and leads to a higher contribution of SiH_3 to film growth than presented. The ratio of the contributions of SiH_3 and SiH_2 increases by a factor of ~6.

[40] J. Perrin, O. Leroy, and M.C. Bordage, Contrib. Plasma Phys. **36**, 1 (1996).

[41] A.A. Howling, L. Sansonnens, J.L.-Dorrier, and Ch. Hollenstein, J. Appl. Phys. **75**, 1340 (1994).

[42] S. Ramalingan, D. Maroudas, and E.S. Aydil, submitted for publication.

[43] Y.B. Kim, K. Stephan, E. Märk, and T. Märk, J. Chem. Phys. **74**, 6771 (1981).

[44] A.A. Radzig, and B.M. Smirnov, *Reference Data on Atoms, Molecules and Ions* (Springer-Verlag, Berlin-Heidelberg, 1985).

[45] S.K. Loh, and J.M. Jasinski, J. Chem. Phys. **95**, 4914 (1991).

[46] J.M. Jasinski, Mater. Res. Soc. Symp. Proc. **165**, 41 (1990).

[47] A. Kono, S. Hirose, and T. Goto, Jpn. J. Appl. Phys., Part 1 **38**, 4389 (1999).

[48] A.H.M. Smets, M.C.M. van de Sanden, and D.C. Schram, Thin Solid Films **343-344**, 281 (1999).

[49] S. Ramalingam, D. Maroudas, and E.S. Aydil, Appl. Phys. Lett. **72**, 578 (1998); J. Appl. Phys. **84**, 3895 (1998).

J. Vac. Sci. Technol. A 18 (5), (2000).

Hydrogenated amorphous silicon deposited at very high growth rates by an expanding Ar-H_2-SiH_4 plasma

W. M. M. Kessels,[a] R. J. Severens,[b] A. H. M. Smets, and B. A. Korevaar
Department of Applied Physics, Eindhoven University of Technology, P.O. Box 513, 5600 MB Eindhoven, The Netherlands

G. J. Adriaenssens
Semiconductor Physics Laboratory, Katholieke Universiteit Leuven, Celestijnenlaan 200 D, B3001 Heverlee-Leuven, Belgium

D. C. Schram and M. C. M. van de Sanden[c]
Department of Applied Physics, Eindhoven University of Technology, P.O. Box 513, 5600 MB Eindhoven, The Netherlands

The properties of hydrogenated amorphous silicon (a-Si:H) deposited at very high growth rates (6–80 nm/s) by means of a remote Ar-H_2-SiH_4 plasma have been investigated as a function of the H_2 flow in the Ar-H_2 operated plasma source. Both the structural and opto-electronic properties of the films improve with increasing H_2 flow, and a-Si:H suitable for the application in solar cells has been obtained at deposition rates of 10 nm/s for high H_2 flows and a substrate temperature of 400 °C. The "optimized" material has a hole drift mobility which is about a factor of ten higher than for standard a-Si:H. The electron drift mobility, however, is slightly lower than for standard a-Si:H. Furthermore, preliminary results on the first solar cells with intrinsic a-Si:H deposited at 7 nm/s are presented. Relating the film properties to the SiH_4 dissociation reactions reveals that optimum film quality is obtained for conditions where H from the plasma source governs SiH_4 dissociation and where SiH_3 contributes dominantly to film growth. Conditions where ion-induced dissociation reactions of SiH_4 prevail and where the contribution of SiH_3 to film growth is much smaller lead to inferior film properties. A large contribution of very reactive (poly)silane radicals is suggested as the reason for this inferior film quality. Furthermore, a comparison with film properties and process conditions of other a-Si:H deposition techniques is presented.

I. INTRODUCTION

Among the presently investigated renewable energy sources, thin film solar cells based on hydrogenated amorphous and/or micro-crystalline silicon technology are a clean and cost-effective alternative for nowadays fossil fuels. In the research to improve their price/performance ratio, special attention has been addressed in the recent years to increase the deposition rate of the intrinsic silicon layer in these solar cells. A higher deposition rate enables a higher throughput without adding more processing equipment and, consequently, large-scale production can be obtained with a reduction of the production costs.

Hydrogenated amorphous silicon (a-Si:H) is usually deposited by "conventional" radio frequency (13.56 MHz) plasma enhanced chemical vapor deposition (rf PECVD) at rates of 0.1–0.3 nm/s. Various efforts has been made to increase the deposition rate while maintaining (reasonable) film quality. These efforts range from investigations of more "extreme" operating conditions (at high power and pressure, working in the γ-regime),[1,2] different reactor geometries (depositing under additional ion bombardment),[3] and other gas mixtures (admixing noble gases[4,5] or using Si_2H_6)[1,6] to developing completely new a-Si:H production techniques. The development of these new production techniques has been initiated by the fact that the increase in deposition rate for rf PECVD is limited as it rapidly goes at the expense of the material quality. A more significant improvement has been obtained by changing the excitation frequency from 13.56 MHz to the very high frequency (VHF) range (30–300 MHz). For this VHF PECVD technique deposition rates up to

---

[a] Electronic mail: w.m.m.kessels@phys.tue.nl

[b] Present address: AKZO-NOBEL Central Research, P.O. Box 9300, 6800 SB Arnhem, The Netherlands

[c] Electronic mail: m.c.m.v.d.sanden@phys.tue.nl

3 nm/s have been reported.[7-9] However, for the production of solar cell devices the deposition rate is in practice usually limited to rates below 1 nm/s.[10,11]

A feature of the aforementioned methods is that they are so-called "direct plasma" techniques. This means that plasma generation and deposition take place in the same region, which makes it difficult or impossible to vary plasma parameters independently. For this reason, in the last decade a lot of research has been devoted to remote plasma techniques, where plasma generation, growth precursor transport, and deposition are geometrically separated. Some examples are: microwave generated plasmas,[12,13] inductively coupled plasmas (ICP),[14-16] and electron cyclotron resonance (ECR) plasmas.[17-19] The deposition rates obtained by these techniques seize also up at ~1 nm/s. However, for some of the techniques the favorable film properties obtained, such as a high stability against light-induced degradation, are of more interest.[12,19]

A technique for which both advantages, i.e., high growth rate and high stability of the a-Si:H deposited, have been reported is hot wire chemical vapor deposition (HWCVD). With this technique, device quality a-Si:H has been obtained at deposition rates in the range of 0.5 to 2 nm/s.[20-23] For films deposited at high substrate temperatures (~400 °C) good electronic properties have been obtained[20,21] while films with a low H content (2–3 at.%) exhibit improved stability against light-induced degradation.[24,25] This property, together with the very different electronic and structural properties,[26-28] are most probably related to the specific growth conditions of HWCVD, such as a high flux of H, a high substrate temperature, and a lack of energetic particle bombardment.[20]

This article describes high rate deposition of a-Si:H using the expanding thermal plasma (ETP). For this remote plasma deposition technique, it has recently been shown that it can produce good quality a-Si:H at deposition rates up to 10 nm/s.[29-31] The technique uses a, in a subatmospheric plasma source created, Ar-H_2 plasma for SiH_4 dissociation in a low-pressure deposition chamber. In this article, the film properties of the a-Si:H deposited will be presented as a function of the H_2 flow in the plasma source and for two different substrate temperatures.

The aim of this article is not only to show that a-Si:H with properties suitable for the application in solar cells can be deposited at rates up to 10 nm/s, but also to relate the a-Si:H properties to the plasma processes and to the contribution of different plasma species to film growth. The production of Si containing ions and radicals and their contribution to film growth in the expanding thermal plasma has been studied in detail by the combination of different plasma diagnostics and has been presented in previous work.[32-37] It has been observed that the plasma processes in the downstream region change drastically when varying the H_2 flow in the plasma source. The dominant SiH_4 dissociation process shifts from ion-induced reactions at zero or low H_2 flows to H abstraction reactions of SiH_4 by H atoms at higher H_2 flows.[32,35,37] This causes a transition from film growth with a large contribution of very reactive (poly)silane radicals at low H_2 flows to film growth with a dominant contribution of SiH_3 radicals at higher H_2 flows.[37] A small contribution of H-poor cationic Si clusters remains rather constant as a function of the H_2 flow.[35] The consequences of this transition in growth precursors for the a-Si:H film properties will be presented and possible relations indicated.

From this study, more insight into the growth of good quality a-Si:H at high deposition rates can be obtained while the results are also relevant for other (low-deposition rate) techniques. From a comparison of the ETP deposited a-Si:H with a-Si:H deposited by rf PECVD and other techniques (HWCVD/other remote plasmas), it is tried to come to general insights with respect to a-Si:H deposition. For example, from similarities in film properties and growth conditions it is possible to address questions such as: "What is the role of ion bombardment?", "Are high substrate temperatures inevitable for obtaining good quality a-Si:H at high deposition rates?", etc.

II. DEPOSITION SETUP AND FILM DIAGNOSTICS

The ETP deposition technique is schematically represented in Fig. 1. The technique is based on the generation of an Ar-H_2 plasma in a thermal plasma source (a cascaded arc), which subsequently expands into a low-pressure chamber where it dissociates the injected SiH_4 gas. The cascaded arc is operated at a dc current of 45 A and a voltage between 70 and 140 V

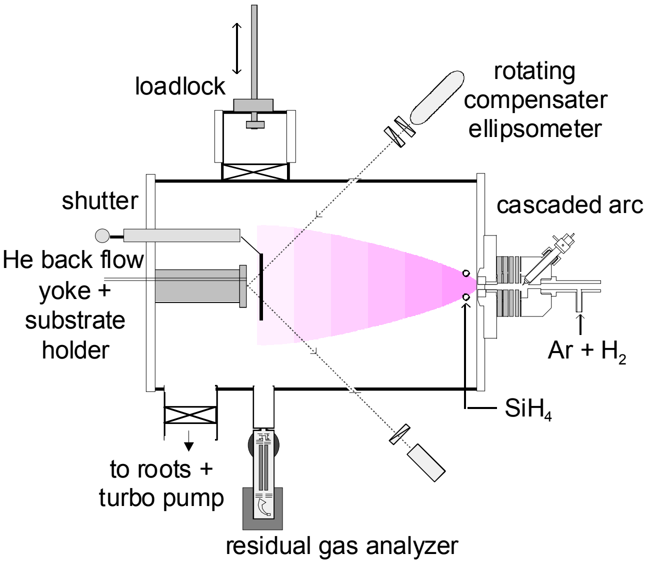

FIG. 1. Schematic representation of the expanding thermal plasma (ETP) deposition system.

depending on the H_2 fraction in the gas mixture. The Ar flow used is 55 sccs (standard cm^3s^{-1}), while the H_2 flow is varied between 0 and 15 sccs. The plasma source pressure is about 400 mbar. Pure SiH_4 is admixed in the low-pressure (0.2 mbar) chamber just behind the source exit by means of an injection ring. The SiH_4 flow is fixed at 10 sccs for the present study.[38]

Up to three substrates can be mounted on a substrate holder, which is placed on a copper yoke in the deposition chamber by means of a loadlock system. The yoke is positioned at 35 cm from the cascaded arc outlet and is resistively heated. Accurate substrate temperature control (100–500 °C) is achieved by means of a He backflow between the yoke and the substrate holder, and between the substrate holder and the substrates.[39] For the present study, substrate temperatures T of 250 and 400 °C have been used. During plasma ignition and admixing of SiH_4, the substrates are screened from the plasma by means of a shutter, which is opened after stabilization of the gases. More details on the deposition setup can be found in Refs. 32 and 35.

Films with a thickness between 500 and 1000 nm have been deposited on 2.5×2.5 cm^2 p-type Si(111) substrates (10–20 Ωcm) and on Corning 7059 glass. The refractive index and deposition rate of the films have been obtained by *in situ* ellipsometry (at 632.8 nm) and *ex situ* infrared transmission spectroscopy. From the analysis of the ellipsometry data using an optical model for the film, also the surface roughness of the films during deposition has been obtained.[40,41] In the model, the surface roughness is represented by a toplayer with a void fraction of 50%. The H content of the films has been determined from the Si-H absorption peaks in the infrared transmission data using re-calibrated values of the proportionality constants:[42] $(1.6\pm0.2)\times10^{19}$ cm^{-2} for the wagging mode at ~640 cm^{-1}, $(9.0\pm1.0)\times10^{19}$ cm^{-2} and $(1.5\pm0.2)\times10^{20}$ cm^{-2} for the stretching modes at ~2000 cm^{-1} and ~2100 cm^{-1}, respectively. The intensity of the absorption I for the two stretching modes has been used to calculate the microstructure parameter $R^*=I_{2100}/(I_{2000}+I_{2100})$. This yields information on how the H is bonded, as isolated SiH (absorption centered at ~2000 cm^{-1}) or as SiH_2 and/or clustered SiH on internal surfaces (absorption centered at ~ 2100 cm^{-1}). Raman spectroscopy with 514.5 nm laser radiation of an Ar^+ laser has been applied to investigate the lattice disorder.

Concerning the opto-electronic properties, the photoconductivity σ_{ph} has been obtained under AM1.5 illumination (100 mW/cm^2) using coplanar Al contacts. The dark conductivity σ_d and its activation energy E_{act} have been determined during the cool down stage after annealing the films at 160 °C for 30 min in vacuum. Transmission-reflection spectroscopy has been used for the analysis of the optical band gap. The Tauc optical band gap E_{Tauc} has been determined from Tauc's equation $(\alpha E)^{1/2} = B(E - E_{Tauc})$ and the Klazes' or cubic band gap E_{cubic} from the Klazes' equation $(\alpha E)^{1/3} = C(E - E_{cubic})$ with B and C material dependent constants.[43] The electron and hole drift mobilities have been obtained from standard time-of-flight (TOF) experiments[44] using 2–4 μm thick a-Si:H films sandwiched between a bottom Cr substrate and a top semi-transparent Cr contact. The electric field applied has been varied between $(0.5–2.5)\times10^4$ Vcm^{-1} for these measurements.

III. RESULTS

A. Deposition rate and structural film properties

Figure 2 shows the deposition rate of the films deposited at substrate temperatures of 250 and 400 °C for different H_2 flows in the cascaded arc plasma source. The deposition rate shows first a steep decrease as a function of the H_2 flow, followed by a slight increase at higher H_2 flows. This behavior is addressed in other articles,[32,35,37] where it was shown that at low H_2 flows SiH_4 dissociation is governed by ion-induced reactions and at high H_2 flows by reactions with atomic H from the plasma source. The deposition rate varies between 6 and 80 nm/s and is much higher than for other deposition techniques. The deposition rate also shows a dependence on the substrate temperature, especially at low H_2 flows. This can mainly be attributed to differences in film density as can be concluded from Fig. 3, where the refractive index of the films is given. The Si density or mass density is about linear in the refractive index of the films in the infrared.[42] After correcting for the film density, the deposition rate in terms of Si atoms deposited per unit of time shows only a slight decrease

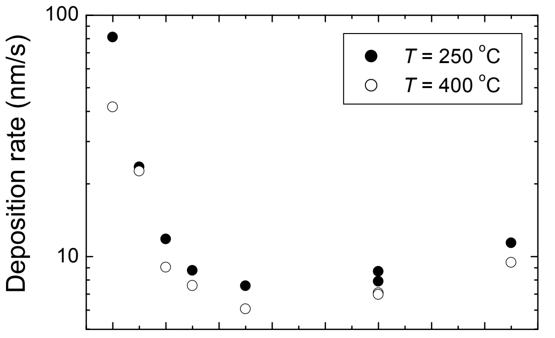

FIG. 2. Deposition rate, determined by *ex situ* infrared transmission spectroscopy and *in situ* ellipsometry, as a function of the H_2 flow in the cascaded arc plasma source for two substrate temperatures.

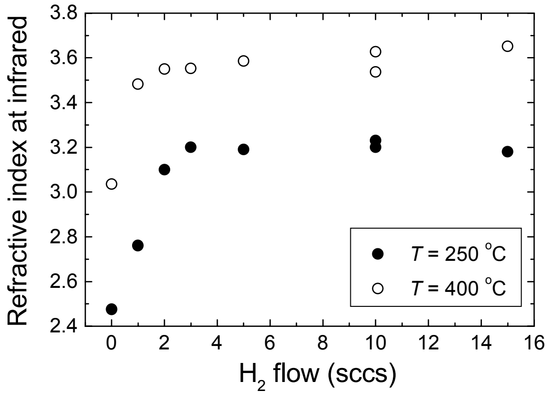

FIG. 3. Refractive index of the films as determined from *ex situ* infrared transmission spectroscopy.

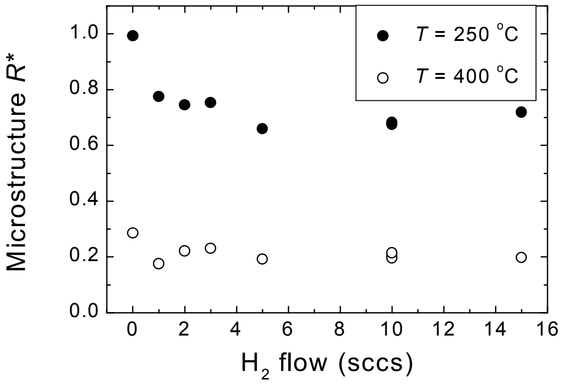

FIG. 5. The microstructure R^* as determined from the ratio of the integrated absorbance at the 2100 cm^{-1} and 2000 cm^{-1} SiH_x stretching modes.

as a function of the substrate temperature.[36] In addition to the fact that the refractive index depends on the substrate temperature, it depends also on the H_2 flow. At low H_2 flows the refractive index is considerably lower meaning that these films contain more H and/or have a considerable void fraction.

Figure 4 shows that the H content of the films deposited at 250 °C is higher than for the films deposited at 400 °C, which is in agreement with the difference in refractive index. For the films deposited at 250 °C the H content is about 17 at.%, while it is about 7 at.% for the films deposited at 400 °C. The microstructure parameter R^*, given in Fig. 5, reveals that mainly the amount of H bonded as clustered SiH and/or SiH_2[45] decreases with increasing temperature. For the different H_2 flows, the data show that for both substrate temperatures the H content is lower and the R^* value is higher at a H_2 flow of 0 sccs. Together with the lower refractive index, this implies that the films deposited with 0 sccs H_2 contain a considerable amount of voids. From these observations it is concluded that the films obtained at very low H_2 flows have inferior structural properties compared to those deposited at high H_2 flows. As will be addressed in more detail in Sec. IV A, this behavior can be attributed to the contribution of different plasma different species to a-Si:H growth. At high H_2 flows, film growth is dominated by SiH_3 radicals which have a relatively low surface reaction probability. At very low H_2 flows on the other hand, there is a large contribution of radicals with surface reaction probabilities close to one. This transition to radicals with a lower surface reactivity when going to higher H_2 flows, is also indicated by the decrease of the surface roughness with increasing H_2 flow as shown in Fig. 6.

Compared to a-Si:H deposited by conventional techniques such as rf PECVD, the ETP deposited a-Si:H distinguishes itself mainly by the much higher deposition rate. Furthermore, a higher substrate temperature is necessary for the ETP technique to

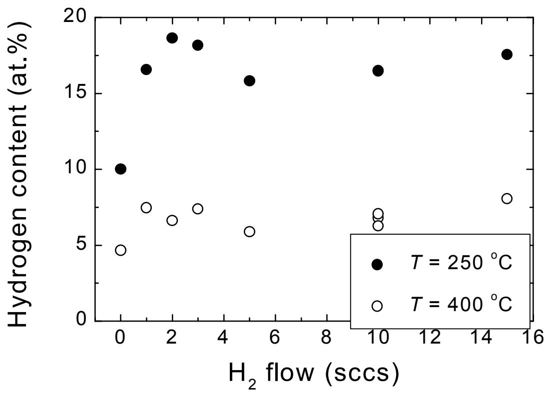

FIG. 4. The H content of the films determined from the SiH_x infrared absorption peaks.

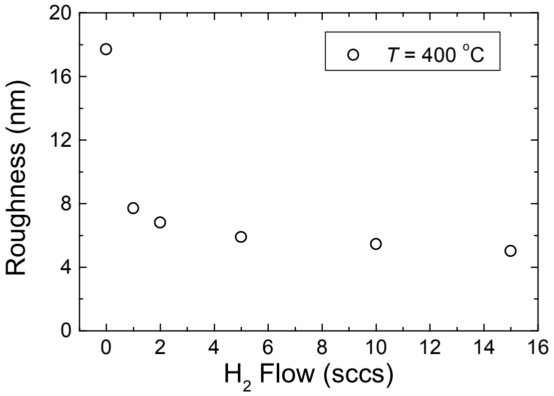

FIG. 6. The surface roughness at a film thickness of 500 nm as determined by *in situ* ellipsometry for films deposited at 400 °C. The roughness has been derived from the ellipsometry data using an optical model of the film in which the surface roughness corresponds with a toplayer containing 50% voids.

obtain the same refractive index and Si mass density: rf PECVD yields usually dense films at substrate temperatures of 250 °C,[43,46] whereas for the films deposited at high rate by the expanding thermal plasma a substrate temperature over 350 °C is required.[29,31,47] The H content and the microstructure parameter R^* for the ETP films deposited at 250 °C are also higher than for "optimized" rf PECVD films which are usually deposited at this substrate temperature. These rf PECVD films contain typically ~10–12 at.% H while the value for R^*<0.1.[43,46]

The H content of the ETP films deposited at 400 °C is lower than for "optimized" rf PECVD material (T=~250 °C) while the R^* value is still higher. Nevertheless, in Sec. III B it will be shown that a substrate temperature of 400 °C yields the "optimized" film quality for the ETP technique. The difference in substrate temperatures yielding optimum film quality leads however to somewhat different optical and electronic properties between the two "optimized" materials as will be addressed in Sec. III B.

The last structural property investigated for the very high rate deposited a-Si:H is the lattice disorder, which is deduced from the Raman Si-Si transverse optical (TO) linewidth. Raman spectra of films deposited with 10 sccs H_2 are given in Fig. 7 for substrate temperatures of 200 and 450 °C. The spectra show only a broad feature at ~475 cm^{-1} indicating that the material is purely amorphous. The half width at half maximum of the Si-Si TO mode is 35 cm^{-1} for the 200 °C sample and 33 cm^{-1} for the 450 °C sample. The corresponding bond-angle distortions[48] are 9° and 8.5°, respectively. These values are also typically found for rf PECVD a-Si:H.[49]

B. Opto-electronic film properties

The AM1.5 photoconductivity σ_{ph} and dark conductivity σ_d of the films are given in Fig. 8. Both σ_{ph} and σ_d are higher for the films deposited at 400 °C, but their ratio σ_{ph}/σ_d (photosensitivity) is lower at this temperature. This lower photosensitivity is mainly due to the higher values of σ_d at 400 °C. Furthermore, it is clear that σ_{ph} decreases for decreasing H_2 flow leading to a very small photosensitivity at low H_2 flows. This implies that also the opto-electronic film properties deteriorate for decreasing H_2 flow in the cascaded arc.

In comparison with rf PECVD a-Si:H, the photosensitivity of the ETP films is rather low: ~10^4 at 250 °C and ~10^3 at 400 °C. For high quality rf PECVD a-Si:H deposited at substrate temperatures around 250 °C, a photosensitivity of ~10^5 is usually reported, with σ_{ph} in the order of 10^{-5} Ω^{-1}cm^{-1} and σ_d preferably <10^{-10} Ω^{-1}cm^{-1}.[43,46] For the ETP films obtained at 250 °C, σ_{ph} is about one order of magnitude smaller. This shows that at the substrate temperatures typically used for a-Si:H deposition the quality of the very high rate deposited ETP material is indeed inferior. This agrees with the lower Si atomic density obtained at 250 °C. The comparison of the ETP films deposited at 400 °C with rf PECVD films produced at 250 °C is however somewhat more complicated. The values of σ_{ph} are slightly smaller than for the "optimized" rf PECVD films, but especially the values of σ_d are higher. The higher values of σ_d can (partially) be attributed to the above-mentioned lower H content of the ETP deposited a-Si:H. This lower H content leads to a lower optical band gap,[46,50,51] and consequently to a smaller activation energy E_{act} of σ_d and therefore to higher values for σ_d itself. The activation energy of σ_d is given in Fig. 9. The typical value of ~0.75 eV at 400 °C is slightly smaller than the usually reported value of ~0.8 eV for rf PECVD a-Si:H. Because σ_d is very sensitive on E_{act} due to the exponential dependence, the smaller value of E_{act} is one reason for the relatively low photosensitivity at 400 °C. For the 250 °C deposited films E_{act} is higher (~0.90 eV) than for rf PECVD films deposited at this temperature, in agreement with their higher H content.

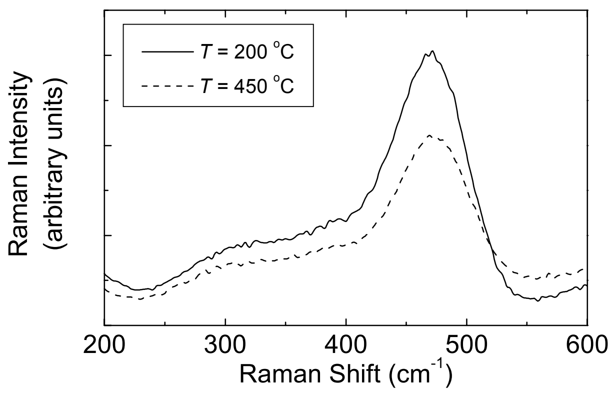

FIG. 7. Raman spectra for films deposited with 10 sccs H_2 at substrate temperatures of 200 and 450 °C.

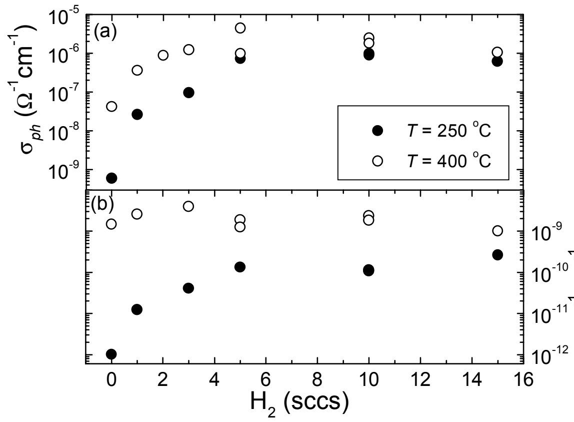

FIG. 8. (a) AM 1.5 photoconductivity σ_{ph} (100 mW/cm^2) and (b) dark conductivity σ_d as a function of the H_2 flow in the cascaded arc.

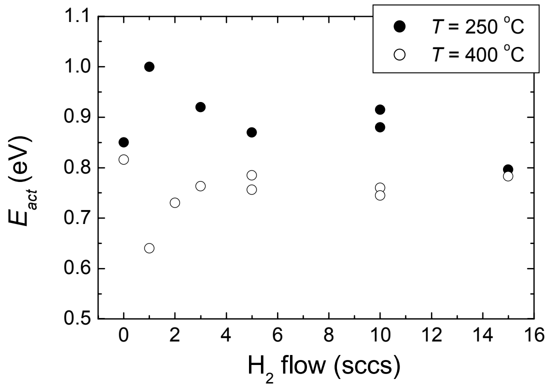

FIG. 9. Activation energy E_{act} of the dark conductivity.

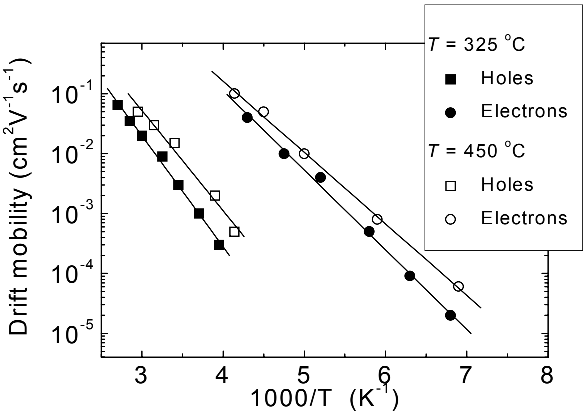

FIG. 10. Electron and hole drift mobility of the a-Si:H for an electric field of 10^4 Vcm^{-1}. The H_2 flow in the arc was 10 sccs and the substrate temperatures were 325 °C and 450 °C.

The optical gap has only been determined for the condition with 10 sccs H_2. The Tauc gap E_{Tauc} is 1.67 eV for films deposited at 400 °C, which is indeed lower than the typical values of 1.7–1.8 eV for rf PECVD a-Si:H.[43,46] For the ETP films deposited at 250 °C, E_{Tauc} is 1.76 eV. The cubic optical gap E_{cubic} is 1.51 eV for the films deposited at 400 °C, which is about twice the value of E_{act} (0.75 eV). This implies that the material does not suffer severely from impurities.[43] Furthermore, the lower bandgap leads to a larger absorption coefficient (α=3.8×10^4 cm^{-1} at 2.0 eV), implying that in solar cells with ETP a-Si:H thinner intrinsic films can be used.

To obtain more insight into the electronic properties, the electron and hole drift mobility have been investigated by means of time-of-flight (TOF) measurements for films deposited with 10 sccs H_2. The deposition rate of these films was 10 nm/s.[38] The mobilities for films deposited at 325 and 450 °C are shown in Fig. 10 as a function of the TOF-analysis temperature and for an electric field of 10^4 Vcm^{-1}. The hole and electron mobility are very weakly dependent on the electric field.[31] For the 325 °C films, the room temperature drift mobilities are 0.70 cm^{2}V^{-1}s^{-1} and 3.7×10^{-3} cm^{2}V^{-1}s^{-1} for the electrons and holes, respectively, and 0.81 cm^{2}V^{-1}s^{-1} and 1.1×10^{-2} cm^{2}V^{-1}s^{-1} for the 450 °C films. The increase of both mobilities with increasing substrate temperature clearly shows that the electronic film properties improve with increasing substrate temperature. The activation energies are 0.29 eV and 0.24 eV for the electrons at 325 °C and 450 °C, respectively, which is higher than the typical value of 0.15 eV.[52] The activation energy of the hole mobility, which is 0.39 eV for both substrate temperatures, is standard.[52] Very remarkable is that the hole drift mobility of the ETP material at 450 °C is about one order of magnitude larger than for standard a-Si:H.[52] The electron drift mobility, however, is about a factor 3 to 6 smaller. The relatively high hole drift mobility, coupled to the only slightly lower electron drift mobility, results in an increased average carrier mobility and hence a higher recombination rate.[53] This yields a second explanation for the relatively low photosensitivity of the material compared to rf PECVD a-Si:H.

Finally, it should be mentioned that also the defect density of the ETP a-Si:H deposited at high substrate temperatures is reasonably low. Post-transit photocurrent analysis of the TOF-experiments, described in detail in Ref. 31, yielded a defect density of ~10^{16} cm^{-3}. In combination with the enhanced hole drift mobility, this suggests that the ETP deposited a-Si:H is suitable for the application in solar cells.

C. Solar cells

First attempts on the fabrication of solar cells with an intrinsic a-Si:H layer deposited by the expanding thermal plasma have been carried out. The fact that the best film properties are obtained at relatively high substrate temperatures complicates the application of the ETP material in the commonly used p-i-n solar cell structure. Deposition of the intrinsic film at substrate temperatures over 300 °C causes severe deterioration of the p-layer and consequently zero solar cell performance. Therefore two different, single junction solar cells have been fabricated: a p-i-n cell with the i-layer deposited at 300 °C has been produced in cooperation with the Delft University of Technology, and a n-i-p cell with the i-layer deposited at 400 °C in cooperation with Utrecht University. In the n-i-p cell, a thermally stable n-layer was used as also applied in HWCVD deposited solar cells.[54] For both cells, the doped layers were prepared in rf PECVD chambers, and the vacuum was broken to deposit the intrinsic a-Si:H films in the ETP setup. The i-layers were deposited with a H_2 flow of 10 sccs and at a deposition rate of 7 nm/s. The p-i-n cell contained a 10 nm thick p-layer deposited on glass

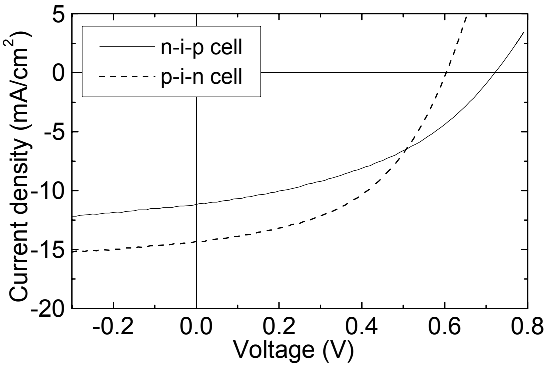

FIG. 11. J-V curves for solar cells with an intrinsic a-Si:H layer deposited by the expanding thermal plasma at a rate of 7 nm/s. During the deposition of the intrinsic layer the H_2 flow in the arc was 10 sccs and the substrate temperature was 300 °C and 400 °C for the p-i-n and n-i-p cell, respectively.

with Asahi SnO_2 and a 20 nm thick n-layer. For the n-i-p cell, a 75 nm thick n-layer deposited on stainless steel at a substrate temperature of 430 °C has been used. The p-layer was 30 nm and the cell was finished with a 40 nm thick indium tin oxide (ITO) top contact. The thickness of the i-layers was 400 and 500 nm for the p-i-n cell and n-i-p cell, respectively, while no optimization of these values has taken place.

The performances of the solar cell devices are listed in Table I and the current-voltage curves are given in Fig. 11. The cell deposited at 300 °C had an initial efficiency of 4.1% (under 100 mW/cm^2 AM1.5 illumination). This p-i-n cell suffered already from degradation of the p-layer as can also be concluded from its relatively low V_{oc}. However, its performance is still better than that of the n-i-p cell, which had an efficiency of 3.3%. This is despite the fact that the properties of the individual i-layer at 400 °C are superior. The lower efficiency can, among other things, be attributed to the fact that for the 400 °C cell the ITO top contact was not optimized for optical transmission. As a reference, the p-i-n cells with the i-layer deposited by rf PECVD and n-i-p cells with the i-layer deposited by HWCVD have record initial efficiencies of 10%[55] and 5.6%,[54] respectively.

Considering the fact that no optimization of the solar cells in their entirety has been carried out, such as tuning of the properties of the doped layers and a refinement of the thickness of the intrinsic a-Si:H layer, these preliminary results on solar cells deposited at a rate of 7 nm/s are promising. Furthermore, we note that transport through air was inevitable (total air exposure time > 12 hrs) and that no light trapping and no special back reflection enhancement techniques were applied.

TABLE I. Performance of single junction solar cells based on two different cell structures. The intrinsic a-Si:H layer has been deposited by the expanding thermal plasma at a rate of 7 nm/s. For the p-i-n cell the thickness was 400 nm, for the n-i-p cell 500 nm, and the substrate temperatures were 300 and 400 °C, respectively.

	p-i-n cell	n-i-p cell
Open circuit voltage V_{oc}	0.61 V	0.72 V
Short circuit current density J_{sc}	14.3 mA/cm^2	11.2 mA/cm^2
Fill-Factor *FF*	0.48	0.42
Efficiency η	4.1%	3.3%

IV. DISCUSSION

A. Relation between the film properties and the growth precursors

In the previous sections, it has been shown that the film properties obtained at no or very low H_2 flow are inferior to those obtained at H_2 flows within the range of 5–15 sccs. This behavior can be related to a change in the plasma processes and film growth precursors when the H_2 flow is varied. By detailed investigations using several plasma diagnostics[32,34,35,37] it is found that for the different H_2 flows two different regions can be distinguished with respect to the SiH_4 dissociation process. At low H_2 flows, SiH_4 is mainly dissociated by reactions induced by ions emanating from the plasma source. By means of charge transfer reactions with ions and dissociative recombination reactions with electrons this leads to a considerable production of SiH_x radicals ($x \leq 2$).[34,35,37] These radicals have a high (surface) reactivity, and they contribute either directly to film growth or react first with SiH_4 to create reactive polysilane radicals (such as Si_2H_x ($x \leq 4$), etc.)[56] before contributing to growth. When the H_2 admixture is increased, the flow of ions from the plasma source reduces drastically, whereas the flow of atomic H from the source increases. This leads to more hydrogen abstraction reactions between SiH_4 and H and consequently to an increasing contribution of SiH_3 to film growth. For H_2 flows $\gtrsim$ 7.5 sccs, film growth is by far dominated by SiH_3 (contribution is estimated at ~90%).[37] The contribution of Si containing positive ions to film growth is less than 10% [35,37] and rather independent of the H_2 flow.[35] Despite the fact that at low H_2 flows SiH_4 dissociation is governed by ions, fast dissociative recombination reactions of the ions with electrons under these conditions lead to a strong reduction of the contribution of the ions at low H_2 flows.[37]

The transition to dominantly SiH_3 when increasing the H_2 flow is corroborated by the dependence of the overall surface reaction probability on the H_2 flow. This overall surface reaction probability depends on the fluxes of different reactive species to the film and on each of their particular surface reaction probabilities. The overall surface reaction probability decreases from ~0.5 to ~0.3 when increasing the H_2 flow from 0 sccs to 15 sccs.[36,37] At the high H_2 flows, the overall surface reaction probability of ~0.3 approaches the values of the surface reaction probability proposed for SiH_3 (0.2–0.3).[36] At low H_2 flows, there is apparently a significant contribution of reactive SiH_x ($x \leq 2$) and polysilane radicals. For these radicals, values of the surface reaction probability within the range of 0.6–1 have been proposed.[36]

From these results, the poorer a-Si:H film quality obtained at low H_2 flows can be understood. Radicals with a high surface reaction probability lead easily to a high surface roughness and columnar film growth because they stick (almost) immediately at their position of impact on the surface (the "microscopic-shadowing" effect).[57] Radicals with a lower surface reaction probability on the other hand, can have multiple reflections on the surface before they actually stick. Radicals such as SiH_3 are therefore capable of filling up so-called "valleys" at the surface[57] causing smoother film growth (On this point we disagree with Doughty *et al.*[58] Without underrating the importance of surface diffusion, a radical that can undergo several reflections has certainly a larger probability of ending up at the "bottom of a valley"). The decreasing surface roughness for increasing H_2 flow is thus in perfect agreement with the increasing contribution of SiH_3. Since voids are more easily incorporated when the surface is rough, a higher contribution of very reactive radicals explains the lower Si atomic density and higher void fraction at very low H_2 flows.

The improvement of the opto-electronic properties with increasing H_2 flow can be understood from the improvement of the electronic transport properties with increasing film density. Porous films are obviously also more susceptible to oxidation when exposed to air. It is also expected that the defect density of the films depends on the species contributing to growth. Furthermore, σ_{ph} and σ_d show somewhat more dependence on the H_2 flow than the structural film properties, especially at a substrate temperature of 400 °C. This suggests that it is easier to compensate for poor structural properties (as caused by the growth precursors) by using high substrate temperatures than for poor electronic performance.

Because the film properties do not show a correlation with the contribution of the cationic Si clusters, no relation between their contribution and the film properties can be extracted from the data. However, it is not excluded that these ions have important implications for the film quality, as has also been discussed in Refs. 33 and 35. Despite the fact that the contribution of the ions is within the range of 5–9%, these H-poor and compact clusters can easily affect the defect density: their contribution is much larger than the defect density in high quality a-Si:H that is in the order of 10^{-6}–10^{-7} of the Si atomic density.[43,46]

It can be concluded that the type of species contributing to a-Si:H growth has important implications for the film properties finally obtained. It has been shown that the quality of the a-Si:H with respect to solar cell applications improves with an increasing contribution of SiH_3. Such a relation is already generally accepted for a-Si:H produced at the commonly used deposition rates, but here this relation is also found for very high rate deposited a-Si:H. It is important to realize that the film quality, in terms of electronic properties, is not necessarily directly related to the contribution of SiH_3. Film properties such as the defect density can also completely be determined by a (small) contribution of other species than SiH_3. Furthermore, the results obtained with the ETP technique imply that a dominant contribution of SiH_3 only is not sufficient to obtain high quality a-Si:H at high deposition rates. Under these conditions, also higher substrate temperatures are required to obtain films with a sufficiently high mass density. This might be related to the absence of a (sufficient) ion bombardment of the film during deposition as will be discussed in the following section.

B. Comparison with a-Si:H deposited by other techniques

In Sec. III, the ETP deposited a-Si:H has been compared to rf PECVD a-Si:H, typically deposited at substrate temperatures between 200 and 300 °C. In this section, we will also compare the material with a-Si:H deposited by other techniques, where in some cases either the material properties or the process conditions show striking similarities. Although such a comparison is afflicted with differences in analyzed film parameters, method of analysis, etc., it is still worth trying to come to some general insights regarding the growth and properties of a-Si:H.

First of all, the relation between the deposition rate and substrate temperature is considered. In the present study, it has been shown that relatively high substrate temperatures are necessary to obtain films of good quality at high deposition rates. The fact that for the expanding thermal plasma higher substrate temperatures are required to obtain dense films with a sufficiently low R^* might be related to the absence of energetic ion bombardment during deposition (sheath potential <2 eV).[33,34] That it is possible to deposit high quality a-Si:H at lower substrate temperatures when sufficient ion bombardment takes place is also suggested by Abelson.[59] Moreover, a relation between the ion energy and both the film density and R^* is indicated by the data of Hamers *et al.*[60] Using rf and VHF PECVD, it was shown that dense films with

$R^*<0.1$ were obtained when 5 eV ion energy was available per Si atom deposited. This observation is consistent with the fact that films with reasonable properties can be obtained at 3 nm/s by rf PECVD when depositing at the cathode and using somewhat higher substrate temperatures (350 °C) than usually.[3] The HWCVD technique on the other hand, is capable of producing very dense films with $R^*=0$ at deposition rates up to 2 nm/s and at relatively low substrate temperatures while ion bombardment is absent.[20,23,24,26] This absence of energetic ion bombardment can possibly be compensated by a large flux of "energetic" H that is thermalized at the filament.[20] Furthermore, it should be noted that the substrate temperatures reported for HWCVD are not always reliable because accurate temperature control is difficult due to the presence of a hot filament.[61,62] In some cases, only the substrate temperature prior to deposition is reported.[63]

Another important effect associated with ion bombardment is the enhancement of the electron and hole drift mobility as reported for rf PECVD a-Si:H for ion energies within an extremely narrow window around 20 eV (T=250 °C).[64,65] The exact values of the mobilities have been under discussion in Refs. 52 and 66. The enhancement of the mobilities can possibly be associated with the ion-energy effects observed in Si^+ beam epitaxy by Rabalais *et al.*[67] Low defect density crystalline silicon was obtained for ion energies within a very narrow window (~20±10 eV) at low substrate temperatures (160 °C). For higher temperatures this window broadened out, particularly at the low-energy side. These observations also suggest that ion bombardment can be interchanged with substrate temperature, at least as long as the typical ion energy is not much larger than the displacement threshold energy causing deleterious effects.

Going back to HWCVD, for the a-Si:H produced by this technique some very interesting properties have been observed. Mahan *et al.*[20] have shown that no severe deterioration of the film properties takes place when going to high substrate temperatures and to a low H concentrations in the films (down to <1% for T>400 °C). For increasing substrate temperature, both σ_{ph} and the electron drift mobility[68] showed only a slight decrease, while an improved stability against light-induced degradation was obtained for films with a H content of 2–3 at.% (T=400 °C prior to deposition).[63] Furthermore, E_{Tauc} and σ_d of the material remained, respectively, high and low when going to low H concentrations.

In comparison with the ETP a-Si:H films deposited at 400 °C, the lower H content and the value of $R^*=0$ for the HWCVD films are remarkable. Because the substrate temperature was 400 °C prior to deposition, this difference suggests that the substrate temperature during the deposition of the HWCVD films was considerably higher than 400 °C. Furthermore, some significant differences have been reported for films deposited by different HWCVD reactors under similar circumstances. The drastic decrease in H content with increasing substrate temperature has been reproduced in several other studies,[62,69] but Feenstra *et al.* found film properties improving with increasing substrate temperature while the H content remained high (9.5 at.%) up to 430 °C.[21] This material showed also no improved stability compared to rf PECVD a-Si:H and values of $R^*\geq0.1$ were reported.[70] Heintze *et al.* reported similar R^* values for films containing 4 at.% H which were obtained at a substrate temperature of 400 °C. These films showed only a slightly improved stability.[69]

Also the observation by Mahan *et al.*[20] that both E_{Tauc} and σ_d remained constant when going to films with a low H concentration is remarkable. This behavior is in contrast with the observations for ETP deposited a-Si:H, but also with the observations for HWCVD a-Si:H films reported by Nelson *et al.*[62] and Heintze *et al.*[69] Mahan *et al.* has attributed the fact that E_{Tauc} remained constant at a relatively high value when going to low H concentrations to improved structural ordering in the HWCVD films.[20,27]

Regarding the improved structural ordering in low H content HWCVD a-Si:H,[20,27] there might be some similarities with the ETP deposited a-Si:H. Although speculative, the higher hole drift mobility in the ETP material as well as the appearance of a steep edge in the band tail states[31] might suggest also a different network bonding, while the enhanced hole drift mobility might be related with the relatively large ambipolar diffusion length in the low H content HWCVD a-Si:H films.[20] For the moment, it can only be mentioned that both techniques show similar values for the half width at half maximum of the Raman Si-Si TO mode,[27] values which are also typically found for rf PECVD a-Si:H.

Another aspect related to R^*, is the fact that H bonded as SiH_2 in the film has been linked with the contribution of higher silane related chemical species and subsequently with light-induced degradation of a-Si:H.[71] The fact that R^* increases with increasing deposition rate,[51,72,73] has been attributed to the higher contribution of these species to film growth, because these kind of species are more created at higher plasma power and/or pressure in rf PECVD (the method usually applied to increase the deposition rate).[71] For the optimized plasma conditions in the expanding thermal plasma (i.e., high H_2 flow), film growth is dominated by SiH_3 and only a very small fraction of higher silanes has been observed.[32,35] The R^* value is nevertheless relatively high, especially at 250 °C. Furthermore, no strong dependence of R^* on the H_2 flow has been observed (see Fig. 5), while the contribution of polysilane radicals presumably increases significantly when going to low H_2 flows.

The ETP technique has some similarities with other remote plasmas, such as the microwave operated "remote hydrogen plasma" (RHP)[12] and the H_2 operated electron cyclotron resonance plasma (H-ECR).[19] These plasmas use also H generated in a H_2 operated source to dissociate SiH_4, and therefore film growth is presumably also dominated by SiH_3 in these techniques. Furthermore, in these plasma also less ion bombardment takes place (this is to a smaller extent valid for H-ECR)[74] and high substrate temperatures (T=~400 °C) are typically used as well. The RHP technique yields however a relatively high H content at this temperature (10 at.%)[12] while R^*=~0.[75] For H-ECR the relatively high E_{Tauc} of 1.74 eV at 450 °C[74] suggests also a relatively high H content. Furthermore, it is suggested that for both techniques there is a relatively high H flux during deposition. It is therefore intriguing that, under similar circumstances as for HWCVD, also an improved stability for the material has been reported.[12,19] The HWCVD material, however, has a H content of 2–3 at.%. with R^*=~0,[20] while the SiH_4 dissociation process and dominant growth precursors are also very different. The SiH_4 is decomposed at a filament yielding mainly Si and H atoms.[61] These radicals can subsequently react with SiH_4 before reaching the substrate. The probability for these reactions, however, is limited due to the relatively low SiH_4 pressure and small distance between filament and substrate (typically ≤5 cm). It is expected that a considerable fraction of the (hot) Si atoms can react with SiH_4 (to mainly H_2SiSiH_2),[61,76] but this is less evident for H. It is rather improbable that H reacts to SiH_3 in the gas phase and the proposed scheme that SiH_3 is created at the a-Si:H surface by H (i.e., H creates a surface dangling bond by H abstraction and this surface dangling bond abstracts subsequently a H atom from SiH_4)[76] is also unlikely because of the very low reactivity of SiH_4 with pristine crystalline Si surfaces.[77,78] It can therefore be excluded that in HWCVD SiH_3 contributes dominantly to film growth. This shows that a dominant contribution of SiH_3 is not a necessary condition for high quality a-Si:H growth.

V. CONCLUSION

The film properties of a-Si:H deposited using the expanding thermal plasma have been investigated for different operating conditions of the plasma source and for two different substrate temperatures. It has been shown that this technique is capable of depositing low-defect density a-Si:H at deposition rates up to 10 nm/s for a substrate temperature of 400 °C and a relatively high H_2 flow in the cascaded arc plasma source. The a-Si:H obtained for these conditions is suitable for application in solar cells but it has somewhat different properties than rf PECVD a-Si:H. The substrate temperature of 400 °C, necessary to obtain dense films at high deposition rates, leads to a relatively low H content of 6–7 at.% and a relatively high microstructure parameter R^* of 0.2. The films have a small Tauc bandgap (~1.67 eV) and a relatively small activation energy of the dark conductivity (~0.75 eV). This is related with the low H content of the films and it explains, at least partially, the relatively high dark conductivity (~2×10^{-9} $\Omega^{-1}cm^{-1}$) of the films. The photoconductivity of the material (~4×10^{-6} $\Omega^{-1}cm^{-1}$) is slightly lower than for "optimized" rf PECVD a-Si:H. This can most probably be attributed to the enhanced hole drift mobility of the material which is about a factor of ten higher than for "optimized" rf PECVD a-Si:H. The enhanced hole drift mobility without the equivalent reduction of the electron drift mobility leads to enhanced recombination.

The results on the first solar cells with the i-layer deposited at 7 nm/s by the expanding thermal plasma show also the potential of very high rate deposited a-Si:H. A simple p-i-n cell with the i-layer deposited at 300 °C yielded an efficiency of 4.1%, despite thermal degradation of the p-layer and a not fully optimized intrinsic a-Si:H layer. Moreover, the cell thickness was not optimized and air exposure was inevitable. The first n-i-p cell, with a thermally stable n-layer and with higher quality intrinsic a-Si:H deposited at 400 °C, yielded an efficiency of 3.3%, despite a non-optimized ITO top contact. These results are encouraging for further solar cell optimization, which will be done in a recently developed solar cell deposition system consisting of a rf PECVD reactor, an expanding thermal plasma reactor, and a sample transfer chamber.

The film properties obtained for the different operating conditions of the plasma source have also been related to the SiH_4 dissociation reactions and species contributing to film growth. The improvement of the properties with increasing H_2 flow added to the Ar in the cascaded arc plasma source can be attributed to an increasing contribution of SiH_3 to film growth. The optimum film quality is obtained for conditions in which SiH_3 is by far dominant (contribution SiH_3 is estimated at ~90%), while conditions with a high contribution of very reactive (poly)silane radicals lead to inferior properties. The high surface reaction probability of these radicals leads to a high surface roughness and a low film density.

ACKNOWLEDGMENTS

The authors greatly acknowledge H.-Z. Song from the University of Leuven for performing the TOF measurements, R. E. I. Schropp and C. H. M. van de

Werf from Utrecht University and E. J. Geluk, B. S. Girwar, and R. A. C. M. M. van Swaaij of the Delft University of Technology for the production and testing of the solar cells. M. J. F. van de Sande, A. B. M. Hüsken, and H. M. M. de Jong are thanked for their skilful technical assistance. This work was supported by The Netherlands Organization for Scientific Research (NWO), The Netherlands Foundation for Fundamental Research on Matter (FOM) and The Netherlands Agency for Energy and the Environment (NOVEM).

[1] J. Perrin, P. Roca i Cabarrocas, B. Allain, and J.-M. Friedt, Jpn. J. Appl. Phys., Part 1 **27**, 2041 (1988).

[2] P. Roca i Cabarrocas, J. Non-Cryst. Solids **164-166**, 37 (1993).

[3] S. Will, H. Mell, M. Poschenrieder, and W. Fuhs, J. Non-Cryst. Solids **227-230**, 29 (1998).

[4] J.C. Knights, R.A. Lujian, M.P. Rosenblum, R.A. Street, D.K. Bieglesen, and J.A. Reimer, Appl. Phys. Lett. **38**, 331 (1981).

[5] H. Meiling, J. Bezemer, R.E.I. Schropp, and W.F. van der Weg, Mater. Res. Soc. Symp. Proc. **467**, 459 (1997).

[6] W. Futako, T. Takagi, T. Nishimoto, M. Kondo, I. Shimizu, and A. Matsuda, Jpn. J. Appl. Phys., Part 1 **38**, 4535 (1999).

[7] M. Heintze and R. Zedlitz, J. Non-Cryst. Solids **164-166**, 55 (1993).

[8] W.G.J.H.M. van Sark, J. Bezemer, E.M.B. Heller, M. Kars, and W.F. van der Weg, Mater. Res. Soc. Symp. Proc. **377**, 3 (1995).

[9] U. Kroll, J. Meier, P. Torres, J. Pohl, and A. Shah, J. Non-Cryst. Sol. **227-230**, 68 (1998).

[10] W.G.J.H.M. van Sark, J. Bezemer, R. van der Heijden, and W.F. van der Weg, Mater. Res. Soc. Symp. Proc. **420**, 21 (1996).

[11] S.J. Jones, X. Deng, T. Liu, and M. Izu, Mater. Res. Soc. Symp. Proc. **507**, 113 (1998).

[12] N.M. Johnson, C.E. Nebel, P.V. Santos, W.B. Jackson, R.A. Street, K.S. Stevens, and J. Walker, Appl. Phys. Lett. **59**, 1443 (1991).

[13] J.M. Jasinski, J. Vac. Sci. Technol. A **13**, 1935 (1995).

[14] M. Goto, H. Toyoda, M. Kitagawa, T. Hirao, and H. Sugai, Jpn. J. Appl. Phys., Part 1 **36**, 3714 (1997).

[15] J.A. Theil and G. Powell, J. Appl. Phys. **75**, 2652 (1994).

[16] K. Yokota, M. Takada, Y. Ohno, and S. Katayama, J. Appl. Phys. **72**, 1188 (1992).

[17] M. Kitagawa, K. Setsune, Y. Manabe, and T. Hirao, Jpn. J. Appl. Phys., Part 1 **27**, 2026 (1988).

[18] M. Zhang, Y. Nakayama, S. Nonoyama, and S. Wakita, J. Non-Cryst. Sol. **164-166**, 63 (1993).

[19] V.L. Dalal, T. Maxson, R. Girvan, and S. Haroon, Mater. Res. Soc. Symp. Proc. **467**, 813 (1997).

[20] A.H. Mahan, J. Carapella, B.P. Nelson, R.S. Crandall, and I. Balberg, J. Appl. Phys. **69**, 6728 (1991).

[21] K.F. Feenstra, C.H.M. van der Werf, E.C. Molenbroek, and R.E.I. Schropp, Mater. Res. Soc. Symp. Proc. **467**, 645 (1997).

[22] A.H. Mahan, R.C. Reedy jr., E. Iwaniczko, Q. Wang, B.P. Nelson, Y. Xu, A.C. Gallagher, H.M. Branz, R.S. Crandall, J. Yang, and S. Guha, Mater. Res. Soc. Symp. Proc. **507**, 119 (1998).

[23] P. Alpuim, V. Chu, and J.P. Conde, J. Appl. Phys. **86**, 3812 (1999).

[24] M. Vanecek, Z. Remes, J. Fric, R.S. Crandall, and A.H. Mahan, *Proceedings of the 12th European Photovoltaic Solar Energy Conference* (Amsterdam, The Netherlands, 1994), p. 354.

[25] D. Kwon, J.D. Cohen, B.P. Nelson, and E. Iwaniczko, Mater. Res. Soc. Symp. Proc. **377**, 301 (1995).

[26] Y. Wu, J.T. Stephen, D.X. Han, J.M. Rutland, R.S. Crandall, and A.H. Mahan, Phys. Rev. Lett. **77**, 2049 (1996).

[27] A.H. Mahan, D.L. Williamson, and T.E. Furtak, Mater. Res. Soc. Symp. Proc. **467**, 657 (1997).

[28] R.S. Crandall, X. Liu, and E. Iwaniczko, J. Non-Cryst. Solids **227-230**, 23 (1998).

[29] R.J. Severens, M.C.M. van de Sanden, H.J.M. Verhoeven, J. Bastiaanssen, and D.C. Schram, Mater. Res. Soc. Symp. Proc. **420**, 341 (1996).

[30] W.M.M. Kessels, A.H.M. Smets, B.A. Korevaar, G.J. Adriaenssens, M.C.M. van de Sanden, and D.C. Schram, Mater. Res. Soc. Symp. Proc. **557**, 25 (1999).

[31] B.A. Korevaar, G.J. Adriaenssens, A.H.M. Smets, W.M.M. Kessels, H.–Z. Song, M.C.M. van de Sanden, and D.C. Schram, J. Non-Cryst. Solids. **266-269**, 380 (2000).

[32] M.C.M. van de Sanden, R.J. Severens, W.M.M. Kessels, R.F.G. Meulenbroeks, and D.C. Schram, J. Appl. Phys. **84**, 2426 (1998); J. Appl. Phys. **85**, 1243 (1999).

[33] W.M.M. Kessels, C.M. Leewis, A. Leroux, M.C.M. van de Sanden, and D.C. Schram, J. Vac. Sci. Technol. A **17**, 1531 (1999).

[34] M.C.M. van de Sanden, W.M.M. Kessels, R.J. Severens, and D.C. Schram, Plasma Phys. Control. Fusion **41**, A365 (1999).

[35] W.M.M. Kessels, C.M. Leewis, M.C.M. van de Sanden, and D.C. Schram, J. Appl. Phys. **86**, 4029 (1999).

[36] W.M.M. Kessels, M.C.M. van de Sanden, R.J. Severens, and D.C. Schram, J. Appl. Phys. **87**, 3313 (2000).

[37] W.M.M. Kessels, M.C.M. van de Sanden, and D.C. Schram, accepted for publication in J. Vac. Sci. Technol. **18**, (2000).

[38] With a H$_2$ flow of 10 sccs typically a deposition rate of 7–8 nm/s is obtained. However, due to a drift in the SiH$_4$ mass flow controller, some measurements, such as the presented TOF-analysis, have been performed on films deposited at somewhat higher rates (~10 nm/s). As shown in a separate study this has no significant influence on the film properties nor on the plasma composition (Ref. 37).

[39] J.W.A.M. Gielen, W.M.M. Kessels, M.C.M. van de Sanden, and D.C. Schram, J. Appl. Phys. **82**, 2643 (1996).

[40] A.H.M. Smets, M.C.M. van de Sanden, and D.C. Schram, Thin Solid Films **343-344**, 281 (1999).

[41] A.H.M. Smets, M.C.M. van de Sanden, and D.C. Schram, submitted for publication.

[42] W.M.M. Kessels, M.C.M. van de Sanden, R.J. Severens, L.J. Van IJzendoorn, and D.C. Schram, Mater. Res Soc. Symp. Proc. **507**, 529 (1998).

[43] R.E.I. Schropp and M. Zeman, *Amorphous and Microcrystalline Silicon Solar Cells: Modeling, Materials and Device Technology* (Kluwer Academic Publishers, Boston 1998).

[44] T. Tiedje, J.M. Cebulka, D.L. Morel, and B. Abeles, Phys. Rev. Lett. **46**, 1425 (1981).

Submitted for publication in J. Appl. Phys.

[45] R.J. Severens, G.J.H. Brussaard, M.C.M. van de Sanden, and D.C. Schram, Appl. Phys. Lett. **67**, 491 (1995).

[46] W. Luft and Y.S. Tsuo, *Hydrogenated Amorphous Silicon Alloy Deposition Processes* (Dekker, New York, 1993).

[47] W.M.M. Kessels, R.J. Severens, M.C.M. van de Sanden, and D.C. Schram, J. Non-Cryst. Solids **227-230**, 133 (1998).

[48] D. Beeman, R. Tsu, and M.F. Thorpe, Phys. Rev. B **32**, 874 (1985).

[49] A.H. Mahan, in *Properties of Amorphous Silicon and its Alloys*, ed. by Tim Searle (Inspec, The Institution of Electrical Engineers, London, 1998), p. 39.

[50] N. Maley, and J.S. Lannin, Phys. Rev. B **36**, 1146 (1987).

[51] C. Manfredotti, F. Fizzotti, M. Boero, P. Pastorino, P. Polesello, and E. Vittone, Phys. Rev. B **50**, 18046 (1994).

[52] G.J. Adriaenssens, in *Properties of Amorphous Silicon and its Alloys*, ed. by Tim Searle (Inspec, The Institution of Electrical Engineers, London, 1998), p. 199.

[53] H. Dersch, L. Schweitzer, and J. Stuke, Phys. Rev. B **28**, 4678 (1983).

[54] K.F. Feenstra, J.K. Rath, C.H.M. van der Werf, Z. Hartman, and R.E.I. Schropp, *Proceedings of the 2nd World Conference on Photovoltaic Energy Conversion* (Vienna, Austria, 1998), p. 956.

[55] M. Zeman, R.A.C.M.M. van Swaaij, E. Schroten, L.L.A. Vosteen, and J.W. Metselaar, Mater. Res. Soc. Symp. Proc. **507**, 409 (1998).

[56] J. Perrin, O. Leroy, and M.C. Bordage, Contrib. Plasma Phys. **36**, 1 (1996).

[57] A. Gallagher, Mater. Res. Soc. Symp. Proc. **70**, 3 (1986), A. Gallagher, Int. J. Solar Energy **5**, 311 (1988).

[58] D.A. Doughty, J.R. Doyle, G.H. Lin, and A. Gallagher, J. Appl. Phys. **67**, 6220 (1990).

[59] J.R. Abelson, Appl. Phys. A **56**, 493 (1993).

[60] E.A.G. Hamers, W.G.J.H.M. van Sark, J. Bezemer, H. Meiling, and W.F. van der Weg, J. Non-Cryst. Solids **226**, 205 (1998).

[61] J. Doyle, R. Robertson, G.H. Lin, M.Z. He, and A. Gallagher, J. Appl. Phys. **64**, 3215 (1988).

[62] B.P. Nelson, Q. Wang, E. Iwaniczko, A.H. Mahan, and R.S. Crandall, Mater. Res Soc. Symp. Proc. **507**, 927 (1998).

[63] A.H. Mahan (private communication).

[64] G. Ganguly and A. Matsuda, Mater. Res Soc. Symp. Proc. **336**, 7 (1994).

[65] K. Kato, S. Iizuka, G. Ganguly, T. Ikeda, A. Matsuda, and N. Sato, Jpn. J. Appl. Phys., Part 1 **36**, 4547 (1997).

[66] J. Kocka, H. Stuchlikova, A. Fejfar, G. Ganguly, I. Sakata, A. Matsuda, and G. Juska, J. Non-Cryst. Solids **227-230**, 229 (1998).

[67] J.W. Rabalais, A.H. Al-Bayati, K.J. Boyd, D. Marton, J. Kulik, Z. Zhang, and W.K. Chu, Phys. Rev. B **53**, 10781 (1996).

[68] S. Dong, Y. Tang, R. Braunstein, R.S. Crandall, B.P. Nelson, and A.H. Mahan, J. Appl. Phys. **82**, 702 (1997), see also comments on electron drift mobility in Ref. 52.

[69] M. Heintze, R. Zedlitz, H.N. Wanka, and M.B. Schubert, J. Appl. Phys. **79**, 2699 (1996).

[70] K.F. Feenstra, PhD Thesis, Utrecht University, The Netherlands (1998).

[71] T. Takagi, R. Hayashi, A. Payne, W. Futako, T. Nishimoto, M. Takai, M. Kondo, and A. Matsuda, Mater. Res. Soc. Symp. Proc. **557**, 105 (1999).

[72] T. Takagi, K. Takechi, Y. Nakagawa, Y. Watabe, and S. Nishida, Vacuum **51**, 751 (1998).

[73] K. Maeda, I. Umezu, and H. Ishizuka, Phys. Rev. B **55**, 4323 (1997).

[74] R.D. Knox, V. Dalal, B. Moradi, and G. Chumanov, J. Vac. Sci. Technol. A **11**, 1896 (1993).

[75] S.E. Ready, J.B. Boyce, N.M. Johnson, J. Walker, and K.S. Stevens, Mater. Res. Soc. Symp. Proc. **192**, 127 (1990).

[76] E.C. Molenbroek, A.H. Mahan, E.J. Johnson, and A.C. Gallagher, J. Appl. Phys. **79**, 7278 (1996).

[77] S.M. Gates, B.A. Scott, D.B. Beach, R. Imbihl, and J.E. Demuth, J. Vac. Sci. Technol. A **5**, 628 (1987).

[78] L.-Q. Xia, M.E. Jones, N. Maity, and J.R. Engstrom, J. Vac. Sci. Technol. A **13**, 2651 (1995).

Cavity ring down detection of SiH_3 in a remote SiH_4 plasma and comparison with model calculations and mass spectrometry

W. M. M. Kessels,[a)] A. Leroux, M. G. H. Boogaarts, J. P. M. Hoefnagels,
M. C. M. van de Sanden,[b)] and D. C. Schram
Department of Applied Physics, Eindhoven University of Technology, P.O. Box 513, 5600 MB Eindhoven, The Netherlands

Spatially resolved SiH_3 measurements are performed by cavity ring down spectroscopy on the SiH_3 $\tilde{A}\,^2A_1 \leftarrow \tilde{X}\,^2A_1$ transition at 217 nm in a remote Ar-H_2-SiH_4 plasma used for high rate deposition of hydrogenated amorphous silicon. The obtained densities of SiH_3 and its axial and radial distribution in the cylindrical deposition reactor are compared with simulations by a two-dimensional axisymmetric fluid dynamics model. The model, in which only three basic chemical reactions are taken into account, shows fairly good agreement with the experimental results and the plasma and surface processes as well as transport phenomena in the plasma are discussed. Furthermore, the SiH_3 density as determined by cavity ring down spectroscopy is in good agreement with the SiH_3 density as obtained by threshold ionization mass spectrometry.

I. INTRODUCTION

Hydrogenated amorphous silicon (a-Si:H) produced by plasma decomposition of SiH_4 is a widely used material with its major applications in thin film solar cells and thin film transistors. For the optimization of the deposition process and the a-Si:H film properties, detailed knowledge on the elementary plasma and surface reactions is essential. Therefore numerous studies on the plasma composition have been carried out, mainly in radio frequency (rf) parallel plate reactors. From this consideration, the plasma processes and the contribution of the different plasma species to film growth are also investigated in the so-called expanding thermal plasma (ETP). This remote plasma deposition technique distinguishes itself mainly by the fact that it is capable of depositing good quality a-Si:H at much higher rates (up to 10 nm/s) than by conventional techniques.[1,2] Apart from the fact that this technique has potential for cost-effective solar cell production, it enables also investigation and verification of film growth mechanisms under more "extreme" conditions. These conditions are rather well-defined (as will be shown below) due to the fact that the remote nature of the technique allows for independent parameter control and variation.

Up to now, the SiH_4 dissociation process and species contributing to film growth in the expanding thermal plasma have been studied by several diagnostics, such as Langmuir probes, ion and threshold ionization mass spectrometry, optical emission spectroscopy, and surface reaction probability measurements.[3-7] These studies have revealed that under "optimized" conditions, the SiH_4 is primarily dissociated by H emanating from the Ar-H_2 operated plasma source

$$H + SiH_4 \rightarrow SiH_3 + H_2 \qquad (1)$$

because electron-induced ionization and dissociation of SiH_4 are insignificant due to the low electron temperature (0.1–0.3 eV).[3,5] Furthermore, it has been shown that the contribution of positive ions $Si_nH_m^+$ (with n up to 10) to film growth is about 6%.[4,5] The contribution of radicals other than SiH_3 is expected to be rather small because the contribution of SiH_3 is estimated at ~90% from threshold ionization mass spectrometry (TIMS) measurements performed at the position of the substrate.[7]

Although mass spectrometry yields directly information relevant for deposition plasmas because it measures the species very close to the wall, it cannot be applied easily and non-intrusively at several positions in the plasma. Spatially-resolved measurements at different positions are useful for the investigation of the generation and loss processes of species in the plasma. For this reason, SiH_3 has recently also been detected by cavity ring down spectroscopy (CRDS) in the ETP setup.[8] In this absorption technique, the $\tilde{A}\,^2A_1 \leftarrow \tilde{X}\,^2A_1$ electronic transition of SiH_3 centered at ~215 nm is used. The corresponding absorption band is diffuse (it ranges from ~200–260 nm) due to the predissociative nature

---

[a)] Electronic mail: w.m.m.kessels@phys.tue.nl
[b)] Electronic mail: m.c.m.v.d.sanden@phys.tue.nl

of the excited state[9,10] and an approximate peak absorption cross-section of 2.4×10^{-21} m^2 at 215 nm has been estimated by Lightfoot *et al.*[10] An important advantage of cavity ring down spectroscopy is its very high sensitivity. The high sensitivity is due to the fact that the technique is based on multipassing and due to the fact that not the change in absolute light intensity is measured like in traditional absorption spectroscopy. Instead, CRDS uses the decay time of a laser light pulse trapped in an optical cavity created by two highly reflective mirrors.[11] Briefly, the decay or ring down time τ_λ of a light pulse at a wavelength λ that is monitored at the exit mirror, depends on the reflectivity of the mirrors R_λ, the length d of the cavity and the possible presence of an absorbing medium with absorption A_λ

$$\tau_\lambda = \frac{d/c}{\left(1 - R_\lambda + A_\lambda\right)} \tag{2}$$

with c the speed of light. For an axisymmetric density profile $n(r)$ with radial coordinate r, the absorption at a lateral position y depends on the cross-section σ_λ of the absorbing species and its line-integrated number density over the absorption path length $2l$

$$A_\lambda(y) = \sigma_\lambda \int_{-l}^{l} n(r)dx = \sigma_\lambda \int_{-l}^{l} n(\sqrt{x^2 + y^2})dx \tag{3}$$

with $l = \sqrt{R^2 - y^2}$ and R the radius of the setup. By comparing the decay time for the cavity with absorbing species with the decay time for the "empty" cavity, the absorption and the (line-integrated) density of the absorbing species can be calculated.

In addition to the measurements described in Ref. 8, in this article the absorption by SiH_3 measured at several axial positions is presented as a function of the SiH_4 flow. Furthermore, also measurements at lateral positions are given enabling a calculation of the spatially resolved SiH_3 density by means of Abel inversion. In Ref. 8, a homogeneous SiH_3 density has been assumed over a path length $2l = 30$ cm.

The measured SiH_3 density and its radial distribution in the cylinder-symmetric deposition chamber are furthermore compared to those obtained by two-dimensional axisymmetric model calculations. These calculations have been performed using the commercial computational fluid dynamics software PHOENICS-CVD.[12] In the model, only the (supposedly) basic gas phase and surface chemical processes are taken into account. It is assumed that H is the only reactive species emanating from the Ar-H_2 operated plasma source and that reaction (1) is the only SiH_4 dissociation process. No ion and electron processes are taken into account, reducing the model basically to a hot, reactive gas model. As concluded from previous studies, this is fairly reasonable, especially as far as the production of SiH_3 is concerned. From this simplified model, better insight into the processes and in the transport phenomena in the reactor can be gained. The simulations, combined with the experimental results on the radial profile of the SiH_3 density, are furthermore helpful for the comparison of the SiH_3 densities obtained by CRDS with those obtained by TIMS at the position of the substrate holder.[7] It will be demonstrated that the densities show good agreement.

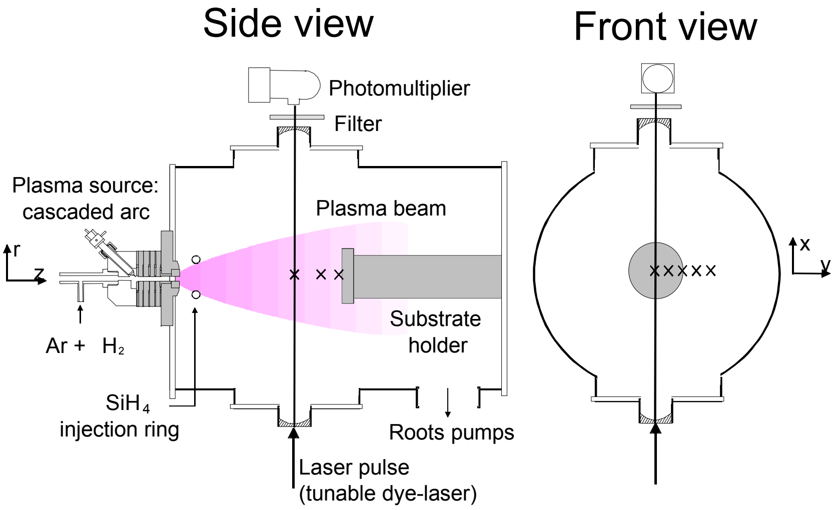

FIG. 1. Schematics of the side and front view of the expanding thermal plasma (ETP) used for a-Si:H deposition together with the cavity ring down spectroscopy setup. The laser beam's axial positions (0.6, 3.6, and 11 cm from the substrate holder) and radial positions (from 0 to 11 cm) at 3.6 cm from the substrate holder are indicated (×). The figure is not to scale.

II. DEPOSITION SYSTEM AND OPTICAL SETUP

A side and front view of the expanding thermal plasma is given in Fig. 1. The setup consists of a cascaded arc plasma source and a downstream deposition chamber. In the cascaded arc a thermal Ar-H_2 plasma is created at a pressure of ~400 mbar using an Ar flow of 55 sccs (standard cubic centimeter per second) and a H_2 flow of 10 sccs. The arc is current controlled at 45 A and the arc voltage is ~140 V. The plasma expands supersonically into the low-pressure deposition chamber (0.2 mbar) leading to a stationary shock at approximately 5 cm from the arc exit. At this distance, pure SiH_4 is added to the plasma by means of an injection ring with a diameter of 7.5 cm. For the experiments reported here, the SiH_4 flow is varied between 0 and 25 sccs. At 35 cm from the arc exit, a substrate holder with a diameter of 10 cm is positioned that can be exchanged by a Hiden Analytical mass spectrometer (PSM Upgrade of EPIC 300) with a similar geometry.[5,7] During processing the reactor with a volume of 180 ℓ is pumped by a stack of two roots blowers and one fore-pump with a total pumping capacity of ~1500 m^3/hr. This leads to a typical residence time of the gas of 0.4–0.5 s. Overnight the reactor is pumped by means of a 450 ℓ/s turbopump reaching a base pressure of 10^{-6} mbar.

For the CRDS measurements, a stable optical cavity is created by two plano-concave mirrors (~97% reflectivity around 217 nm, –100 cm radius of curvature, 2.5 cm diameter) at a distance of 108 cm apart. The mirrors are mounted on flexible bellows and a very small Ar flow is used to protect them against deposition. The lateral and axial position can be set by means of a sliding vacuum seal. The measurements reported here have been performed at axial positions of 0.6, 3.6 and 11 cm from the substrate (see side view Fig. 1). For an axial position of 3.6 cm, lateral measurements have been performed from 0 to 11 cm from the axis (see front view Fig. 1).

Laser radiation from a Nd:YAG pumped dye laser (Spectra-Physics DCR-11/Sirah PrecisionScan-D) is introduced into the cavity. Operated on Coumarine 440 and frequency-doubled with a BBO crystal, the dye laser delivers radiation with a tunable wavelength between 214 and 227 nm, an estimated bandwidth of 0.2 cm^{-1}, and a typical pulse energy of 10 μJ. A wavelength scan is given in Ref. 8, but in this study the laser wavelength has been kept at 217 nm. The output intensity behind the exit mirror is measured through a narrow bandpass filter (10 nm) with a photomultiplier (Hamamatsu R928) and a digital 500 Ms/s, 100 MHz oscilloscope (Tektronix TDS340a). For all measurements, an average over 64 laser shots is taken and from the resulting transient signal the ring down time τ is determined from a weighted least-squares fit of the logarithm of the transient data. In the measurements described here, τ is first determined for an Ar-H_2 plasma, which did not show any absorption, and then for the Ar-H_2-SiH_4 plasma containing SiH_3. Furthermore, no absorption due to SiH_4 has been observed in agreement with the literature (onset absorption at ~170 nm).[10]

III. MODEL

Two-dimensional axisymmetric simulations of the stationary gas flows, transport phenomena, and gas phase and surface reactions in the downstream deposition reactor have been carried out with the commercial computational fluid dynamics software PHOENICS-CVD.[12] A description of the modeling of the transport phenomena and chemical reactions of multi-component gas mixtures and the applied numerical methods can be found in Refs. 13 and 14. First, a description of the reactor and the processes taken into account in the model will be presented as well as the simplifications and assumptions used. Secondly, some typical gas flow phenomena in the reactor as calculated by the model will be illustrated.

As mentioned above, the reactor has been assumed to be axisymmetric (see Fig. 2). This has as a main consequence that the outlet towards the pumping system has been assumed to be located along the complete side of the reactor for one axial position. The total area of the outlet has been set equal to its actual value. Another important simplification is that the supersonic region has been left out of the model. The model starts 5 cm from the arc exit at the position of the SiH_4 injection ring. For all species one uniform inlet area has been assumed, which has been set equal to the estimated beam area at that position (supersonic expansion under 45°). Therefore only subsonic flows have been taken into account, while the inlet conditions (as defined below) have been taken from experimental data in the region of the shock. Although this is a good approximation because the conditions before the shock are not influenced by the conditions downstream, it causes some deviations in the radial, subsonic outer region of the shock, because this region

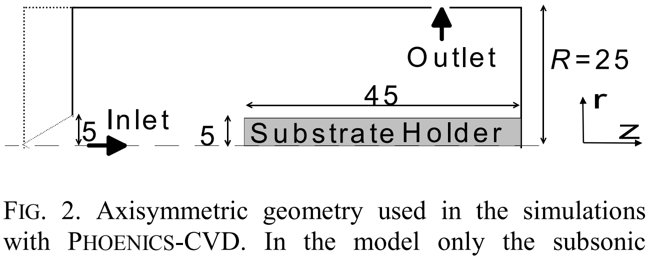

FIG. 2. Axisymmetric geometry used in the simulations with PHOENICS-CVD. In the model only the subsonic expansion is taken into account reducing the length of the reactor in the model by 5 cm as indicated. The dimensions are given in centimeters.

is not taken into account in the model (see Fig. 2). For the calculation domain, a non-uniform cylindrical grid has been used with 25 grid points in the radial and 40 grid points in the axial direction. The grid is locally refined near the inlet, the substrate, the outlet, and the reactor walls. Grid independence of the results has been checked by using a 50×80 grid for some representative situations. The differences were smaller than 5%.

In the model, only five species (Ar, H_2, H, SiH_4, SiH_3) are considered, while no electrons and ions have been taken into account. This is a fairly good approximation for the experimental conditions described, i.e., with significant H_2 dilution, as concluded from previous experimental investigations of the plasma.[3,5,7] At the inlet, Ar, H_2, H, and SiH_4 are introduced in the reactor with an axial velocity of 800–850 m/s and a quadratic velocity profile in radial direction. At the inlet a single gas temperature equal to 3000 K has been assumed for the mixture. These values for the velocity and temperature have been derived from laser-induced fluorescence (LIF) measurements on Ar.[15] The Ar flow is 55 sccs, whereas the H and H_2 flow at the inlet are calculated from the initial H_2 flow of 10 sccs and the H_2 dissociation degree α. The inlet pressure has been set at ~0.23 mbar,[16,17] and varies slightly with the actual total gas flow. At the outlet, the flow has a radial velocity of typically 16 m/s as determined by the pumping capacity. All walls are isothermal and maintained at a temperature of 500 K, except for the substrate holder, which has been set at 700 K. This is approximately equal to the typical substrate temperature during deposition (400 °C).[1,2]

The only gas phase reaction taken into account in the model is reaction (1), in which SiH_3 is produced by hydrogen abstraction of SiH_4. Based on the results of Goumri *et al.*[18] for temperatures T in the range of 290–660 K, the rate of this reaction has been set at $1.8\times10^{-16}\exp(-1925/T)$ m^3s^{-1} for the complete temperature interval in the model.

For H and SiH_3 surface reactions have been implemented. H can recombine at the walls by the reaction

$$H(g) + H(s) \rightarrow H_2(g) \qquad (4)$$

with recombination coefficient γ. It is assumed that γ is independent of the wall temperature and for simulations with only Ar-H_2, γ has been set equal to 0.2, the value proposed for stainless steel.[19] For simulations with SiH_4 (i.e., with deposition and consequently a-Si:H covered walls) γ is set equal to 1.[19]

SiH_3 can get lost at the surface by deposition while simultaneously splitting off gaseous H_2:

$$SiH_3(g) \rightarrow a\text{-}Si{:}H(s) + H_2(g). \qquad (5)$$

For this reaction, a sticking probability s of SiH_3 equal to the surface reaction probability β has been assumed, i.e., $s=\beta$. Recombination of SiH_3 with H at the surface forming gaseous SiH_4[20-22] is not included in the calculations described, but it has been checked that this has negligible implications for the calculated SiH_3 and SiH_4 density when the SiH_4 consumption is small. In the presented calculations β is taken 0.3 and assumed to be surface temperature independent.[6] Reaction (1) and (5) imply that for every Si atom deposited 1.5 gaseous H_2 molecules are generated. In reality, for the heated substrate holder almost 2 gaseous H_2 molecules are generated per Si deposited and for the relatively cold walls approximately 1 gaseous H_2 molecule.[3]

Before running simulations with SiH_4, first the value of the dissociation degree α of the H_2 emanating from the arc has to be set. On the value of α it can be decided from simulations with only Ar and H_2 by comparing the calculated H density with the one determined by two-photon-absorption laser-induced fluorescence (TALIF) in an Ar-H_2 plasma.[23] The calculated H densities for α=2% and α=5% are given in Fig. 3. The H densities obtained for α=2% show good agreement with the experimentally obtained densities, especially at small z values. The difference for larger z values can possibly be attributed to the different reactor geometry (e.g., the chamber diameter is 32 cm instead of 50 cm) and the absence of a substrate holder in the reactor wherein the TALIF measurements were performed. Concerning the radial H densities, the behavior of the experimental and simulated densities show very good agreement, i.e., flat profiles in the center of the reactor. In the following sections, results of simulations with both α=2% and α=5% will be presented, because a better agreement with the experimental data is obtained for

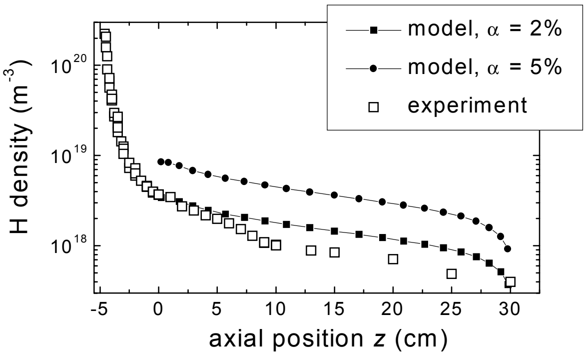

FIG. 3. Experimental axial H density as determined by two-photon laser-induced fluorescence (Ref. 23), compared with the calculated H densities for two values of the H_2 dissociation degree α. The experimental values are obtained in a reactor with a slightly different geometry and cascaded arc and for slightly different plasma conditions (50 sccs Ar, 8.3 sccs H_2, and 40 A arc current). The model starts at 5 cm from the arc outlet that is situated at z=-5 cm.

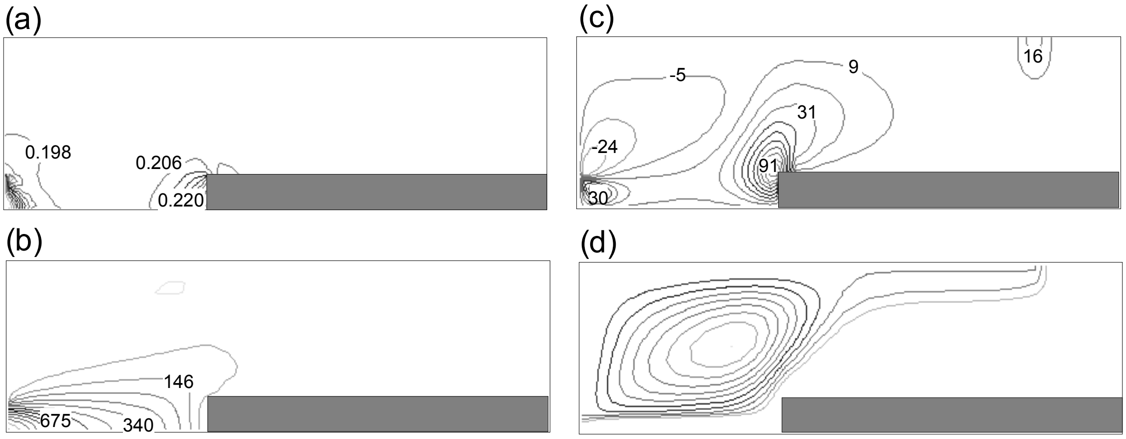

FIG. 4. The calculated iso-lines for the (a) static pressure, (b) axial, and (c) radial velocity, as well as for the (d) streamlines for a condition typically used for a-Si:H deposition. The pressure is given in mbar, the velocity in m/s.

values of α slightly larger than 2%. Small differences in α for the two setups might be caused by the aforementioned differences in reactor geometry as well as the slightly different operating conditions used for the TALIF measurements. The TALIF measurements were performed with an Ar flow of 50 sccs, a H_2 flow of 8.3 sccs, and an arc current of 40 A.

In Fig. 4, results of a simulation for standard conditions, i.e., with 10 sccs SiH_4 and a substrate temperature of 700 K, are given. The presented pressure, axial and radial velocity fields and streamlines yield insight into the gas flows in the reactor. The pressure at the inlet (0.23 mbar) and in front of the substrate holder (0.22 mbar) are slightly higher than the global pressure of 0.20 mbar in the rest of the reactor. The slightly higher pressure in front of the substrate holder that extends ~5 cm upstream indicates a flow stagnation zone. This can also be seen from the velocity contour plots. The axial velocity decreases from ~850 m/s at the inlet to zero just in front of the substrate holder where it is partly converted into radial velocity. At the corner of the substrate holder, a radial velocity up to ~100 m/s is generated. The radial velocity iso-lines and streamlines indicate also a recirculation zone with a flow velocity of less than 25 m/s. Furthermore, the radial velocity is ~16 m/s at the outlet of the reactor towards the pumps. These observations and values are typical for all conditions considered in this work and they are not seriously influenced by the chemical reactions taking place.

IV. RESULTS AND DISCUSSION

A. Cavity ring down measurements

1. Lateral scan and radial density profile

Before addressing the absorption by SiH_3 and its local density for different SiH_4 flows, first information on the radial distribution of SiH_3 has to be obtained. Therefore the absorption has been measured for different lateral positions y at an axial position of 3.6 cm from the substrate holder. Unfortunately, due to practical limitations, measurements could only be performed at this axial position and for lateral positions ranging from 0 to 11 cm. At 3.6 cm from the substrate holder, it is not expected that the SiH_3 density is affected by the substrate holder due to surface loss of SiH_3. The typical gradient length of the SiH_3 density towards the surface is smaller than 3 cm as calculated from its diffusivity[24] and surface reaction probability.[6] The SiH_3 density, however, can slightly be affected by the stagnation of the plasma beam in front of the substrate holder (see Sec. IV B).

In Fig. 5, the absorption $A_\lambda(y)$ at λ=217 nm is given as a function of y for a SiH_4 flow of 10 sccs. The data have been averaged over ten separate measurements and the error bars have been calculated from the standard deviation. For an axisymmetric density profile, the density $n(r)$ of SiH_3 at radial position r can be calculated from $A_\lambda(y)$ by Abel inversion of Eq. (3)[25]

$$n(r) = \frac{-1}{\sigma_\lambda \pi} \int_r^R \frac{1}{(y^2 - r^2)^{1/2}} \frac{dA_\lambda(y)}{dy} dy \qquad (6)$$

with R is the radius of the setup. For practical evaluation of Eq. (6), the lateral profile of the absorption is fitted by means of a sum of two Gaussians, both centered at y=0. The advantage of this method is that Gaussians are invariant to Abel inversion making the calculation straightforward. The fit is given in Fig. 5, where it has been imposed that the lateral absorption profile drops to zero at y=R. Other procedures for carrying out the inversion[25,26] are not useful due to the fact that only a few data points are available and only for a limited part of the profile. Concerning the fit in Fig. 5, it should be taken into

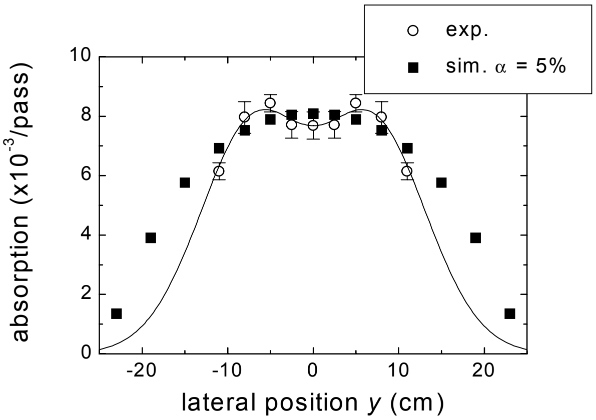

FIG. 5. The absorption $A(y)$ as measured at lateral positions ranging from 0 to 11 cm and at a distance of 3.6 cm from the substrate holder. The SiH_4 flow is 10 sccs. For Abel inversion, the lateral profile has been fitted by a sum of two Gaussians while imposing zero absorption at the radius of the setup $y=R=25$ cm. For presentation purposes, at $y<0$ the same values are given as for $y>0$. Furthermore, the lateral absorption profile as calculated from the simulated SiH_3 density (i.e., product of line-integrated density and cross-section) with $\alpha=5\%$ is given for the same axial position (see Sec. IV B).

account that it does not describe the data points perfectly and that it is certainly not unique. Nevertheless, it is believed that it gives a reasonable description of the profile, although in the interpretation of the deduced radial SiH_3 density distribution these uncertainties should be kept in mind.

In Fig. 6, the radial profile of the SiH_3 density as calculated from the fit in Fig. 5 is given. For the calculation of the density, the cross-section at 217 nm has been assumed equal to the one reported for 215 nm. This is validated by the broad nature of the SiH_3 absorption peak.[8,10] In addition to a decrease in density in the outward direction due to outward diffusion and surface loss, the radial profile is hollow at the axis. This was actually already evident from the lateral absorption profile. The hollow profile is most probably caused by a temperature effect: a higher gas temperature at the axis in a (nearly) isobaric reactor [see Fig. 4(a)] leads to a lower SiH_3 density at the axis. As already mentioned, it is not expected that the SiH_3 density at a distance of 3.6 cm from the substrate is directly influenced by loss of SiH_3 at the substrate holder. Model calculations presented in Sec. IV B corroborate this interpretation. Simulated radial SiH_3 profiles show also a reduced density at the axis due to a higher gas temperature, albeit to a smaller extent.

Lateral absorption profiles for other SiH_4 flows showed, within the experimental error, a similar dependence of the absorption on the lateral position as in Fig. 5 for 10 sccs SiH_4. There might be some indications that the profile is slightly more hollow at

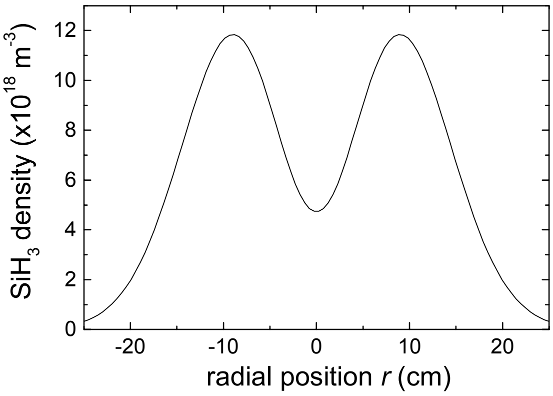

FIG. 6. Radial distribution of the SiH_3 density $n(r)$ as obtained from the Abel inversion of the lateral absorption profile in Fig. 5. The distance to the substrate holder is 3.6 cm.

low SiH_4 flows, but within the accuracy the radial distribution of SiH_3 in Fig. 6 is expected to be representative for all conditions.

2. SiH_4 flow series at different axial positions

In Fig. 7, the absorption by SiH_3 is given as a function of the SiH_4 flow for three different axial positions, 11, 3.6, and 0.6 cm from the substrate holder. The experimental uncertainty in the measurements is less than 15%, as estimated from the reproducibility. The trend and the absolute magnitude of the absorption are roughly the same for the three positions, although the absorption at 11 cm from the substrate holder is slightly lower than for the other two positions. The trend of the absorption for increasing SiH_4 flow is furthermore similar to the one observed in the SiH_3 density as determined by threshold ionization mass spectrometry[7] (see Sec. IV

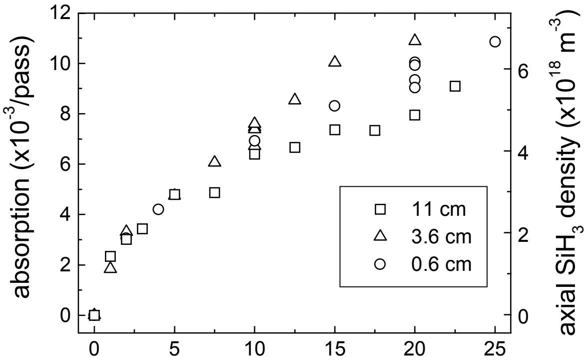

FIG. 7. The absorption $A(y=0)$ by SiH_3 as measured at three axial positions (given in centimeters from the substrate holder) for different SiH_4 flows. At the right ordinate, the axial ($r=0$) density of SiH_3 at a distance of 3.6 cm from the substrate holder is given as determined from the radial distribution in Fig. 6.

C for a direct comparison). On the right ordinate of Fig. 7, also the axial (r=0) SiH_3 density is given for the position of 3.6 cm from the substrate holder. As mentioned above, it should be kept in mind that the radial distribution, and thus the axial density, is very sensitive to the fit of the lateral profile and the errors in the lateral absorption values. This complicates a conclusive interpretation of the exact local SiH_3 density. For the other axial positions, no information on the radial distribution of SiH_3 is available. However, it is expected that the scale at the right ordinate of Fig. 7 gives a rough indication of the magnitude of the axial density at these positions. The densities are in fairly good agreement with the estimated densities in Ref. 8 where a homogeneous distribution of SiH_3 over 30 cm was assumed. More insight into the SiH_3 density at different axial positions can be obtained from the simulations, which are addressed next.

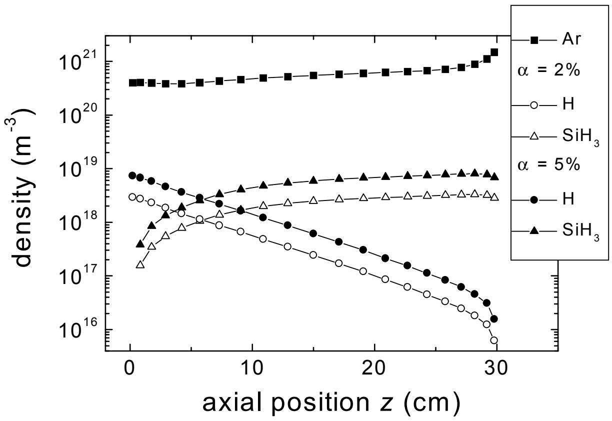

FIG. 8. The axial density of Ar, H, and SiH_3 obtained from the simulations with PHOENICS-CVD for initial H_2 dissociation degrees α of 2% and 5%.

B. Model calculations

In this section, the results obtained from simulations with PHOENICS-CVD will be presented, concentrating mainly on the SiH_3 density and its spatial distribution (i.e., axial and radial density profiles). From the comparison with the experimental results, it is possible to test whether the principal processes in the expanding thermal plasma for a-Si:H deposition can be reduced to the three chemical reactions taken into account into the model. The simulations are also helpful in the interpretation and understanding of the experimental data.

In Fig. 8, the axial densities of Ar, H and SiH_3 are given as a function of the axial position z for the condition with 10 sccs SiH_4. For H and SiH_3, data are given for both α=2% and α=5% as only these densities are influenced significantly by the value of α within this range. In Fig. 9, the corresponding radial profiles of the gas temperature, Ar density, H density, and SiH_3 density are given for axial positions of 0.6, 3.6 and 11 cm from the substrate holder. For SiH_3, the radial density deduced from the experimental data is also presented. On the basis of these figures several comments can be made:

- The axial Ar density increases slightly for increasing z due to the gradually decreasing gas temperature. Just in front of the substrate holder, the Ar density shows a sharper increase due to a temperature jump (from 1500 to 700 K within 3 cm) and due to stagnation of the plasma beam (pressure increases from 0.20 mbar to 0.22 mbar). The density of SiH_3 increases while the density of H decreases with increasing z due to, respectively, production and loss by reaction (1). The density of both reactive species decreases in front of the substrate due to surface loss. The surface loss seems to have only a small effect, however in terms of density this effect is obscured by the temperature jump and stagnation pressure. When considering the relative densities or concentrations of the species, the effect of surface loss is much clearer. Furthermore, it is noteworthy that between the cases with α=2% and α=5% only differences in the absolute magnitude of the H and SiH_3 density are observed.
- Comparing the H density with the one in Fig. 3 for the Ar-H_2 case, reveals that for α=2% the H density in front of the substrate holder has been decreased from ~4×10^{17} to ~7×10^{15} by admixing 10 sccs SiH_4. This shows that reaction (1) is fast enough to consume almost all H within the transit from the injection ring to the substrate holder. The SiH_3 density close to the substrate holder is about a factor of ~300 higher than the corresponding H density, while the difference in thermal flux is a factor of ~50. This suggests that the interaction of H with the a-Si:H surface during deposition is limited compared to the interaction of SiH_3 for the ETP technique.
- For the radial profiles at different axial positions, the distribution of the Ar density is opposite to the distribution of the gas temperature. This is also expected because the downstream region is nearly isobaric and Ar is largely the majority species. This means that the gas mixture properties are not significantly influenced by the chemistry occurring. Furthermore, the influence of the substrate holder, causing a homogeneous gas temperature in its vicinity, can be clearly seen.
- The radial distributions of H and SiH_3 are strongly influenced by surface loss of these radicals at the side walls of the reactor. The profile for the H density is much narrower than for SiH_3, which can be attributed to the higher diffusivity of H. For species with a considerable surface loss probability, a larger diffusivity causes a larger gradient length. Or, in other

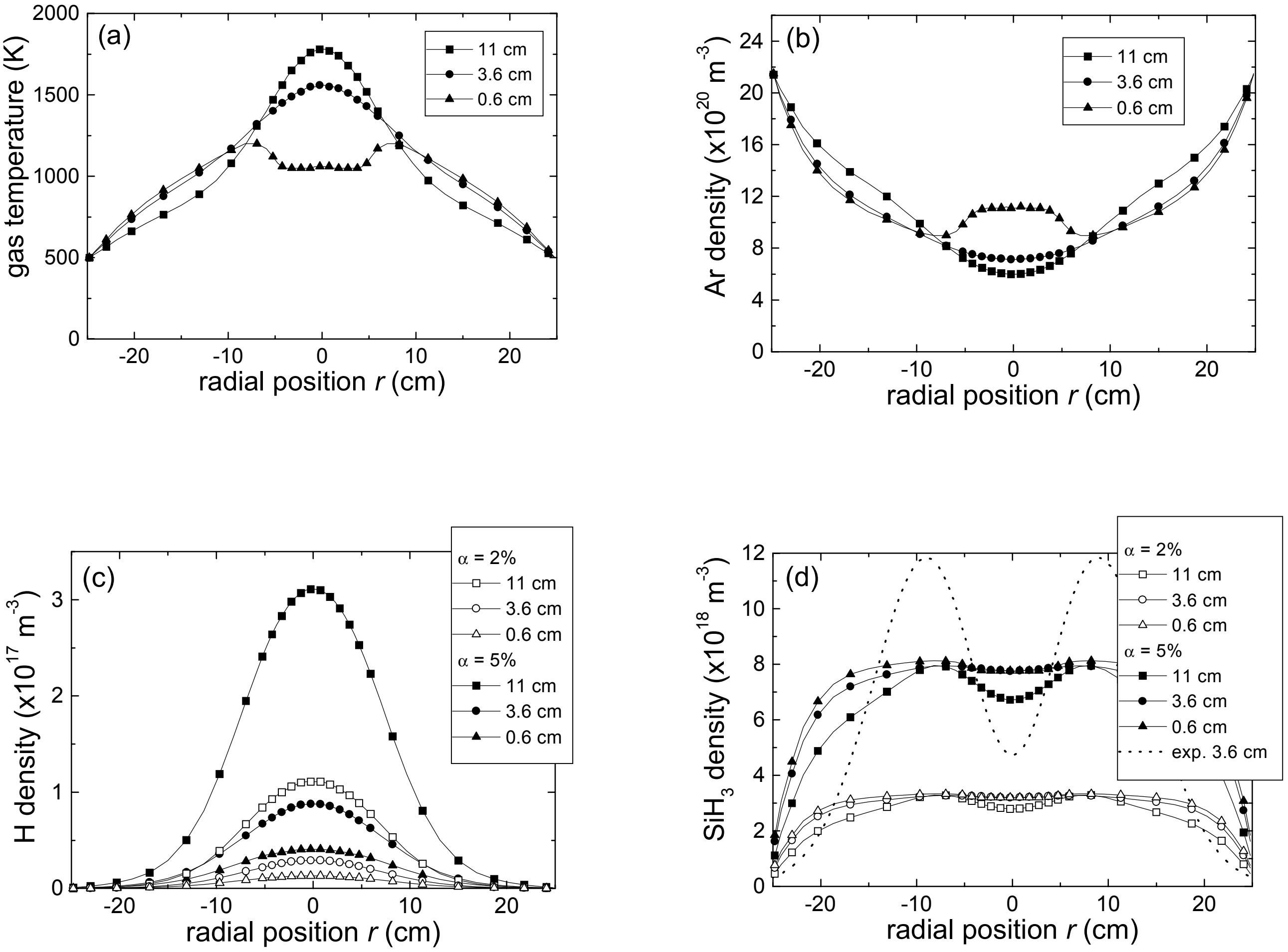

FIG. 9. Radial profiles of the (a) gas temperature, (b) Ar density, (c) H density, and (d) SiH_3 density for axial positions of 0.6, 3.6, and 11 cm from the substrate holder. Where different, the values are given for both α=2% and α=5%. In (d) also the radial distribution of SiH_3 as deduced from the experiments is presented.

words, surface loss affects densities up to a larger distance from the wall. In axial direction, this effect is not observed because the density at the axis is not determined by diffusion but by convection in the beam with a velocity of hundreds of m/s. This is true up to positions close to the substrate holder, where the transport to the substrate is finally taken over by diffusion.

- For the radial distribution of the H density, no significant influence of the substrate holder is observed for the three axial positions. For SiH_3, a hollow profile is observed at 11 cm due to the higher gas temperature at the axis, while at 3.6 cm from the substrate holder the density is more expanded in radial direction and nearly flat. The nearly flat profile is mainly caused by the fact that the substrate holder influences the gas temperature at this position, leading to a rather homogeneous temperature and SiH_3 density. For 0.6 cm, this effect is even more pronounced.
- The comparison of the simulated radial distribution with the experimentally determined distribution at 3.6 cm from the substrate holder, reveals some distinct differences. The simulated profile is nearly flat in the center while the Abel inverted experimental profile is hollow. Hollow profiles are also observed in the simulated data, but only at a larger distance from the substrate holder (e.g., at 11 cm) and much less pronounced. Leaving the accuracy of the radial density profile as deduced by Abel inversion out of consideration for the moment, this might suggest that in the experiment the gas temperature at 3.6 cm is not yet influenced significantly by the substrate holder. Such a difference might be caused by a too large heat conductivity of the gas mixture in the simulations. Diffusion is, however, accurately taken into account in the simulations by the Stefan-Maxwell diffusion model.[13] Furthermore, the heat conductivity depends on the composition of the plasma, but a slightly different composition and the presence of other minority species (radicals, ions, electrons) cannot explain the difference. To reduce the computational effort, thermal diffusion has not been included for the results presented, but it has been verified that the inclusion of

this effect (on the basis of the rigid spheres approximation) leads to differences smaller than 5%. Another striking difference, which is possibly related to the difference in radial profile at r=0, is that the simulated profile is considerably broader than the experimental radial profile (note that its width is mainly determined by the absorption at y=11 cm in Fig. 5). In this case, the thermal conductivity can also play a role: a lower thermal conductivity would create a smaller thermal gradient length at the wall leading to a higher gas temperature in the region between the axis and the wall and therefore to a higher diffusivity of SiH_3. This high diffusivity causes a larger gradient length for the SiH_3 density and thus a narrower profile. The radial distribution of SiH_3 is furthermore influenced by the wall temperature, whereby a higher wall temperature leads to a somewhat narrower profile (again by higher diffusivity). This effect, however, cannot account for the full difference. Another possibility is that the SiH_3 density is affected by radical-radical reactions, which are not yet taken into account in the model. For example, by

$$SiH_3 + SiH_3 \rightarrow SiH_2 + SiH_4. \qquad (7)$$

For the SiH_3 densities presented, the reaction time of SiH_3 for this reaction is typically several milliseconds,[24] meaning that reaction (7) can become very important in the recirculation zone where the diffusivity and the gas flow velocity is rather low.

- An interesting question is how SiH_3 radicals from the center of the beam reach the side wall of the reactor. The radicals can either diffuse directly over the total radius of the setup or diffuse to the recirculating flow in the vortex [See Fig. 4(d)]. Here, by following the streamlines, they can be transported by convection to the region close to the wall, which they can finally reach by diffusion. On the basis of calculations of the diffusion time and the velocity of the recirculating flow, direct diffusion seems to be most important. This is in agreement with the fact that the profile of the SiH_3 density increases in width when going from 11 cm to 3.6 and 0.6 cm from the substrate holder.
- In terms of (line-integrated) SiH_3 density, a better agreement with the experimental data is obtained for α=5%. For this value, the line-integrated density is roughly equal to the experimental one while for α=2% it is a factor ~2.5 smaller. This comparison relies strongly on the absorption cross-section of SiH_3, which is quoted as an approximate value.[10] A factor 2.5 higher dissociation degree for H_2 in the a-Si:H deposition setup, is not inconceivable on the basis of the aforementioned differences in setup and conditions. Moreover, the experimental accuracy of the TALIF measurements and the assumptions in the model are of concern. A higher rate for reaction (1), however, has no influence, because the amount of H is almost fully consumed by this reaction. Furthermore, α=5% yields also better agreement in SiH_4 consumption. For 10 sccs SiH_4, the experimentally obtained SiH_4 consumption is ~10–12%,[7] while if all H is consumed by reaction (1) it is 10% for α=5%. In the simulations presented below only results will be given with α=5%.

Instead of comparing radial density distributions, it is also possible to avoid the procedure of Abel inversion and to compare simulated line-integrated SiH_3 densities or "absorptions" with the experimental values. This is actually the only solid comparison that can be made as no interpretation of the experimental data is involved. In Fig. 5, the calculated absorption for α=5% is included in the lateral absorption profile at 3.6 cm from the substrate holder. The main differences are that the calculated lateral absorption profile does not show a dip in the center and that it drops less fast to zero. These differences are rather significant and are not within the experimental uncertainty of the data. Yet, the discrepancy is reduced compared to the one in the radial density distributions in Fig. 9(d). This illustrates the effect of the deduction of the radial SiH_3 distribution from the data in Fig. 5 by Eq. (6).

By calculating the "absorption" from the simulated SiH_3 density, it is possible to make a comparison with the experimentally obtained absorption at different axial positions and for different SiH_4 flows. In the simulations, the radial distribution of SiH_3 is dependent on the SiH_4 flow: at low SiH_4 flows a hollow profile is obtained (for 1 sccs SiH_4, the density in center is reduced by ~25% of its maximum value), while at high SiH_4 flows the profile is flat in the center. This behavior is in agreement with the earlier mentioned indication that the lateral absorption profiles show a somewhat larger dip at the axis at low SiH_4 flows than for 10 sccs SiH_4 in Fig. 5. In Fig. 10, the calculated absorption at 11, 3.6 and 0.6 cm is given

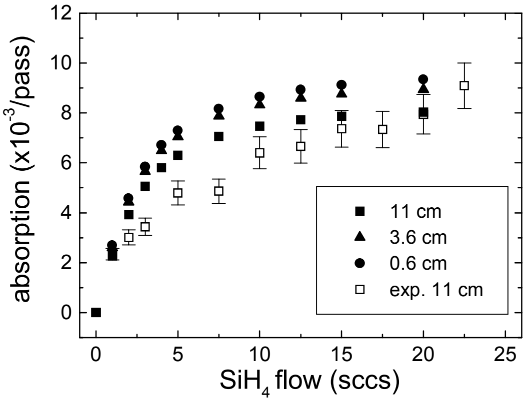

FIG. 10. Absorption by SiH_3 at 11, 3.6, and 0.6 cm from the substrate holder as calculated from the simulations with α=5%. The experimentally obtained absorption values at 11 cm (see Fig. 7) are given for comparison.

given as a function of the SiH_4 flow. The experimental values at 11 cm are given for comparison. The simulated "absorption" at 11 cm is smaller than at positions closer to the substrate holder, whereas the absorptions at 3.6 and 0.6 cm are nearly identical. This is in fairly good agreement with the experiments (see Fig. 7) and it shows that especially between 11 and 3.6 cm there is still a considerable production of SiH_3 by reaction (1). The dependence of the absorption on the SiH_4 flow is also in rough agreement, although there is a significant difference at low SiH_4 flows. The calculated absorption shows a steeper increase with SiH_4 flow leading to higher values at low SiH_4 flows. Furthermore, the simulated values show a clear saturation at high SiH_4 flows, while for the experiments this behavior is less apparent. In the simulations, the saturation is due to the fact that almost all H is consumed by reaction (1) at high SiH_4 flows. This effect might also explain the fact that the SiH_3 density in Fig. 7 and in Ref. 7, as well as the SiH_4 consumption in Ref. 7, flatten off for high SiH_4 flows. Apart from some other marginal phenomena (e.g., ion-molecule reactions[4]), this means that the SiH_4 consumption and SiH_3 production in the ETP technique is limited by the amount of H available for the present plasma settings.[7]

C. Comparison with mass spectrometry

Now that insight has been obtained into the radial distribution of SiH_3, it is possible to make a comparison between the SiH_3 densities obtained from CRDS and those obtained by threshold ionization mass spectrometry (TIMS).[7] TIMS has revealed the axial (r=0) SiH_3 density close to the substrate holder (mass spectrometer). For a quantitative comparison, we need to know the SiH_3 density at this position from the CRDS measurements. The absorption by SiH_3 at a distance of 0.6 cm from the substrate holder has been determined, however, at this position no experimental information on the radial distribution is present. Two approaches can be followed to estimate the axial SiH_3 density at this position. First, the axial density at 3.6 cm from the substrate holder (as given in Fig. 7) can be used by assuming that the absolute magnitude of this density is not affected severely when coming closer to the substrate. This assumption seems reasonable on the basis of the simulated data in Fig. 9, where the SiH_3 density decreases only slightly just in front of the substrate holder. In the second approach, the axial density profile at 3.6 cm from the substrate holder can be taken, whereby it is assumed that when coming closer to the substrate the dip in density (which is presumably due to the gas temperature) diminishes or disappears. This assumption is reasonable on the basis of the fact that very close to the substrate holder, the gas temperature is dictated by the substrate holder as also shown in the simulations (albeit up to a larger distance from the substrate holder). The SiH_3 density very close to the substrate holder is therefore expected to level out due to the homogeneous gas temperature. It is estimated that this leads to a rather homogeneous SiH_3 density over the area of the substrate holder, which is almost a factor two larger than the axial density at 3.6 cm in Fig. 7. This method is less sensitive for the actual depth of the dip in Fig. 6 obtained from the Abel inversion procedure.

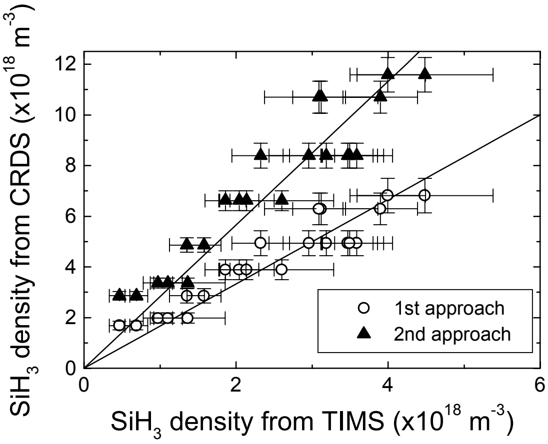

FIG. 11. The axial SiH_3 density as obtained by cavity ring down spectroscopy (CRDS) as a function of the SiH_3 density determined from threshold ionization mass spectrometry (TIMS). For the CRDS measurements, two approaches for the determination of the absolute axial density at the position of the substrate have been used as described in the text.

For both approaches, the axial SiH_3 density from the CRDS measurements close to the substrate is given in Fig. 11 as a function of the density obtained by TIMS. The densities show a very good correlation, also in absolute magnitude. This is especially true for the first approach, whereas the expectedly more realistic second approach gives also a fairly good agreement when considering the accuracy of the calibration procedure for the TIMS measurements.[7] In any case, a quantitative agreement within a factor of 2–3 is observed. Finally it is noted that in this comparison it is assumed that the radial distribution of SiH_3 does not depend on the SiH_4 flow. A slightly more hollow profile for low SiH_4 flows, as might be suggested by the experiments and which is observed in the simulations, would lead even to a better agreement.

V. CONCLUSIONS

Cavity ring down spectroscopy has been applied to detect SiH_3 in an Ar-H_2-SiH_4 plasma generated by the expanding thermal plasma setup. Measurements have been performed at different axial and lateral positions and for different SiH_4 flows. The obtained SiH_3

densities and spatial distributions have been compared with two-dimensional, axisymmetric simulations performed by a fluid dynamics model. The experimentally determined axial SiH_3 density in front of the substrate holder has furthermore been compared to the SiH_3 density obtained by threshold ionization mass spectrometry.

The CRDS measurements reveal an increasing absorption and consequently increasing SiH_3 density with increasing SiH_4 flow and with increasing distance from the plasma source. The simulations yield good agreement with these results showing that for the presented plasma settings the downstream processes in the reactor can roughly be described by one basic gas-phase and two basic surface chemical reactions. This means that for "optimized" conditions in the expanding thermal plasma, ion and electron reactions can be neglected as important SiH_4 dissociation processes, and that the production of SiH_3 can be fully explained by hydrogen abstraction from SiH_4 by H emanating from the Ar-H_2 operated plasma source. There exist some differences in the experimental and simulated radial distribution of SiH_3, but these can probably be attributed to simplifications in the model and to the fact that the experimental distribution is deduced from only a few lateral absorption measurements. Agreement in the absolute SiH_3 density can be obtained for reasonable settings in the model. The absolute density is mainly sensitive to the H_2 dissociation degree at the position of SiH_4 injection: depending on the accuracy of the absorption cross-section for SiH_3, a slightly higher dissociation degree has to be assumed than obtained by experiments for slightly different conditions in a different setup. Furthermore, the axial SiH_3 density in front of the substrate holder determined by TIMS shows good agreement with the SiH_3 density obtained by CRDS and the simulated density at this position. The quantitative agreement depends again on the absorption cross-section, the radial distribution of SiH_3 just in front of the mass spectrometer, as well as on the accuracy of the calibration procedure of the mass spectrometry measurements. Nevertheless, an agreement within a factor of 2–3 is obtained.

All together, cavity ring down spectroscopy, mass spectrometry and the simulations reveal identical SiH_3 densities within approximately a factor of 2–3. For the condition with 10 sccs SiH_4, a SiH_3 density of $4–8\times10^{18}$ m^{-3} is obtained in front of substrate holder. With reasonable assumptions for the sticking probability of SiH_3 (0.1–0.3 [6]) and its thermal velocity, this density can explain the a-Si:H deposition rate of ~7 nm/s obtained for this plasma setting. Furthermore, it has to be noted that a possibly inhomogeneous radial SiH_3 density due to a spatial distribution in gas temperature is partly compensated by this temperature when the homogeneity of the deposition flux or deposition rate is considered.

The absorption determined from the line-integrated, simulated SiH_3 density shows roughly the same dependence on the SiH_4 flow as the experimental values, except for some differences at low SiH_4 flows. The calculated absorption saturates at high SiH_4 flows due to full consumption of H. An almost full consumption of H is therefore most probably also the reason why the measured SiH_3 density and SiH_4 consumption flatten off at large SiH_4 flows. It shows that the rate for H reacting with SiH_4 is fast enough to consume all H and that at high SiH_4 flows the amount of H available is the limiting factor for SiH_4 dissociation in the expanding thermal plasma.

In summary, the spatially resolved CRDS measurements and the fluid dynamics model with only the basic chemical reactions have revealed more insight into the plasma and surface reactions and the gas flow dynamics during a-Si:H deposition. The model has also proven to be very helpful for the interpretation of the experimental data while the experiments yield a test of the basic assumptions of the model. In future work, both the model and experimental information will be extended.

ACKNOWLEDGMENTS

P. J. Böcker is thanked for the development of the cavity ring down software and his contribution to the experiments and S. Mazouffre is thanked for providing the TALIF measurements. The authors greatly acknowledge M. J. F. van de Sande, J. F. C. Jansen, A. B. M. Hüsken, and H. M. M. de Jong for their skilful technical assistance. This work was supported by The Netherlands Organization for Scientific Research (NWO-prioriteit), The Netherlands Foundation for Fundamental Research on Matter (FOM), and The Netherlands Agency for Energy and the Environment (NOVEM).

[1] W.M.M. Kessels, A.H.M. Smets, B.A. Korevaar, G.J. Adriaenssens, M.C.M. van de Sanden, and D.C. Schram, Mater. Res. Soc. Symp. Proc. **557**, 25 (1999).

[2] B.A. Korevaar, G.J. Adriaenssens, A.H.M. Smets, W.M.M. Kessels, H.–Z. Song, M.C.M. van de Sanden, and D.C. Schram, J. Non-Cryst. Solids **266-269**, 380 (2000).

[3] M.C.M. van de Sanden, R.J. Severens, W.M.M. Kessels, R.F.G. Meulenbroeks, and D.C. Schram, J. Appl. Phys. **84**, 2426 (1998), J. Appl. Phys. **85**, 1243 (1999).

[4] W.M.M. Kessels, C.M. Leewis, A. Leroux, M.C.M. van de Sanden, D.C. Schram, J. Vac. Sci. Technol. A **17**, 1531 (1999).

[5] W.M.M. Kessels, C.M. Leewis, M.C.M. van de Sanden, and D.C. Schram, J. Appl. Phys. **86**, 4029 (1999).

[6] W.M.M. Kessels, M.C.M. van de Sanden, R.J. Severens, and D.C. Schram, J. Appl. Phys. **87**, 3313 (2000).

Submitted for publication in J. Vac. Sci. Technol. A.

[7] W.M.M. Kessels, M.C.M. van de Sanden, and D.C. Schram, accepted for publication in J. Vac. Sci. Technol. A **18**, (2000).

[8] M.G.H. Boogaarts, P.J. Böcker, W.M.M. Kessels, D.C. Schram, and M.C.M. van de Sanden, accepted for publication in Chem. Phys. Lett.

[9] G. Olbrich, Chem. Phys. **101**, 381 (1986).

[10] P.D. Lightfoot, R. Becerra, A.A. Jemi-Alade, and R. Lesclaux, Chem. Phys. Lett. **180**, 441 (1991).

[11] A. O'Keefe and D.A.G. Deacon, Rev. Sci. Instrum. **59**, 2544 (1988); *Cavity Ring down Spectroscopy- a new technique for trace absorption measurements*, eds. K.W. Busch and M.A. Busch (American Chemical Society, Washington, 1998).

[12] PHOENICS-CVD is a product of CHAM Ltd., 40 High Street, Wimbledon Village, London SW19 5AU, England. Electronic mail: jrh@cham.co.uk. It is described in detail in The Phoenics Journal **8** (1995).

[13] C.R. Kleijn and K.J. Kuijlaars, The Phoenics Journal **8,** 404 (1995).

[14] K.J. Kuijlaars, C.R. Kleijn, and H.E.A. van den Akker, The Phoenics Journal **8,** 439 (1995).

[15] R. Engeln, N. Sadeghi, S. Mazouffre, and D.C. Schram, to be published.

[16] M.C.M. van de Sanden, R. van den Bercken, and D.C. Schram, Plasma Sources Sci. Technol. **3**, 511 (1994).

[17] R.F.G. Meulenbroeks, R.A.H. Engeln, M.N.A. Beurskens, R.M.J. Paffen, M.C.M. van de Sanden, J.A.M. van der Mullen, and D.C. Schram, Plasma Sources Sci. Technol. **4**, 74 (1995).

[18] A. Goumri, W.-J. Yuan, L. Ding, Y. Shi, and P. Marshall, Chem. Phys. **177**, 233 (1993).

[19] P. Kae-Nune, J. Perrin, J. Jolly, and J. Guillon, Surf. Sci. **360**, L495 (1996)

[20] A. Gallagher, Mater. Res. Soc. Symp. Proc. **70**, 3 (1986).

[21] A. Matsuda, K. Nomoto, Y. Takeuchi, A. Suzuki, A. Yuuki, and J. Perrin, Surf. Sci. **227**, 50 (1990).

[22] J. Perrin, M. Shiratani, P. Kae-Nune, H. Videlot, J. Jolly, and J. Guillon, J. Vac. Sci. Technol. A **16**, 278 (1998).

[23] S. Mazouffre, M.G.H. Boogaarts, J.A.M. van der Mullen, and D.C. Schram, Phys. Rev. Lett. **84**, 2622 (2000).

[24] J. Perrin, O. Leroy, and M.C. Bordage, Contrib. Plasma Phys. **36**, 1 (1996).

[25] H.R. Griem, *Plasma Spectroscopy*, (McGraw-Hill Book Company, New York, 1964).

[26] W. Lochte-Holtgreven, in *Plasma Diagnostics*, ed. by W. Lochte-Holtgreven (North-Holland Publishing Company, Amsterdam, 1968).

Improvement of hydrogenated amorphous silicon properties with increasing contribution of SiH_3 to film growth

W. M. M. Kessels,[a] M. G. H. Boogaarts, J. P. M. Hoefnagels,
M. C. M. van de Sanden,[b] and D. C. Schram
Department of Applied Physics, Eindhoven University of Technology, P.O. Box 513, 5600 MB Eindhoven, The Netherlands

From cavity ring down spectroscopy and threshold ionization mass spectrometry measurements in a remote Ar-H_2-SiH_4 plasma it is clearly demonstrated that the properties of hydrogenated amorphous silicon (a-Si:H) strongly improve with increasing contribution of SiH_3 to film growth. The measurements corroborate the proposed dissociation reactions of SiH_4 for different plasma conditions and it is shown that solar grade quality a-Si:H can be obtained at deposition rates up to 10 nm/s under conditions where film growth is by far dominated by SiH_3.

For hydrogenated amorphous silicon (a-Si:H) deposited by means of plasma decomposition of SiH_4, it is commonly accepted that the high quality of the films is directly related to a dominant contribution of SiH_3 to film growth.[1,2] This relation is mainly attributed to the relatively low sticking probability of SiH_3 and its high surface mobility on an almost fully hydrogenated a-Si:H surface. To obtain more evidence for the aforementioned relationship, also for the less studied, but technological very interesting conditions of high rate deposition, the contribution of SiH_3 to film growth has been investigated for the expanding thermal plasma (ETP) and related to the film properties obtained. With this remote deposition technique solar grade a-Si:H can be obtained at deposition rates up to 10 nm/s,[3,4] and, as will be shown in this article, for conditions where film growth is by far dominated by SiH_3.

The ETP technique is based on the dissociation of SiH_4 in a low-pressure deposition chamber by means of an Ar-H_2 plasma generated in a high-pressure operated cascaded arc plasma source.[5,6] Recently, it was shown that the film properties obtained by this technique depend strongly on the amount of H_2 admixed in the cascaded arc.[3] Figure 1 shows that the deposition rate decreases drastically when a small H_2 flow is admixed, whereas the film quality, here only illustrated by the photoconductivity, improves significantly. This behavior has been attributed to the dissociation processes of SiH_4 and the radicals generated. Due to the low electron temperature in the downstream deposition chamber,[5,6] SiH_4 dissociation is governed by reactions with reactive ionic and atomic particles emanating from the cascaded arc. At very low H_2 flows these are mainly Ar^+,[6] which leads to dissociative charge transfer reactions with SiH_4 followed by (fast) dissociative recombination with electrons

$$Ar^+ + SiH_4 \rightarrow SiH_n^+ + pH_2 + qH + Ar \quad (n\leq 3,\ 4=n+2p+q) \tag{1}$$

$$SiH_n^+ + e \rightarrow SiH_m + sH_2 + rH \quad (m\leq 2,\ n=m+2s+r).$$

This leads dominantly to SiH_m ($m\leq 2$) radicals which are highly reactive, both with the a-Si:H surface as with SiH_4 (leading to reactive polysilane radicals).[5,7] When increasing the H_2 flow, the amount of ions from the cascaded arc decreases considerably and mainly H emanates from the arc as reactive species. Therefore

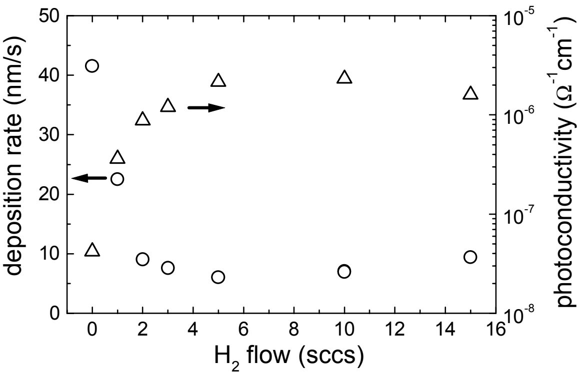

FIG. 1. Deposition rate and AM1.5 photoconductivity (100 mW/cm^2) for a-Si:H films deposited at a substrate temperature of 400 °C and with an Ar and SiH_4 flow of 55 and 10 sccs, respectively, an arc current of 45 A, and a chamber pressure of 0.20 mbar. The H_2 flow in the Ar-H_2 operated cascaded arc plasma source has been varied.

---

[a] Electronic mail: w.m.m.kessels@phys.tue.nl
[b] Electronic mail: m.c.m.v.d.sanden@phys.tue.nl

the reaction[5,7]

$$H + SiH_4 \rightarrow SiH_3 + H_2 \qquad (2)$$

takes over at high H_2 flows. The improvement of the film properties with increasing H_2 flow has therefore been attributed to the transition from a high contribution of very reactive (poly)silane radicals to a dominant contribution of SiH_3 to film growth. Furthermore, the drastic decrease in deposition rate at low H_2 flows can be understood from the fast diminishing importance of the efficient ion-induced reactions, while the gradual increase at higher H_2 flows can be attributed to an increasing H flow from the cascaded arc. Ion-molecule reactions play also a role, but the contribution of $Si_nH_m^+$ ions to film growth is small (<10%) and almost independent of the H_2 flow.[6] The contribution of the ions is therefore not responsible for the observed trend in film quality. The above-mentioned reaction pathway has been proposed on the basis of several plasma diagnostic investigations reported previously.[5-7] In this article, clear evidence will be presented by direct SiH_3 measurements using cavity ring down absorption spectroscopy (CRDS) and threshold ionization mass spectrometry (TIMS).

The CRDS and TIMS measurements have been performed under experimental conditions identical to those in Fig. 1. With CRDS, the line-of-sight integrated absorption by SiH_3 has been measured for an axial position of 0.6 cm from the substrate holder. This was done by probing the SiH_3 $\tilde{A}\ {}^2A_1 \leftarrow \tilde{X}\ {}^2A_1$ transition which has a broad absorption band ranging from ~200–260 nm due to the predissociative nature of the upper state.[8] In Fig. 2, the parts of the absorption spectrum measured with CRDS are given for two different conditions and compared with the spectrum reported by Lightfoot *et al.*[8] The experimental setup and procedure for the CRDS measurements are presented in detail in Ref. 9. The line-integrated density of SiH_3 is calculated from the absorption cross-section estimated for 215 nm (2.4×10^{-21} m^2),[8] while the local axial value of the density is estimated from Abel inverted lateral absorption profiles yielding the radial distribution of SiH_3.[10] The TIMS measurements have been performed with a Hiden Analytical mass spectrometer at the position of the substrate.[7]

In Fig. 3, the axial density of SiH_3 as obtained by CRDS and TIMS is given as a function of the H_2 flow for positions close to the substrate. For high H_2 flows, both techniques yield a gradually increasing SiH_3 density with increasing H_2 flow as is expected from reaction (2) and from the increasing deposition rate in Fig. 1. At very low H_2 flows, where SiH_4 dissociation is governed by ion-induced reactions, the relatively high SiH_3 density can be understood from the very high SiH_4 consumption (up to 60%)[7] and deposition rate. Under these conditions, a significant amount of SiH_3 can be produced by H generated in reactions (1). The small discrepancy between the TIMS and CRDS data in relative behavior at low H_2 flows can most probably be attributed to experimental error in the TIMS measurements caused by clogging of the mass spectrometer's orifice due to the very high deposition rate at low H_2 flows. A significant contribution to the absorption signal by other plasma species at very low H_2 flows is not expected because the measured parts of the spectrum perfectly overlap with the absorption band reported in the literature for all H_2 flows (see Fig. 2). This makes also a possible influence of absorption or scattering by dust particles in the plasma, as observed in, e.g., radio-frequency (rf) SiH_4 plasmas,[11] improbable.

Concerning the differences in absolute density, these can, among others things, be attributed to the fact that the densities refer to different positions from the substrate holder. The SiH_3 density in front of the

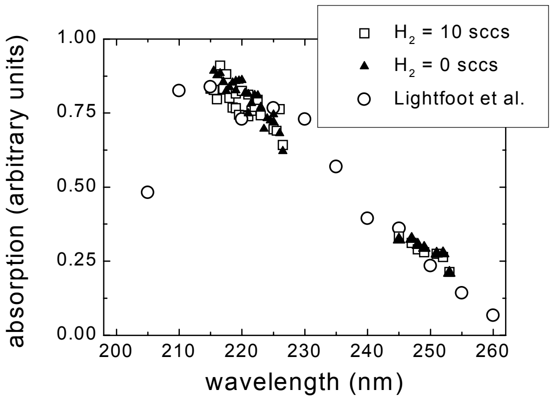

FIG. 2. Parts of the (normalized) SiH_3 absorption spectrum as measured by cavity ring down spectroscopy for a H_2 flow of 0 and 10 sccs. The absorption spectrum reported by Lightfoot *et al.* (Ref. 8) is given for comparison.

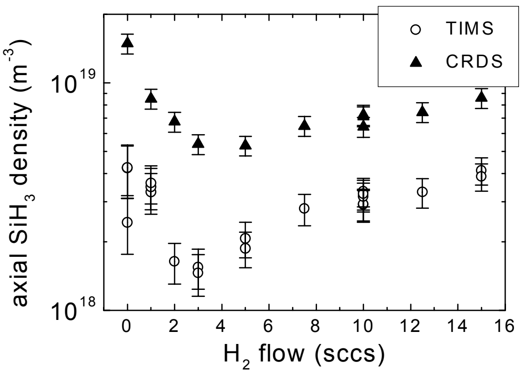

FIG. 3. The axial SiH_3 density as obtained from threshold ionization mass spectrometry (TIMS) and cavity ring down spectroscopy (CRDS) as a function of the H_2 flow. The TIMS data refer to the position of the substrate while the CRDS data refer to a distance of 0.6 cm from the substrate.

substrate can decrease due to surface loss of SiH_3 and therefore lead to a lower density in the TIMS measurements. Furthermore, for both techniques the absolute scale of the density suffers also from experimental uncertainty. For CRDS, this is mainly due to the procedure for obtaining the radial distribution of SiH_3 in order to calculate the local density,[10] as well as due to the uncertainty in absorption cross-section, which is only an approximate value (an upper limit).[8] The accuracy of the absolute density determined by TIMS is limited considerably by estimations made in the calibration procedure.[7] It has to be stressed that the relative values are reliable, as also indicated by the experimental error.

The uncertainty in the absolute scale of the SiH_3 density n_{SiH3} close the substrate, complicates an accurate calculation of the *absolute* value of the contribution of SiH_3 to film growth by the expression[12]

$$\text{contribution of } SiH_3 = \tfrac{1}{4} n_{SiH3} v \frac{s}{1-\beta/2} \frac{1}{N_{Si}} \frac{1}{R_{dep}}. \quad (3)$$

Where v is the thermal velocity of SiH_3 in front of the substrate, s and β the SiH_3 sticking and surface reaction probability, respectively, R_{dep} the deposition rate, and N_{Si} the Si atomic density in the film (dependent on plasma settings). Moreover, the parameters in Eq. (3) are not all known with a high accuracy (especially v, s, and β) preventing precise determination of the contribution of SiH_3 within a factor of two.

Therefore another method is used to calculate the absolute contribution of SiH_3. Because at high H_2 flows (>5 sccs) mainly H emanates from the arc as reactive species, it is very plausible that the increase in deposition rate between 10 and 15 sccs H_2 in Fig. 1 is caused by an increase of the H flow (ion flow from the arc is very small and decreases with H_2 flow)[6] and consequently by an increase in the SiH_3 production by reaction (2). This increase in SiH_3 production between 10 and 15 sccs H_2 is observed in both the TIMS and CRDS measurements, meaning that the (identical) relative *increase* in TIMS and CRDS signal can be related directly with the relative *increase* in deposition rate. From this relation, the absolute contribution of SiH_3 can be calculated with a much higher accuracy, as no information about the absolute densities is required. It only needs to be assumed that v, s, and β are independent of the H_2 flow, but these assumptions would be used when applying Eq. (3) as well. Furthermore, it is important to note that the latter method would give the same *relative* dependence of the SiH_3 contribution on the H_2 flow. For the method proposed here, the uncertainty in the contribution is mainly determined by the reproducibility of the plasma conditions since the CRDS, TIMS, and deposition rate measurements have been performed at different times.

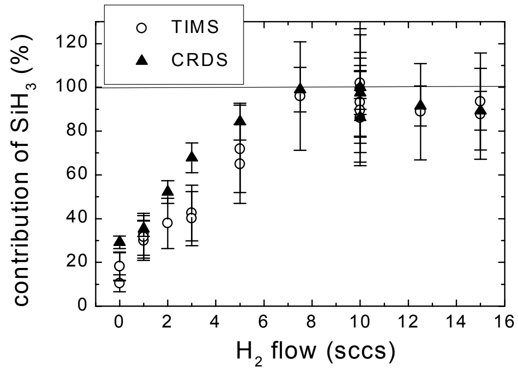

FIG. 4. The contribution of SiH_3 to a-Si:H film growth as calculated from the CRDS and TIMS measurements.

As shown in Fig. 4, the contribution of SiH_3 increases with increasing H_2 flow and saturates for flows larger than ~7.5 sccs. This is in perfect agreement with the proposed SiH_4 dissociation mechanisms. At very low H_2 flows, the ion-induced reactions lead mainly to radicals other than SiH_3, whereas the contribution of SiH_3 to film growth increases with increasing H flow and decreasing ion flow from the cascaded arc when going to higher H_2 flows. For the H dominated conditions, where the optimal film properties are obtained, the contribution of SiH_3 is dominant and about constant. From Fig. 4, it is estimated that film growth is approximately 90% due to SiH_3 with a balance by a small contribution of other (poly)silane radicals and ions. This high contribution of SiH_3 is in very good agreement with the value for the surface reaction probability (~0.3) obtained at high H_2 flows[7] and the contribution of SiH_3 is higher than the reported contribution of SiH_3 to a-Si:H growth in low power rf plasmas.[12,13]

In summary, two diagnostic techniques have been applied independently for SiH_3 detection and have revealed similar results for the SiH_3 density and the contribution of SiH_3 to a-Si:H film growth. The results corroborate the proposed reaction mechanisms in the expanding thermal plasma and a direct correlation between a-Si:H film quality and the contribution of SiH_3 to film growth is unambiguously shown. Furthermore, it is demonstrated that solar grade quality a-Si:H can be obtained at deposition rates up to 10 nm/s for conditions in which film growth is by far dominated by SiH_3.

The authors gratefully acknowledge P. J. Böcker and B. H. P. Broks for their contribution to the measure-ments and M. J. F. van de Sande, J. F. C. Jansen, A. B. M. Hüsken, and H. M. M. de Jong for their technical assistance. This work was supported by The Netherlands Organization for Scientific Research

(NWO), The Netherlands Foundation for Fundamental Research on Matter (FOM) and The Netherlands Agency for Energy and the Environment (NOVEM).

[1] A. Gallagher, Mater. Res. Soc. Symp. Proc. **70**, 3 (1986).

[2] A. Matsuda, J. Vac. Sci. Technol. A **16**, 365 (1998).

[3] W.M.M. Kessels, A.H.M. Smets, B.A. Korevaar, G.J. Adriaenssens, M.C.M. van de Sanden, and D.C. Schram, Mater. Res. Soc. Symp. Proc. **557**, 25 (1999).

[4] B.A. Korevaar, G.J. Adriaenssens, A.H.M. Smets, W.M.M. Kessels, H.–Z. Song, M.C.M. van de Sanden, and D.C. Schram, J. Non-Cryst. Solids. **266-269**, 380 (2000).

[5] M.C.M. van de Sanden, R.J. Severens, W.M.M. Kessels, R.F.G. Meulenbroeks, and D.C. Schram, J. Appl. Phys. **84**, 2426 (1998).

[6] W.M.M. Kessels, C.M. Leewis, M.C.M. van de Sanden, and D.C. Schram, J. Appl. Phys. **86**, 4029 (1999).

[7] W.M.M. Kessels, M.C.M. van de Sanden, and D.C. Schram, accepted for publication in J. Vac. Sci. Technol. A **18**, (2000).

[8] P.D. Lightfoot, R. Becerra, A.A. Jemi-Alade, and R. Lesclaux, Chem. Phys. Lett. **180**, 441 (1991).

[9] M.G.H. Boogaarts, P.J. Böcker, W.M.M. Kessels, M.C.M. van de Sanden, and D.C. Schram, accepted for publication in Chem. Phys. Lett.

[10] W.M.M. Kessels, A. Leroux, M.G.H. Boogaarts, J.P.M. Hoefnagels, M.C.M. van de Sanden, and D.C. Schram, submitted for publication.

[11] H. Toyoda, M. Goto, M. Kitagawa, T. Hirao, and H. Sugai, Jpn. J. Appl. Phys. Part 2 **34**, L448 (1995).

[12] P. Kae-Nune, J. Perrin, J. Guillon, and J. Jolly, Plasma Sources Sci. Technol. **4**, 250 (1995).

[13] N. Itabashi, N. Nishiwaki, M. Magane, S. Naito, T. Goto, A. Matsuda, C. Yamada, and E. Hirota, Jpn. J. Appl. Phys, Part 2 **29**, L505 (1990).

Cavity ring down study of the densities and kinetics of Si and SiH in a remote Ar-H_2-SiH_4 plasma

W. M. M. Kessels,[a)] J. P. M. Hoefnagels, M. G. H. Boogaarts,
D. C. Schram, and M. C. M. van de Sanden[b)]

Department of Applied Physics, Center for Plasma Physics and Radiation Technology, Eindhoven University of Technology, P.O. Box 513, 5600 MB Eindhoven,The Netherlands

Cavity ring down absorption spectroscopy is applied for the detection of Si and SiH radicals in a remote Ar-H_2-SiH_4 plasma used for high rate deposition of device quality hydrogenated amorphous silicon (a-Si:H). The formation and loss mechanisms of SiH in the plasma are investigated and the relevant plasma chemistry is discussed using a simple one-dimensional model. From the rotational temperature of SiH typical gas temperatures of ~1500 K are deduced for the plasma, whereas total ground state densities in the range of 10^{15}–10^{16} m^{-3} for Si and 10^{16}–10^{17} m^{-3} for SiH are observed. It is demonstrated that both Si and SiH have only a minor contribution to a-Si:H film growth of ~0.2% and ~2%, respectively. From the reaction mechanisms in combination with optical emission spectroscopy data, it is concluded that Si and SiH radicals initiate the formation of hydrogen deficient polysilane radicals. In this respect, Si and SiH can still have an important effect on the a-Si:H film quality under certain circumstances.

I. INTRODUCTION

Basic understanding of the growth process of the industrially widely applied material hydrogenated amorphous silicon (a-Si:H) from SiH_4 plasmas requires a detailed analysis of the plasma reactions, plasma composition, and contribution of plasma species to film growth. In addition to the long-lived SiH_3 radical, which is generally accepted to be the main precursor for a-Si:H film growth in most types of plasmas, also very reactive and thus short-lived radicals such as SiH_2, SiH and Si are of interest. Due to their high gas phase and surface reactivity, these radicals have generally a low density in the plasma, but they can nevertheless still have a significant effect on the film properties.

The investigation of these low-density radicals requires very sensitive diagnostic techniques. In addition to mass spectrometry,[1-3] laser-induced fluorescence (LIF) based techniques,[4-11] ultraviolet absorption spectroscopy,[12-14] and intracavity[15,16] and infrared laser absorption techniques,[17,18] recently also cavity ring down absorption spectroscopy (CRDS) has been introduced in the field of SiH_4 plasmas. This sensitive, and relatively easy-to-apply diagnostic[19] has already been used for the detection of SiH_3,[20-22] SiH_2,[16] and nanometric Si-based particles.[23] Compared to the LIF based techniques, the advantage of CRDS is that absolute radical densities can easily and sensitively be determined from the measurements without an elaborate calibration procedure. A disadvantage, however, is that an Abel inversion procedure is necessary to obtain spatially resolved information. In addition to the previous CRDS measurements of SiH_3, in this article we will present CRDS measurements of Si and SiH in the expanding thermal plasma.

The expanding thermal plasma (ETP) is a remote plasma technique, which is capable of depositing device quality a-Si:H at rates up to 10 nm/s.[24-26] Besides the study of the a-Si:H film properties obtained by the ETP technique, also the plasma chemistry and the contribution of plasma species to film growth are fully investigated. In previous articles, it has been demonstrated that the dissociation of SiH_4 in the ETP is either governed by ion-induced reactions for a purely Ar operated plasma source or by atomic hydrogen reactions when relatively high H_2 flows are added to the Ar.[3,27] For all plasma conditions, the deposition process is dominated by neutral species.[27] It has been shown that at high H_2 flows (>7.5 sccs), the deposition rate can almost completely be explained by the contribution of SiH_3 radicals to film growth (estimated contribution ~90%).[3,22] The formation of SiH_3 is due to the hydrogen abstraction reaction

$$H + SiH_4 \quad \rightarrow \quad SiH_3 + H_2 \qquad (1)$$

by H emanating from the cascaded arc plasma source. For these conditions, the best film properties for the application of the a-Si:H in, e.g., thin film solar cells,

---

[a)] Electronic mail: w.m.m.kessels@phys.tue.nl

[b)] Electronic mail: m.c.m.v.d.sanden@phys.tue.nl are obtained at deposition rates up to 10 nm/s.[23-25] When going to the ion dominated region by reducing the H_2 flow in the cascaded arc, the contribution of SiH_3 to film growth decreases[3,22] and relatively poor a-Si:H film properties are obtained.[23,25] This change has been attributed to the fact that Ar^+ induced dissociation of SiH_4 leads primarily to the production of very reactive radicals such as SiH_2, SiH, and Si. In this article, the role of SiH and Si under different conditions will be addressed by means of absolute density measurements. Furthermore, their contribution to film growth will be presented.

After a presentation of the experimental setup in Sec. II, the procedure for the SiH and Si measurements and their absolute density determination will be discussed in Sec. III. In Sec. IV A, the production and loss mechanisms of the radicals will be considered and in Sec. IV B, their density and contribution to film growth as a function of the H_2 flow in the Ar-H_2 operated plasma source will be presented. Finally, the conclusions will be given in Sec. V.

II. DEPOSITION SYSTEM AND OPTICAL SETUP

The ETP setup is extensively described in Refs. 27 and 28 and is only briefly presented here. In a cascaded arc plasma source an Ar or Ar-H_2 plasma is created at subatmospheric pressure (~400 mbar). At the arc outlet, the plasma expands into a low-pressure deposition chamber (~0.20 mbar) where SiH_4 is admixed to the plasma by an injection ring. The cascaded arc is current-controlled at 30–75 A and is typically operated on an Ar flow of 55 sccs (i.e., standard cm^3 s^{-1}) and H_2 flows varying between 0 and 15 sccs. The electron temperature in the expansion is very low (~0.1–0.3 eV) and depending on the H_2 flow, the cascaded arc acts therefore predominantly as an Ar^+ ion source (at no and very low H_2 flows) or as a H source with a small contribution of mainly H^+ ions (H_2 flow ≥5 sccs).[27-29] The dissociation of the injected SiH_4, at flows between 0.5 and 10 sccs, is therefore either Ar^+ or H dominated, depending on the H_2 flow.[3]

For the CRDS measurements, an optical cavity has been created with its axis at 3.6 cm from the substrate holder by two highly-reflective mirrors (Laser Optik, –100 cm radius of curvature, 2.5 cm diameter).[20,21] For the SiH measurements, mirrors with a reflectivity of 99.6% at 414 nm have been used and for the Si measurements mirrors with a reflectivity of 98.2% at 251 nm. The mirrors have been positioned 108 cm apart on flexible bellows and protected against deposition by a small Ar flow.[20,21] Laser radiation has been produced by means of a tunable dye laser (Sirah PrecisionScan-D) pumped by a frequency-tripled (355 nm) Nd:YAG-laser (Spectra-Physics/Quanta Ray DCR-11, 5 ns pulse duration, 10 Hz repetition rate). For the SiH measurements, the dye laser has been operated on an Exalite 411 dye solution yielding radiation in the range of 405–414 nm with a laser linewidth of 3 pm. For the Si measurements, the dye laser has been operated on a Coumarine 503 dye solution and the radiation has been frequency-doubled with a BBO crystal to obtain radiation in the range of 245–255 nm. For both wavelength regions, only the oscillator and the preamplifier of the dye laser have been used, resulting typically in 10 μJ light pulses. In order to avoid optical saturation, the laser intensity has further been reduced by using one or two filters before it is introduced into the cavity. At the other side of the cavity, the light leaking out at the second mirror has been passed through a filter (20 nm width around 425 nm for SiH, 10 nm width around 250 nm for Si) and has been measured by a photomultiplier (Hamamatsu R928). A digital 500 Ms/s, 100 MHz oscilloscope (Tektronix TDS340a), triggered by the Nd:YAG laser, has been used to measure the photomultiplier signal and transients have been averaged over 16 or 64 laser shots. From a weighted least-squares fit of the logarithm of the transient data, the ring down time τ_λ at a laser wavelength λ has been determined which is equal to[19]

$$\tau_\lambda = \frac{d/c}{(1 - R_\lambda + \sigma_\lambda \int n\,dl)}. \qquad (2)$$

Where d is the length of the cavity, c the speed of light, and R_λ the reflectivity of the mirrors. The product of the cross-section σ_λ and the line-integrated density of the absorbing species $\int n\,dl$ forms the absorption. In the experiments described, for every measurement τ has first been determined either without SiH_4 gas or without plasma, and then for the SiH_4 containing plasma. From the difference in τ for both situations, the absorption by Si or SiH has been calculated. The calculation of their total density from the absorption values is addressed in Sec. III. No absorption by the SiH_4 gas has been observed at the wavelengths investigated.

III. SiH AND Si MEASUREMENTS AND ABSOLUTE DENSITY DETERMINATION

The SiH radical has been measured on the $A\ ^2\Delta \leftarrow X\ ^2\Pi$ electronic transition around 414 nm. A part of the absorption spectrum as measured for an arc current of 66 A and a H_2 and SiH_4 flow of 0 sccs and 2 sccs, respectively, is given in Fig. 1. The stepsize in laser wavelength was 5×10^{-4} nm, and for every wavelength τ has been measured without and with SiH_4

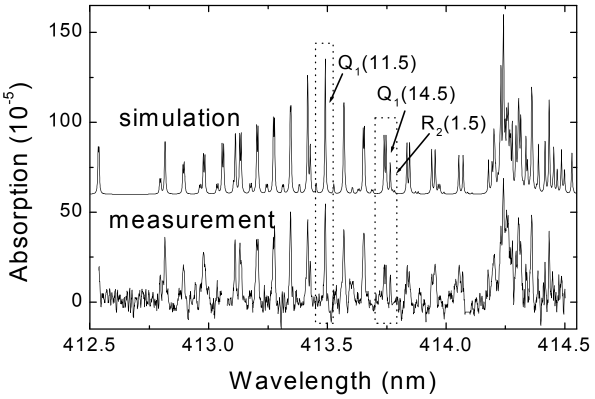

FIG. 1. Part of the measured and simulated spectrum of the A $^2\Delta \leftarrow$ X $^2\Pi$ transition of SiH in the expanding thermal plasma. In the simulations only the v'=0 ← v"=0 transitions are taken into account and the spectrum is shifted vertically for clarity. The plasma settings are: 55 sccs Ar, 2 sccs SiH$_4$, 0 sccs H$_2$, and an arc current of 66 A. The rotational temperature determined from the simulation is 1800±300 K and the laser linewidth is 3 pm. The rotational lines used to determine the SiH density [Q$_1$(11.5), Q$_1$(14.5), and R$_2$(1.5)] and rotational temperature [ratio Q$_1$(14.5) and R$_2$(1.5)] are indicated.

plasma. The measured absorption by SiH in Fig. 1 has been corrected for a small, broadband background absorption, which will be addressed below. In Fig. 1, also the simulated spectrum of the SiH A $^2\Delta$ (v'=0) ← X $^2\Pi$(v"=0) band is given as calculated by the program LIFBASE.[30] The simulation has yielded a rotational temperature of 1800±300 K for SiH in this particular condition. Assuming the kinetic gas temperature equal to this rotational temperature in the calculation of the Doppler broadening yields a laser linewidth of 3 pm.

The SiH density measurements presented below have been performed by scanning over the Q$_1$(11.5) rotational line at 413.46 nm and the Q$_1$(14.5) and R$_2$(1.5) rotational lines at 413.72 and 413.75 nm, respectively (see Fig. 1). The Q$_1$ lines split up in two Λ–doubling components but these are not resolved for the Q$_1$(11.5) case. The rotational temperature for the different plasma conditions has been extracted from the relative magnitude of the Q$_1$(14.5) and R$_2$(1.5) lines, which have been measured in one scan. The SiH density in a particular sublevel has been determined by using the Einstein absorption coefficient calculated from LIFBASE.[30] The total ground state density of SiH has been determined from the relative population densities of the measured sublevels using the measured rotational temperature and an estimated vibrational temperature. The vibrational temperature has been assumed equal to the average of the rotational temperature (~1500 K) and the vibrational temperature determined from optical emission spectroscopy (OES) on excited SiH (~3000 K).[3] It is expected that these values form the lower and upper limit, respectively, of the vibrational temperature of ground state species. This estimation introduces an uncertainty of ~20% in the absolute density. It has been found that the total SiH densities derived from both the Q$_1$(11.5) line and the combination of Q$_1$(14.5) and R$_2$(1.5) lines are in agreement within a factor of 2–3. In the calculation of these absolute densities from the line-of-sight CRDS measurements a homogeneous SiH density over 30 cm has been assumed. This assumption on the absorption path length has been based on Abel inverted, lateral CRDS measurements of SiH$_3$.[21] Although the SiH$_3$ density showed a more complex radial dependence, the assumption of a homogeneous distribution over 30 cm leads to a good estimate of the SiH$_3$ density in the center of the reactor.

To determine the ground state Si density, the Si(3p^2 ^{3}P$_0$) and Si(3p^2 ^{3}P$_1$) densities have been measured using the transitions Si(4s ^{3}P$_1$ ← 3p^2 ^{3}P$_0$) at 251.4 nm, Si(4s ^{3}P$_2$ ← 3p^2 ^{3}P$_1$) at 250.7 nm, and Si(4s ^{3}P$_1$ ← 3p^2 ^{3}P$_1$) at 251.9 nm. These measurements have been performed by scanning the laser over the different absorption lines. A background absorption by SiH$_3$ radicals has been observed as will be discussed below. Furthermore, special attention has been addressed to the determination of τ under these strongly absorbing conditions.

The densities in the specific states have been determined from the absorption corrected for the SiH$_3$ background using the Einstein absorption coefficients.[31] For the calculation of the Doppler broadening a gas kinetic temperature equal to the rotational temperature of SiH has been used, and a laser linewidth of ~1.4 pm. The density of Si has again been assumed to be homogeneously distributed over 30 cm. The values for the Si(3p^2 ^{3}P$_1$) density as determined from the two transitions showed very good agreement. The total ground state density of Si has been determined from the densities in the two sublevels taking into account their statistical weight and relative populations.[31] For this calculation thermal equilibrium has been assumed. For the relatively high gas temperature in the ETP this means that the three Si ground state sublevels 3p^2 ^{3}P$_0$, ^{3}P$_1$, and ^{3}P$_2$ are almost equally populated per statistical weight, whereas the populations of the sublevels 3p^2 ^{1}D$_2$ and ^{1}S$_0$ are negligibly small. Although this is a reasonable assumption because direct electron excitation processes are insignificant in the ETP technique due to the low electron temperature,[13] preferential population of sublevels, e.g., by recombination reactions of ions with electrons (see Sec. IV A) cannot totally be excluded. The total ground state Si density determined from the Si(3p^2 ^{3}P$_0$) density and from the

Si($3p^2\,^3P_1$) density (average value) showed agreement within 50%.

As mentioned above, a broad background absorption has been observed for both the SiH and Si radical measurements. The background absorption for the Si measurements around 251 nm can be attributed to absorption by SiH_3 on the $\tilde{A}\,^2A_1 \leftarrow \tilde{X}\,^2A_1$ transition centered at 215 nm and with a broad absorption peak ranging from 200–260 nm.[32] The broadband absorption by SiH_3 within the region 247–253 nm together with the SiH_3 measurements within the range 215–227 nm have actually been used to determine the SiH_3 density in the plasma.[22] The measurements at both wavelength regions fitted perfectly to the SiH_3 absorption band measured by Lightfoot et al.[32] The SiH_3 densities determined by CRDS showed furthermore a very good correlation with threshold ionization mass spectrometry measurements of SiH_3.[3,21,22] It is therefore established that the broadband absorptions measured around 220 nm and around 250 nm are due to SiH_3.

The origin of the relatively small, broadband absorption observed in the SiH measurements and ranging at least from 407 to 414 nm is still unclear. The broadband absorption within this wavelength region showed also some correlation with the SiH_3 absorption values (and thus also with the mass spectrometry measurements). For this reason, we have extensively considered the possibility of Rayleigh scattering and absorption by Si dust particles in the plasma.[16,23] Such particles could lead to the apparent CRDS absorption values within the three wavelength regions ("absorption" for 10 sccs H_2 and 10 sccs SiH_4: 6.9×10^{-3} at 217 nm, 2.1×10^{-3} at 250 nm, and 3.0×10^{-4} at 413 nm) because the scattering and absorption cross-sections for such particles decrease with increasing wavelength. For different assumptions on size and optical constants of dust particles, the apparent "absorption" due to scattering and absorption by such particles has been examined. This, however, revealed a significant different dependence on the wavelength as the one experimentally observed. The above-mentioned agreement of the absorptions in the regions 215–227 nm and 245–253 nm with the literature SiH_3 absorption band showed at least much better agreement. Moreover, the broadband absorptions at all the three wavelength regions appeared and disappeared instantaneously (time resolution is ~1 s) when the SiH_4 flow was switched on and off. The absorptions reached also immediately their steady state value. Such a fast generation of particles without a continuous increase in scattering and absorption due to growth of the particles on a longer time scale is very improbable. This is especially the case for the ETP technique with its low electron temperature. The low electron temperature makes negative ion formation rather improbable while also confinement of negatively charged particles in the plasma is inefficient due to the low sheath potential. Furthermore, we recall the very good agreement between the SiH_3 densities determined from CRDS and from mass spectrometry.[21] Due to the large variety in possible plasma species a broadband absorption by other species, potentially related to the SiH_3 density, is certainly possible.

IV. RESULTS AND DISCUSSION

A. Production and loss mechanisms of SiH

In order to obtain clear insight into the production and loss mechanisms of SiH, but also of SiH_2 and Si as will be discussed below, a well-defined investigation of the SiH density has been carried out as a function of the SiH_4 flow. This investigation has been performed for conditions with a pure Ar operated plasma source. The reason is that it is expected that SiH in the ETP technique is mainly created by ion-induced reactions rather than from subsequent radical-radical reactions.[3,25,27] This investigation under ion-dominated plasma source conditions has been performed with different arc current settings, which basically yield different flows of ions from the plasma source.[28]

Figure 2 shows the SiH density as a function of the SiH_4 flow for 45 and 75 A arc currents. Furthermore, for 30 A and 66 A the SiH density is given at 5 sccs and 7.5 sccs SiH_4. The trend in SiH density in Fig. 2 confirms our expectations based on previously proposed reaction processes in the ETP technique,[3,25,27] but we have tried to gain a better and more quantitative confirmation by means of a simple plug down model. In this one-dimensional model,[33-35]

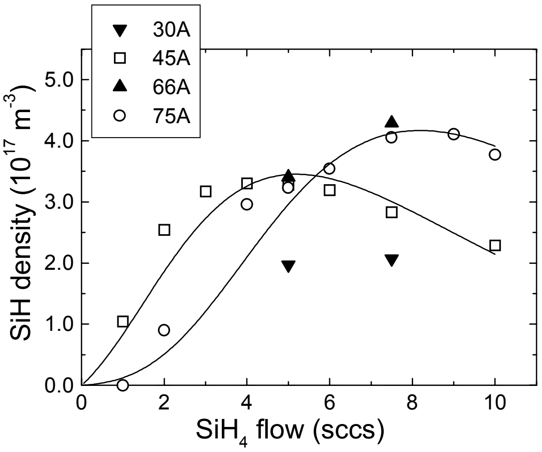

FIG. 2. The total ground state SiH density for different arc currents as a function of the SiH_4 flow. The Ar and H_2 flows are 55 sccs and 0 sccs, respectively. A vibrational temperature of 2300 K has been assumed. The solid lines represent SiH densities for 45 A and 75 A arc current as simulated by a simple model. For further explanation refer to text.

several reactions are taken into account for an axial flow of Ar^+ and SiH_4 from the arc outlet and injection ring towards the substrate holder. At the substrate holder, the species either deposit or disappear into the background. Based on experimental observations, the axial velocity is set to decrease with increasing distance from the plasma source. The velocity is ~800 m/s at the position of the SiH_4 injection ring and ~100 m/s at the position of the CRDS measurements (i.e., at 3.6 cm from substrate holder). Furthermore, expansion of the beam in radial direction is taken into account. In Fig. 2, the simulated densities of SiH are shown and apparently the production and loss of SiH can be understood from the following reactions in the plasma.

Ar^+ ions emanating from the cascaded arc react with SiH_4 by means of dissociative charge transfer

$$Ar^+ + SiH_4 \quad \rightarrow \quad Ar + SiH_x^+ + pH + qH_2 \qquad (3)$$

with $x \leq 3$ and $x+p+2q = 4$. This reaction with a total rate of 3.9×10^{-17} $m^{-3}s^{-1}$ leads to SiH_3^+, SiH_2^+, SiH^+, and Si^+ with branching ratios of 0.78, 0.12, 0.08, and 0.02, respectively, at thermal ion energies.[36,37] Because the flow of ions and electrons from the arc is very high for a pure Ar operated source,[27] these silane ions will almost immediately undergo dissociative recombination with electrons (reaction rate is 1.8×10^{-13} m^3s^{-1}).[27,37] For SiH_3^+ and SiH_2^+ this can lead to SiH radicals by

$$SiH_3^+/SiH_2^+ + e \quad \rightarrow \quad SiH + rH + sH_2 \qquad (4)$$

with $r+2s = 1$ or $r+2s = 2$. In general, the dissociative recombination of SiH_x^+ ions can also lead to SiH_2 and Si radicals.[3] The branching ratios are however unknown and it is also unclear in which form the hydrogen (H or H_2) is split off. Furthermore, the energy produced in the recombination process can lead to electronic excitation of SiH.

Reaction (4) leads to a strong reduction of the ion and electron density. However, for conditions with high Ar^+ flows and low SiH_4 flows, SiH can be lost by a subsequent charge transfer reaction. For example, by

$$SiH + Ar^+ \quad \rightarrow \quad Si^+ + H + Ar. \qquad (5)$$

This reaction, with a similar rate as reaction (3), explains the slower onset of the SiH density at 75 A compared with the one at 45 A.

Another loss mechanism of SiH occurs at sufficiently high SiH_4 flows where the SiH density starts to decrease with increasing SiH_4 flow. This can be explained by reactions between SiH and SiH_4

$$\begin{aligned} SiH + SiH_4 \quad &\rightarrow \quad Si_2H_5^* && (6a) \\ &\rightarrow \quad Si_2H_3 + H_2. && (6b) \end{aligned}$$

The rate for this reaction is ~5×10^{-17} m^3s^{-1} at the pressure of 0.2 mbar in the downstream region.[8] We expect the production of the hydrogen deficient Si_2H_3 radical to be the dominant channel, because $Si_2H_5^*$ needs collisional stabilization. Some pressure dependence of the reaction rate has been observed by Nomura *et al.*, however, only for pressures higher than 0.25 mbar. For lower pressures the reaction rate appears to be constant.[8]

Furthermore, charge transfer reactions between Ar^+ and H_2 are taken into account because at lot of H_2 is produced in the SiH_4 dissociation processes. The ArH^+ created by the charge transfer reaction can subsequently recombine with electrons.[38] This process leads to an additional reduction of the ion and electron density.

As can be seen in Fig. 2, the model with these reactions reproduces the observed trends in SiH density very well. At 45 A, the SiH density increases with increasing SiH_4 flow up to the point at which the SiH_4 flow is approximately equal to the Ar^+ flow from the arc. From that point, reaction (6) becomes significant and the SiH density decreases with increasing SiH_4 flow. The trend at 75 A is similar but due to reaction (5) the SiH density is lower at low SiH_4 flows. Furthermore, a higher SiH density is reached at sufficiently high SiH_4 flows and the loss of SiH by reaction (6) becomes only apparent at higher SiH_4 flows. In addition to the fact that more Ar^+ ions emanate from the arc at 75 A, also the higher depletion of SiH_4 for this condition[28] plays a role. The data points for 30 and 66 A are also consistent with the predictions by the model.

The agreement with the experiments is obtained by realistic input parameters in the model. The ion flows of 2.5 sccs and 7.5 sccs for 45 A and 75 A, respectively, are in fairly good agreement with the values determined by Langmuir probe measurements (the ion flows in Ref. 28 are overestimated by 30–40%).[27] The reaction rates in the model are furthermore equal to the literature values within a factor of 2–4. Considering the assumptions in the model, this is a fairly good agreement. Some difference might also be expected from the fact that the gas temperature in the ETP technique is significantly higher than the temperatures for which the reaction rates have been determined (typically between 300 and 500 K). The agreement in absolute density is obtained by adjusting the (unknown) branching ratios for the recombination reactions of SiH_x^+ [reaction (4)].

In Fig. 3, the rotational temperatures are shown that correspond to the density measurements in Fig. 2. The rotational temperature of ground state species in the plasma is usually equal to kinetic gas temperature, and from this it is obvious that the gas temperature (at 3.6 cm from the substrate holder) is relatively high in

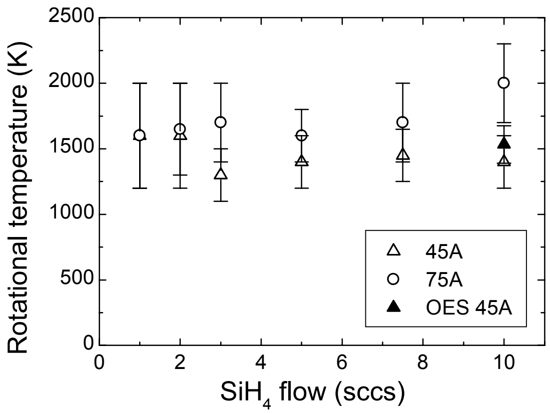

FIG. 3. The SiH rotational temperature corresponding to the SiH densities in Fig. 2. The temperature refers to a position of 3.6 cm from the substrate holder and 32 cm from the cascaded arc outlet. The rotational temperature determined by optical emission spectroscopy (OES) on electronically excited SiH (Ref. 3) is given for comparison for the condition with 10 sccs SiH_4 and 45 A arc current.

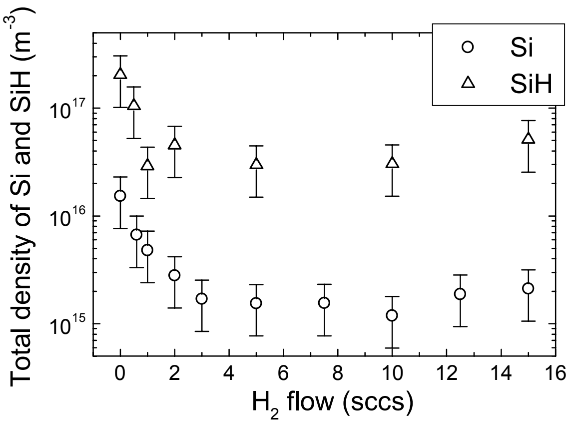

FIG. 4. The total Si and SiH densities as a function of the H_2 flow in the cascaded arc plasma source. The arc current is 45 A. The Si density has been determined from the Si($3p^2\ {}^3P_0$) and Si($3p^2\ {}^3P_1$) ground state densities. The Ar flow and SiH_4 flow are 55 sccs and 10 sccs, respectively. The densities refer to a position of 3.6 cm from the substrate holder and 32 cm from the cascaded arc outlet.

the ETP technique. The temperature of typically 1500 K is in good agreement with other temperature measurements.[39,40] No significant dependence of the temperature on the SiH_4 flow has been observed, but it appears that the gas temperature is slightly higher at higher arc currents and thus higher plasma powers. In Fig. 3, also the rotational temperature of electronically excited SiH is given as obtained by optical emission spectroscopy (OES). There is a good agreement with the CRDS data but this can be pure coincidence. The rotational distribution of excited species as measured in emission can be completely determined by their creation mechanism while full thermalization of excited SiH by collisions within its radiative lifetime (534 ns) is improbable.

Finally, we will argue that the production and loss of SiH_2 and Si in the expanding thermal plasma is governed by similar reactions as for SiH.[3] The reason for this is that SiH_2 and Si, in contrast with SiH_3, can also be created by the dissociative recombination reaction of SiH_x^+, $x \leq 3$ with electrons [reaction (4)]. Furthermore, SiH_2 and Si are known to be also rather reactive with SiH_4.[14,37]

B. Si and SiH density and their contribution to a-Si:H film growth

In Sec. IV A, it has been concluded that SiH, as well as Si, are produced in reactions initiated by Ar^+ from the cascaded arc. This has important implications for the production of SiH and Si as a function of the H_2 flow added to the Ar in the arc. As discussed in Sec. I, there is a large ion flow from the arc at low H_2 flows and it is therefore expected that a significant amount of SiH_4 is dissociated into SiH and Si in this case. Increasing the H_2 flow on the other hand, leads to a drastic decrease of the ion flow[27,28] and a much smaller production of SiH and Si is expected under these circumstances.[3,22] The smaller production rate can lead to a decreasing importance of these radicals for film growth and can possibly explain the improvement of the a-Si:H film quality with increasing H_2 flow.[25] Here we will investigate the contribution of SiH and Si to film growth. From this study, we will test the above-mentioned hypothesis and investigate whether the contribution of these radicals can (partially) compensate for the observed decreasing contribution of SiH_3 to film growth for decreasing H_2 flows.[3,22]

In Fig. 4, the total densities of Si and SiH are given as determined by the procedures described in Sec. III for a SiH_4 flow of 10 sccs and an arc current of 45 A. The total ground state Si density has been determined from both the Si($3p^2\ {}^3P_0$) and Si($3p^2\ {}^3P_1$) density.

The density of Si and SiH show the same dependence on the H_2 flow. The Si and SiH density are both higher at very low H_2 flows, which can be understood from the higher ion flows from the cascaded arc for these conditions. The Si density is about one order of magnitude lower than the SiH density. This can possibly be attributed to a lower production rate of Si [determined by the branching ratios of reactions (3) and (4)] but also to a higher loss rate of Si. The rate for the reaction

$$\mathrm{Si} + \mathrm{SiH_4} \rightarrow \mathrm{Si_2H_2} + \mathrm{H_2} \qquad (7)$$

is $3.5\times10^{-16}\ \mathrm{m^3s^{-1}}$ [14] and consequently larger than the rate of reaction (6) for SiH. For reaction (7) no pressure dependence of the reaction rate has been observed for the pressures of interest and therefore primarily production of Si_2H_2 is expected.[14] Furthermore, it is important to note that the absolute density of Si is about three and the absolute density of SiH is about two orders of magnitude lower than the density of SiH_3 in the expanding thermal plasma. For comparison, at the typical flow of 10 sccs H_2 in the arc the SiH_3 density is $\sim 4–8\times 10^{18}$ m^{-3}.[3,21,22]

The lower density of Si and SiH is also reflected in their contribution to film growth as shown in Fig. 5. The contribution of Si and SiH has been determined from their density n_{SiHx} by the expression[1]

$$\text{contribution}_{SiHx} = \tfrac{1}{4} n_{SiHx} v \frac{s}{1-\beta/2} \frac{1}{N_{Si}} \frac{1}{R_{dep}} \qquad (8)$$

with v the thermal velocity of Si and SiH close to the substrate, s and β their sticking and surface reaction probability, respectively, R_{dep} the deposition rate,[3,25] and N_{Si} the Si atomic density in a-Si:H (depending on plasma settings).[25] For SiH s=β=~0.95 [41,42] and for Si it is generally assumed that s=β=~1 on the basis of its hydrogen deficiency.[1,43] We note that the uncertainty in the density but also the uncertainty in the other parameters in Eq. (8), introduces a rather large uncertainty in the contribution of Si and SiH to film growth.[22] Furthermore, we have used the Si and SiH density determined at a distance of 3.6 cm from the substrate holder.[22]

As can be seen in Fig. 5, SiH and Si have only a relatively small contribution to film growth of ~2% and ~0.2%, respectively. Such a minor contribution has been expected for high H_2 flows at which SiH_3 radicals dominate film growth, but apparently the contribution of Si and SiH is almost independent of the H_2 flow. Only at 0 sccs H_2, there is a slightly higher contribution of SiH and Si, but the small increase can certainly not compensate for the reduced SiH_3 contribution.[3,22]

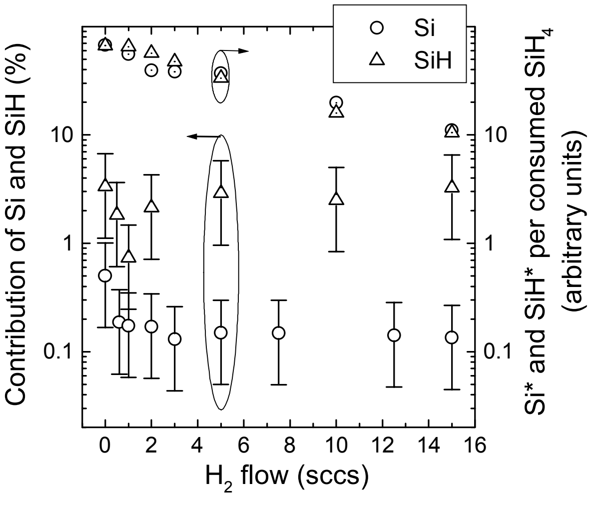

FIG. 5. Contribution of Si and SiH to a-Si:H film growth as determined from the densities in Fig. 4. In the figure, also the emission intensities of Si* (4s $^1P_1 \rightarrow 3p^2$ $^1S_0$, 390.6 nm) and SiH* ($A^2\Delta \rightarrow X^2\Pi$, ~414 nm) per unit of time and per consumed SiH_4 molecule are given in arbitrary units (Ref. 3).

The observation that the contribution of SiH and Si to the growth flux is very weakly dependent on the H_2 flow is surprising because at low H_2 flows many more ions emanate from the plasma source. As mentioned above, it is therefore expected that reactions (3) and (4) are relatively more important at low H_2 flows. As discussed in Ref. 3, there is also evidence for the higher production rate of Si and SiH from optical emission spectroscopy data. We will briefly repeat the argumentation for this evidence. In the ETP technique, the electron temperature is too low to lead to a significant excitation of Si and SiH radicals in the plasma. Therefore, the only way to obtain electronically excited Si and SiH (i.e., Si* and SiH*) is the dissociative recombination step [reaction (4)] following the dissociative charge transfer reaction between an ion and SiH_4. This implies that emission by radiative decay of these species actually indicates the recombination of SiH_x^+ ions with electrons and that the emission intensity actually represents the number of dissociative recombination events.[3] In Fig. 5, the emission intensity of Si* and SiH* per unit of time is given (in arbitrary units), while this intensity is also corrected for the amount of SiH_4 consumed at every plasma setting. This correction is performed by dividing the emission intensity by the SiH_4 consumption or, equivalently, by the deposition rate.[3] Figure 5 shows that at low H_2 flows, there is indeed relatively more Si* and SiH* emission than at high H_2 flows. The emission intensity per consumed SiH_4 decreases by a factor of 7 when going from 0 sccs H_2 to 15 sccs H_2.[3] This decrease suggests that the relative production rate of Si and SiH radicals is higher (i.e., per consumed SiH_4) at low H_2 flows. However, considering the weak H_2 flow dependence of the Si and SiH contribution to film growth, it implies also that the loss rate of Si and SiH radicals, e.g., by reactions with SiH_4, is relatively higher at low H_2 flows.

As concluded from Fig. 2, at 10 sccs SiH_4 and 45 A arc current, the SiH density is already significantly affected by the reaction of SiH with SiH_4 [reaction (6)]. For Si, this is probably even more important because reaction (7) has a larger rate than reaction (6). We therefore expect that at 3.6 cm from the substrate holder, and thus 32 cm from the arc outlet, a significant amount of the Si and SiH produced has already reacted to (hydrogen deficient) disilane radicals. For the conditions with no or very low H_2

flows, it is expected that a relatively larger part of the recombination reactions takes place at a position closer to the SiH_4 injection ring. At this position a strong recombination of the ions will take place until the ion and electron density have sufficiently been reduced.[27] Under these circumstances, the Si and SiH radicals have consequently on the average a longer pathway through the SiH_4 gas and therefore they can undergo relatively more reactions with SiH_4. This is a plausible reason for a relatively stronger loss of Si and SiH at very low H_2 flows and consequently for the weak H_2 flow dependence of their contribution to film growth.

As already mentioned, the contribution of Si and SiH cannot compensate for the decreasing contribution of SiH_3 for decreasing H_2 flows in the arc.[3,22] Therefore, the decreasing contribution of SiH_3 has to be compensated by other neutral species.[27] On the basis of the presented results, we conclude that at these low H_2 flows in the arc, the a-Si:H film growth is probably for a large part governed by reactive, hydrogen deficient disilane and possibly even trisilane or polysilane radicals. This kind of radicals is created from the Si, SiH, and also SiH_2 radicals by, for example, reaction (6) and (7). The hydrogen deficient disilane radicals are most probably also very reactive with SiH_4 leading consequently to polysilane radical formation. A large contribution of very reactive radicals at very low H_2 flows has also been indicated by overall surface reaction probability measurements.[3,44] The overall surface reaction probability, which depends on the flux of different species to the substrate and on each of their surface reaction probabilities, increases with decreasing H_2 flow. At high H_2 flows the value of the overall surface reaction probability is ~0.3, which is approximately equal to the surface reaction probability for SiH_3. The value of ~0.5 at 0 sccs H_2, however, suggests a significant contribution of more reactive plasma species.[3,44] A relatively large contribution of reactive polysilane radicals is therefore also a plausible reason for the relatively poor film properties obtained at very low H_2 flows. Their reactive nature leads to columnar film growth with a high surface roughness and high film porosity.[25]

V. CONCLUSIONS

Cavity ring down absorption spectroscopy has been applied for the detection of Si and SiH radicals in the expanding thermal plasma. Absolute densities have been determined and the contribution of Si and SiH to film growth has been calculated. The rotational temperature of SiH revealed furthermore information about the gas temperature in the plasma. A typical temperature of ~1500 K has been observed.

From a study of the SiH density for different arc currents and as a function of the SiH_4 flow, the reaction mechanisms governing the production and loss of SiH and Si have been investigated. By means of a simple one-dimensional model, it has been demonstrated that Si and SiH are created by the combination of dissociative charge transfer and dissociative recombination reactions induced by ions emanating from the plasma source. At relatively high SiH_4 flows, the reaction of Si and SiH with SiH_4 is an important loss mechanism. On the basis of the low pressure in the downstream plasma, it is expected that these reactions lead mainly to the formation of hydrogen deficient disilane radicals.

The density of Si and SiH and their contribution to film growth have also been investigated for different H_2 flows in the cascaded arc plasma source. It has been shown that Si and SiH have only a minor contribution: the a-Si:H film growth is approximately 2% due to SiH and 0.2% due to Si radicals from the plasma. Furthermore, for both radicals the contribution to film growth is almost independent of the H_2 flow. The SiH_4 dissociation reactions indicate that relatively more Si and SiH is produced at very low H_2 flows than at high H_2 flows and this is corroborated by optical emission spectroscopy measurements on electronically excited Si and SiH. The very weak H_2 flow dependence of their contribution has therefore been attributed to a higher relative loss of these radicals by reactions with SiH_4 at low H_2 flows. As a consequence, it is expected that the herein-created hydrogen deficient disilane and possibly polysilane radicals are very important for film growth at very low H_2 flows. This can account for the relatively high overall surface reaction probability and relatively poor film quality obtained under these conditions.

ACKNOWLEDGMENTS

The authors gratefully acknowledge B. H. P. Broks for his contribution to the measurements and Dr. R. Engeln for his help and the fruitful discussions. M. J. F. van de Sande, J. F. C. Jansen, A. B. M. Hüsken, and H. M. M. de Jong are thanked for their skilful technical assistance. Dr. W. C. M. Berden from the group of Prof. Dr. G. J. M. Meijer from the University of Nijmegen is acknowledged for providing us the CRDS mirrors for Si detection. This work has been supported by The Netherlands Organization for Scientific Research (NWO), The Netherlands Foundation for Fundamental Research on Matter (FOM) and The Netherlands Agency for Energy and the Environment (NOVEM).

[1] P. Kae-Nune, J. Perrin, J. Guillon, and J. Jolly, Plasma Sources Sci. Technol. **4**, 250 (1995).
[2] Y. Yasaka and K. Nishimura, Plasma Sources Sci. Technol. **7**, 323 (1998).
[3] W.M.M. Kessels, M.C.M. van de Sanden, and D.C. Schram, accepted for publication in J. Vac. Sci. Technol. A **18**, (2000).
[4] R.M. Roth, K.G. Spears, and G. Wong, Appl. Phys. Lett. **45**, 28 (1984).
[5] Y. Matsumi, T. Hayashi, H. Yoshikawa, and S. Komiya, J. Vac. Sci. Technol. A **4**, 1786 (1986).
[6] Y. Takubo, Y. Takasugi, and M. Yamamoto, J. Appl. Phys. **64**, 1050 (1988).
[7] D. Mataras, S. Cavadias, and D. Rapakoulias, J. Vac. Sci. Technol. A **11**, 664 (1993).
[8] H. Nomura, K. Akimoto, A. Kono, and T. Goto, J. Phys. D. **28**, 1977 (1995).
[9] M. Hertl, N. Dorval, O. Leroy, J. Jolly, and M. Péalat, Plasma Sources Sci. Technol. **7**, 130 (1998).
[10] A. Kono, S. Hirose and T. Goto, Jpn. J. Appl. Phys., Part 1 **38**, 4389 (1999).
[11] M. Hertl and J. Jolly, J. Phys. D **33**, 381 (2000).
[12] K. Tachibana, H. Tadokoro, H. Harima, and Y. Urano, J. Phys. D **15**, 177 (1982).
[13] M. Sakakibara, M. Hiramatsu, and T. Goto, J. Appl. Phys. **69**, 3467 (1991).
[14] T. Tanaka, M. Hiramatsu, M. Nawata, A. Kono, and T. Goto, J. Phys. D **27**, 1660 (1994).
[15] K. Tachibana, T. Shirafuji, and Y. Matsui, Jpn. J. Appl. Phys., Part 1 **31**, 2588 (1992).
[16] A. Campargue, D. Romanini, and N. Sadeghi, J. Phys. D **31**, 1168 (1998).
[17] Y. Yamamoto, H. Nomura, T. Tanaka, M. Hiramatsu, M. Hori, and T. Goto, Jpn. J. Appl. Phys., Part 1 **33**, 4320 (1994).
[18] Shiratani, H. Kawasaki, T. Fukuzawa, Y. Watanabe, Y. Yamamoto, S. Suganuma, M. Hori, and T. Goto, J. Phys. D **31**, 776 (1998).
[19] *Cavity Ring down Spectroscopy - a new technique for trace absorption measurements*, eds. K.W. Busch and M.A. Busch (American Chemical Society, Washington, 1998).
[20] M.G.H. Boogaarts, P.J. Böcker, W.M.M. Kessels, D.C. Schram, and M.C.M. van de Sanden, accepted for publication in Chem. Phys. Lett.
[21] W.M.M. Kessels, A. Leroux, M.G.H. Boogaarts, J.P.M. Hoefnagels, M.C.M. van de Sanden, and D.C. Schram, submitted for publication.
[22] W.M.M. Kessels, M.G.H. Boogaarts, J.P.M. Hoefnagels, M.C.M. van de Sanden, and D.C. Schram, submitted for publication.
[23] F. Grangeon, C. Monard, J.-L. Dorrier, A.A. Howling, Ch. Hollenstein, D. Romanini, and N. Sadeghi, Plasma Sources Sci. Technol. **8**, 448 (1999).
[24] W.M.M. Kessels, R.J. Severens, A.H.M. Smets, B.A. Korevaar, G.J. Adriaenssens, D.C. Schram, and M.C.M. van de Sanden, submitted for publication.
[25] W.M.M. Kessels, A.H.M. Smets, B.A. Korevaar, G.J. Adriaenssens, M.C.M. van de Sanden, and D.C. Schram, Mater. Res. Soc. Symp. Proc. **557**, 25 (1999).
[26] B.A. Korevaar, G.J. Adriaenssens, A.H.M. Smets, W.M.M. Kessels, H.–Z. Song, M.C.M. van de Sanden, and D.C. Schram, J. Non-Cryst. Solids. **266-269**, 380 (2000).
[27] W.M.M. Kessels, C.M. Leewis, M.C.M. van de Sanden, and D.C. Schram, J. Appl. Phys. **86**, 4029 (1999).
[28] M.C.M. van de Sanden, R.J. Severens, W.M.M. Kessels, R.F.G. Meulenbroeks, and D.C. Schram, J. Appl. Phys. **84**, 2426 (1998); J. Appl. Phys. **85**, 1243 (1999).
[29] S. Mazouffre, M.G.H. Boogaarts, J.A.M. van der Mullen, and D.C. Schram, Phys. Rev. Lett. **84**, 2622 (2000).
[30] J. Luque and D.R. Crosley, *Lifbase: Database and Spectral Simulation Program (Version 1.5)*, SRI international report MP 99-009 (1999).
[31] A.A. Radzig, B.M. Smirnov, *Reference Data on Atoms, Molecules and Ions* (Springer-Verlag, Berlin-Heidelberg, 1985).
[32] P.D. Lightfoot, R. Becerra, A.A. Jemi-Alade, and R. Lesclaux, Chem. Phys. Lett. **180**, 441 (1991).
[33] R.F.G. Meulenbroeks, R.A.H. Engeln, M.N.A. Beurskens, R.M.J. Paffen, M.C.M. van de Sanden, J.A.M. van de Mullen, and D.C. Schram, Plasma Source Sci. Technol. **4**, 74 (1995).
[34] W.M.M. Kessels, C.M. Leewis, M.C.M. van de Sanden, and D.C. Schram, J. Vac. Sci. Technol. A **17**, 1531 (1999).
[35] R. Engeln, K.G.Y. Letourneur, M.G.H. Boogaarts, M.C.M. van de Sanden, and D.C. Schram, Chem. Phys. Lett. **310**, 405 (1999).
[36] E.R. Fisher and P.B. Armentrout, J. Chem. Phys. **93**, 4858 (1990).
[37] J. Perrin, O. Leroy, and M.C. Bordage, Contrib. Plasma Phys. **36**, 1 (1996).
[38] R.F.G. Meulenbroeks, M.F.M. Steenbakkers, Z. Qing, M.C.M. van de Sanden, and D.C. Schram, Phys. Rev. E **49**, 2272 (1994).
[39] G.M.W. Kroesen, D.C. Schram, A.T.M. Wilbers, and G.J. Meeusen, Contrib. Plasma Phys. **31**, 27 (1991).
[40] R.F.G. Meulenbroeks, R.A.H. Engeln, J.A.M. van der Mullen, and D.C. Schram, Phys. Rev. E **53**, 5207 (1996).
[41] P. Ho, W.G. Breiland, and R.J. Buss, J. Chem. Phys. **91**, 2627 (1989).
[42] P.R. McCurdy, K.H.A. Bogart, N.F. Dalleska, and E.R. Fisher, Rev. Sci. Instrum. **68**, 1684 (1997).
[43] A. Gallagher, Mater. Res. Soc. Symp. Proc. **70**, 3 (1986).
[44] W.M.M. Kessels, M.C.M. van de Sanden, R.J. Severens, and D.C. Schram, J. Appl. Phys. **87**, 3313 (2000).

In situ probing of surface hydrides on hydrogenated amorphous silicon using attenuated total reflection infrared spectroscopy

W. M. M. Kessels
Department of Applied Physics, Eindhoven University of Technology, P.O. Box 513, 5600 MB Eindhoven, The Netherlands

Denise C. Marra
Department of Chemical Engineering, University of California Santa Barbara, Santa Barbara, California 93106

M. C. M. van de Sanden
Department of Applied Physics, Eindhoven University of Technology, P.O. Box 513, 5600 MB Eindhoven, The Netherlands

Eray S. Aydil[a)]
Department of Chemical Engineering, University of California Santa Barbara, Santa Barbara, California 93106

An *in situ* method based on attenuated total reflection Fourier transform infrared spectroscopy (ATR-FTIR) is presented for detecting surface silicon hydrides on plasma deposited hydrogenated amorphous silicon (a-Si:H) films and for determining their surface concentrations. Surface silicon hydrides are desorbed by exposing the a-Si:H films to low energy ions from a low density Ar plasma and by comparing the infrared spectrum before and after this low energy ion bombardment absorptions by surface hydrides can sensitively be separated from absorptions by bulk hydrides incorporated into the film. An experimental comparison with other methods that utilize isotope exchange of the surface hydrogen with deuterium showed good agreement and the advantages and disadvantages of the different methods are discussed. Furthermore, the determination of the composition of the surface hydrogen bondings on the basis of literature data on hydrogenated crystalline silicon surfaces is presented, and the quantification of the hydrogen surface coverage is discussed.

I. INTRODUCTION

Investigation of plasma-surface interactions in plasma deposition of materials and the effect of these interactions on the deposited film properties requires knowledge of both the plasma and surface composition. While there have been many studies on the identity and concentration of gas phase species in SiH_4 containing discharges used for deposition of hydrogenated amorphous silicon (a-Si:H), studies on the composition of the surface during deposition are scarce. For a-Si:H, the hydrogen coverage of the surface is expected to influence the film quality through its effect on the interaction mechanisms of radicals impinging on the surface with the film. Surface reactions can also affect[1,2] the incorporation of dangling bonds, leading to electronic defects, and the incorporation of hydrogen which influences the opto-electronic properties of the material such as the absorption coefficient and the optical bandgap.[3,4] Furthermore, the interaction of atomic hydrogen from the plasma with the film affects the film morphology,[3,4] and it is believed that hydrogen in the film plays an important role in the photo-induced degradation of the electronic properties, the so-called Staebler-Wronski effect.[4-6]

Information on silicon surface hydrides (SiH_x, $x \leq 3$) can be obtained through surface sensitive infrared absorption spectroscopy (in all its diversities), preferentially by *in situ* and real-time monitoring of the film growth. The study of the surface hydrides is made difficult by the fact that the weak absorptions due to surface Si-H vibrational modes cannot easily be discerned from the strong absorption by SiH_x bonds in the a-Si:H bulk film. This problem can be partially solved by studying the absorption during the initial stages of film growth for ultra-thin a-Si:H films.[7-11] These experiments have indicated that mainly higher hydrides (SiH_2 and SiH_3) are present in the film during initial film growth, but one cannot distinguish

---

[a)] Corresponding author. Electronic mail: aydil@engineering.ucsb.edu whether these higher hydrides are present at the substrate-film interface and/or at the film-vacuum interface (the surface) for thicker films. In fact, these experiments do not reveal information about the surface composition and coverage under steady-state film growth conditions. In an attempt to resolve this information, Miyoshi *et al.* deposited a-Si:H on as grown a-Si:H films and analyzed the infrared spectra with respect to the spectrum of the as grown films.[12] However, in spectra collected this way possible changes in the bulk SiH$_x$ bonds cannot be distinguished from changes in the newly deposited film and interactions of the plasma with the underlying film are obscured. This problem can be avoided by using methods that rely on isotope substitution. For example, Toyoshima *et al.* were able to detect the surface hydrides by depositing a-Si:D from a SiD$_4$ plasma on top of an a-Si:H film.[13,14] In such an experiment, the removal of the surface hydrides initially present on the a-Si:H surface is not obscured by SiD$_x$ absorptions in the newly deposited a-Si:D film. A similar technique relies on the exposure of a-Si:H films to atomic deuterium while monitoring the decrease in SiH$_x$ absorption due to the replacement of surface hydrides with their deuterated counterparts.[11,12,15] This method also reveals the interactions of atomic deuterium (hydrogen) with a-Si:H films, which are not limited only to hydrogen substitution at the surface.[16] A new method, recently applied to study the surface hydrides on amorphous and nanocrystalline silicon films,[17] is the removal of the surface hydrides by low-energy (~20 eV) ion bombardment using a low ion density Ar plasma. The absorption by the hydrides before and after this Ar plasma was measured by attenuated total reflection Fourier transform infrared spectroscopy (ATR-FTIR). In this article, this technique is described in greater detail and the influence of the Ar plasma on the film is determined. Furthermore, a comparison between this technique and above-mentioned methods using isotope substitution is given. The validity of the different techniques in terms of probing the surface hydrides is discussed along with their applicability and accuracy.

II. EXPERIMENTAL SETUP

The experiments were conducted in an inductively coupled plasma (ICP) reactor at 13.56 MHz[17,a)] and the conditions for deposition, ion-bombardment assisted desorption of the surface hydrides and the isotope exchange experiments with D$_2$ are listed in Table I. For all conditions, the reflected power was less than 5% and the base pressure in the reactor was 10^{-7} Torr.

The ATR-FTIR setup is described in detail in Ref. 17. Briefly, GaAs (100) ATR crystals[b)] were used to extend the spectral range of the study down to 800 cm^{-1}. The number of total reflections at each side is 35, leading to a sensitivity in reflectance R of $\Delta R/R \approx 1.4\times10^{-5}$ per reflection. The resolution of the spectrometer was set at 4 cm^{-1} and spectra were collected in the range 750–4000 cm^{-1}. However, this study focuses on the regions containing the stretching vibrations of the hydrides (“deuterides”). This is around 2100 cm^{-1} for hydrogen and 1500 cm^{-1} for deuterium. No polarization dependent studies have been performed and the detected (unpolarized) infrared radiation intensity is about equal for both polarizations for the angle of incidence used in this study.[18]

III. PROBING OF SURFACE HYDRIDES USING ION-BOMBARDMENT ASSISTED DESORPTION

A. Procedure and identification of surface hydrides

Approximately 200 Å thick a-Si:H films were deposited on ATR crystals and infrared spectra of the films were monitored in real time. At 200 Å the ratio of the absorption by bulk hydrides at ~2000 cm^{-1} (attributed to isolated SiH) and ~2100 cm^{-1} (attributed to SiH$_2$ and clustered SiH at internal surfaces) had already reached a steady state. Following the deposition, a reference spectrum was collected by averaging 1000 scans which results in a total collection time of nearly 7 minutes. Subsequently, an Ar plasma was ignited for 2 s, using the pulse mode of a programmable rf power supply, and a spectrum with 1000 scans was collected with respect to the reference spectrum that was taken immediately after deposition. The 2 s long Ar plasma exposures were usually

TABLE I. Experimental conditions for deposition of a-Si:H, ion-bombardment assisted desorption of the surface hydrides by an Ar plasma, and the isotope exchange experiments with an Ar-D$_2$ plasma.

	deposition	ion bombardment	isotope exchange
Ar flow (sccm)	50	50	50
Ar/SiH$_4$ (1%) flow (sccm)	50		
D$_2$ flow (sccm)			5
Power (W)	50	100	50
Pressure (mTorr)	40	20	40

[a)] See addendum, Figure A.1.

[b)] See Addendum, Figure A.2.

repeated up to a total exposure time of 10 s, collecting an infrared spectrum each time with respect to the reference spectrum of the as deposited film. This procedure is schematically illustrated in Fig. 1 and as will be shown below the spectrum taken after 10 s of Ar plasma exposure gives a very good indication of the hydrides initially present on the surface.

Figure 2 shows the spectrum of the surface silicon hydrides for a film deposited at 230 °C obtained using the method described above with 10 s Ar plasma exposure. Note that this spectrum is collected with respect to the reference spectrum of the as deposited film and only shows the changes that have taken place due to the Ar plasma exposure. The absorption is expressed in absorbance (=-ln(I/I_{ref}), where I/I_{ref} is the ratio of the infrared radiation intensity after and before ion bombardment, respectively). Thus negative values of absorbance correspond to absorbing species removed from the film while positive values of absorbance correspond to newly generated absorptions. The absorption band between ~2070 and ~2150 cm^{-1} is therefore due to surface hydrides removed by ion bombardment. The peak centered at ~1970 cm^{-1} is related to Ar plasma induced changes in the bulk a-Si:H, which appear at lower wavenumbers and are much broader. Fortunately, these absorptions do not interfere with the higher frequency surface hydride modes. The absorption between 2070 and 2150 cm^{-1} shows some features and it can be deconvoluted into several narrow Gaussians with a full width at half maximum in the range of 6–14 cm^{-1}. Although sometimes on the level of noise, the features are expected to correspond to different configurations of hydrogen present at the surface and are therefore narrow. This has been supported by the fact that the features were consistently present, for all sputtering times and also under different plasma conditions and substrate temperatures. In fact, the exact deconvolution procedure involved an iterative approach in which multiple spectra were fitted using non-linear least-squares optimization with different numbers of peaks. The total number of peaks and their positions were decided based on the need to include them to reproduce the features consistently observed in different spectra. Although some influence of noise cannot be excluded, it is believed that by far most of the features are real and that the deconvolution is appropriate. This is also corroborated by the agreement between the peak positions (within the resolution) and those obtained by numerous infrared absorption spectroscopy experiments on hydrogenated crystalline silicon (c-Si) surfaces of various crystal orientations and surface reconstructions.[19-29,c)] These studies are also used for assigning the different absorption peaks due to the different silicon hydride configurations present on the surface. Some of the assignments are still under debate, but most literature agrees on the following division. Absorption peaks at wavenumbers between ~2070 cm^{-1} and ~2100 cm^{-1} correspond to silicon monohydrides (SiH) on the surface, between ~2100 cm^{-1} and ~2130 cm^{-1} to silicon dihydrides (SiH_2), and between ~2130 cm^{-1} and ~2150 cm^{-1} to silicon trihydrides (SiH_3). A complication is

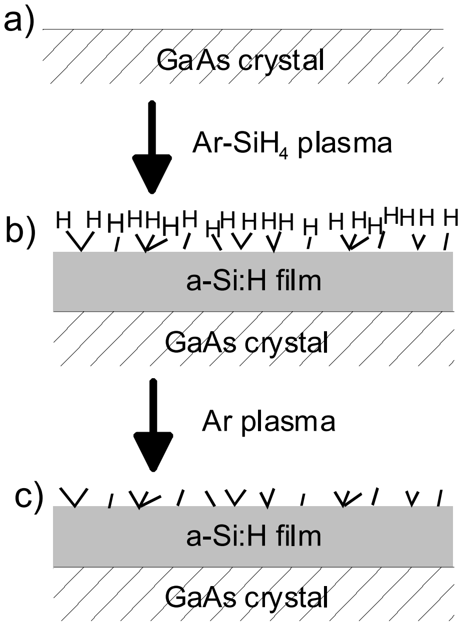

FIG. 1. Schematic representation of the method used for probing surface and bulk hydrides in a-Si:H by ATR-FTIR. Hydrogen in both the bulk and on the interfaces is probed by taking a spectrum (b) during or after deposition with respect to a spectrum (a) of a clean crystal. Surface hydrides are probed by taking a spectrum (c) after ion bombardment, using an Ar plasma, with respect to a spectrum (b) of the film after deposition. In the text, spectrum (b) is referred to as the reference spectrum.

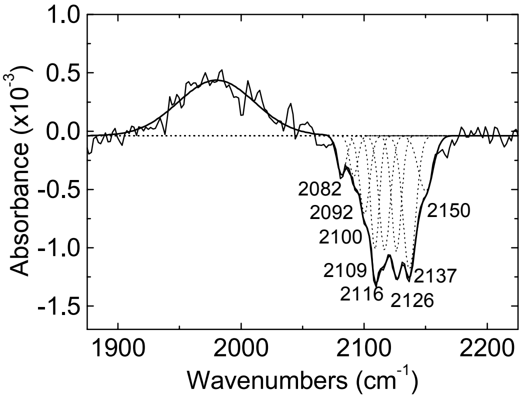

FIG. 2. Infrared spectrum of the surface hydrides SiH_x (2075 cm^{-1}–2150 cm^{-1}) on an a-Si:H film deposited at 230 °C. The absorbance band is deconvoluted into several narrow Gaussian peaks (positions are indicated) corresponding to different configurations of Si-H bonds on the surface as described in the text. The broad peak centered at ~1970 cm^{-1} corresponds to Ar plasma induced changes in the bulk hydrides.

[c)] See addendum, Table A.I.

the observation of SiH_2 vibrations at 2091 cm^{-1} (symmetric stretch) and 2097 cm^{-1} (isolated) on the Si(100)-(3×1) and -(1×1) surface,[23] and the observation of SiH_3 vibrations at 2126 cm^{-1} (asymmetric stretch) on the Si(111)-(7×7) surface.[24] Yet these are exceptions to the aforementioned division, which is expected to give a good approximate indication of the surface composition. For a-Si:H some controversy about the assignment of surface Si-H stretching modes still exists in the literature, but the majority of the studies are in approximate agreement with the above-mentioned assignments.[11,12,14,15] Some minor discrepancies exist for the assignment of absorptions around 2100 cm^{-1},[11,14] but cases in which absorptions by SiH are assumed to have higher wavenumbers than absorptions by SiH_2 (at, respectively, 2115 cm^{-1} and 2091 cm^{-1})[30] may be erroneous on the basis of the data available for hydrogenated c-Si.[19-29]

The composition of the a-Si:H surface in terms of mono-, di- and trihydrides is obtained by adding the total integrated absorbances peaking in the three aforementioned regions. This lumping of absorptions makes the determination of the surface composition less sensitive to the details of the deconvolution procedure. In terms of absorbance, the dihydride mode is dominant on the a-Si:H surface at 230 °C as can be seen in Fig. 2.[17,31] Expressed in absorbance, the distribution of hydrogen in the different hydrides is approximately 13% in SiH, 51% in SiH_2, and 36% in SiH_3. Whether the surface contains mainly SiH_2 at 230 °C depends on the relative oscillator strengths for the different stretching modes at the surface. To our knowledge this information is not available for SiH_x bondings at the surface. The oscillator strengths for bulk hydrides are available, but not completely unambiguous. For the ratio of oscillator strengths of the stretching modes at ~2000 cm^{-1} and at ~2100 cm^{-1} values ranging between 1 and 3 have been proposed.[32-35] On the other hand, for hydrogen stretching modes in silane gases, it is found that the oscillator strength per Si-H bond is roughly the same for all the silanes.[36] Thus the distribution of the SiH_x absorbance may be presumed to be representative and a good approximation of the surface composition. For the a-Si:H surface at 230 ºC, this would mean that 26% of the surface Si atoms are bonded to one hydrogen atom (SiH), 50% to two hydrogen atoms (SiH_2), and 24% to three hydrogen atoms (SiH_3). In this way, the final composition of the surface can be determined reproducibly within 5% accuracy as calculated from the standard deviation of experiments carried out at least in triplicates.

B. Effect of Ar plasma exposure time

The influence of the plasma exposure time on the spectra and the selection of an exposure time of 10 s for the determination of the surface composition are addressed next. Ideally the films should be exposed to the Ar plasma only for the time necessary to remove all the hydrides present on the surface.[37] This time is however not easily defined and we have explored the optimum Ar plasma exposure time by studying the changes in the infrared spectrum of the surface as a function of the exposure time. Figure 3 shows the integrated absorbances as a function of Ar plasma exposure time for the three wavenumber regions mentioned above for a film deposited at 160 °C. During the first 10 s of Ar plasma exposure only the surface hydrides (only SiH_2 and SiH_3 are present at 160 °C)[31] are removed. This is evidenced by slight increases in their absorbances with increasing exposure time, while their relative distribution remains roughly constant. However, when the film is exposed to the Ar plasma longer than 10 s, a rather abrupt increase in absorbance is observed along with an increase in contribution from wavenumbers < 2100 cm^{-1}. The latter is due to the appearance of a broad absorption at these lower wavenumbers and this corresponds to removal of bulk-like SiH_x bonds. This indicates that at these longer times, not only the surface hydrides are desorbed, but that H is removed from the subsurface or from the bulk of the film as well. In fact, bulk SiH_x bonds have absorptions centered at ~2015 cm^{-1} and ~2100 cm^{-1} for films deposited at 160 °C and the fact that after 16 min. of Ar plasma exposure the SiH absorption is still not centered at ~2015 cm^{-1} but at slightly higher wavenumbers, indicates that still no real bulk a-Si:H has been sputtered but only the presumably hydrogen-

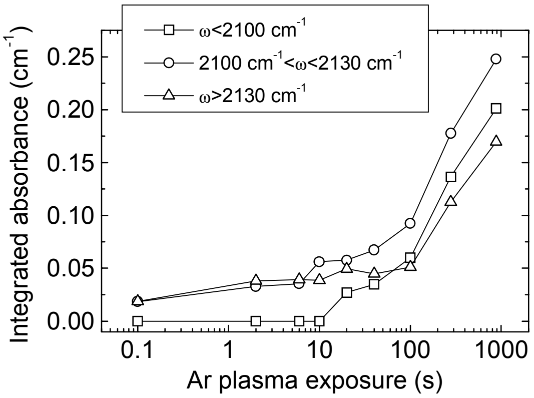

FIG. 3. Influence of the Ar plasma exposure time on the total integrated absorbance. For exposure times ≤ 10 s the regions of the spectrum with wavenumbers ω below 2100 cm^{-1}, between 2100 and 2130 cm^{-1}, and above 2130 cm^{-1} correspond to surface mono-, di- and trihydrides, respectively. For longer times broad absorptions appear below 2100 cm^{-1} and around 2100 cm^{-1}, corresponding to isolated SiH, and SiH_2 and clustered SiH in bulk a-Si:H, respectively. This indicates that subsurface or bulk hydrogen is removed as well after ~10 s of Ar plasma exposure. The film used for this experiment was deposited at 160 °C.

rich subsurface layer. It can be concluded that up to ~10 s of Ar plasma exposure only the surface hydrides are removed. This conclusion is corroborated by spectroscopic ellipsometry measurements where for Ar plasma exposure times up to 10 s no changes in the film thickness have been observed.[38] Figure 3 shows that even for shorter Ar plasma exposure times a good indication of the surface composition can be obtained, but at ~10 s the best signal-to-noise ratio is achieved because the absorbance corresponding with the removed surface hydrides is at maximum. The integrated absorbance at this time will correspond approximately with the total amount of hydrogen present on the surface, i.e., the hydrogen surface coverage. Yet an accurate determination of this coverage will suffer from the difficulty in determining exactly the integrated absorbance corresponding to surface hydrides. This will be discussed in Sec. V. Finally, it should be noted that the time of Ar plasma exposure necessary to remove only the surface hydrides depends strongly on the properties of the plasma used for ion-bombardment assisted desorption. Under the presented conditions, the ion energy and flux are approximately 20 eV and 2×10^{15} $cm^{-2}s^{-1}$, respectively.[31] Thus a 10 s Ar plasma exposure corresponds to an ion dose of 2×10^{16} cm^{-2}, which is in the expected order of magnitude to remove approximately one monolayer of adsorbates.

IV. COMPARISON WITH METHODS USING ISOTOPE SUBSTITUTION

A. Deposition of a-Si:H on a-Si:D

In this section the method of probing the surface hydrides by Ar ion bombardment as described in Sec. III is compared with other methods presented in the literature. First a comparison is made with the method used by Toyoshima *et al.*[14,39] who obtained the surface composition by depositing a-Si:H on an a-Si:D film, while monitoring the surface deuterides removed from the initial surface. In the present study, SiD_4 was not available to exactly duplicate this procedure, and a-Si:D films were created by exposing a-Si:H films to an Ar-D_2 plasma for one minute. This leads to an exchange of the hydrogen in a large fraction of the film and certainly in the top most regions as evidenced by infrared spectra taken in real time. Subsequently, a-Si:H was deposited onto this film and information on the surface composition was obtained. The surface spectra can not directly be compared with those of Toyoshima *et al.*[39] because the Ar-D_2 plasma treatment can also induce other changes in the bulk and at the surface, such as deuterium insertion in Si-Si bonds and a-Si:H etching.[16] For the present purpose, which is to compare different methods for obtaining the surface composition, the effect of these changes are made irrelevant by comparing the surface spectrum obtained by this method with a spectrum obtained by ion bombarding an a-Si:D film prepared by Ar-D_2 plasma treatment as well. Information about the assignments of the absorption peaks in the stretching region has been obtained from data available for deuterated c-Si surfaces.[20-22,d)]

The spectrum for the surface silicon deuterides, obtained by exposing an a-Si:D film deposited at 230 °C to an Ar plasma for 10 s, is shown in Fig. 4 [spectrum (a)]. The spectra obtained by depositing a-Si:H on top of the a-Si:D are shown in the same figure: spectrum (b) and spectrum (c) correspond to a-Si:H deposition times of 4 s and 28 s, respectively. Comparison of the spectra shows that spectrum (b), recorded after 4 s of a-Si:H deposition on a-Si:D, resembles spectrum (a) both in absolute magnitude of absorbance and in peak positions. On the other hand, spectrum (c), recorded after 28 s of a-Si:H deposition on a-Si:D, shows a much higher magnitude of absorbance and, more importantly, peak positions different from those in spectrum (a) and (b). In spectrum (c), the dominant absorption is centered at 1528 cm^{-1} instead of 1534 cm^{-1}, as is the case for both spectrum (a) and (b). Furthermore, the shoulder at higher wavenumbers is less pronounced in spectrum (c). From a comparison with a spectrum of bulk a-Si:D [spectrum (d)], which has broad absorption peaks centered at 1475 and 1525 cm^{-1}, it can be concluded that during the 28 s of deposition in spectrum (c) the underlying a-Si:D bulk is influenced by the SiH_4 plasma. The fact that the absorption peaks are not yet centered at the positions of the bulk deuterides indicates that only the less dense, and probably deuterium-rich, region close to the surface is influenced. Apparently, depositing a-Si:H on top of an a-Si:D film does eventually not only remove the surface

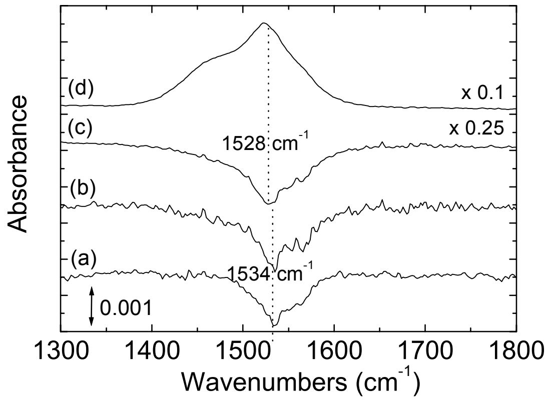

FIG. 4. Comparison between the infrared surface spectrum of an a-Si:D film deposited at 230 °C obtained (a) by Ar ion-bombardment assisted desorption, and by depositing a-Si:H on top of the a-Si:D film (b) for 4 s, and (c) for 28 s. An infrared spectrum (d) of bulk a-Si:D is given for comparison.

[d)] See addendum, Table A.I.

deuterides, but also induces changes in the bulk a-Si:D. This can occur by hydrogen diffusion or by penetration of the film by radicals or ions from the plasma. These changes are not observable for short deposition times when the SiH_4 plasma has only had time to affect the surface. Indications for bulk modification appear already after 7 s. This illustrates that caution is required when this method is applied: when the film is exposed too long to the SiH_4 plasma (i.e., $\gtrsim$7 s for the present experimental conditions and consequently more sensitive to time than Ar ion bombardment), not only the deuterides on the surface are removed but also the underlying film is changed. This can complicate the determination of the surface composition when using this method.

From spectrum (a) and (b) the surface composition of the a-Si:D film at 230 °C can be determined by deconvoluting the SiD_x absorption band with absorption peaks centered at 1510, 1525, 1535, and 1550–1570 cm^{-1}. These absorptions are attributed to SiD, SiD_2/SiD_3, SiD_2 and SiD_3 stretching modes, respectively.[20-22] As both SiD_2 and SiD_3 contribute to the absorption at 1525 cm^{-1}, the absorbance at this position is divided among SiD_2 and SiD_3 on the basis of the ratio of their absorbances at 1535 and 1550–1570 cm^{-1}, respectively. For the surface composition of the a-Si:D films at 230 °C this means that, in terms of absorbance, ~15% of the surface deuterium is bonded as SiD, ~35% as SiD_2 and ~50% as SiD_3. Compared to the a-Si:H surface at 230 °C, the a-Si:D surface contains relatively more SiD_3 at the expense of SiD_2. This can possibly be attributed to the preparation method of the a-Si:D film (Ar-D_2 exposure of a-Si:H) causing also insertion of deuterium in Si-Si bonds at the surface.

We note that, if one assumes that spectrum (c) shows a pure "surface spectrum" with no contribution of the bulk, one would draw most probably roughly the same conclusion about the dominant bonding configuration of the surface deuterides, yet on a wrong basis. This can lead to erroneous interpretations, especially in attempts to quantify the surface composition. In conclusion, this method also requires a careful examination of the influence of deposition time (more so than for the ion-bombardment assisted desorption method) as changes in the bulk are easily induced.

B. D/H exchange by Ar-D_2 plasma exposure

Another method of probing the surface hydrides on a-Si:H is by replacing them by atomic deuterium generated from a D_2 plasma.[11,12,15] We investigated this method by exposing an a-Si:H film deposited at 230 °C to an Ar-D_2 plasma for different amounts of time. In Fig. 5, the spectra of this film taken after 0.2 s [spectrum (b)] and after 7 s [spectrum (c)] of Ar-D_2 plasma exposure are given. It is expected that for a properly chosen exposure time, atomic deuterium will replace the hydrogen atoms on the surface, and that the corresponding decrease in absorbance due to the removed hydrides yields an indication of the composition of the surface. On the other hand, the increased absorbance due to the newly created surface deuterides does not give a good indication of the surface composition because atomic deuterium can also induce other changes at the surface.[16] This has no implications for the absorbance corresponding to the disappeared hydrides as this region of the spectrum shows only what has been removed from the surface. However, that this technique does not work out properly can be seen in Fig. 5. The comparison between the spectrum taken after 0.2 s Ar-D_2 plasma [spectrum (b)] and the one taken after 10 s Ar plasma exposure [spectrum (a)] shows a discrepancy in the positions of the (dominant) absorbances. The main peak in spectrum (a) is positioned at 2112 cm^{-1}, while the main peak after deuterium substitution is positioned at 2102 cm^{-1}. This shift to lower wavenumbers is also observed for longer exposure times [e.g., in spectrum (c)] and implies that hydrogen in the bulk is affected by the Ar-D_2 plasma exposure. Deuterium substitution is apparently much faster than the removal of the surface hydrides by ion bombardment or by deposition. The fact that the total absorbance of spectrum (b) is roughly of the same order of magnitude as for spectrum (a) implies that modifications in the bulk occur before the hydrogen on the surface is completely substituted by deuterium. This fast bulk change is possibly due to fast diffusion of deuterium in a-Si:H and/or to deuterium ions in the Ar-D_2 plasma which can easily penetrate the film. Because of this simultaneous modification of the bulk, spectra showing only the surface hydrides cannot be obtained by an Ar-D_2 plasma, not even when the exposure time is decreased. An interaction by deuterium

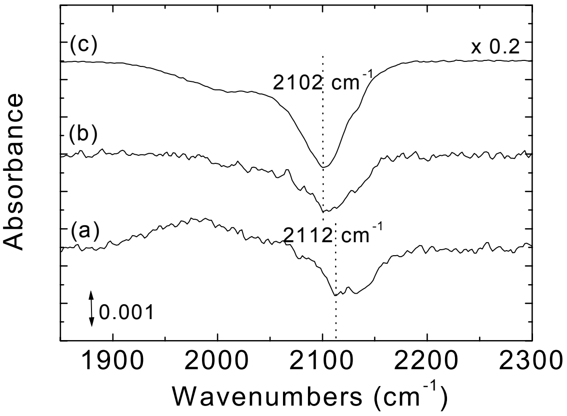

FIG. 5. Comparison between infrared surface spectrum of an a-Si:H film deposited at 230 °C obtained (a) by Ar ion-bombardment assisted desorption, and by exposing the a-Si:H to an Ar-D_2 plasma (b) for 0.2 s, and (c) for 7 s.

deuterium ions can be circumvented by using atomic deuterium, e.g., created on a hot filament. However, thus far atomic deuterium used for probing the surface hydrides has mainly been created by plasmas.[11,12,15]

V. DISCUSSION

From the results, it can be concluded that absorptions by surface hydrides and by bulk hydrides can be distinguished by comparing infrared spectra before and after applying an Ar plasma and that this method gives an accurate and unambiguous representation of the surface composition. For the experimental conditions used, this method is easier to apply than the techniques using isotope substitution. The surface deuterium removal by depositing a-Si:H on top of an a-Si:D film is also a viable method for determining the surface hydride composition and results obtained using this method are in good agreement with the ion-bombardment assisted desorption method. However, this technique is more sensitive to exposure time due to fast deuterium substitution in the bulk. Probing the surface composition by hydrogen substitution with an Ar-D_2 plasma is complicated for the same reason, however hydrogen substitution in the bulk can occur on an even shorter time-scale and even before all surface hydrides have been replaced. This method was therefore not feasible. Furthermore, using an Ar plasma to probe the surface hydrides has a practical advantage of eliminating the need for D_2 or, very expensive, SiD_4. Moreover, the technique can also be used in a broad range of (plasma) deposition and surface modification processes, even in cases where isotope substitution experiments are unfeasible, e.g., in the study of fluorine surface termination. A disadvantage common to all three techniques is that no real time information on the surface composition during film growth is obtained. In all three cases the film deposition has to be stopped to take a reference infrared spectrum. Complications can arise especially when thermal hydrogen desorption from the surface takes place. The time between deposition and probing of the surface can, however, be shortened by using a technique with enhanced sensitivity like attenuated total reflection infrared spectroscopy in our case.

Concerning the determination of the surface composition by Ar ion bombardment, the best accuracy has been obtained after an Ar plasma exposure of 10 s. This corresponds roughly with the time necessary to completely remove the hydrides from the surface (see Fig. 3). Although easier than for the methods using isotope substitution, it is still difficult to decide accurately on the time necessary to remove exactly all surface hydrogen. This complicates the determination of the hydrogen surface coverage from the infrared absorbance. Another problem in the calculation of the surface coverage is the lack of knowledge about oscillator strengths or proportionality constants of the different hydride configurations. As mentioned in Sec. III, the exact determination of the surface composition in terms of mono-, di-, and trihydrides is even not possible without making assumptions about the relative oscillator strengths of the surface hydrides. In the literature, estimations of the hydrogen surface coverage of a-Si:H have utilized either information about oscillator strengths in bulk a-Si:H or information on hydrogenated c-Si surfaces. Katiyar *et al.*,[9] Toyoshima *et al.*,[14] and Von Keudell *et al.*[40] have all used data on the stretching mode at 2100 cm^{-1} as deduced by, for example, Langford *et al.*[32] The proportionality constant A between hydrogen areal density N_H and the total integrated absorbance [$\int(\alpha/\omega)d\omega$, α is absorption coefficient, ω is frequency] is taken in the range 1.4×10^{20}–2.2×10^{20} cm^{-2}. On the other hand, Marra *et al.*[17] have used the absorbance due to the stretching mode at 2086 cm^{-1} of hydrogen on an ideally terminated Si(111) surface as presented by Jakob *et al*:.[29] the integrated absorbance ($\int \alpha d\omega$) due to one monolayer of hydrogen (N_H= 7.83×10^{14} cm^{-2}) is 2.27×10^{-3} cm^{-1}. The corresponding proportionality constant A, with a correction for the difference in the definition of integrated absorbance (i.e., with division by ω), is 7.20×10^{20} cm^{-2}. This is about a factor of 3 to 5 larger than for hydrogen in the bulk. This difference is rather significant when the hydrogen coverage of the surface is calculated. For example, when the proportionality constant of bulk hydrogen underestimates the proportionality constant of surface hydrogen, then conclusions in the literature about one monolayer of hydrogen on the surface ("fully passivated surface")[9,14,40] refer in fact to 3 to 5 monolayers of hydrogen.

The difference in proportionality constants can be understood from its definition:[32,36]

$$A = \frac{c\, n\, \mu\, \omega}{2\pi^2 {e_S^*}^2} \tag{1}$$

where c is the speed of light, n the refractive index, μ the reduced mass and e_S^* the effective charge of the dipole in the solid. The latter is related by a local field correction, depending on the electronic dielectric constant of the medium, to the effective charge e_G^* of the same oscillator in a gas molecule.[36] Both the effective charge of the dipole and the refractive index in Eq. (1) can differ for the surface hydrides compared to those in the bulk. Since the refractive index is lower in the surface region (about 40% estimated from Bruggeman's effective medium theory assuming 50% voids), this will lead to a smaller A and therefore can not account for the difference. The effective charge, on the other hand, increases with the electronic dielectric constant of the medium. For the 2100 cm^{-1} absorption peak in a-Si:H, reported values of the effective charge are ~0.3–0.4,[32,35] while it is ~0.1 for silane gases. The effective charge for the surface hydrides on ideally terminated Si(111) calculated by Jakob *et al.* is 0.120±0.05.[29] This, combined with the correction for the refractive index, explains the difference between the proportionality constants derived for hydrogen in bulk a-Si:H and on the surface of c-Si. It does still not clarify the exact value of the effective charge for hydrides on the a-Si:H surface and the corresponding proportionality constant, but nevertheless it suggests that applying the proportionality constants for bulk hydrogen gives most probably an underestimation of the hydrogen areal density. Using the values given by Jakob *et al.*,[29] the amount of hydrogen removed from the surface of the film in Fig. 2 is 6.7×10^{14} cm^{-2}, corresponding to an equivalent coverage of 0.85 monolayer on a Si(111) surface. Applying the proportionality constants for hydrogen in bulk a-Si:H, the hydrogen removed would yield only 0.1–0.3 monolayers. This for a-Si:H unexpected low coverage,[41] together with the evidence in Fig. 3 that after ~10 s Ar plasma exposure approximately all surface hydrides are removed, indicates that the proportionality constants for bulk hydrogen are inappropriate for the calculation of the hydrogen coverage of the surface. Calculations using this data[9,14,40] probably referred to hydrogen within a few monolayers from the surface, which comports with the observation (see Sec. IV) that with the isotope exchange techniques the subsurface region is easily probed as well.[14]

A last aspect important for the determination of the surface coverage is that for amorphous films such as a-Si:H, the surface is not well defined. It may therefore not be appropriate to talk about the surface coverage in terms of monolayers, but in terms of a two dimensional concentration which can be converted to equivalent monolayer coverage on well-defined surfaces. Furthermore, it should be taken into account that the surface site density and thus the hydrogen coverage increases with increasing surface roughness and can therefore depend on, e.g., the substrate temperature and film thickness.[31] This complicates the determination of the surface coverage of hydrogen as a function of substrate temperature in order to draw conclusions about the surface dangling bond density as done in Ref. 14.

VI. CONCLUSIONS

A recently developed method[17] to determine the surface silicon hydride composition on plasma deposited a-Si:H by means of *in situ* attenuated total reflection infrared spectroscopy has been studied in detail. In this method, absorptions due to surface hydrides are distinguished from absorptions by hydrides in the bulk by removing the hydrogen at the surface with an Ar plasma and by comparing the infrared spectra of the film taken before and after ion bombardment. Herein, the influence of Ar plasma exposure has been investigated, and from this, the time necessary to remove only surface hydrides has been established. The determination of the surface composition in terms of mono-, di-, and trihydrides on the basis of data available for hydrogenated c-Si surfaces is addressed and the quantification of the hydrogen surface coverage by using data from ideally hydrogen terminated c-Si surfaces and from bulk a-Si:H has been discussed.

Furthermore, the method of Ar ion-bombardment assisted desorption has been compared with other techniques using isotope substitution. A good agreement has been found with the method in which a-Si:H is deposited on a-Si:D to reveal the surface deuterides. However, it is shown that the Ar ion bombardment method is preferable for the experimental conditions used, particularly in comparison with isotope substitution by means of an Ar-D_2 plasma. In this case, fast substitution of bulk hydrogen has been observed even before the substitution of surface hydrogen was completed. Another advantage of the ion-bombardment assisted desorption method is that it is applicable in a much wider range of (plasma) deposition and surface modification processes.

ACKNOWLEDGMENTS

This material is based upon work supported under a National Science Foundation Graduate Fellowship. This work was supported by the NSF/DOE Partnership of Plasma Science and Engineering Award (DMR 97–13280). *In situ* ATR-FTIR was developed with support from the National Science Foundation Young Investigator Award (ECS 94–57758). W. K. acknowledges the Netherlands Organization for Scientific Research (NWO) and the Center for Plasma Physics and Radiation Technology (CPS) for their financial support. The authors thank Professor D. C. Schram, Professor D. Maroudas and Dr. S. Ramalingam for the fruitful discussions.

[1] A. Matsuda, Plasma Phys. Control. Fusion **39**, A431 (1997).

[2] M.C.M. van de Sanden, W.M.M. Kessels, R.J. Severens, and D.C. Schram, Plasma Phys. Control. Fusion **41**, A365 (1999).

[3] W. Luft and Y.S. Tsuo, *Hydrogenated Amorphous Silicon Alloy Deposition Processes* (Dekker, New York, 1993).

[4] R.A. Street, *Hydrogenated Amorphous Silicon* (Cambridge University Press, New York, 1991).

[5] M. Stutzman, W.B. Jackson, and C.C. Tsai, Phys. Rev. B **32**, 23 (1985).

[6] H.M. Branz, Phys. Rev. B **59**, 5498 (1999).

[7] Y. Toyoshima, K. Arai, A. Matsuda, and K. Tanaka, Appl. Phys. Lett. **56**, 1540 (1990).

[8] N. Blayo and B. Drevillon, J. Non-Cryst. Solids **137-138**, 771 (1991).

[9] M. Katiyar, Y.H. Yang, and J.R. Abelson, J. Appl. Phys. **77**, 6247 (1995).

[10] J. Knobloch and P. Hess, Appl. Phys. Lett. **69**, 4041 (1996)

[11] S. Miyazaki, H. Shin, Y. Miyoshi, and M. Hirose, Jpn. J. Appl. Phys. **34**, 787 (1995)

[12] Y. Miyoshi, Y. Yoshida, S. Miyazaki, and M. Hirose, J. Non-Cryst. Solids **198-200**, 1029 (1996).

[13] Y. Toyoshima, K. Arai, A. Matsuda, and K. Tanaka, Appl. Phys. Lett. **57**, 1028 (1990).

[14] Y. Toyoshima, K. Arai, A. Matsuda, and K. Tanaka, J. Non-Cryst. Solids, **137-138**, 765 (1991).

[15] R. Nozawa, H. Takeda, M. Ito, M. Hori, and T. Goto, J. Appl. Phys. **85**, 1172 (1999).

[16] C.-M. Chiang, S.M. Gates, S.S. Lee, M. Kong, and S.F. Bent, J. Chem. Phys. B **101**, 9537 (1997).

[17] D.C. Marra, E.A. Edelberg, R.L. Naone and E.S. Aydil, J. Vac. Sci. Technol. A **16**, 3199 (1998).

[18] N.J. Harrick, *Internal Reflection Spectroscopy* (Wiley, New York 1967).

[19] Y.J. Chabal, G.S. Higashi, and S.B. Christman, Phys. Rev. B **28**, 4472 (1983).

[20] Y.J. Chabal and K. Raghavachari, Phys. Rev. Lett. **53**, 282 (1984).

[21] Y.J. Chabal, and K. Raghavachari, Phys. Rev. Lett. **54**, 1055 (1985).

[22] V.A. Burrows, Y.J. Chabal, G.S. Higashi, K. Raghavachari, and S.B. Christman, Appl. Phys. Lett. **53**, 998 (1988).

[23] Y.J. Chabal, G.S. Higashi, K. Raghavachari, and V.A. Burrows, J. Vac. Sci. Technol. A **7**, 2104 (1989).

[24] K.J. Uram and U. Jansson, J. Vac. Sci. Technol. B **7**, 1176 (1989).

[25] U. Jansson and K.J. Uram, J. Chem. Phys. **91**, 7978 (1989).

[26] K.J. Uram and U. Jansson, Surf. Sci. **249**, 105 (1991).

[27] Y.J. Chabal, in *Internal Reflection Spectroscopy: Theory and application*, edited by F.M. Mirabella, Jr. (Dekker, New York, 1993), p. 191.

[28] P. Jakob, P. Dumas, and Y.J. Chabal, Appl. Phys. Lett. **59**, 2968 (1991).

[29] P. Jakob, Y.J. Chabal, and K. Raghavachari, Chem. Phys. Lett. **187**, 325 (1991).

[30] J.A. Glass Jr., E.A. Wovchko, and J.T. Gates Jr., Surf. Sci. **348**, 325 (1996).

[31] D.C. Marra, W.M.M. Kessels, M.C.M. van de Sanden, K. Kashefizadeh, and E.S. Aydil, submitted for publication.

[32] A.A. Langford, M.L. Fleet, B.P. Nelson, W.A. Lanford, and N. Maley, Phys. Rev. B **45**, 13367 (1992).

[33] C. Manfredotti, F. Fizzotti, M. Boero, P. Pastorino, P. Polesello, and E. Vittone, Phys. Rev. B **50**, 18047 (1994).

[34] W.M.M. Kessels, M.C.M. van de Sanden, R.J. Severens, L.J. van IJzendoorn, and D.C. Schram, Mater. Res. Soc. Symp. Proc. **507**, 529 (1998).

[35] W. Beyer and M.S. Abo Ghazala, Mat. Res. Soc. Symp. Proc. **507**, 601 (1998).

[36] M.H. Brodsky, M. Cardona, and J.J. Cuomo, Phys. Rev. B **16**, 3556 (1977).

[37] The a-Si:H surface is not very well defined and it is not excluded that Si atoms bonded to the surface hydrogen are desorbed. This has no direct implications for the interpretation of the data.

[38] D.C. Marra, E.A. Edelberg, R.L. Naone, and E.S. Aydil, Appl. Surf. Sci. **133**, 148 (1998).

[39] Y. Toyoshima, Thin Solids Films **234**, 367 (1993).

[40] A. von Keudell and J.R. Abelson, Phys. Rev. B **59**, 5791 (1999).

[41] S. Yamasaki, T. Umeda, J. Isoya, and K. Tanaka, J. Non-Cryst. Solids **227-230**, 83 (1998).

Addendum: *In situ* probing of surface hydrides on hydrogenated amorphous silicon using attenuated total reflection infrared spectroscopy

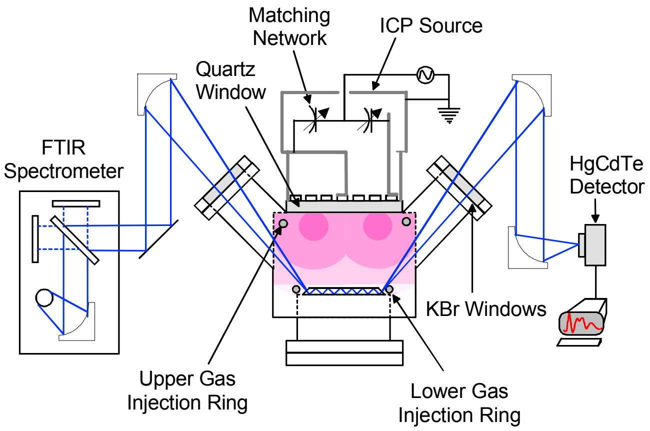

FIG. A.1. Schematic of the 13.56 MHz driven inductively coupled plasma (ICP) reactor with the attenuated total reflection Fourier transform infrared spectroscopy setup. In the upper gas injection ring Ar or Ar-H_2/D_2 is injected and in the lower injection ring Ar-SiH_4 (1%).

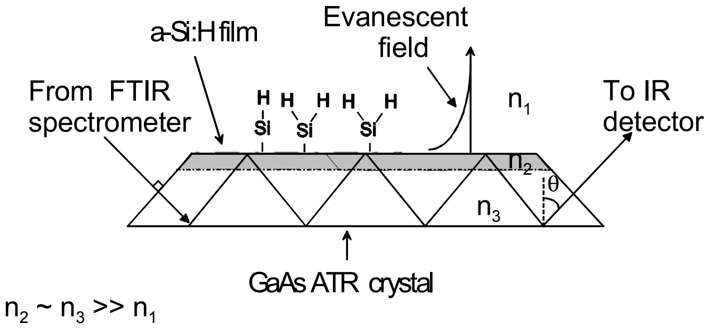

FIG. A.2. Schematic of the attenuated total reflection crystal (50 mm×10 mm×0.7 mm) with a thin film of a-Si:H. The actual number of reflections is 35 per side. The use of a GaAs crystal has as advantage that it has a high transmission down to relatively low frequencies (~750 cm^{-1}) while its refractive index is approximately equal to the refractive index of a-Si:H. Therefore almost no refraction occurs at the interface GaAs/a-Si:H, while total reflection takes place at the interface a-Si:H/vacuum. This leads to a linear behavior of the absorbance in the film over the film thickness. The surface hydrides are detected in the evanescent electric field.

TABLE A.I. Frequency assignments of hydrides and deuterides on different crystalline silicon surfaces.

frequency (cm^{-1})	mode	crystal orientation and surface reconstruction (preparation method)	Ref.
Deuterides SiD_x			
1507	*Mas*	Si(111), flat (HF prepared)	2
1512	*Miso*	Si(111), flat (HF prepared)	2
1516	*Miso′*	Si(111), flat (HF prepared)	2
1516	*Dss*	Si(100)-(1×1) and -(3×1) (UHV prepared)	4
1517	*Mss*	Si(111), flat (HF prepared)	2
1519	*Mas*	Si(100)-(2×1) (UHV prepared)	1
1522.5	*Dss*	Si(111), flat (HF prepared)	2
1526	*Diso*	Si(100)-(1×1) and -(3×1) (UHV prepared)	4
1526	*Dsa*	Si(100)-(1×1) and -(3×1) (UHV prepared)	4
1528	*Mss*	Si(100)-(2×1) (UHV prepared), highly strained surface	1
1530	*Tss*	Si(111), flat (HF prepared)	2
1533.5	*Diso*	Si(111), flat (HF prepared)	2
1544.5	*Das*	Si(111), flat (HF prepared)	2
1550	*Tiso*	Si(111), flat (HF prepared)	2
1559	*Tas*	Si(111), flat (HF prepared)	2

Submitted for publication in J. Vac. Sci. Technol. A.

TABLE A.I. (Continued)

Hydrides SiH_x			
2072	*Mas*	Si(111), flat (HF prepared)	2
2072		Si(100), flat and stepped (HF prepared)	3
2073	*M*	Si(111)-(7×7) (UHV prepared), low H coverage	12
2076	*M-normal*	Si(111)-(7×7) (H_2 and Si_2H_6 adsorption)	5,6
2077	*M*	Si(111)-(7×7) and -(1×1) (UHV prepared), low H coverage	12
2077	*Miso*	Si(111), flat (HF prepared)	2
2078.75		Si(111), (almost) ideally terminated	9
2080	*Miso*	Si(100), flat and stepped (HF prepared)	3
2082	*M*	Si(111)-(7×7) and -(1×1) (UHV prepared), high H coverage	12
2083	*Mss*	Si(111), flat (HF prepared)	2
2083.7	*M*	ideally H terminated Si(111) (HF prepared)	8,9,10
2085	*Miso'*	Si(111), flat (HF prepared)	2
2086	*M-tilted*	Si(111)-(7×7) (H_2 and Si_2H_6 adsorption)	5,6
2087.5	*Mas*	Si(100)-(2×1) (UHV prepared), highly strained surface	1
2088	*M*	Si(111)-(7×7) (UHV prepared), high H coverage	12
2090		Si(100), flat and stepped (HF prepared)	3
2090	*M*	Si(100)-(1×1) and -(3×1) (UHV prepared)	4
2091.3	*Dss*	Si(100)-(1×1) and -(3×1) (UHV prepared)	4
2093	*Miso*	Si(100)-(2×1) (UHV prepared), highly strained surface	1
2093	*M'*	Si(100)-(1×1) and -(3×1) (UHV prepared)	4
2095	*M-tilted*	Si(111)-(7×7) (H_2 and Si_2H_6 adsorption)	5,6
2095	*Mas*	Si(100)-(1×1) and -(3×1) (UHV prepared)	4
2096	*M*	Si(111)-(7×7) (H_2 and Si_2H_6 adsorption)	5,7
2097.3	*Diso*	Si(100)-(1×1) and -(3×1) (UHV prepared)	4
2098.8	*Mss*	Si(100)-(2×1) (UHV prepared), highly strained surface	1
2099	*Mss''*	Si(111), stepped (HF prepared)	3
2101	*Mss*	Si(100)-(1×1) and -(3×1) (UHV prepared)	4
2103.8	*Das*	Si(100)-(1×1) and -(3×1) (UHV prepared)	4
2106	*Das*	Si(100)-(2×1) (UHV prepared), highly strained surface	1
2106	*Dss*	Si(111)-(7×7) (H_2 and Si_2H_6 adsorption)	5,6
2106.5	*Dss*	Si(111), flat (HF prepared)	2
2107		Si(100), flat and stepped (HF prepared)	3
2111	*Diso*	Si(111), flat (HF prepared)	2
2112	*Dss*	Si(100)-(2×1) (UHV prepared), highly strained surface	1
2112	*Diso*	Si(100), flat and stepped (HF prepared)	3
2115.5	*Das*	Si(111), flat (HF prepared)	2
2117		Si(100), flat and stepped (HF prepared)	3
2119	*Das*	Si(111)-(7×7) (H_2 and Si_2H_6 adsorption)	5,6
2126	*Tas*	Si(111)-(7×7) (H_2 and Si_2H_6 adsorption)	5
2130	*Tas*	Si(111)-(7×7) (Si_2H_6 adsorption)	7
2130	*Tss*	Si(111), flat (HF prepared)	2
2130		Si(100), flat and stepped (HF prepared)	3
2137	*Tiso*	Si(111), flat (HF prepared)	2
2137	*Tiso*	Si(100), flat and stepped (HF prepared)	3
2139	*Tas*	Si(111), flat (HF prepared)	2
2140		Si(100), flat and stepped (HF prepared)	3
2143	*T*	Si(111)-(7×7) (H_2 and Si_2H_6 adsorption)	5,6
2154	*Tss*	Si(111)-(7×7) (H_2 and Si_2H_6 adsorption)	5
2154	*Tss*	Si(111)-(7×7) (Si_2H_6 adsorption)	7

M: monohydride; *D*: dihydride; *T*: trihydride; *iso*: isolated; *as*: asymmetric; *ss*: symmetric.

[1] Y.J. Chabal and K. Raghavachari, Phys. Rev. Lett. **53**, 282 (1984) .

[2] V.A. Burrows, Y.J. Chabal, G.S. Higashi, K. Raghavachari, and S.B. Christman, Appl. Phys. Lett. **53**, 998 (1988).

[3] Y.J. Chabal, G.S. Higashi, K. Raghavachari, and V.A. Burrows, J. Vac. Sci. Technol. A **7**, 2104 (1989).

[4] Y.J. Chabal, and K. Raghavachari, Phys. Rev. Lett. **54**, 1055 (1985).

[5] K.J. Uram and U. Jansson, J. Vac. Sci. Technol. B **7**, 1176 (1989).

[6] U. Jansson and K.J. Uram, J. Chem. Phys. **91**, 7978, (1989).

[7] K.J. Uram and U. Jansson, Surf. Sci. **249**, 105 (1991).

[8] Y.J. Chabal, in *Internal Reflection Spectroscopy: Theory and application*, ed. by F.M.Mirabella, Jr. (Dekker, New York, 1993), p. 191.
[9] P. Jacob, Y.J. Chabal, and K. Raghavachari, Chem. Phys. Lett. **187**, 325 (1991).
[10] P. Jakob, P. Dumas, and Y.J. Chabal, Appl. Phys. Lett. **59**, 2968 (1991).
[12] Y.J. Chabal, G.S. Higashi, and S.B. Christman, Phys. Rev. B **28**, 4472 (1983).

In situ infrared study of the role of ion flux and substrate temperature on a-Si:H surface composition

Denise C. Marra
Department of Chemical Engineering, University of California Santa Barbara, Santa Barbara, California 93106

W. M. M. Kessels and M. C. M. van de Sanden
Department of Applied Physics, Eindhoven University of Technology, P.O. Box 513, 5600 MB Eindhoven, The Netherlands

Keyvan Kashefizadeh and Eray S. Aydil[a)]
Department of Chemical Engineering, University of California Santa Barbara, Santa Barbara, California 93106

The surface composition of hydrogenated amorphous silicon films has been investigated using *in situ* attenuated total reflection Fourier transform infrared spectroscopy. The fraction of SiH_x (x=1–3) on the surface is reported for films deposited at 40–370 °C and with varying plasma power. A series decomposition reaction set in which $SiH_3 \rightarrow SiH_2 \rightarrow SiH$ is proposed to explain the surface coverage dependence on temperature and dangling bond density. Enhancing the incident ion flux during growth is shown to promote decomposition reactions by generating the necessary dangling bonds.

I. INTRODUCTION

Plasma enhanced chemical vapor deposition (PECVD) from silane is typically used for growing hydrogenated amorphous silicon (a-Si:H) films since it yields good quality films for industrial applications at low temperatures. The extent of hydrogenation is a critical factor in determining the quality and stability of the films, as it affects both the microstructure and the defect density. Varying the substrate temperature is a simple way to modify the hydrogen content in the films. At low temperature, excess H is typically incorporated into the bulk resulting in a porous structure and poor electronic properties. Electronic performance also suffers at high temperatures (>350 °C) possibly due to defects created by thermal desorption of H_2(g). The film microstructure and defect density also depend on the properties of the discharge. In principle, the discharge parameters can be adjusted to enhance material properties provided that the mechanism of H incorporation is understood. The goal is to achieve a balance between defect passivation and excess hydrogenation that leads to porosity and degradation. One way to achieve this balance is by studying the reactions that govern the deposition and H incorporation. *In situ* diagnostic tools based on infrared spectroscopy, such as infrared reflection-absorption spectroscopy,[1] attenuated total reflection Fourier transform infrared spectroscopy (ATR-FTIR),[2-5] and multiple internal reflection (MIR) –FTIR[2,3] are perfectly suited to studying such processes. While *in situ* MIR-FTIR can be used to monitor the silicon hydride bonding in the growing film in real time as well as to delineate the hydrogen depth profile in the as-deposited film,[6] ATR-FTIR can be used to identify the corresponding surface composition.[7,8] From an accurate assessment of the surface composition, and in conjunction with information in the literature gleaned from gas phase and theoretical investigations, one can infer the relevant surface reactions during the a-Si:H growth process.

A number of research groups have investigated silicon hydride composition on a-Si:H surfaces and near surfaces *in situ* using such techniques as infrared phase modulated ellipsometry (IRPME),[9,10] infrared reflection absorption spectroscopy (IR-RAS),[1,11] IR-RAS combined with optical cavity substrates,[12] and ATR-FTIR.[7,8,13-16] In particular, a study of the surface hydride coverage as a function of temperature using *in situ* IR-RAS and isotope exchange has been reported by Toyoshima *et al.* for plasma deposited a-Si:H films.[1] In these studies, it was found that at low temperatures, the surface is predominantly covered with SiH_3 and SiH_2 and as the temperature is increased, the surface monohydride composition becomes increasingly more dominant. The instability of higher hydrides at elevated temperatures has been studied extensively on crystalline silicon (c-Si) surfaces,[17-22] and it has been shown to be highly

---

[a)] Corresponding author. Electronic mail: aydil@engineering.ucsb.edu dependent on the dangling bond density.[19] A similar dependence on dangling bond coverage for hydride stability on a-Si:H surfaces has been proposed[8,19,23] and will be addressed in this article.

For this study, we employ *in situ* attenuated total reflection Fourier transform infrared spectroscopy (ATR-FTIR) to probe the surface species on a-Si:H films deposited by an inductively coupled plasma from SiH_4 diluted in Ar. Making use of the enhanced spectral resolution of the ATR-FTIR technique and applying a brief Ar plasma pulse to desorb surface hydrides, we determine the fractional coverage in terms of silicon mono-, di-, and trihydrides on the surface. Through investigation of the surface composition as a function of the substrate temperature and ion bombardment during deposition, we deduce the reactions that are likely to be responsible for the observed surface coverage. Furthermore, under select operating conditions, knowledge of the surface species provides insight into the primary growth precursor(s).

II. EXPERIMENT

The experiments were conducted in an inductively coupled plasma (ICP) deposition reactor equipped with *in situ* ATR-FTIR and *in situ* spectroscopic ellipsometry (SE). A complete description of the infrared apparatus and the ICP deposition chamber appears in a previous publication.[8] The plasma is excited by applying radio frequency (rf) power at 13.56 MHz to a 6 in. diameter planar coil placed on a quartz window 8 in. above the substrate platen. The chamber pressure is regulated using a throttle valve and is independent of the gas flow. During deposition, the reactor pressure was maintained at 40 mTorr with 50 sccm of SiH_4 (1% in Ar) fed from an injection ring surrounding the substrate holder and an additional 50 sccm of Ar fed from a gas injection ring directly below the coil. The temperature of the stainless steel substrate electrode is regulated by a feedback controller with a 300 W ring heater and a thermocouple placed immediately below the sample. The substrate temperature ranged from 40 to 370 ^{o}C, and the rf power to the ICP source was 25, 50, and 100 W at each temperature studied. The electrode was left floating for these experiments. Based on ion energy distribution function measurements in a similar reactor, we expect the ion energies to range from 10–50 eV with a peak at approximately 15 eV under these conditions.[24,25]

The substrate was a GaAs ATR crystal dimensioned to allow approximately 35 reflections from the film/vacuum interface. The selection of GaAs enables detection of the low frequency deformation modes of the higher hydrides. Furthermore, since the index of refraction is similar to that of the a-Si:H, the beam passes through the growing film approximately 70 times enhancing the IR signal. Although not reported here, the bulk deposition was monitored in real time using MIR-FTIR. By probing the surface at different deposition times, we determined an adequate thickness of film such that the surface species were independent of the underlying substrate. In other words, these data are not representative of the surface composition during nucleation, but rather at steady state. For this, as few as ~50–100 Å are needed, and we chose 6 minutes of deposition (~200 Å) for convenience.

Multiple passes of the infrared beam through the crystal substrate and through the growing film greatly enhance the signal due to the surface hydrides, however, it is still necessary to decouple the surface modes from the strong bulk signal. To isolate the surface signal, we expose the deposited film to a 100 W Ar plasma for 10 s in 2 s intervals to remove the surface hydrides by ion-bombardment assisted desorption.[7,8] The validity of this method of studying the surface coverage was previously established,[7] and the effects of this brief plasma pulse were investigated and the conditions selected such that sputtering of and evolution of H from the bulk film was minimal.[15] As further support, in a study of hydrogen and disilane adsorption on ion-roughened Si (100), Gong *et al.* showed that low energy ions (50 eV Ar^+) could be used to sputter the silicon surface incurring little damage to the bulk film.[26]

The film thickness and index of refraction were measured using *in situ* spectroscopic ellipsometry.[27-29] Atomic force microscopy was used to determine the surface roughness of films grown under select conditions to understand how the morphology might affect the IR absorbance intensity. The ion flux to the surface was determined from Langmuir probe measurements in Ar discharges without silane to avoid film deposition on the probe. Since we typically use 0.5 sccm of SiH_4 in 99.5 sccm of Ar, the measured ion flux in pure Ar will be approximately the same as that during deposition.

III. EXPERIMENTAL OBSERVATIONS

A. Temperature Dependence of Surface Composition

The infrared spectra displaying the SiH stretching modes of SiH_x species on surfaces of a-Si:H films deposited at 50 W and at several substrate temperatures are shown in Fig. 1. Since the infrared spectrum of the deposited film is used as the reference, the surface species desorbed by ion bombardment are identified by a decrease in absorbance. The infrared assignments of the surface silicon hydride stretching vibrational frequencies are

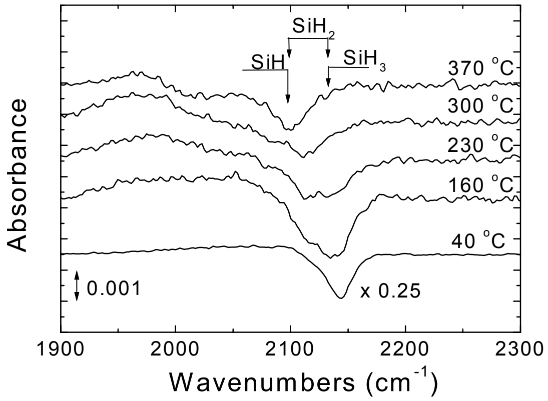

FIG. 1. Infrared spectra of the surface of a-Si:H films deposited at varying substrate temperatures. The range of frequencies corresponding to SiH, SiH_2 and SiH_3 stretching vibrations are indicated with arrows. A shift from higher to lower hydrides with increasing temperature is evident. The collection time for each spectrum was approximately 7 min with a spectral resolution of 4 cm^{-1}.

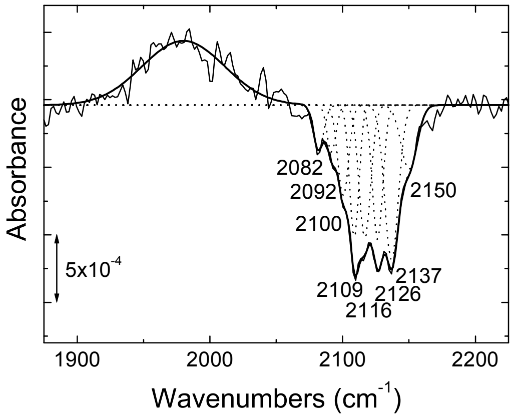

FIG. 2. The surface infrared spectrum of the a-Si:H film deposited at 230 °C. The film was exposed to 10 s of a 100 W Ar plasma to remove the surface hydrides and the as-deposited film was used as the reference spectrum. The features of the stretching region have been fit with 8 narrow Gaussian peaks that can be attributed to SiH, SiH_2, and SiH_3 on the surface.

made based on those of H on c-Si as described in a previous publication.[8] According to the literature for Si-H on various c-Si surface reconstructions,[30-34] the surface monohydride in different bonding environments is associated with vibrational frequencies ranging from 2069 to 2100 cm^{-1}. Since a preferred orientation is not expected for the amorphous surface, it is not surprising to find a distribution of peaks associated with hydrogen in various bonding environments. The wide span of frequencies for the higher hydrides also reflects the complexity of the amorphous surface, and absorption peaks in the range from 2101 to 2129 cm^{-1} are ascribed to SiH_2 on the surface, while SiH_3 is responsible for peaks appearing from 2130 to 2150 cm^{-1}. The broad shape increasing in absorbance and centered at 1970 cm^{-1} is attributed to SiH[35] or Si-H-Si[36] vibrations in the bulk. The formation of these species during Ar plasma treatment was consistently detected, and does not alter the conclusions of this work.

In Fig. 1, a clear shift of the SiH_x absorption band towards lower frequencies with increasing deposition temperature is evident and indicative of a shift from tri- and di-hydride dominated coverage to mono-hydride coverage. The relative concentration of the various surface silicon hydrides can be extracted by deconvoluting the various stretching mode contributions to this band. For example, the stretching region of the infrared spectrum of the film deposited at 230 °C has been deconvoluted using multiple narrow Gaussian peaks as shown in Fig. 2. The individual absorption peaks used to fit this band are shown as dotted lines. The frequencies of these peaks were selected based on their consistent appearance in the spectra of films deposited under various conditions and at different Ar sputtering times. The spectra in the stretching region can also be fit reasonably well using several broader peaks, however the consistently observed fine features can only be captured if we use the narrow (6–14 cm^{-1}) absorption line shapes as shown in Fig. 2. The hydride coverage data can be extracted from either fitting procedure with some loss in accuracy when the broad peak method is employed. We report the surface composition in terms of the fraction of SiH_x (x=1, 2, or 3) by summing the integrated absorption intensities of the individual peaks that have been assigned to a particular hydride species. We divide by the number of Si-H bonds per silicon hydride species such that we report the fraction of SiH_x bound as SiH, SiH_2 or SiH_3. In the absence of data to the contrary, we assume that the absorption cross sections of the surface mono-, di- and tri-hydride species are the same.[15]

Using the above quantification procedure, the surface coverage of silicon hydrides as a function of substrate temperature is displayed in Fig. 3. As can be concluded from the raw spectra of Fig. 1, the fraction of SiH_3 on the surface decreases monotonically with increasing temperature, while the fraction of SiH on the surface increases. These data are consistent with a thermally activated, series decomposition reaction from an SiH_3 precursor (as shown below), where $SiH_3 \rightarrow SiH_2 \rightarrow SiH$. For such a process, one would expect a maximum in the intermediate concentration, and, in fact, the fraction of surface SiH_2 undergoes a maximum with increasing substrate temperature as seen in Fig. 3. Similar temperature dependence was reported by Toyoshima *et al.* on a-Si:H surfaces[1] and has been widely reported for both SiH_3 and disilane on c-Si.[17-22] The temperature range at which SiH_3 and

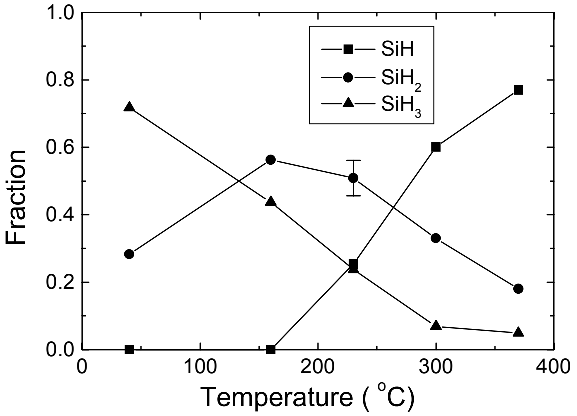

FIG. 3. The fraction of SiH, SiH_2 and SiH_3 on the surface as a function of substrate temperature as determined from Gaussian fitting of the infrared data. Values of the absorption cross section for the Si-H stretching mode are assumed to be the same for the silicon hydrides. For clarity, only one error bar is indicated and equal to one standard deviation of three separate experiments; others are similar.

SiH_2 on c-Si became unstable was found to be highly dependent on the coverage.[19] Thus, one would expect a similar effect on the amorphous surface depending on the prevalence of dangling bonds. In fact, Chiang *et al.* prepared a-Si:H films that were monohydride-terminated at temperatures as low as 200 °C,[23] while Marra *et al.* found SiH_2 not only stable, but dominant on the surface during plasma deposition of a-Si:H at 230 °C.[8] This disparity is likely due to the availability of dangling bonds during growth.

B. Effect of ion bombardment

To test the hypothesis that the stability of higher hydrides depends on the dangling bond density[8,19] and that the presence of dangling bonds affects the surface coverage during plasma deposition, we investigated the effect of incident ion flux on the surface composition. At each temperature of interest, the surface spectra were recorded for films deposited using different plasma powers. Based on Langmuir probe measurements, at 40 mTorr, we found that the ion density increases linearly with increasing plasma power as shown in Fig. 4. The corresponding ion flux to the surface, shown on the right ordinate of Fig. 4, was computed assuming an electron temperature of 2 eV and that Ar^+ and ArH^+ are the dominant ions.[37] One of the principal effects of the ion bombardment during deposition is the physical sputtering of hydrogen and silicon hydrides to form dangling bonds. [e.g., see reactions (8) and (9) in Sec. IV B] Therefore, to study the influence of surface dangling bonds on the surface composition, we varied the ion flux during deposition by adjusting the plasma power.

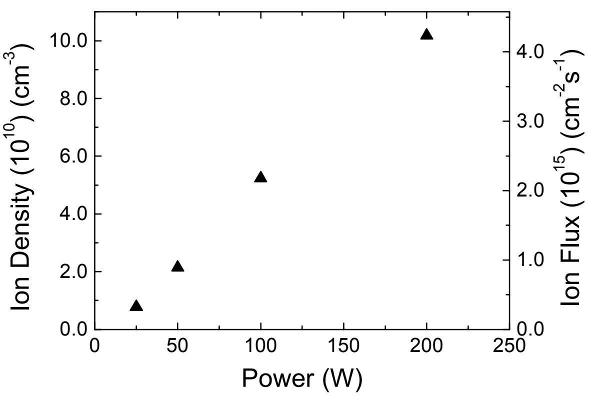

FIG. 4. Increase in ion density as a function of the plasma power as determined by Langmuir probe measurements. The corresponding ion flux is shown on the right ordinate.

The surface infrared spectra were collected and deconvoluted as described in the preceding section. Based on these assignments, the power dependence of the surface hydride coverage for films deposited at several different substrate temperatures is shown in Fig. 5. At low temperature, Fig. 5(a), the surface composition is independent of the plasma power, hence the ion flux. However, as the temperature increases, the effect of ion bombardment becomes increasingly more significant until very high temperature (370 °C) upon which the effect of ion flux again becomes negligible.

IV. DISCUSSION

A. Surface composition and surface reactions

1. Temperature dependence

Since the gas phase composition is independent of the substrate temperature, the temperature dependence of the surface composition, as shown in Fig. 3, can provide information about the reactions that occur on the surface during a-Si:H growth and may even aid in identification of the dominant precursor. The surface coverage at low temperature is most indicative of precursors from the gas phase since the thermal energy is insufficient to activate many of the surface reactions that lead to dissociation and H expulsion from the film. In fact, a-Si:H films grown at low temperature typically contain more SiH_2 and SiH_3 relative to films grown at higher substrate temperatures. On the surface at 40 °C, we find predominantly SiH_3 and this is consistent with the belief that SiH_3 is the principal precursor to the deposition.[38-41] Explicitly, the infrared spectrum of the surface of the film deposited at 40 °C is shown in Fig. 6 with the SiH_3 stretching vibration centered at 2143

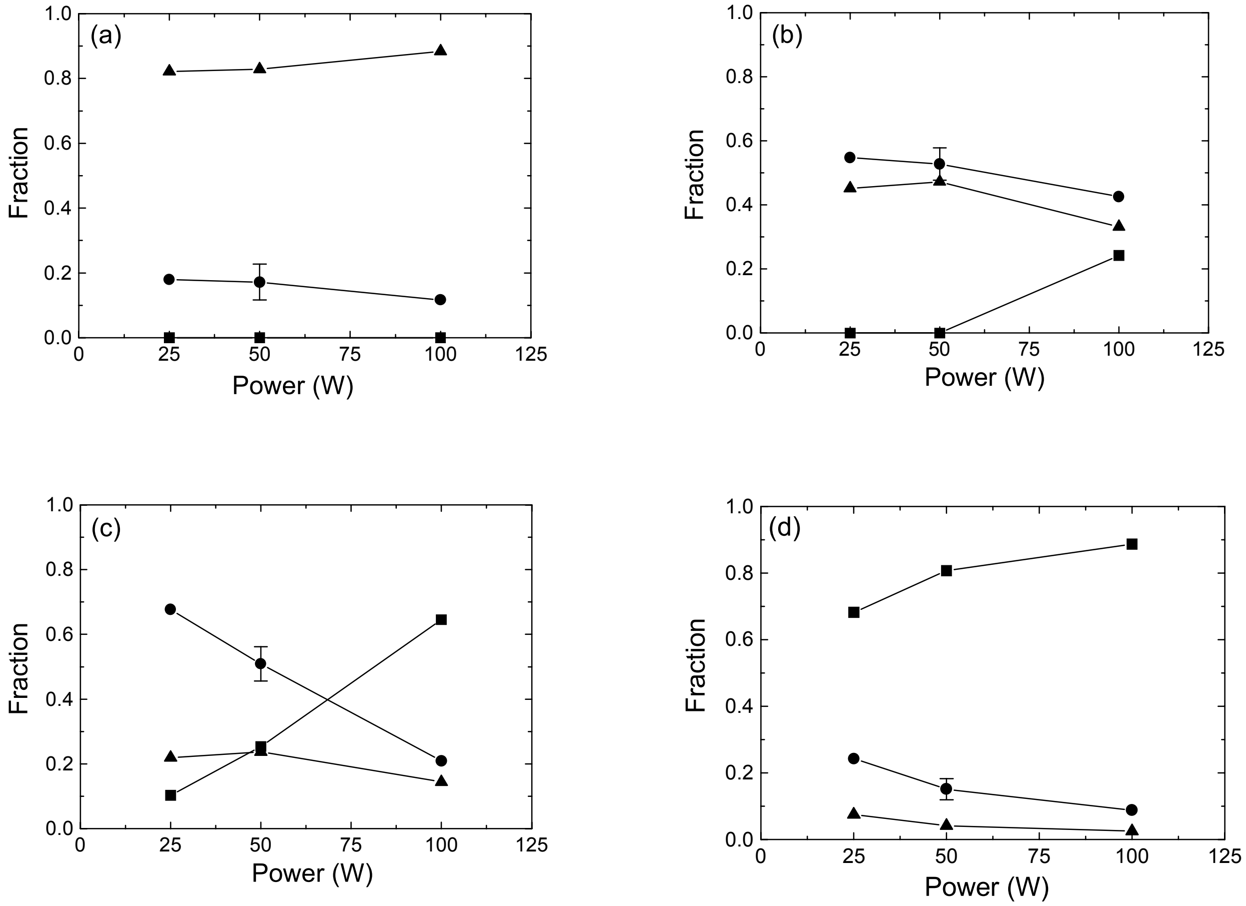

FIG. 5. Fraction of silicon hydrides on the a-Si:H surface as function of power for several substrate temperatures, (a) 40 °C, (b) 160 °C, (c) 230 °C, and (d) 370 °C. Symbols: square - SiH; circle - SiH_2; triangle - SiH_3.

cm^{-1}, and the corresponding symmetric and degenerate deformation modes at 870 and 915 cm^{-1}. The presence of SiH_2 is also evidenced by deformation modes at 850 and 893 cm^{-1} and stretching motions appearing as a shoulder at 2122 cm^{-1}. Quantitative analysis of the stretching region shows that approximately 30% of the surface hydrides are bound as SiH_2. A surface composed of 70% SiH_3 with the balance SiH_2 could conceivably be produced by deposition from SiH or SiH_2 precursors with sequential insertion of atomic H. However, in a previous publication, we showed that the rate of H insertion was much slower than the rate of SiH_3 adsorption.[8] Specifically, H insertion could not account for the overwhelming SiH_3 signal even at higher temperature. Thus, we conclude that at least 70% of the Si brought onto the surface is by SiH_3 and SiH_3 is the dominant precursor to a-Si:H deposition in our reactor. Incident SiH_3 can adsorb directly onto surface dangling bonds as follows,

$$\mathrm{SiH}_{3(g)} + \_{}_{(s)} \rightarrow \mathrm{SiH}_{3(s)}, \qquad (1)$$

where '_' represents a dangling bond and (g) and (s) denote gas phase and surface species, respectively. In addition, SiH_3 radicals have been shown to insert into strained Si–Si bonds,[42,43]

$$\mathrm{SiH}_{3(g)} + \mathrm{Si-Si}_{(s)} \rightarrow \mathrm{Si-SiH_3-Si}_{(s)}, \qquad (2)$$

where the surface SiH_3 produced via reaction (2) can remain over coordinated or create a dangling bond by reducing its Si bonds. In this way, both reactions (1) and (2) can be responsible for the overwhelming presence of SiH_3 on the surface at room temperature. However, at elevated temperature, an additional process becomes important: the over coordinated SiH_3 can transfer H to an adjacent Si atom to form lower silicon hydrides.[43]

The fraction of SiH_2 found on the a-Si:H surface can be produced by several reactions: either directly by adsorption of impinging SiH_2 radicals,

$$\mathrm{SiH}_{2(g)} + \_{}_{(s)} \rightarrow \mathrm{SiH}_{2(s)}, \qquad (3)$$

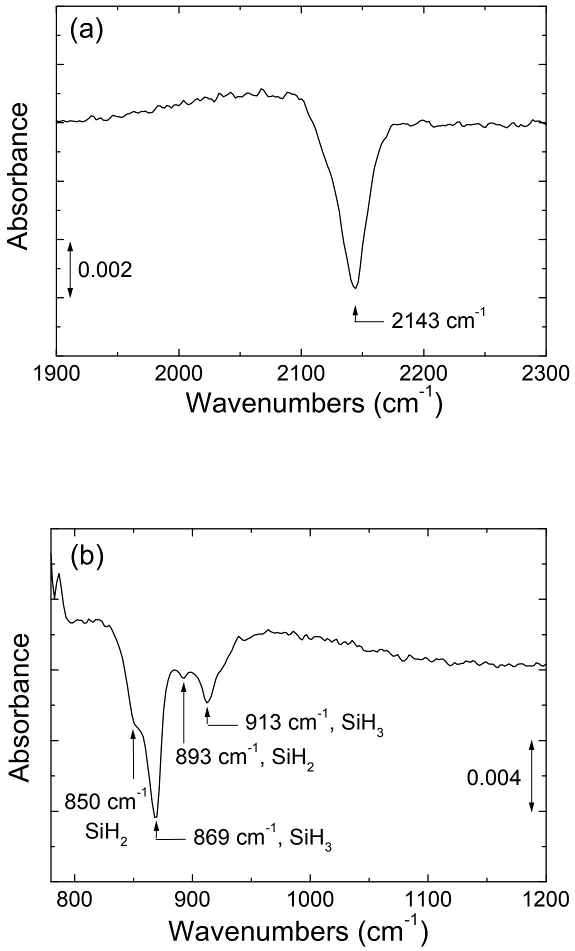

FIG. 6. Infrared spectrum of the surface of the a-Si:H film deposited at 40 °C. The (a) stretching and the (b) deformation regions indicate many SiH_3 species in close proximity on the surface.

or by dissociation or abstraction. The dissociation of adjacent SiH_3 species is expected to proceed according to the reaction,

$$2\,\mathrm{SiH}_{3(s)} \rightarrow \mathrm{SiH}_{2(s)} + \mathrm{SiH}_{4(g)}\,, \tag{4}$$

provided that the thermal energy is sufficient to activate this reaction. The more general form of this reaction between neighboring SiH_3 and SiH_x (x=1,2, or 3) on Si (111) was proposed by Olander *et al.*[17] and is supported by the work of several others on c-Si and porous silicon surfaces.[44] Our IR data suggest that reaction (4) may be activated but slow at 40 °C based on the observation of some SiH_2 with a large percentage of SiH_3 on the surface.

The small fraction of SiH_2 detected on the surface of the film grown at 40 °C could also be generated by the abstraction of H by SiH_3 radicals from the gas phase, where

$$\mathrm{SiH}_{3(g)} + \mathrm{SiH}_{3(s)} \rightarrow \mathrm{SiH}_{2(s)} + \_{}_{(s)} + \mathrm{SiH}_{4(g)}\,. \tag{5}$$

This exothermic reaction is expected to free up sites for precursor adsorption at all temperatures. A relatively low activation barrier for abstraction equal to 0.092 eV was computed by Ramalingam *et al.* using molecular-dynamics simulations of a-Si:H deposition from SiH_3 radicals at 500 and 773 K.[22] These simulations show that reaction (5) is the dominant mechanism of H removal/dangling bond formation in the absence of ion bombardment.[43] Ramalingam and coworkers also observed reaction (4) during the high temperature a-Si:H growth simulations as well as during MD simulations of SiH_3 impinging on pristine Si (001) surfaces, however, reaction (5) was found to be much more prevalent.[43]

Based on these theoretical studies, we expect reaction (5) to be more frequent than reaction (4) during a-Si:H deposition in our reactor. However, due to a lack of measurement of the fluxes of species impinging on the surface, we are unable to address the relative importance of reaction (3). Even though we have verified the prevalence of SiH_3 in the discharge, we can not exclude the presence of SiH_2 except by invoking arguments that have been used previously by Gallagher.[45] Specifically, the high reactivity of SiH_2 in the gas phase limits its flux to the substrate.

As the substrate temperature increases, additional surface reactions become activated. According to the literature concerning the stability of higher hydrides on c-Si,[19,21,46] when active sites are present on the surface at elevated temperatures, decomposition of SiH_3 can proceed by the following reaction pathway resulting in surface SiH_2 and SiH,

$$\mathrm{SiH}_{3(s)} + \mathrm{Si\_}_{(s)} \rightarrow \mathrm{SiH}_{2(s)} + \mathrm{SiH}_{(s)}\,. \tag{6}$$

Since the coordination of the SiH_2 on the amorphous surface is not known, only the general form of the reaction is shown. An additional dangling bond in the vicinity of the initial surface SiH_3 may be required in order to achieve four-fold coordination of the SiH_2. The absence of $SiH_{(s)}$ on the surface at low temperature suggests that reaction (6) does not occur at 40 °C and that the barrier to this reaction, regardless of the coordination of the products, is high relative to those of reactions (4) and (5). In a similar manner, the dihydride is known to decompose at high temperatures in the presence of dangling bonds by

$$\mathrm{SiH}_{2(s)} + \mathrm{Si\_}_{(s)} \rightarrow 2\,\mathrm{SiH}_{(s)}\,. \tag{7}$$

As was the case for reaction (6), the coordination of the products is intentionally unspecified. Based on behavior of SiH_2 concentration displayed in Fig. 3, the onset of this reaction appears to be near 200 °C at the dangling bond density associated with these plasma conditions.

Gates *et al.* and Wang *et al.* cited reaction (6) for the decomposition of adsorbed SiH_3 in separate studies of disilane decomposition on Si (001) surfaces at low coverage.[19,21] Neither group found evidence for reaction (4). On Si (001) at room temperature, Wang *et al.* found the stability of SiH_3 to be on the order of minutes. This group was able to compare the number of surface SiH with that of SiH_2 through direct counting using scanning tunneling microscopy (STM) and found an equal amount of each, also consistent with formation by reaction (6).[21] Using static secondary-ion mass spectroscopy (SSIMS), Gates *et al.* reported decomposition of SiH_3 via reaction (6) at temperatures as low as 200 K but ranging as high as 600 K.[19] The availability of dangling bonds was cited as the reason for the variation in temperature.

2. Power dependence

The results of the influence of power on the surface composition confirm the importance of reactions (6) and (7) during a-Si:H growth. By increasing the ion flux, hence the rate of dangling bond generation, we were able to promote these decomposition reactions and accelerate the transition from higher hydride- to SiH-dominated surface coverage, as shown in Fig. 5. The surface coverage data at 160 ^{o}C [Fig. 5 (b)], suggest that reaction (6) requires the high dangling bond density associated with high ion exposure at 100 W. When the temperature is increased to 230 ^{o}C, shown in Fig. 5 (c), there is some SiH on the surface even at 25 W indicating that decomposition via reaction (6) has just begun to proceed. The higher fraction of SiH_2 versus SiH on the surface under these conditions reveals that there is another mechanism of formation for the dihydride – most likely abstraction by incident SiH_3 [reaction (5)] or the Langmuir-Hinshelwood type abstraction [reaction (4)]. However, as the power is increased to 100 W, the surface composition changes from primarily SiH_2 coverage to mainly SiH indicating the progression of reactions (6) and (7). At 370 ^{o}C, the thermal energy is sufficient to enable both reactions to proceed even at 25 W.

For all films, independent of surface temperature, more dangling bonds are created in the presence of increased ion bombardment. Above 160 ^{o}C any increase in the ion flux is sufficient to create the dangling bonds required to promote the decomposition reactions. These reactions result in SiH dominance on the surface as shown in Figs. 5 (c) and (d). In contrast, when the thermal energy is insufficient, the surface coverage remains constant despite substantial increases in ion bombardment and the corresponding dangling bond density on the surface. For example, at 40 ^{o}C, the SiH_3-rich surface is preserved even when the ion flux is increased by a factor of 7. Unfortunately we were unable to measure the surface composition at higher plasma power since further increase in ion bombardment caused substantial heating of the ATR crystal. For example, with the electrode temperature set at 40 ^{o}C and the plasma power at 200 W, the film temperature measured by IR was 200 ^{o}C by the time the surface had reached steady state. The 100 W plasma did not cause such severe heating of the substrate. The "40 ^{o}C" film may be as high as 90 ^{o}C during the 100 W deposition; however, this is apparently not high enough to activate any additional reactions since the surface is identical at 25 and 100 W. During deposition at 25 W the temperature rises to 60 ^{o}C. Ion bombardment at higher set point temperatures does not increase the substrate temperature since the ring heater can adjust to deliver less power than required to maintain the set point.

Figure 5 clearly establishes the fact that enhanced dissociation in the gas phase can not be responsible for the increase in lower hydrides on the surface at high power and high temperatures. Any change in dissociation in the discharge would be independent of the substrate temperature, and as such, the surface coverage would reflect this change at all temperatures. Instead, the low temperature SiH_3 surface coverage is preserved over the entire range of plasma power verifying that the shift to lower hydrides at high temperature and high power is a result of surface reactions.

While the effect of ion flux on the surface spectra has provided strong evidence for the importance of reactions (6) and (7) during a-Si:H deposition, none of the experiments has provided convincing evidence for reaction (4). Furthermore, no conclusive evidence could be obtained through a directed experiment in which an a-Si:H film was deposited at 40 ^{o}C followed by heating to 370 ^{o}C in an attempt to promote reaction (4). After heating to 370 ^{o}C, we expected to find a surface composed of fewer SiH_3 with many SiH and SiH_2. If reaction (4) were activated, then adjacent SiH_3 would have been depleted leaving SiH_2 and dangling bonds. Remaining SiH_2 and SiH_3 could then react with these newly formed dangling bonds resulting in SiH on the surface. Instead, the surface after heating was identical to that of the deposited film indicating that reaction (4) does not occur on our a-Si:H surfaces. However, the uncertainty arises from the possibility of the a-Si:H bulk providing an infinite source of H. In this scenario, surface H are removed via reaction (4) or a similar, H_2 desorption process and the desorbed surface H are subsequently replenished by subsurface H. The aforementioned experiment would not be able to detect this H transfer since the reference spectrum is collected just prior to Ar sputtering, i.e., after H motion out of the bulk. Bulk multiple internal reflection infrared spectra collected during the high-temperature annealing step, reveal that H bound as SiH_x (x=1–3) at internal surfaces preferentially desorb upon heating. The signal from the surface (film/vacuum) species is overwhelmed by this strong signal therefore we can not determine whether surface has been desorbed as well. The vibrational frequencies of H at internal surfaces are also surface-like, adding to the difficulty. In addition, if the surface modes were replenished as H released from the subsurface diffused out of the film, the IR spectra would not detect any change in surface bonding.

At this point, we are unable to say with certainty whether or not reaction (4) is a source of H removal from our a-Si:H films. Despite its occurrence on c-Si surfaces,[18,20] reaction (4) may be precluded on our surfaces by the orientation or the proximity of SiH_3 being unfavorable for reaction. Differences in local bonding environments between a-Si:H and Si(001) surfaces for example, are expected to strongly influence reaction probabilities. Similarly, this work can not exclude a thermally activated reaction in which adjacent Si atoms cross link and release H_2.[47,48]

B. Role of ions on surface reactions

Higher hydride decomposition reactions (6) and (7) can not proceed unless dangling bonds are available. During a-Si:H growth in our deposition reactor, creation of active sites is expected to occur via ion bombardment in addition to abstraction by incident SiH_3 [reaction (5)] and possibly reaction (4). Specifically, physical sputtering of the surface hydrides by incident ions could reduce hydrogen density and generate dangling bonds via

$$\text{ion} + \mathrm{SiH}_{x(\mathrm{s})} \rightarrow \mathrm{SiH}_{x-y(\mathrm{s})} + y\,\mathrm{H}_{(\mathrm{g})} + y\,\_{(\mathrm{s})}\,. \qquad (8)$$

Additionally, the silicon atom itself may be dislodged by the ion,

$$\text{ion} + \mathrm{SiH}_{x(\mathrm{s})} \rightarrow \mathrm{SiH}_{x(\mathrm{g})} + \_{(\mathrm{s})}\,, \qquad (9)$$

where the majority of ions in our discharge are Ar^+ and ArH^+.[37]

The relative importance of ion bombardment reactions (8) and (9) versus adsorption and abstraction reactions (1) and (5) depends on the yields for reactions (8) and (9), the probabilities for adsorption and abstraction, as well as on the ratio of the ion flux to the radical precursor flux. In the limit that the ion flux is much greater than the flux of SiH_3 radicals, one expects a high dangling bond density on the surface. In contrast, when the flux of SiH_3 is much greater than the ion flux, one expects the surface to be almost completely passivated. For the conditions of this study, we can compute a rough estimate of the dangling bond coverage on the a-Si:H surface during deposition. Having shown that SiH_3 is our dominant precursor and H insertion is slow, we assume that adsorption of SiH_3 onto dangling bonds [reaction (1)] is the dominant means by which surface dangling bonds are passivated. Defect (dangling bond) generation occurs via abstraction of H by SiH_3 [reaction (5)] as well as by ion bombardment reactions (8) and (9). Thus, the areal dangling bond density, σ_{db}, on the a-Si:H surface at steady state can be estimated by the following equation:

$$\frac{d\sigma_{db}}{dt} = P_{ab} F_S \theta_{\mathrm{H}} + Y I_+ \theta_{\mathrm{H}} - P_{ad} F_S \theta_{db} = 0 \qquad (10)$$

where F_S and I_+ are the fluxes of SiH_3 radicals and incident ions, respectively, and Y represents the sputtering yield of H atoms per incident ion. The probabilities of abstraction [reaction (5)] and adsorption [reaction (1)] are given by P_{ab} and P_{ad}, respectively. The fractional defect coverage, θ_{db}, is related to the fractional H coverage, θ_{H}, via

$$\theta_{\mathrm{H}} + \theta_{db} = 1\,. \qquad (11)$$

Equation (10) is similar to that presented by Matsuda to describe the dangling bond steady state balance on the a-Si:H surface during growth.[41] In that work, films were deposited in the absence of additional Ar and the term accounting for the generation of defects through ion bombardment was omitted. Furthermore, since we did not heat our substrates above 370 °C, we are able to neglect defect generation due to H_2 desorption.

According to equation (10), the surface H coverage is

$$\theta_{\mathrm{H}} = \frac{1}{1 + \frac{P_{ab}}{P_{ad}} + \frac{Y I_+}{P_{ad} F_s}}\,. \qquad (12)$$

The probability of adsorption of SiH_3 onto a dangling bond is 1, therefore, the second term in the denominator is approximately equal to P_{ab}. The third term represents the competition between the creation of defects via ion damage and the passivation of dangling bonds by precursors for film growth. If we assume that SiH_3 is the precursor for growth, we can estimate the net flux of SiH_3 from the deposition rate measured by spectroscopic ellipsometry. Using the atomic density of c-Si (5×10^{22} cm^{-3}) and the measured growth rate, we find the net SiH_3 flux for the 50 W plasma to be 2.2×10^{14} cm^{-2}s^{-1} for a deposition rate of 26 Å/min at 230 °C. This estimation represents the lower bound of the SiH_3 flux. Assuming a sticking probability of 0.26 for the SiH_3, a more realistic estimate of the incident SiH_3 flux is 8.5×10^{14} cm^{-2}s^{-1}. The ion flux can be obtained from the Langmuir probe data of Fig. 4; and in the 50 W discharge, I_+ is approximately equal to F_s. Thus, the last term in the

TABLE I. Parameters used to estimate the dangling bond coverage on the surface of the a-Si:H film deposited at 50 W and 230 °C according to Eq. (12).

P_{ad}	1
P_{ab}	0.05 [43]
Y	0.05 H per ion [15]
I_{+}	8.9×10^{14} $\mathrm{cm^{-2}s^{-1}}$
F_S	8.5×10^{14} $\mathrm{cm^{-2}s^{-1}}$

denominator is on the order of the sputter yield. The sputtering yield for ions impinging on the a-Si:H surface, estimated from the decrease in integrated absorbance due to H sputtering by plasma,[15] is approximately 0.05 H per ion. The probability of abstraction of H from a-Si:H surfaces by SiH_3 radicals has been computed by Ramalingam *et al.* and is also found to be on the order of 5%. A summary of the values used to estimate the defect coverage on the a-Si:H surface deposited at 230 °C and 50 W is given in Table I, and the corresponding dangling bond coverage on the a-Si:H surface is approximately 0.1. This coverage is sufficiently low to limit the rates of reactions involving dangling bonds.

In an earlier work we proposed that the stability of higher hydrides on the a-Si:H surface at temperatures as high as 230–300 °C was due to a lack of dangling bonds on the surface.[8] Indeed, recent molecular dynamic simulations of a-Si:H deposition from SiH_3 precursor by Ramalingam *et al.* showed that most surface Si atoms are either four-fold or over coordinated with a few under coordinated Si atoms scattered on the surface.[43] However, these dangling bonds determined the reactivity of the surface and the reaction mechanism of SiH_3 adsorption and decomposition on the surface. The silicon hydride composition as a function of substrate temperature for these simulated films is reported in Ref. 43 and compared with the experimental results herein. The temperature dependence of the surface hydrides is in good agreement with that for surfaces grown at 25 W with limited ion bombardment in that the film growth simulated at 500 K has predominantly SiH_2 on the surface while the film at 773 K has mainly SiH. There did not seem to be a significant difference between the dangling bond coverage of the films grown at the two temperatures despite the fact that the silicon hydride distribution was not the same.

C. H coverage

In a related study, Toyoshima *et al.* used IR-RAS and D/H isotope exchange technique to sample the surface species on plasma deposited a-Si:H films from 25 to 500 °C.[1] They reported a constant value for the total surface hydride integrated absorption intensity for temperatures below 380 °C and attributed this observation to a fully hydrogen-terminated surface. At higher temperature (>380 °C), the integrated absorption intensity falls off due to hydrogen desorption. This decrease in integrated absorption is correlated with an increase in growth rate consistent with the creation of more active sites. However, according to the MD simulations of Ramalingam and coworkers, it is possible to have a small, but finite dangling bond density on the surface while maintaining a constant H coverage.[43]

For our films, the total integrated absorption intensity for the surface as a function of temperature is shown in Fig. 7(a). On the right ordinate, we have converted the total integrated absorbance into concentration using the absorbance [$\int A(\nu)\mathrm{d}\nu = 2.27\times10^{-3}\ \mathrm{cm^{-1}}$ per reflection] for 1 monolayer (ML) of H in the form of silicon monohydride on Si (111) reported by Jakob *et al.*[49] and as described in a separate publication.[15] The total hydrogen coverage appears to be approximately constant above 160 °C, and we compute an average H surface concentration of $5.7\times10^{14}\ \mathrm{cm^{-2}}$ for films grown in the range of 230–370 °C. This corresponds to 0.72 ML equivalent of full coverage on ideally terminated Si (111). At 40 °C, however, we have sputtered 3.1 ML equivalent H on ideally terminated Si (111). It is important to note that unlike the Si(111) surface, our a-Si:H surface consists of mono-, di-, and tri-hydrides, and we have assumed that the absorption cross section for all silicon hydrides are the same. Thus, the relatively high integrated Si-H stretching absorbance at 40 °C is artificially inflated by the double and triple counting due to the di- and tri-hydrides. Similar reasoning accounts for the slightly lower Si-H absorption intensity of the surface at 160 °C that has relatively fewer trihydrides. Figure 7(b) displays the absorbance data of Fig. 7(a) corrected for the number of Si-H bonds per SiH_x (x=1,2,3) (i.e., by division by the number of bonds). The total SiH_x coverage is also shown. When the absorbance is corrected for the number of Si-H bonds per SiH_x, the surface H density is constant, within experimental error, as a function of temperature in the range 160 to 370 °C. The larger SiH_x density at 40 °C could be due to a large absorption cross section for the SiH_3 stretch as compared with SiH and SiH_2. Alternatively, or even in addition, the high Si-H absorption intensity may be due to a relatively high surface roughness at 40 °C that would effectively increase the surface area.

Although we can not directly measure the absorption cross section of the various SiH_x modes, we can determine whether the surface roughness can account for the enhanced absorbance at low temperature. To do so, we measured the surface roughness using atomic force microscopy (AFM). These measurements indicate that the film deposited

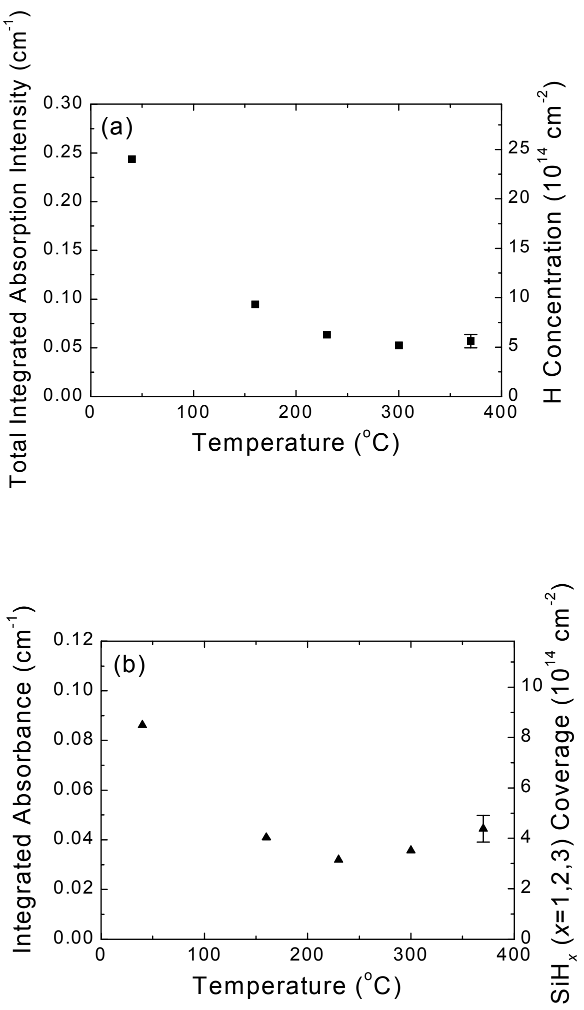

FIG. 7. (a) The temperature dependence of the integrated absorption intensity of all surface silicon hydrides. The absolute surface H concentration is shown on the right ordinate. All films were deposited for 6 min. In (b), the integrated absorbance has been corrected for the number of Si-H bonds in each SiH$_x$ (x = 1,2,3). The corresponding SiH$_x$ coverage is reported on the right ordinate

at 40 °C is indeed rougher than the films grown at higher temperatures. The height images obtained by AFM of the surface of films deposited for 5 minutes at 40 °C (a) and at 230 °C (b) are displayed in Fig. 8. According to spectroscopic ellipsometric measurements, the film thickness is 190 and 163 Å for the films grown at 40 and 230 °C, respectively. Based on the AFM data in Fig. 8, the film deposited at 40 °C is rougher than the film deposited at 230 °C and the corresponding RMS roughness values are 0.49 nm and 0.20 nm respectively measured over an area of 1 μm × 1 μm. The respective maximum feature heights for the images shown are 5.0 nm and 2.8 nm.

To determine whether the measured variance in the surface area is commensurate with the strong absorbance at 40 °C, we prepared films with identical surface compositions but having varying degrees of roughness. To do so, we exploited the fact that the surface roughness, as determined using AFM, grows as the film thickness increases. The AFM height image of a film grown at 230 °C for 15 min is shown in Fig. 8 (c). This image should be compared with that of the film grown at 230 °C for 5 min as shown in Fig. 8 (b). Though visual interpretation of the AFM images is quite adequate in this case, the RMS roughness is plotted on the right ordinate of Fig. 9 and shown to increase with deposition time. The corresponding integrated absorption intensity for the total hydrogen coverage on the surface is shown on the left ordinate.

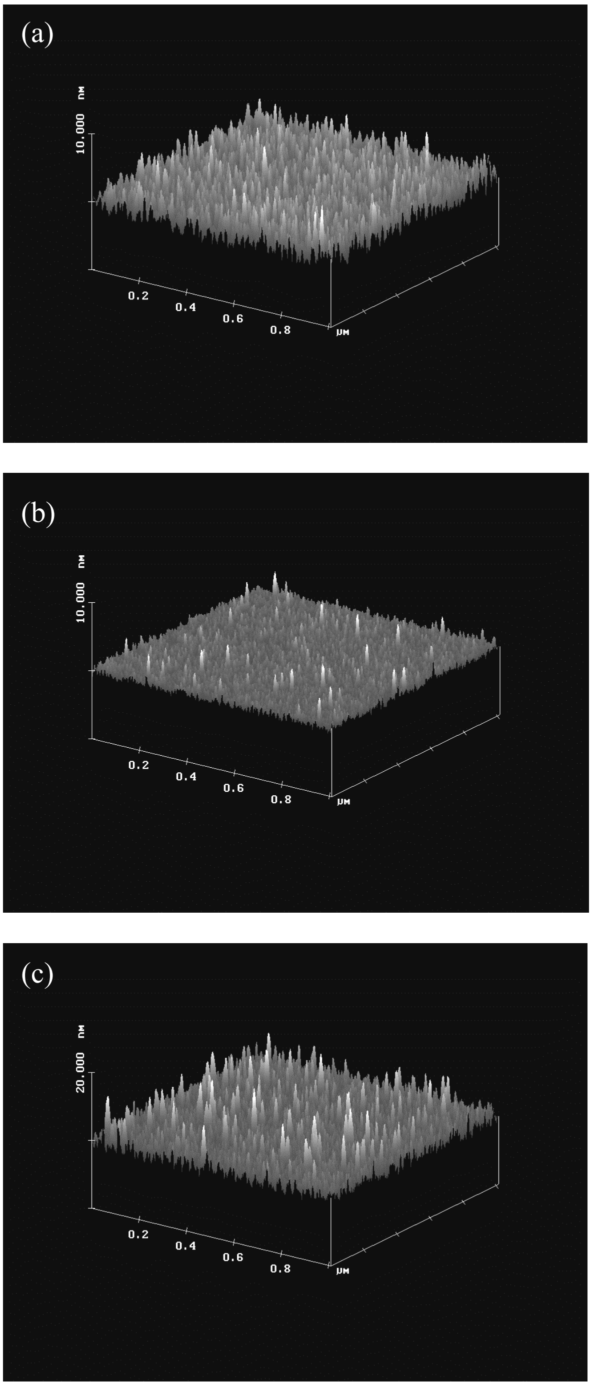

FIG. 8. AFM height images of the surface of a-Si:H deposited for (a) 5 minutes at 40 °C, (b) 5 minutes at 230 °C, and (c) 15 minutes at 230 °C. The z scale of (c) has been expanded relative to the scales of the x and y directions to enhance clarity of the surface features.

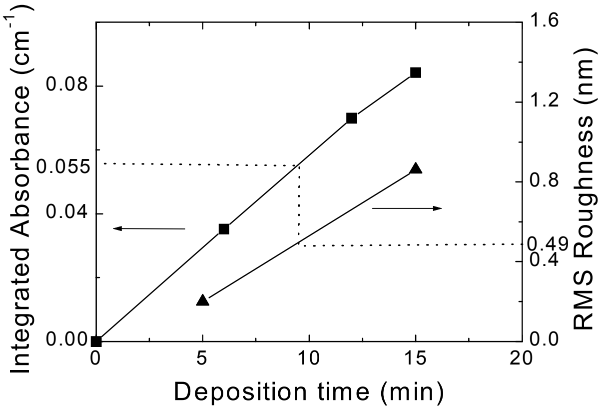

FIG. 9. Integrated absorption intensity for the total surface hydride coverage as a function of deposition time for films deposited at 230 °C. On the right ordinate, the RMS roughness as measured by AFM is shown to increase throughout the deposition. The solid lines are included as a guide for the eye.

Films deposited in the range of 6–20 minutes (240 to 640 Å thick) had identical surface compositions and only the total absorption intensity changed. Thus, the total hydride removal (detected as integrated absorption intensity) is found to increase with increasing film thickness/surface roughness.

It is useful to consider the integrated absorption intensity and roughness of the film deposited at 40 °C in relation to those properties of the films grown for 5 and 15 minutes at 230 °C. Because the fractional silicon hydride coverage of the two films grown at the same temperature is identical, the increase in integrated absorbance can be attributed to the increase in surface area due to roughening during growth. For the following discussion, let us assume that the SiH_x (x=1,2,3) absorption cross sections are identical, therefore the integrated absorbance intensity is independent of surface coverage and depends only on the degree of roughness. To deposit a film at 230 °C having a RMS roughness on the order of that of the surface deposited at 40 °C (0.49 nm) would require almost 10 minutes deposition. The integrated absorbance [corrected for the number of Si-H bonds per SiH_x (x=1,2,3)] corresponding to ~10 minutes growth at 230 °C would be ~0.055 as indicated by the dotted line in Fig. 9. This value is almost identical to the integrated absorbance (also corrected for the number of Si-H bonds) measured for the surface of the film grown for 5 minutes at 40 °C (0.054) and having the RMS roughness of 0.49 nm. Thus, we can conclude that the enhanced integrated absorbance for the film deposited at 40 °C can be ascribed to the increased surface roughness. This analysis indicates that the assumption of approximately equal absorption cross sections for the various silicon hydrides is valid.

It is worth noting that if the raw integrated absorption intensity is used for this analysis without correction for the number of Si-H bonds per SiH_x, then a completely different conclusion is reached. Due to the triple counting for the SiH_3-rich surface at 40 °C, the corresponding RMS roughness can not account for the inflated absorption intensity. In this way, the absorption cross section of SiH_3 would incorrectly appear to be larger than SiH and SiH_2.

The constant integrated absorbance for surfaces of films deposited in the range 160 to 370 °C is consistent with the data of Toyoshima *et al.*,[1] however our observation of higher integrated absorbance at 40 °C is not in accordance with their data. Although it may be possible that their deposition method affords an additional smoothening mechanism at 40 °C, this seems unlikely since their surface is also largely dominated by SiH_3 species. It is more probable that limitations inherent in the IR-RAS technique are responsible for the observation of Toyoshima *et al.* of identical integrated absorbance at 40 °C as at the higher temperatures. In the IR-RAS technique, polarization dependence of detection sensitivity restricts detection to the modes in which H displacement is perpendicular to the surface. In contrast to c-Si, the orientation of Si-H bonds on the poorly-defined amorphous surface is random, therefore, many bonds are undetectable by this technique.

It should be noted that the oscillator strengths of the silicon hydride species on a-Si:H surfaces are not known, and we have used values reported by Jakob *et al.* for H on c-Si surfaces to determine absolute values for surface H-coverage.[49] Furthermore, although we have tested the sputtering method carefully for validity and reproducibility,[15] we can not be certain that we have removed *exactly* the surface layer, no more, no less. These uncertainties are inherent to detecting surface adsorbates on amorphous hydrogenated silicon surfaces *in situ*. Assuming the oscillator strengths are independent of temperature and coverage, we can compare the relative hydride coverage as a function of temperature and deduce the reactions as was done in this article.

V. CONCLUSIONS

Using *in situ* ATR-FTIR we report on the surface coverage of plasma deposited a-Si:H over a range of substrate temperature and plasma power. At low temperature and in the range of ion flux investigated, the thermal energy is insufficient to activate silicon hydride decomposition reactions. At low temperature, the surface is primarily covered by SiH_3, most likely in close proximity to each other. This observation of predominantly SiH_3 on the surface, combined with a relatively slow H insertion rate,[8] supports the hypothesis that SiH_3 is the dominant precursor to a-Si:H deposition.[38-40] At higher temperatures and in the presence of dangling bonds, decomposition of SiH_3 and SiH_2 proceeds via reactions (6) and (7) resulting in fewer higher hydrides on the surface. By increasing the ion flux and thereby generating more dangling bonds on the surface, these decomposition reactions were accelerated and the surface was composed of fewer higher hydrides than at lower temperatures. In both the low and high temperature limits, however, the dangling bond density, and hence, the ion bombardment, had negligible effect on the surface composition.

We found that the integrated absorption intensity scales with increasing deposition time, hence with film roughness. The silicon hydride composition, however, is independent of the surface roughness within the parameters investigated. Furthermore, we provide evidence that the absorption cross section is constant for SiH_x (x=1,2,3) on the a-Si:H surface.

ACKNOWLEDGMENTS

This research was supported by the NSF/DOE Partnership for Basic Plasma Science and Engineering (Award No. DMR 97–13280) and the Camille and Henry Dreyfus Foundation. D. M. acknowledges support from the National Science Foundation predoctoral fellowship program. W. K. acknowledges the Netherlands Organization for Scientific Research (NWO) and the Center for Plasma Physics and Radiation Technology (CPS) for financial support. Many thanks are due Dr. D. Maroudas, Dr. S. Ramalingam, S. Agarwal, and S. Sriraman for insightful discussions.

[1] Y. Toyoshima, K. Arai, A. Matsuda, and K. Tanaka, J. Non-Cryst. Solids **137-138**, 765 (1991).

[2] N. J. Harrick, *Internal Reflection Spectroscopy* (Wiley, New York, 1967).

[3] Y. J. Chabal, Surf. Sci. Rept. **8**, 211 (1988).

[4] E. S. Aydil, R. A. Gottscho, and Y. J. Chabal, Pure & Appl. Chem. **66**, 1381 (1994).

[5] E. S. Aydil, and R. A. Gottscho, Solid State Technol. **40**, 181 (1997).

[6] B. F. Hanyaloglu, D. C. Marra, and E. S. Aydil, (unpublished).

[7] D. C. Marra, E. A. Edelberg, R. L. Naone, and E. S. Aydil, Appl. Surf. Sci. **133**, 148 (1998).

[8] D. C. Marra, E. A. Edelberg, R. L. Naone, and E. S. Aydil, J. Vac. Sci. Technol. **A 16**, 3199 (1998).

[9] N. Blayo, and B. Drevillon, Appl. Phys. Lett. **59**, 950 (1991).

[10] N. Blayo, and B. Drevillon, J. Non-Cryst. Solids **137&138**, 775 (1991).

[11] R. Nozawa, H. Takeda, M. Ito, M. Hori, and T. Goto, J. Appl. Phys. **85**, 1172 (1999).

[12] M. Katiyar, Y. H. Yang, and J. R. Abelson, J. Appl. Phys. **77**, 6247 (1995).

[13] S. Miyazaki, H. Shin, Y. Miyoshi, and M. Hirose, Jpn. J. Appl. Phys. **34**, 787 (1995).

[14] S. S. Lee, M. J. Kong, S. F. Bent, C.-M. Chiang, and S. M. Gates, J. Phys. Chem. **100**, 20015 (1996).

[15] W. M. M. Kessels, D. C. Marra, M. C. M. van de Sanden, and E. S. Aydil, submitted for publication.

[16] H. Fujiwara, Y. Toyoshima, M. Kondo, and A. Matsuda, Phys. Rev. B **60**, 13598 (1999).

[17] D. R. Olander, M. Balooch, J. Abrefah, and W. J. Siekhaus, J. Vac. Sci. Technol. **B 5**, 1404 (1987).

[18] S. M. Gates, R. R. Kunz, and C. M. Greenlief, Surf. Sci. **207**, 364 (1989).

[19] S. M. Gates, C. M. Greenlief, and D. B. Beach, J. Chem. Phys. **93**, 7493 (1990).

[20] C. C. Cheng, and J. J. T. Yates, Phys. Rev. B **43**, 4041 (1991).

[21] Y. Wang, M. J. Bronikowski, and R. J. Hamers, Surf. Sci. **311**, 64 (1994).

[22] S. Ramalingam, D. Maroudas, E. S. Aydil, and S. P. Walch, Surf. Sci. **418**, L8 (1998).

[23] C.-M. Chiang, S. M. Gates, S. S. Lee, M. Kong, and S. F. Bent, J. Phys. Chem. **B 101**, 9537 (1997).

[24] E. A. Edelberg, A. Perry, N. Benjamin, and E. S. Aydil, Rev. Sci. Instrum. **70**, 2689 (1999).

[25] E. A. Edelberg, A. Perry, N. Benjamin, and E. S. Aydil, J. Vac. Sci. Technol. **A 17**, 506 (1999).

[26] B. Gong, S. Jo, G. Hess, P. Parkinson, and J. G. Ekerdt, J. Vac. Sci. Technol. **A 16**, 1473 (1998).

[27] D. E. Aspnes, J. Vac. Sci. Technol. **18**, 289 (1981).

[28] K. Vedam, J. McMarr, and J. Narayan, Appl. Phys. Lett. **47**, 339 (1985).

[29] B. Johs, D. Meyer, G. Cooney, H. Yao, P. G. Snyder, J. A. Woollam, J. Edwards, and G. Maracas, Mater. Res. Soc. Symp. Proc. **216**, 5989 (1991).

[30] Y. J. Chabal, in *Internal Reflection Spectroscopy: Theory and Applications*, J. Francis M. Mirabella, Ed. (Marcel Dekker, Inc., New York, 1993) p. 191.

[31] Y. J. Chabal, and K. Raghavachari, Phys. Rev. Lett. **53**, 282 (1984).

[32] V. A. Burrows, Y. J. Chabal, G. S. Higashi, K. Raghavachari, and S. B. Christman, Appl. Phys. Lett. **53**, 998 (1988).

[33] U. Jansson, and K. J. Uram, J. Chem. Phys. **91**, 7978 (1989).

[34] K. J. Uram, and U. Jansson, J. Vac. Sci. Technol. B **7**, 1176 (1989).

[35] Y. J. Chabal, G. S. Higashi, and S. B. Christman, Phys. Rev. B **28**, 4472 (1983).

[36] L. C. Snyder, J. W. Moskowitz, and S. Topiol, Phys. Rev. B **26**, 6727 (1982).

[37] S. Agarwal, (private communication, 1999).

[38] R. Robertson, and A. Gallagher, J. Appl. Phys. **59**, 3402 (1986).

[39] N. Itabashi, N. Nishiwaki, M. Magane, S. Naito, T. Goto, A. Matsuda, C. Yamada, and E. Horita, Jpn. J. Appl. Phys., Part 2 **29**, L505 (1990).

[40] J. R. Abelson, Appl. Phys. A **56**, 493 (1993).

[41] A. Matsuda, J. Vac. Sci. Technol. **A 16**, 365 (1998).

[42] A. von Keudell, and J. R. Abelson, Phys. Rev. B **59**, 5791 (1999).

[43] S. Ramalingam, S. Sriraman, D. C. Marra, D. Maroudas, and E. S. Aydil, submitted for publication.

[44] J. A. Glass, Jr., E. A. Wovchko, and J. T. Yates, Jr., Surf. Sci. **348**, 325 (1996).

[45] A. Gallagher, J. Appl. Phys. **63**, 2406 (1988).

[46] K. J. Uram, and U. Jansson, Surf. Sci. **249**, 105 (1991).

[47] G. H. Lin, J. R. Doyle, M. He, and A. Gallagher, J. Appl. Phys. **64**, 188 (1988).

[48] W. M. M. Kessels, R. J. Severens, M. C. M. van de Sanden, and D. C. Schram, J. Non-Cryst. Solids **227-230**, 133 (1998).

[49] P. Jakob, P. Dumas, and Y. J. Chabal, Appl. Phys. Lett. **59**, 2968 (1991).

On the growth mechanism of hydrogenated amorphous silicon

W. M. M. Kessels[a] and A. H. M. Smets
Department of Applied Physics, Center for Plasma Physics and Radiation Technology,
Eindhoven University of Technology, P.O. Box 513, 5600 MB Eindhoven, The Netherlands

D. C. Marra and E. S. Aydil
Department of Chemical Engineering, University of California Santa Barbara,
California 93106-5080, USA

D. C. Schram and M. C. M. van de Sanden[b]
Department of Applied Physics, Center for Plasma Physics and Radiation Technology,
Eindhoven University of Technology, P.O. Box 513, 5600 MB Eindhoven, The Netherlands

The kinetic growth model for hydrogenated amorphous silicon (a-Si:H) from SiH_3 radicals in SiH_4 plasmas is reviewed on the basis of recently obtained experimental and computational data. New surface reactions are considered and their implications for the a-Si:H film growth mechanism are discussed. Furthermore, from the experimentally observed substrate temperature dependence of the bulk hydrogen content and the composition of the a-Si:H surface hydrides, it is concluded that surface processes play an important role in hydrogen elimination from the film during the growth process.

I. INTRODUCTION

Hydrogenated amorphous silicon (a-Si:H) is a widely used material with applications in devices such as solar cells, thin film transistors (TFTs), detectors, photoreceptors, and light emitting diodes (LEDs). Throughout the last two decades, the aim at improving the a-Si:H material properties for its specific applications has initiated numerous studies in order to understand the a-Si:H film growth mechanism from SiH_4 plasmas.[1-18] In this article, we will give a short review of the most important growth models, while concentrating mainly on the kinetic growth model in which SiH_3 is considered to be the dominant growth precursor. An extension of our understanding of the film growth reaction mechanisms will be given on the basis of recent experimental investigations as well as on the basis of simulations and calculations rapidly emerging from the availability of strong computational power. Finally, we will focus on data of the bulk and surface hydrogen content and composition in order to clarify the ‘riddle’ with respect to H elimination from the film during growth.

II. REVIEW OF a-Si:H GROWTH MODELS

One kind of models for a-Si:H growth is based on a thermodynamic approach. Herein hydrogen equilibration during deposition is used to explain the defect concentration and properties of a-Si:H and its alloys as a function of, e.g., the substrate temperature T_s and deposition rate R_d. In this model, which is initiated by the work of Winer and Street,[7-10] no detailed surface chemical reactions are taken into account nor does the model describe how film growth actually takes place. The formation of dangling bonds, the principle defects in a-Si:H, is attributed to the breaking of weak Si-Si bonds (with an exponential distribution in the valance band-tail) by mobile H that is released from Si-H bonds:[7]

$$\text{H + weak bond} \leftrightarrow \text{Si-H + broken bond.} \qquad (1)$$

The density of weak bonds in a-Si:H is determined by reactions which convert weak bonds in the subsurface region into strong bonds. These conversion reactions are assumed to be mediated by H diffusion and they are the rate limiting step in network equilibration. At sufficiently high T_s, H diffusion is fast enough to redistribute between alternative bonding sites and to equilibrate the distribution of Si-Si and Si-H bonds, thereby minimizing the concentration of weak and dangling bonds. Herein the minimum weak-bond density is determined by the network constraint causing a minimum disorder in a-Si:H (thermal disorder). Street has described this process in terms of the hydrogen density of states and the hydrogen

---

[a] Electronic mail: w.m.m.kessels@phys.tue.nl
[b] Electronic mail: m.c.m.v.d.sanden@phys.tue.nl

Accepted for publication in Thin Solid Films.

chemical potential.[9,10] At too low T_s, the insufficient H mobility does not allow the network to equilibrate and the film structure and H content to be determined by the hydrogen chemical potential. Consequently, a large amount of weak bonds are "frozen" into the network. At too high temperatures on the other hand, thermal disorder will lead to a higher weak bond density than optimal, manifested by an increased valence-band tail slope. These two processes explain the U-shape dependence of the defect density in a-Si:H on T_s.[7] The optimal film quality is obtained when the average rate of H diffusion is equal to the deposition rate R_d. The surface layer, as formed by the attachment of SiH_x radicals, is disordered and has an excess amount of H. The final structure is therefore determined by the motion and elimination of the excess H and the reduction of structural order, whereby a large fraction of bonded H must redistribute in the time in which a few atomic layers of the film are grown. Consequently, at higher R_d a higher T_s is required, which is generally observed.

Although the thermodynamic approach has been successful in explaining several experimental observations, it has also a number of drawbacks. An overview of the drawbacks is given in Ref. 12 by Ganguly *et al.*, but a particular major weakness of the model is that it does not explain how film growth actually takes place. Furthermore, the model is also rather vague about H elimination in the growth zone.

A model in which the surface reactions of the species contributing to growth are taken into account is the kinetic growth model initially developed by Gallagher,[2] Perrin,[4] and Matsuda.[3,5] In this model, referred to as the 'MGP model' for brevity, SiH_3 is assumed to be the only growth precursor. This assumption is based on the (presumed) dominance of this radical in plasmas leading to device quality a-Si:H. The basic reactions of SiH_3 within this model are illustrated in Fig. 1(a).

The central assumption in the MGP model is that SiH_3 reaching the a-Si:H surface can go in a weakly adsorbed (physisorbed) state forming a three center Si-H-Si bond on a surface SiH_x site.[2] The probability for this process is the surface reaction probability β. The SiH_3 radical in this weakly adsorbed state can subsequently diffuse over the surface by hopping from one to another surface H atom. During this surface diffusion, SiH_3 can either abstract a surface H atom to create a surface radical site (dangling bond) and gaseous SiH_4, or stick on a surface dangling bond (chemisorption) and contribute to film growth. Another possibility is that the SiH_3 radical reacts with another physisorbed SiH_3 forming gaseous Si_2H_6. The (macroscopic) probability for sticking is s while the probability for the formation of the gaseous species is γ $(=\gamma_{SiH4}+\gamma_{Si2H6})$. Desorption from the physisorbed state is expected to be unimportant on the basis of energetic considerations such that $\beta=s+\gamma$. At the commonly used substrate temperatures T_s, film growth in this model is therefore balanced by precursor mediated sticking of SiH_3 and precursor mediated H abstraction by SiH_3. At high T_s (>400 °C and depending on R_d),[17] surface dangling bond creation can also occur by thermal desorption of surface H forming gaseous H_2. This process, however, will not be considered here.

The MGP model gives a good description of a-Si:H growth under conditions in which SiH_3 is the predominant growth precursor. The model accounts for the fact that at low T_s two SiH_3 radicals are necessary per growth step[3] and that conformal deposition profiles are obtained in step-coverage experiments (implying a low sticking probability of the species leading to growth).[19] Furthermore, the

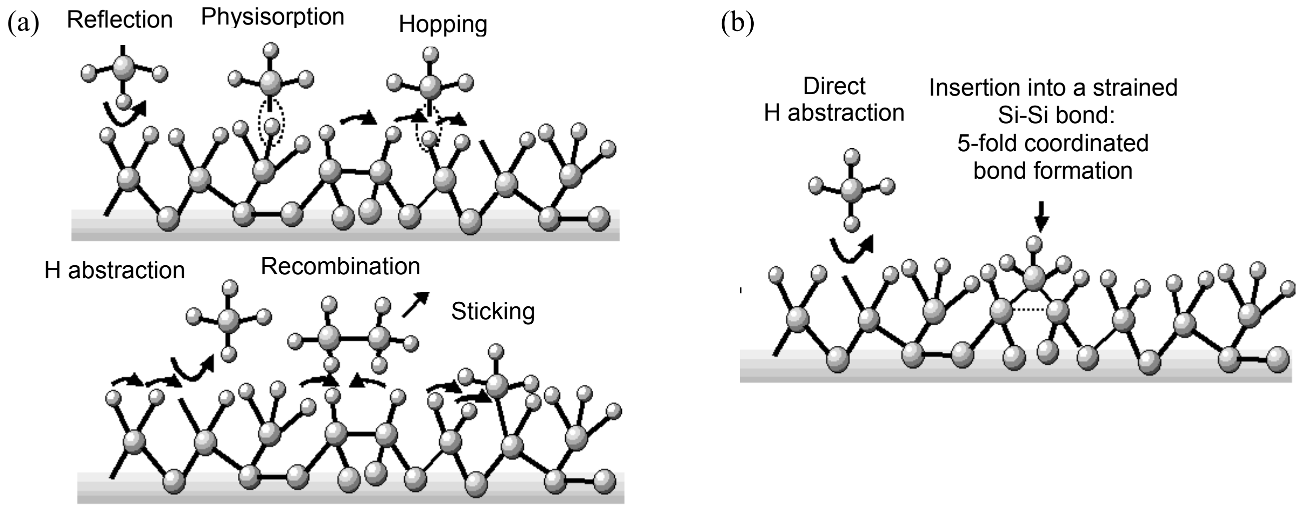

FIG. 1. Schematic representation of the surface reactions during a-Si:H film growth from SiH_3 radicals. (a) Basic reactions as proposed in the MGP model, (b) extended set of possible reactions as proposed from recent studies. For further explanation see text.

occurrence of surface diffusion can account for a smoothening mechanism that explains the relatively low and temperature dependent surface roughness of a-Si:H.[20-22] That precursor mediated film growth is necessary for an almost fully hydrogenated surface[23] with a low fractional dangling bond coverage θ_{db} can be illustrated by considering the balance equation for θ_{db} in the case that no precursor state is present. Assuming direct abstraction of surface H and direct sticking on surface dangling bonds by SiH_3 from the gas phase with probability P_{ab} and P_s, respectively, yields

$$d\theta_{\mathrm{db}}/dt = \Gamma_{\mathrm{SiH}_3}\theta_{\mathrm{H}} P_{ab} - \Gamma_{\mathrm{SiH}_3}\theta_{\mathrm{db}} P_s \tag{2}$$

with θ_H the fractional H coverage (θ_H=1-θ_{db}), and Γ_{SiH3} the flux of SiH_3 per surface site. In steady state $(d\theta_{\mathrm{db}}/dt = 0)$, this equation reduces to

$$\theta_{\mathrm{db}} = \frac{1}{1 + P_s/P_{ab}}. \tag{3}$$

Using β=~0.28 for SiH_3[15] with s=~0.09[5] and assuming P_s=1 (no barrier for chemisorption) yields P_{ab}=~0.09 and θ_{db}=~0.09. This value for θ_{db} is much higher than expected (and measured, as will be discussed in Sec. III), especially when θ_{db} is assumed to be directly related to the very low bulk defect density N_d.[12] Note that P_{ab} is actually fixed by the experimentally determined "macroscopic" sticking probability s of SiH_3 because abstraction is balanced by sticking. By introducing a precursor mediated state, it can be accounted for both s=~0.09 and θ_{db}<<0.09 because much more sites than on the basis of θ_{db} are available for SiH_3 to adsorb: $\theta_{db}P_s$ in Eq. (2) becomes $\theta_{db}P_s$ + a large factor due to sticking after multiple hops. The passivation of dangling bonds by sticking can still be very fast because the surface diffusing SiH_3 can sample many surface sites per unit of time.[4,12]

The MGP model has been used to explain the substrate temperature independent β and s of SiH_3 (yielding insight into the Arrhenius type of thermally activated surface reactions) at the commonly used substrate temperatures,[5,15] and the catalytic effect of B_2H_6 addition which drastically enhances the deposition rate.[4] In the work of Ganguly and Matsuda, it is also tried to directly link θ_{db} with the bulk defect density N_d under the assumption that dangling bonds on the surface layer become statistically a part of the bulk.[12,13] This assumption is based on the observations that at low substrate temperatures N_d is independent of the SiH_3 growth flux, whereas at temperatures higher than the onset for thermal desorption of hydrogen from the surface N_d can be reduced by going to a higher SiH_3 growth flux ("precursor assisted defect suppression").[12,13] This hypothesis has implications for the thermal activation of the surface reactions as will be addressed below. Furthermore, attempts have been made to include more hydrogen deficient radicals with a higher surface reactivity[11,14] while Perrin *et al.* have included reactions with atomic H from the plasma.[15] For the assumptions made, the inclusion of these reactions by atomic H was found to have only important consequences when going from the deposition of a-Si:H to the deposition of microcrystalline silicon (μc-Si:H).

III. NEW INSIGHTS INTO a-Si:H GROWTH

In this section, results of recent a-Si:H growth studies will be summarized. The implications for the MGP model will be considered and on the basis of newly proposed surface reactions it is tried to solve some inconsistencies in the model.

Experiments that are very relevant for the growth model of a-Si:H are the *in situ* and real time dangling bond density measurements during film growth by Yamasaki *et al.*[24] From electron spin resonance (ESR) measurements, a dangling bond density of ~2×10^{17} m^{-2} was observed for room temperature a-Si:H in a surface layer with a thickness of ~5 nm. This corresponds roughly with θ_{db} = ~10^{-2}–10^{-3}. Although this value of θ_{db} is still low in comparison with one obtained when only direct reactions are considered (see Sec. II), it is much higher than expected when assuming a direct relation between θ_{db} and N_d.[12,13] Furthermore, no strong substrate temperature dependence has been observed up to 200 °C in contrast to the case of N_d.[25] The latter discrepancy, but especially the unphysical values for the activation energies and the pre-exponential factors which have to be assumed for the rates of the surface reactions, have lead Robertson to conclude that the surface reactions do not directly determine N_d.[18] Instead, he proposes that N_d is determined by weak bonds in a defect pool process (also at low T_s) in which H elimination plays an important role as will be discussed in Sec. IV.

A radically different view on a-Si:H growth has recently been proposed by Von Keudell and Abelson.[26] Although, to our opinion, not incontestably proven, they concluded from their experiments that SiH_3 does not first abstract H atoms from the a-Si:H surface before sticking. Instead, they proposed that SiH_3 can also insert into strained Si-Si bonds on the surface [see Fig. 1(b)]. This mechanism yields another explanation for the low surface dangling bond density during deposition than the assumption of a precursor mediated state because in this case sticking of SiH_3 does not necessarily require dangling bonds. They proposed that this insertion reaction is dominant during a-Si:H film growth.[26] Evidence for such a reaction has recently been obtained from molecular-dynamics studies of SiH_3 impinging on a Si(100)-(2×1) surface by Ramalingam *et al.* In these studies, SiH_3 was observed to insert into strained dimer bonds forming a five-fold coordinated bond.[27] It is unclear yet how this reaction would lead to stationary film growth, because the number of strained bonds on the surface is expected to be limited and furthermore it is a self-limiting process. It is also unclear how film growth by this insertion reaction would account for the temperature independence of s. When the presence of strained bonds on the a-Si:H surface has a similar dependence on T_s as for crystalline Si,[26] the availability of these "growth sites" is strongly temperature dependent leading consequently to a strongly temperature dependent deposition rate. Film growth by insertion of SiH_3 into strained bonds, however, might explain the relatively slow onset (within ~50 s) of the surface dangling bond density at initial film growth as observed by Yamasaki *et al.* in his time-resolved ESR study.[24] This slow onset is in contrast with the very fast rise (within 1 s) of the dangling bond density when exposing the a-Si:H to a H_2 plasma where direct abstraction of surface hydrogen by atomic H from the plasma is known to take place.[28]

An inconsistency in the MGP model is the fact that the model predicts that the probability for Si_2H_6 formation γ_{Si2H6} decreases with increasing T_s for temperatures <400 °C while β and also s (necessarily equal to the probability for SiH_4 formation γ_{SiH4}) are observed to be temperature independent.[5] As pointed out by Van de Sanden *et al.*, an Eley-Rideal type of reaction for the creation of surface dangling bonds, would more naturally explain the substrate temperature independence of the growth flux (i.e., R_d in terms of Si atoms per unit of time).[17] By including direct abstraction of surface hydrogen by atomic H from the plasma, Van de Sanden *et al.* demonstrated that the temperature independent growth flux can be explained and that the model can also account for the proper temperature dependence and order of magnitude of θ_{db} (i.e., with physical values for the activation energies and pre-exponential factors).[17] A direct H abstraction reaction by SiH_3 has recently been observed by Ramalingam *et al.* in molecular-dynamics simulations of SiH_3 impinging on hydrogenated silicon surfaces [see Fig. 1(b)].[27,29] The creation of SiH_4 and a surface dangling bond was observed in an exothermic reaction with a small activation energy barrier of ~0.09 eV (it is expected that this barrier can easily be overcome by the kinetic energy of SiH_3). Because sticking is completely governed by the abstraction reaction by SiH_3 from the gas phase, this type of reaction mechanism naturally explains the temperature independence of s, also for conditions with an almost pure SiH_3 flux, i.e., without the abundant presence of atomic H in the plasma (see Sec. IV). The direct abstraction reaction by SiH_3 has recently also been observed in calculations by Parsons. These calculations, which were performed on a very small cluster (Si_4H_9), revealed an activation energy of ~0.4 eV.[30]

Also in the case of direct abstraction of H by SiH_3 the surface dangling bond density can remain very low, for example, by a hot precursor state of SiH_3 similar as proposed for passivation of dangling bonds on flat crystalline Si during H dosing.[28,31] In such a Kisliuk type of adsorption mechanism,[32] the incident radical becomes dynamically trapped in highly excited states above its diffusion barrier and consequently the radical can sample several surface sites prior to sticking. Furthermore, in addition to the direct H abstraction reaction by SiH_3, some surface mobility of SiH_3 on a-Si:H has been observed in the molecular-dynamics studies of Ramalingam *et al.*[27] SiH_3 incident on a surface containing only 50% hydrogen migrated for 3 ps over the surface (squared displacement almost 1 nm^2) before attaching itself to a dangling bond. For almost hydrogen-free surfaces, the incident SiH_3 attached practically immediately. The state of this surface mobile SiH_3 does however not seem to resemble the three center bond for SiH_3 on a surface H atom as assumed in the MGP model. Moreover, in the above-mentioned cluster calculations by Parsons,[30] no evidence for such a three center bond has been observed. Conclusive proof can however not be extracted from these calculations on a very small cluster.

Another aspect of film growth that has been addressed repeatedly is the evolution of the surface roughness during film growth.[20-22] The surface of a-Si:H is actually extraordinary smooth and this smoothness does not naturally follow from surface diffusion of SiH_3 only.[33] This can simply be seen from the fact that when surface dangling bond creation is random on the surface, film growth will be random as well since in the MGP model the radicals can only stick at these dangling bonds. Therefore SiH_3 needs to have a higher probability to find a dangling bond at steps and valleys at the surface in order to lead to smooth film growth. If film growth is ruled by both H abstraction and sticking by physisorbed SiH_3, this means that there is, e.g., preferential abstraction of H at kink-like and step-like surface sites.[20,21] In the case of direct abstraction from the gas phase and precursor mediated sticking, this would imply that surface dangling bonds need to gather in some way at steps and valleys (where they are possibly more stable because the hydrogen atoms present can be "shared" by several bonds). The gathering of dangling bonds at these sites can, for example, take place by surface diffusion of dangling bonds. Such a process might also be suggested by the relatively high activation energy (~1 eV)[22] for the "diffusion ruling mechanism" when compared to the proposed activation energy for surface diffusion of a weakly adsorbed SiH_3 (0.3–0.4 eV).[3,4,15]

Recently, it has been realized that an important aspect of film growth which is not addressed elaborately in the current growth models is the incorporation of H into the a-Si:H bulk or, perhaps more appropriate, the elimination of H from the a-Si:H during growth.[16,18,34] In addition to the fact that the H content is important for the structural and optical film properties, understanding of the underlying reactions for H elimination (preferentially on a microscopic scale) might also yield more insight into the incorporation of defects into the film.[17,18] This aspect of film growth, which might be independent of how SiH_3 actually attaches to the film, will be considered in the next section.

IV. H ELIMINATION DURING a-Si:H GROWTH FROM SiH_3

An unsolved, but fascinating problem in a-Si:H growth is how SiH_3 radicals containing 75 at.% H can lead to an a-Si:H film with typically a H content of ~25–5 at.% (for T_s ranging from ~100–400 °C). In the thermal equilibrium model addressed in Sec. II, H atoms are expected to be eliminated during the redistribution between alternative bonding sites in the growth zone. This redistribution is governed by diffusion and therefore T_s needs to be high enough.[7-10] As a consequence, at higher R_d even a higher T_s is necessary for fast enough equilibration. Although this seems a reasonable description, the elimination mechanism itself is not identified. In the MGP model, a cross-linking reaction has been proposed in which two Si-H bonds in the (sub)surface region are converted into a Si-Si bond and gaseous H_2.[2] This reaction is also rather undefined because it has not been taken into account that the H elimination step should have only a very small activation energy.[16,18,34] Robertson has recently addressed this weakly activated process of H elimination in a hydrogen chemical potential "picture". The microscopic H elimination reaction was identified with the rearrangement of H_2* configurations in a region close to the surface where the barrier for rearrangement is reduced by the presence of weak bonds.[18] This leads to a process with a lower activation energy, however not to the activation energy of 0.1–0.2 eV observed for H elimination as reported below.

Here, we will present an alternative point of view on H elimination that is based on experimental results. First, the H content will be considered for films deposited under better defined conditions than those used by Robertson.[18] The a-Si:H films have been deposited by the expanding thermal plasma (ETP) technique[35] for deposition rates varying over two orders of magnitude. The plasma conditions have been chosen such that 1) film growth is dominated by SiH_3 (~90% SiH_3 as concluded from three independent measurements, see Fig. 2 and Ref. 35), 2) the flux of H from the plasma is very low compared to the flux of SiH_3,[36] and 3) ion bombardment is absent.[37] The latter is known to suppress H incorporation.[38] The H content of the films is shown in Fig. 3. The H content decreases with increasing T_s but increases with increasing R_d as predicted by the thermal equilibrium model. In order to calculate the activation energy for H elimination, an underlying mechanism needs to be assumed for the process. This mechanism can be relatively general and the microscopic reaction does not need to be specified. Following a similar approach as by Kampas and Griffith,[1] we assume that the H content is determined by the fact whether SiH_3 arriving at the surface cross-links under the formation of H_2 or not (see for more details Ref. 34). The

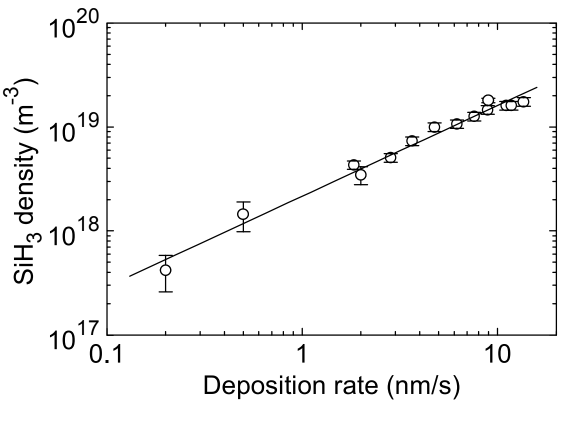

FIG. 2. SiH_3 density close to the substrate as a function of the deposition rate in the expanding thermal plasma. The line with slope ~1 indicates that the deposition rate is linear in the SiH_3 density.

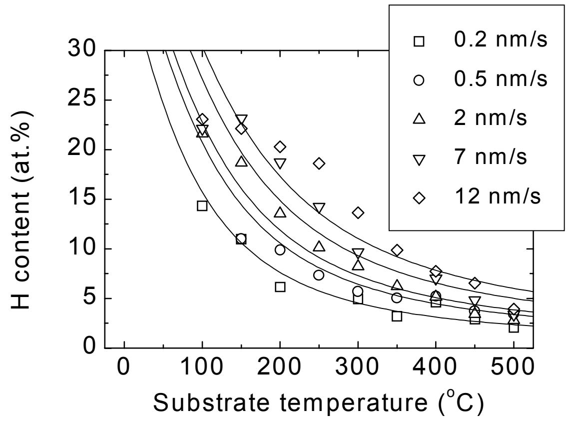

FIG. 3. Bulk H concentration versus the substrate temperature for five different deposition rates in the expanding thermal plasma. The solid lines originate from the fit, see text for further explanation.

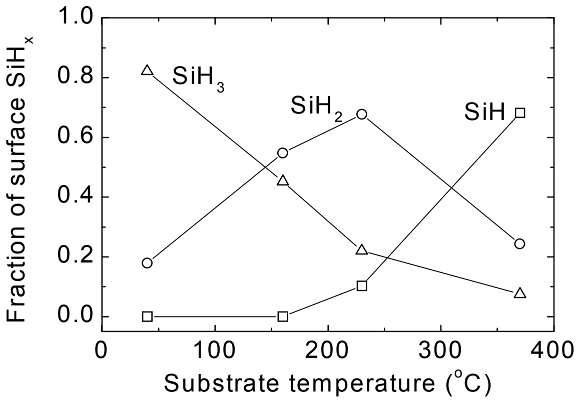

FIG. 4. Fraction of surface Si atoms bonded as SiH$_x$ ($x \leq 3$) as a function of the substrate temperature. The a-Si:H films have been deposited by a "remote" inductively coupled Ar-SiH$_4$ plasma at a plasma power of 25 W.

probability for cross-linking is assumed to be thermally activated by an Arrhenius expression.[34,39] From fitting the data in Fig. 3, an activation energy of 0.13±0.02 eV has been determined for cross-linking. This activation energy, which is indeed very small, has been assumed to be independent of R_d. Therefore only the pre-exponential factor of the Arrhenius expression depends on R_d. This deposition rate dependent pre-factor can be interpreted in terms of a time-scale necessary for the cross-linking reaction, which cannot be satisfied when the deposition rate becomes too high.

Next we will consider experiments in which the composition of the surface hydrides on the a-Si:H surface during film growth have been determined *in situ*.[38] These experiments have been performed on a-Si:H deposited using an inductively coupled plasma reactor under somewhat less well-defined conditions as for Fig. 3. However, there are strong indications that also in this case SiH$_3$ is the dominant growth precursor[38] and we consider data obtained under conditions where the influence of ion bombardment is limited (i.e., at low plasma power). In Fig. 4, the fraction of surface Si atoms bonded to different amounts of H is given. The data in Fig. 4 clearly show the presence of a thermally activated process leading to a transition from dominant SiH$_3$ at low T_s to SiH$_2$, and finally to SiH at high T_s. Calculation of the activation energy for the decomposition reaction of SiH$_3$ into SiH$_2$ using the same underlying mechanism as mentioned above yields 0.21±0.04 eV. Remarkably, this activation energy matches fairly well the value of the activation energy obtained from the bulk H content data, especially when taking the experimental error and the somewhat arbitrarily chosen underlying mechanism into account.

We will now argue that this surface hydride decomposition process has important implications for the H elimination during a-Si:H film growth. We claim that if one understands the decomposition of SiH$_3$ on the surface into SiH$_2$, one understands (at least partially) the elimination of H during film growth. The reason for this is that an a-Si:H surface with only SiH$_2$ *strictly speaking does not need a subsurface H elimination process*: the H atoms of surface SiH$_2$ will not be incorporated into the film because both H atoms will be abstracted during the deposition process in order to create active sites for further film growth.[40] On the average, every surface Si atom needs to end up in the film with two backbonds (for surface SiH$_2$ these are two Si-Si backbonds) in order to retain conservation of surface sites (see, e.g., Fig. 1). So we expect that the fairly good agreement between the activation energies given above is not a coincidence but indicates the importance of surface reactions for the H elimination process. This conclusion is in contrast with the (need for a) subsurface process as proposed by Robertson.[18] It is furthermore noteworthy that Toyoshima *et al.*[23] have observed a similar change in the surface hydrides as in Fig. 4 and that the importance of surface reactions is in agreement with observations that the H rich surface layer exists of only one or a few monolayers.[41]

Although we have presented some evidence for a surface process, the microscopic mechanism for conversion of SiH$_3$ into SiH$_2$ has not been clarified yet. In Ref. 34, we postulated a simple surface process. Herein the chemical energy released during chemisorption of SiH$_3$ on a dangling bond is used to lower the energy barrier for cross-linking of the SiH$_3$ with a neighboring surface SiH$_x$ site while splitting of gaseous H$_2$. Without claiming verity for this particular process, its occurrence might be supported by the fact that Si-H stretch vibrations have a relatively long lifetime[42,43] and remain highly localized[44] whereby the bulk vibrational energy flows directly to bend vibrations, rather than to other stretch states or to host phonons.[42,44] Because these Si-H vibrations are expected to be excited at chemisorption[4] this can lead to the built up of a considerable amount of energy in these vibrations.[45] This energy can possibly be used in the cross-linking step. Another possibility is that surface dangling bonds are involved in the decomposition reactions of surface SiH$_3$ and SiH$_2$. In Ref. 38 for example, a clear influence of surface dangling bonds, as created by ion bombardment, on the decomposition reactions of surface hydrides was observed.

V. CONCLUSIONS

The kinetic model for a-Si:H film growth by SiH$_3$ has been reviewed on the basis of new experimental and computational data. The significance of understanding the H elimination process during growth has been emphasized and the importance of surface processes has been discussed. Although our insight in possible surface reactions has been greatly enlarged, it can be concluded that the growth mechanism of a-Si:H is still not conclusively revealed and that dedicated and detailed studies remain necessary.

ACKNOWLEDGMENTS

Fruitful discussions with Dr. S. Ramalingam, Dr. D. Maroudas, Dr. A. von Keudell, and Dr. J. R. Robertson are acknowledged. C. Smit, B. A. Korevaar, Dr. M. G. H. Boogaarts, and J. P. M. Hoefnagels are thanked for their contributions to the measurements. This work was supported by The Netherlands Organization for Scientific Research (NWO), The Netherlands Foundation for Fundamental Research on Matter (FOM) and The Netherlands Agency for Energy and the Environment (NOVEM).

[1] F.J. Kampas and R.W. Griffith, Appl. Phys. Lett. **39**, 407 (1981).

[2] A. Gallagher, Mater. Res. Soc. Symp. Proc. **70**, 3 (1986).

[3] A. Matsuda and K. Tanaka, J. Appl. Phys. **60**, 2351 (1986).

[4] J. Perrin, Y. Takeda, N. Hirano, Y. Takeuchi, and A. Matsuda, Surf. Sci. **210**, 114 (1989).

[5] A. Matsuda, K. Nomoto, Y. Takeuchi, A. Suzuki, A. Yuuki, and J. Perrin, Surf. Sci. **227**, 50 (1990).

[6] S. Veprek and M. Heintze, Plasma Chem. Plasma Process. **11**, 335 (1990).

[7] K. Winer, Phys. Rev. B **41**, 7952 (1990).

[8] K. Winer, Phys. Rev. B **41**, 12150 (1990).

[9] R.A. Street, Phys. Rev. B **43**, 2454 (1991).

[10] R.A. Street, Phys. Rev. B **44**, 10610 (1991).

[11] J.-L. Guizot, K. Nomoto, and A. Matsuda, Surf. Sci. **244**, 22 (1991).

[12] G. Ganguly and A. Matsuda, Phys. Rev. B **47**, 3661 (1993).

[13] A. Matsuda, Plasma Phys. Control. Fusion **39**, A431 (1997).

[14] A. Matsuda, J. Vac. Sci. Technol. A **16**, 365 (1998).

[15] J. Perrin, M. Shiratani, P. Kae-Nune, H. Videlot, J. Jolly, and J. Guillon, J. Vac. Sci. Technol. A **16**, 278 (1998).

[16] M.C.M. van de Sanden, W.M.M. Kessels, R.J. Severens, and D.C. Schram, Plasma Phys. Control. Fusion **41**, A365 (1999).

[17] M.C.M. van de Sanden, W.M.M. Kessels, A.H.M. Smets, B.A. Korevaar, R.J. Severens, and D.C. Schram, Mater. Res. Soc. Symp. Proc. **557**, 13 (1999).

[18] J. Robertson, J. Appl. Phys. **87**, 2608 (2000).

[19] C.C. Tsai, J.C. Knights, G. Chang, and B. Wacker, J. Appl. Phys. **59**, 2998 (1986).

[20] M. Kondo, T. Ohe, K. Saito, T. Nishimiya, A. Matsuda, J. Non-Cryst. Solids **227-230**, 890 (1998).

[21] A.J. Flewitt, J. Robertson, and W.I. Milne, J. Appl. Phys. **85**, 8032 (1999).

[22] A.H.M. Smets, D.C. Schram, and M.C.M. van de Sanden, Mater. Res. Soc. Symp. Proc. **609**, A7.6.1 (2000).

[23] Y. Toyoshima, K. Arai, A. Matsuda, and K. Tanaka, J. Non-Cryst. Solids **137-138**, 765 (1991).

[24] S. Yamasaki, T. Umeda, J. Isoya, K. Tanaka, J. Non-Crys. Solids **227-230**, 83 (1998).

[25] S. Yamasaki, Mater. Res. Soc. Symp. Proc. **609**, A1.1.1 (2000).

[26] A. Von Keudell and J.R. Abelson, Phys. Rev. B **59**, 5791 (1999).

[27] S. Ramalingam, D. Maroudas, and E.S. Aydil, J. Appl. Phys. **86**, 2872 (1999).

[28] W. Widdra, S.I. Yi, R. Maboudian, G.A.D. Briggs, and W.H. Weinberg, Phys. Rev. Lett. **74**, 2074 (1995).

[29] S. Ramalingam, D. Maroudas, E.S. Aydil, and S.P. Walch, Surf. Sci. Lett. **418**, L8 (1998).

[30] G.N. Parsons, J. Non-Cryst. Solids **266-269**, 23 (2000).

[31] A. Dinger, C. Lutterloh, and J. Küppers, Chem. Phys. Lett. **311**, 202 (1999).

[32] P. Kisliuk, J. Phys. Chem. Solids **3**, 95 (1957).

[33] D.A. Doughty, J.R. Doyle, G.H. Lin, and A. Gallagher, J. Appl. Phys. **67**, 6220 (1990).

[34] W.M.M. Kessels, R.J. Severens, M.C.M. van de Sanden, and D.C. Schram, J. Non-Cryst. Solids **227-230**, 133 (1998).

[35] W.M.M. Kessels, A.H.M. Smets, J.P.M. Hoefnagels, M.G.H. Boogaarts, D.C. Schram, and M.C.M. van de Sanden, Mater. Res. Soc. Symp. Proc. **609**, A4.2.1 (2000).

[36] W.M.M. Kessels, A. Leroux, M.G.H. Boogaarts, J.P.M. Hoefnagels, M.C.M. van de Sanden, and D.C. Schram, submitted for publication

[37] W.M.M. Kessels, C.M. Leewis, M.C.M. van de Sanden, and D.C. Schram, J. Appl. Phys. **86**, 4029 (1999).

[38] D.C. Marra, W.M.M. Kessels, M.C.M. van de Sanden, K. Kashefizadeh, and E.S. Aydil, submitted for publication.

[39] Different from the calculation in Ref. 33, here an Arrhenius expression of the form $\alpha T^n \exp(-E_a/kT)$ with n=0 has been assumed with α the pre-factor, T the substrate temperature, E_a the activation energy, and k the Boltzmann constant.

[40] This is of course only in the ideal case. Due to the amorphous network, H will still be incorporated when the surface contains only SiH_2. It is however plausible that at even higher substrate temperatures when there is dominantly SiH on the surface the probability for H incorporation is even lower.

[41] G.H. Lin, J.R. Doyle, M. He, and A. Gallagher, J. Appl. Phys. **64**, 188 (1988).

[42] P. Guyot-Sionnest, P. Dumas, Y.J. Chabal, G.S. Higashi, Phys. Rev. Lett. **64**, 2156 (1990).

[43] P. Guyot-Sionnest, P.H. Lin, and E.M. Miller, J. Chem. Phys. **102**, 4269 (1995).

[44] C.W. Rella, M. van der Voort, A.V. Akimov, A.F.G. van der Meer, and J.I. Dijkhuis, Appl. Phys. Lett. **75**, 2945 (1999).

[45] C.G. van der Walle, J. Non-Cryst. Solids **227-230**, 111 (1998).

Accepted for publication in Thin Solid Films.

Remote Plasma Deposition of Hydrogenated Amorphous Silicon Plasma Processes, Film Growth, and Material Properties

Summary

In this thesis work, plasma and surface processes during the deposition of hydrogenated amorphous silicon (a-Si:H) have been studied and related to the a-Si:H material properties in order to obtain a better understanding of a-Si:H film growth. This knowledge enables improved optimization of the deposition process as well as of the a-Si:H film quality.

Experiments have been performed using the expanding thermal plasma, a remote plasma deposition technique that allows for independent parameter studies with a large freedom in operating conditions. The technique is based on the dissociation of SiH_4 in a low-pressure reactor by an Ar-H_2 plasma that expands from a cascaded arc plasma source operated at subatmospheric pressures. The expanding thermal plasma technique is capable of depositing a-Si:H at rates up to 10 nm/s, i.e., 10–100 times faster than with conventional deposition techniques. A part of the work has been devoted to the investigation of the a-Si:H material properties obtained under different conditions, and it has been demonstrated that a-Si:H suitable for the application in thin film solar cells can be deposited at these high rates. The major part of the work, however, has been devoted to the investigation of the dissociation processes of the SiH_4 gas and the contribution of the different plasma species to film growth. By relating these results to the material properties, a good understanding of the deposition process in the expanding thermal plasma has been obtained. Furthermore it has also lead to generally relevant, fundamental insights into the conditions under which (high-rate) deposition of good quality a-Si:H is possible.

The remote nature of the deposition technique allows for a separate analysis of the reactive species emanating from the plasma source that induce the dissociation of SiH_4. Therefore, these species have been investigated for different operating conditions of the source, and from the results, SiH_4 dissociation processes have been hypothesized. Subsequently, the proposed reaction scheme has systematically been verified and further refined by investigations of the Ar-H_2-SiH_4 plasma using several, newly-implemented, diagnostic techniques. Hydrogen-poor cationic silicon clusters, $Si_nH_m^+$, have been measured using ion mass spectrometry and Langmuir probe measurements while silane radicals SiH_x ($x \leq 3$) have been detected by means of threshold ionization mass spectrometry (SiH_3 and SiH_2), cavity ring down absorption spectroscopy (SiH_3, SiH and Si) and optical emission spectroscopy (SiH* and Si*). Furthermore, information about the contribution of the different species to film growth has been obtained from surface reaction probability measurements with the aperture-well technique. The combination of these measurements has revealed clear insight into the reactions taking place in the plasma and has yielded quantitative information about the contribution of the different species to the film growth for different plasma settings. It is, for example, found that for all conditions investigated, the a-Si:H deposition process is dominated by neutrals and a direct relation between the contribution of SiH_3 radicals to the film growth and the film quality has been demonstrated. The best film properties are obtained for conditions at which film growth is by far dominated by SiH_3 while films with inferior properties are obtained under conditions at which there is a large contribution of very reactive (poly)silane radicals. The conditions at which SiH_3 dominates the film growth have also been studied by two-dimensional fluid dynamics model calculations, which have been compared to spatially resolved SiH_3 measurements. The model has proven to be a very helpful tool for the interpretation of the experimental data and it has also yielded a better understanding of the gas flow dynamics in the expanding thermal plasma.

In addition to the plasma composition, the nature of the a-Si:H surface is also important for the film growth processes. Therefore, a new method for *in situ* analysis of the hydrogen surface composition during growth has been further developed and tested in cooperation with the University of California Santa Barbara. Using this technique, which is based on attenuated total reflection infrared spectroscopy, the surface coverage of the different hydrides has been determined for a-Si:H deposited using various substrate and plasma conditions in an inductively

coupled plasma reactor. This study has yielded information on thermally activated and ion-induced surface reactions during a-Si:H film growth.

The atomistic mechanisms during the a-Si:H growth process have also been addressed. The prevailing kinetic growth model for a-Si:H has been reviewed and, in particular, the incorporation of hydrogen in a-Si:H and its dependence on the substrate temperature and the deposition rate have been considered. It is argued that hydrogen elimination reactions play a crucial role with respect to the film quality and it is demonstrated that these reactions take place, at least partially, at the surface. It appears that the dominance of SiH_3 to the film growth together with sufficient elimination of hydrogen are key elements for obtaining good quality a-Si:H at high deposition rates.

Finally, it can be concluded that the combined study of the plasma processes, film growth mechanisms, and material properties has provided valuable new insights in the plasma deposition process of a-Si:H in general.

Remote Plasma Deposition of Hydrogenated Amorphous Silicon Plasma Processes, Film Growth, and Material Properties

Samenvatting

In het werk, beschreven in dit proefschrift, zijn plasma- en oppervlakteprocessen die plaatsvinden tijdens de depositie van gehydrogeneerd amorf silicium (a-Si:H) onderzocht en gerelateerd aan de materiaaleigenschappen, teneinde tot een beter begrip van de groei van a-Si:H films te komen. Dit maakt een verdere optimalisatie van zowel het depositieproces als van de kwaliteit van het a-Si:H mogelijk.

Experimenten zijn uitgevoerd met het expanderend thermisch plasma, een *remote* plasmadepositietechniek die zich leent voor onafhankelijke parameterstudies met daarbij een grote vrijheid in plasmacondities. De techniek is gebaseerd op de dissociatie van SiH_4 in een lage-druk reactor door een Ar-H_2 plasma dat expandeert vanuit een op sub-atmospherische druk bedreven plasmabron (cascadeboog). Met deze techniek is het mogelijk om a-Si:H te deponeren met groeisnelheden tot 10 nm/s, hetgeen 10–100 keer sneller is dan met de gebruikelijke depositietechnieken. Een gedeelte van het onderzoek is gewijd aan de eigenschappen van het materiaal verkregen met deze methode. Daarbij is het aangetoond dat a-Si:H gedeponeerd met zulke hoge groeisnelheden toepasbaar is in dunne-film zonnecellen. Het merendeel van het onderzoek betreft echter de dissociatieprocessen van het SiH_4 gas en de bijdragen van de verschillende plasmadeeltjes aan depositie. Door deze resultaten te relateren aan de materiaaleigenschappen, is een goed beeld verkregen van het depositieproces in het expanderend thermisch plasma. Daarnaast heeft het ook geleid tot een beter, algemeen inzicht in de fundamentele omstandigheden waaronder (snelle) depositie van hoge kwaliteit a-Si:H mogelijk is.

Het feit dat de creatie van het plasma geometrisch gescheiden plaatsvindt van de dissociatie van SiH_4 en het depositieproces, maakt het mogelijk om de reactieve deeltjes, die uit de plasmabron komen en die de dissociatie van SiH_4 initiëren, apart te onderzoeken. Deze deeltjes zijn daarom onderzocht voor verschillende plasmacondities en aan de hand van de resultaten zijn de verwachte dissociatieprocessen van SiH_4 opgesteld. Door middel van nieuw geïmplementeerde diagnostieken is het veronderstelde reactieschema vervolgens systematisch geverifiëerd en verfijnd aan de hand van studies aan het Ar-H_2-SiH_4 plasma. Waterstof-arme kationische silicium clusters, $Si_nH_m^+$, zijn gemeten met ionen-massaspectrometrie en Langmuir-sondes terwijl silaan radicalen SiH_x ($x \leq 3$) bestudeerd zijn met behulp van *threshold ionization* massaspectrometrie (SiH_3 and SiH_2), *cavity ring down* absorptiespectroscopie (SiH_3, SiH and Si) en optische emissiespectroscopie (SiH* and Si*). Verder is er informatie verkregen over de bijdragen van verschillende deeltjes aan het depositieproces door oppervlakte-reactiekans metingen met behulp van de *aperture-well* techniek. De combinatie van deze metingen heeft geleid tot een goed begrip van de reacties die plaatsvinden in het plasma en kwantitatieve informatie is verworven over de bijdragen van de verschillende deeltjes aan depositie voor verscheidende plasmacondities. Zo is bijvoorbeeld aangetoond dat voor alle bestudeerde omstandigheden het depositieproces gedomineerd wordt door neutralen en dat er een directe relatie bestaat tussen de bijdrage van SiH_3 aan het depositieproces en de materiaalkwaliteit. De beste materiaaleigenschappen worden verkregen onder condities waarbij het depositieproces verreweg gedomineerd wordt door SiH_3, terwijl materiaal met minderwaardige eigenschappen verkregen wordt onder condities waarbij zeer reactieve (poly)silaan radicalen een grote bijdrage tot groei hebben. De condities, waarbij het groeiproces gedomineerd wordt door SiH_3, zijn tevens bestudeerd aan de hand van berekeningen met een twee-dimensionaal vloeistofmodel, waarvan de resultaten vergeleken zijn met plaatsopgeloste SiH_3 metingen. Het is gebleken dat het model zeer nuttig is voor de interpretatie van de experimentele data terwijl het ook tot een beter inzicht heeft geleid in de gasstromen in het expanderend thermisch plasma.

Naast de samenstelling van het plasma is ook de aard van het oppervlak van a-Si:H van belang voor de processen die plaatsvinden tijdens de groei van a-Si:H. Daarom is in samenwerking met de Universiteit van Californië Santa Barbara een nieuwe methode ontwikkeld en getest voor de *in situ* analyse van de samenstelling van de waterstofverbindingen aan het oppervlak. Met behulp van deze techniek, die gebaseerd is op *attenuated total reflection* infrarood spectroscopie, is de oppervlaktebedekking van de verschillende waterstofverbindingen bepaald voor a-Si:H gedeponeerd met een inductief gekoppeld plasma voor verschillende substraattemperaturen en plasmacondities. Dit onderzoek heeft informatie opgeleverd over thermisch geactiveerde en ion-geïnduceerde oppervlaktereacties die plaatsvinden tijdens de groei van a-Si:H.

Verder zijn ook de atomaire mechanismen die plaatsvinden tijdens het a-Si:H groeiproces behandeld. Het gangbare, kinetische groeimodel voor a-Si:H is besproken. In het bijzonder, zijn de inbouw van waterstof in a-Si:H tijdens de groei en de invloed van de substraattemperatuur en de groeisnelheid daarop in beschouwing genomen. Het is beredeneerd dat reacties die tot waterstofeliminatie leiden een cruciale rol spelen wat betreft de materiaalkwaliteit en het is aangetoond dat deze reacties tenminste deels plaatsvinden op het oppervlak. Het blijkt dat een SiH_3 gedomineerd groeiproces samen met voldoende eliminatie van waterstof een belangrijke rol spelen in het verkrijgen van hoge kwaliteit a-Si:H bij hoge groeisnelheden.

Tenslotte kan geconcludeerd worden dat de combinatie van onderzoek aan plasmaprocessen, groeiprocesmechanismen en materiaaleigenschappen heeft geleid tot nieuwe en waardevolle inzichten in het plasmadepositieproces van a-Si:H in het algemeen.

List of other publications related to this work

In addition to the journal articles presented in this thesis (see Part B of this thesis), other publications related to this work are:

- Hydrogen incorporation during deposition of a-Si:H from an intense source of SiH_3
  M.C.M. van de Sanden, R.J. Severens, W.M.M. Kessels, F. van de Pas, L.J. van IJzendoorn, and D.C. Schram, Mater. Res. Soc. Symp. Proc. **467**, 621 (1997).

- Diagnostics of deposition plasmas
  D.C. Schram, M.C.M. van de Sanden, R.J. Severens, and W.M.M. Kessels, J. Phys. IV France **8**, Pr7-217 (1998).

- Plasma chemistry aspects of a-Si:H deposition using an expanding thermal plasma
  M.C.M. van de Sanden, R.J. Severens, W.M.M. Kessels, R.F.G. Meulenbroeks, and D.C. Schram, J. Appl. Phys. **84**, 2426 (1998).

- Hydrogen in a-Si:H deposited by an expanding thermal plasma: a temperature, growth rate and isotope study
  W.M.M. Kessels, M.C.M. van de Sanden, R.J. Severens, L.J. van IJzendoorn, and D.C. Schram, Mater. Res. Soc. Symp. Proc. **507**, 529 (1998).

- Plasma and surface chemistry effects during high rate deposition of hydrogenated amorphous silicon
  M.C.M. van de Sanden, W.M.M. Kessels, R.J. Severens, and D.C. Schram, Plasma Phys. Control. Fusion **41**, A365 (1999).

- Remote silane plasma chemistry effects and their correlation with a-Si:H film properties
  W.M.M. Kessels, A.H.M. Smets, B.A. Korevaar, G.J. Adriaenssens, M.C.M. van de Sanden, and D.C. Schram, Mater. Res. Soc. Symp. Proc. **557**, 25 (1999).

- The role of H in the growth mechanism of PECVD a-Si:H
  M.C.M. van de Sanden, W.M.M. Kessels, A.H.M. Smets, B.A. Korevaar, R.J. Severens, and D.C. Schram, Mater. Res. Soc. Symp. Proc. **557**, 13 (1999).

- High hole drift mobility in a-Si:H deposited at high growth rates for solar cell application
  B.A. Korevaar, G.J. Adriaenssens, A.H.M. Smets, W.M.M. Kessels, H.–Z. Song, M.C.M. van de Sanden, and D.C. Schram, J. Non-Cryst. Solids. **266-269**, 380 (2000).

- Analysis of time-of-flight photocurrents in a-Si:H deposited by expanding thermal plasma
  G.J. Adriaenssens, H.-Z. Song, V.I. Arkhipov, E.V. Emelianova, W.M.M. Kessels, A.H.M. Smets, B.A. Korevaar, and M.C.M. van de Sanden, Journal of Optoelectronics and Advanced Materials **2**, 31 (2000).

- Modeling of the formation of cationic silicon clusters in a remote Ar-H_2-SiH_4 plasma
  A. Leroux, W.M.M. Kessels, D.C. Schram, and M.C.M. van de Sanden, J. Appl. Phys. **88**, 537 (2000).

- Relation between growth precursors and film properties for plasma deposition of a-Si:H at rates up to 100 Å/s
  W.M.M. Kessels, A.H.M. Smets, J.P.M. Hoefnagels, M.G.H. Boogaarts, D.C. Schram, and M.C.M. van de Sanden, Mater. Res. Soc. Symp. Proc. **609**, A4.2.1 (2000).

- Cavity ring down detection of SiH_3 in a remote Ar-H_2-SiH_4 plasma
  M.G.H. Boogaarts, P.J. Böcker, W.M.M. Kessels, D.C. Schram, and M.C.M. van de Sanden, accepted for publication in Chem. Phys. Lett.

- High growth-rate deposition of silicon-rich a-$Si_xN_yH_z$-films for photovoltaic applications
  W.M.M. Kessels, T. Lauinger, J.D. Moschner, D.C. Schram, and M.C.M. van de Sanden, submitted for publication.

Dankwoord/Acknowledgments

Knowledge is in the end based on acknowledgment.

Ludwig Wittgenstein

Dit proefschrift was natuurlijk nooit tot stand gekomen zonder de hulp en steun van vele anderen. Ik wil daarom iedereen die een bijdrage heeft geleverd hartelijk bedanken.

Erg veel dank gaat uit naar Richard van de Sanden die naast een "perfecte" begeleider inmiddels ook een goede vriend is. Richard, ik ben je erg dankbaar voor alle dingen die ik van je geleerd heb, ook voor die dingen die niet meteen met "mijn onderzoek" te maken hadden. Het wederzijdse enthousiasme en het intense contact (*in de trein van acht uur voor onze* "*werkbespreking*" *en niet te vergeten het bijna dagelijkse telefoontje:* "*het zal Richard wel weer zijn…*") hebben geleid tot een enorme motivatie en, al is het aan anderen om daarover te oordelen, een hoge productiviteit.

Verder ben ik veel dank verschuldigd aan Daan Schram, mijn eerste promotor en de groepsleider. Onze discussies en jouw visie op de plasmafysische en plasmachemische processen zijn zeer inspirerend en altijd een aanleiding om de zaken ook eens van een andere kant te bekijken. Ook ben ik erg ingenomen met de wijze waarop je iedereen bij het reilen en zeilen van de groep betrekt en met de mogelijkheden en vrijheid die je biedt. Dit, samen met de inspanningen van de andere groepsleden, heeft geleid tot de uiterst prettige en uitzonderlijke sfeer in de groep.

Cruciaal voor het onderzoek was ook de technische ondersteuning van Ries van de Sande, Jo Jansen, Bertus Hüsken en Herman de Jong. Ries wil ik extra bedanken. Zonder zijn snelle en vakkundige reparaties als er weer iets kapot ging ("*heeft hij dat gedaan?*") en zijn fantastische ontwerpen voor als we weer iets nieuws verzonnen hadden ("*voor jou doe ik alles…*"), was dit werk niet mogelijk geweest. Ook onze secretaresse Jeanne Loonen ben ik zeer dankbaar voor haar hulp en gezelligheid ("*nog nieuws…?*"). En jullie zijn nog niet van mij af…

En dan het "Depo 2 team": René Severens, Arno Smets (*onze knakenman… bedankt voor de vele "onderhoudswerkzaamheden" aan de opstelling*), Bas Korevaar, Maarten Boogaarts, Alain Leroux, Chiel Smit, Edward Hamers en Johan Hoefnagels. Bedankt voor de hechte samenwerking die zeer vruchtbaar is gebleken en die ons op de kaart van de a-Si:H wereld heeft gezet! Ook naar mijn andere collega's van ETP (inmiddels te veel om allemaal op te noemen) gaat mijn dank uit voor de fantastische tijd in de afgelopen jaren en hun behulpzaamheid op allerlei gebied (*ik denk dat ik nog maar even in de groep blijf…*). Verder wil ik deze kans aangrijpen om ook de collega's van EPG te bedanken.

De geleverde bijdragen van de afstudeerders Suzanne van Egmond, Christian Leewis, Paul Böcker, Johan Hoefnagels en de stagairs Niels van der Beek, Igor Aarts, Frank Hammen en Bart Broks waren ook onontbeerlijk voor het tot stand komen van dit proefschrift. Ik ben erg blij dat ik met jullie samen heb mogen werken en bedankt voor het begrip dat jullie toonden wanneer ik mijn eisen m.b.t. de experimenten weer eens verder opvoerde ("*dat is een mooi resultaat…, nu zou ik dit nog willen…*"). Dit geldt ook voor Cas Smits, Ivo Thomas en René ter Riet die mij tijdelijk in mijn werkzaamheden ondersteunden. Furthermore, I am very grateful for the contributions to the work by my international friends Luc Gabella, Guiseppina Toto, and Cosimo Vitarella. Thanks a lot, guys!

I also want to acknowledge the people from UCSB in Santa Barbara, especially Eray Aydil and Shyam Ramalingam, and, of course, Denise Marra. Denise, thank you for the pleasant time during the measurements, your patience and enthusiasm, and, of course, the proofreading. Thank you all for the fruitful cooperation and your hospitality. It was really a pleasure!

Although mostly acknowledged in the articles, I want to thank once again all the other people (national and international) who have contributed in some way to the investigations presented.

Naast bovengenoemde mensen zijn ook mijn vrienden, kennissen, ex-huisgenoten en natuurlijk de mannen en vrouw van Fysisch Genootschap Nwyvre erg belangrijk geweest voor mij in de afgelopen jaren. Ik heb een geweldige tijd gehad (*naast de talloze traditionele activiteiten, denk ik in het bijzonder aan de wekelijkse borrel, het stappen met (Z)Addo en de Hut op zondag*). Proost!

Tenslotte wil ik mijn eigen Katinka bedanken voor haar liefde en steun. Ze zag het vaak met lede ogen aan dat ik van 's ochtends vroeg tot 's avonds laat in de weer kon zijn met wat ik mijn hobby noem ("*als ik dat af heb, heb ik meer tijd*"… *Niet dus!*) maar zorgde er in al die tijd toch voor dat ik niets tekort kwam. Jouw bijdrage is van onschatbare waarde!

Curriculum Vitae

12 April 1973

Born in Venlo, The Netherlands.

June 1991

Diploma Atheneum, Bouwens van der Boije College, Helden-Panningen.

September 1991 – August 1996

Student Applied Physics, Eindhoven University of Technology.

Four months (summer 1995) traineeship in the group of Prof. M. Fitaire at the Laboratoire de Physique des Gaz et des Plasmas, Université Paris XI.

Master thesis project in the group Equilibrium and Transport in Plasmas.

September 1996 – June 2000

PhD student, Center for Plasma Physics and Radiation Technology, Department of Applied Physics, Eindhoven University of Technology.

Three months (spring 1999) working visit to the group of Prof. E. S. Aydil at the Department of Chemical Engineering, University of California Santa Barbara.

John Coburn and Harold Winters Student Award in Plasma Science and Technology, American Vacuum Society 1999.

July 2000 – Present

Post-doctoral researcher, Center for Plasma Physics and Radiation Technology, Department of Applied Physics, Eindhoven University of Technology.